Simulering af selektivitet i fiskeredskaber

Del 1: Hovedrapport

Udarbejdet af: Bent Herrmann, Ludvig A. Krag, Rikke P. Frandsen, Bo Lundgren, Niels Madsen og Karl-Johan Stæhr

DTU Aqua

2008

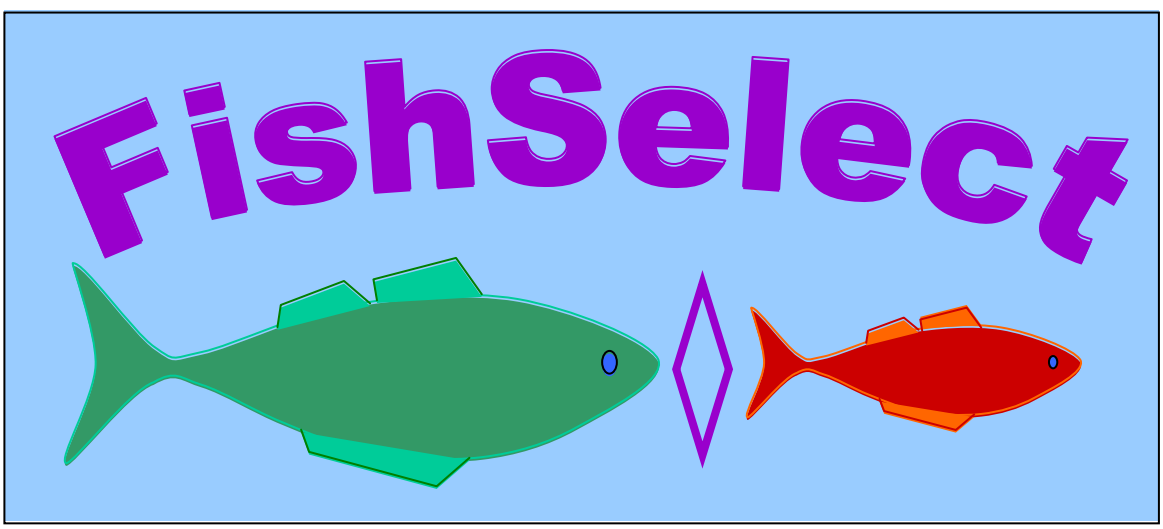

Forord

Denne rapport redegør gennem en kortfattet hovedrapport og gennem en række mere fyldestgørende bilag i appendiks for det arbejde og de resultater, der er opnået i delprojektet ”redskabsselektivitet”. Delprojektet indgår som et selvstændigt element i projektet ”Forvaltningsplaner og dansk fiskeri - Projekt under udviklingsprogrammet for bæredygtigt fiskeri og selektive fangstmetoder”.

Denne projektrapport omhandler udelukkende det gennemførte arbejde i delprojektet om redskabsselektivitet i den samlede projektperiode (2006-2007). Delprojektet omtales herefter blot som ”projektet” samt den mere præcise projekttitel ”Simulering af selektivitet i fiskeredskaber”. Hovedrapporten er skrevet på dansk mens bilagene er skrevet på engelsk. Hovedrapporten består af et resumé efterfulgt af fire kapitler omhandlende de udviklede metoder og værktøjer samt resultater opnået med anvendelse af disse. Hovedrapporten afsluttes med en diskussion, der også indeholder forslag til hvordan der kan arbejdes videre med metoderne og deres anvendelse på konkrete problemstillinger. Appendiksdelen gennemgår i langt større detaljeringsgrad emnerne omtalt i hovedrapporten og dokumenterer bedre det udførte arbejde og de opnåede resultater. Af praktiske årsager er hovedrapport og appendiksdel indbundet i to separate bind.

Projektet ”Simulering af selektivitet i fiskeredskaber” er gennemført af personale fra ”Fiskeriteknologisektionen” Institut for Akvatiske Ressourcer, Danmarks Tekniske Universitet placeret i NordSøen Forskerpark i Hirtshals. Til fremstilling og design af forsøgs- og måleudstyr er der brugt intern assistance fra det mekaniske værksted under instituttet og vedr. specificering og anskaffelse af IT og elektronisk udstyr desuden assistance fra instituttets IT-afdeling. Personale fra andre afdelinger ved instituttet har i forskelligt omfang desuden været behjælpelig med fremskaffelse af og opbevaring af de levende fisk og jomfruhummere der er anvendt i projektet. Eksternt har F.G. O’Neill fra FRS, Aberdeen, Skotland bidraget til arbejdet der rapporteres.

Hos Fiskeriteknologisektionen har følgende medarbejdere bidraget til gennemførelse af projektets videnskabelige indhold og til afrapporteringen af dette:

Bent Herrmann, Ludvig A. Krag, Rikke P. Frandsen, Bo Lundgren, Niels Madsen, Karl-Johan Stæhr.

Yderligere oplysninger om ”Simulering af Redskabsselektivitet” kan indhentes fra projektlederen (Bent Herrmann). For oplysninger om hovedprojektet hvori delprojektet indgår henvises til den overordnede projektleder (Eskild Kirkegaard).

Hirtshals januar 2008

Indholdsfortegnelse

Resumé

Mål og planlagt indhold

I henhold til projektkontrakten har vi i projektet udviklet en selektionsmodel der, baseret på viden om fiskenes morfologi og eksisterende redskabsselektionsdata, gør det muligt at vurdere et redskabs selektivitet. Et delmål er at blive i stand til at udarbejde en designguide, der, for de vigtigste danske arter, beskriver de selektive egenskaber for forskellige typer redskaber. Guiden skal bl.a. bruges til at rådgive om optimal sammenhæng mellem redskabets selektivitet og mindstemålet på de respektive arter. Der vil blive etableret en database med de nødvendige morfologiske data.
Projektet er delt op i tre hovedaktiviteter:

1. Indsamling af data. Laboratorieforsøg, der identificerer de morfologiske karakteristika, der er afgørende for maskepenetrering for forskellige arter. Udvikling af effektiv måleprocedure baseret på vision-teknologiske og mekaniske metoder. Derefter gennemføres morfologimålinger på et større antal individer.
2. Udvikling af selektionssimuleringsværktøj. Et værktøj, der kan beregne selektionen med anvendelse af morfologiske data, fiskeadfærd og redskabsdesign samt redskabets respons på fysiske parametre som fangstmængde og andre relevante parametre for slæbet. Simuleringsværktøjet evalueres ved sammenligning mellem eksisterende eksperimentelle data og modelberegninger.
3. Prognoseberegninger. Der udvikles en prognosemodel, der kan beregne et fartøjs forventede fangst samt de forventede driftsøkonomiske konsekvenser ved designændringer i fangstposen.

Faktisk projektindhold og opnåede resultater.

Der er udviklet en metodik og tilhørende værktøjer til at identificere, opsamle og analysere morfologiske parametre af vigtighed for maskepassage. Måleproceduren omfatter anvendelse af et specialudviklet konturværktøj (MorphoMeter), scanning af værktøjet og digital billedbehandling i et specialudviklet dataopsamlings-, analyse og simuleringsprogram FISHSELECT. Programmet indeholder faciliteter, der muliggør forudsigelse af de basale selektive egenskaber for maskepaneler med forskelligt design (masker af forskellig størrelse og facon). Programmet kan anvendes til at udarbejde en designguide og undersøge om der er et fornuftigt forhold mellem de eksisterende mindstemål og størrelsen hvorover fisken eller skaldyret forventes tilbageholdt af det anvendte paneldesign under givne forhold. Med paneldesign henvises her til de net-paneler trukne redskab er sammen sat af. Metoden åbner også for nye muligheder til at optimere fremtidige paneldesigns til anvendelse i trukne fiskeredskaber.

Der er foretaget dataindsamling for torsk, rødspætte, kuller, pighvar, rødtunge, gråtunge samt jomfruhummer. Der foreligger databaseoplysninger for de morfologiske egenskaber for alle arterne på nær for jomfruhummer. Oparbejdning af data for torsk og rødspætte er fuldt afsluttet og der foreligger designguides for disse arter for følgende masketyper: diamant, kvadrat, rektangel og heksagonal samt ristsystemer. For kuller, pighvar og

rødtunge foreligger en designguide for diamantmasker. For gråtunge og jomfruhummer har det inden for projektets rammer ikke været muligt helt at færdiggøre dataanalysen. Der har nationalt været en del presseomtale af projekts metoder og foreløbige resultater. Der har været international præsentation af metode og foreløbige resultater i ICES regi' (posters og symposium præsentation). Internationalt er der udtrykt interesse for at adoptere metoden. Der foreligger 3 manuskripter til videnskabelige artikler for foreløbig 1: metode, 2: anvendelse på torsk og 3: anvendelse på rødspætte.
Der har også været arbejdet med alternative metoder til bestemmelse af de morfologiske grunddata.

PRESEMO, der er et computerprogram, der simulerer og visualiserer fangstprocesserne i et trawls fangstpose, er blevet videreudviklet og testet op mod eksperimentelle selektionsdata for kuller (på basis af eksisterende morfologiske data) som beskrivelse for rundfisk. Der blev opnået ret god overensstemmelse. Resultaterne er dokumenteret i en videnskabelig artikel, der forudsiger hvordan selektionen i fangstposer af diamant masker afhænger af maskestørrelse, antal masker i omkredsen, trådtykkelsen samt af den akkumulerede fangstmængde.

PRESEMO er bl.a. blevet udvidet med en prognosedel, der kan sammenligne forventede fangstmængder under og over mindstemålet for forskellige fangstposedesigns (forskellig maskevidde, antal masker i omkredsen og netpanelernes trådtykkelse). Det har ikke inden for projektets rammer været muligt at videreudvikle PRESEMO på basis af de FISHSELECT data, der er indsamlet i projektet. PRESEMO har i projektperioden været præsenteret på en international konference samt været inddraget i internationalt rådgivningsarbejde.

FISHSELECT og PRESEMO er begge bygget op omkring en grafisk brugerflade og kan begge afvikles på en PC med hurtig CPU under et Microsoft Windows operativsystem. Begge software-værktøjer er velafprøvede og fungerer teknisk robust og stabilt. Udviklede måle- og hjælpe-værktøjer er gennemprøvede og forefindes i funktionsduelige eksemplarer. Til gennemførelse af de tidskrævende simuleringskørsler samt til dataopsamling er der anskaffet IT-udstyr og andet nødvendigt elektronisk udstyr.

Det vurderes at de udviklede metoder, værktøjer og de hermed opnåede resultater nu er på et sådan niveau at det vil være hensigtsmæssigt at inddrage dette i rådgivningen om tekniske reguleringer i fiskeriet. Samt i forbindelse med udvikling af nye selektive fiskeredskaber. Forskningsmæssigt forventes metodernes anvendelse at kunne bidrage til større viden om fundamentale processer involveret i størrelsesselektion i trukne fiskeredskaber.

Kapitel 1: Beskrivelse af FISHSELECT metodik og værktøjer

FISHSELECT er en metodik til at bestemme og beskrive de morfologiske betingelser, der afgør om fisk og krebsdyr kan trænge gennem masker og ristsystemer i trukne fiskeredskaber. FISHSELECT er baseret på en kombination af laboratorieforsøg med friskfangede levende individer, data opsamling, data analyse og computer simulering. FISHSELECT software-værktøjet, der er udviklet som en del af projektet understøtter alle disse opgaver. Værktøjets faciliteter er beskrevet i appendiks A9, mens metodikken og det matematiske grundlag herfor er beskrevet i detaljer i appendiks A1.
De fire hovedelementer (a til d) i FISHSELECT metodikken beskrives efterfølgende kort. Et overblik for metoden fremgår også af posteren i appendiks A12.

a. <u>Forsøg i laboratoriet og data indsamling.</u>

For hvert individ registreres længde og vægt. Facon og størrelse af de tværsnit på individerne som potentielt kan have betydning for om individet kan trænge igennem masker og ristsystemer registreres også. Dette gøres ved at bruge et specialudviklet konturværktøj "mekanisk MorphoMeter" som tager af aftryk af fiskens facon i et valgt tværsnit (se appendiks A1 afsnit 11 samt appendiks A12, der også beskriver arbejdet med udvikling af en alternativ metode). Ved hjælp af en scanner og digital billedanalyse digitaliseres informationen fra MorphoMeteret i en computer. Tværsnitsdataene parameteriseres og beskrives efterfølgende automatisk på basis af nogle grundlæggende geometriske former. Ved regressionsanalyse relateres parameterværdierne for tværsnitsbeskrivelserne og deres varians til længden af individerne. Alle data opsamles og analyseres i FISHSELECT software-værktøjet. Fig. 1. illustrerer denne proces.

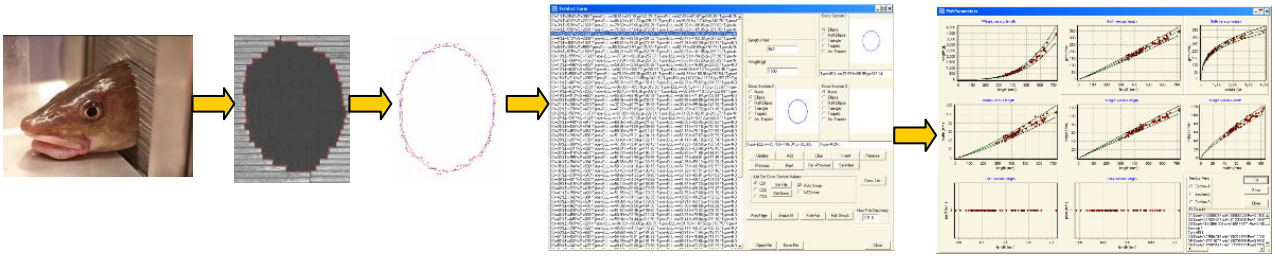

Fig. 1. Processen for tværsnitsmåling: aftryk af tværsnit med MorphoMeter, scanning/billedanalyse, tværsnitsparametrisering, dataformatering, regressionsanalyse (fra venstre).

Plader med huller af forskellig størrelse og facon bruges til at imitere et stort antal masker af forskellig størrelse og facon (Appendiks A10 beskriver det praktiske arbejde omkring implementering af pladerne samt med at relatere deres geometrier til "rigtige" masker). For hver maske og hvert individ undersøges og registreres det om individet kan trænge igennem masken under indflydelse af tyngdekraften alene. Fig. 2 illustrerer denne proces.

Fig. 2. Gennemtrængningsforsøg og dataregistrering (gennemfald – ikke gennemfald).

b. Simulering af laboratorieforsøg med maske gennemtrængning.

I FISHSELECT-softwaren er der indbygget modelerings- og simuleringsfaciliteter, som kan anvende de morfologiske beskrivelser af individtværsnittene og informationer om maskegeometrier. Med disse faciliteter simuleres gennemtrængnings-forsøgene. Desuden inkluderes anvendelse af data fra et eller flere tværsnit for hvert individ og mulighed for forskellige måder til og niveauer for deformation og komprimering af tværsnit under forsøg på at trænge igennem masker. Ved automatisk at generere sammenligningsparametre, der angiver hvor godt de eksperimentelle resultater stemmer overens med de tilsvarende simulerede data, bestemmes hvilken passagemodel, der bedst forklarer maske gennemtrængningen for en specifik art. Passagemodellen kan være baseret på et enkelt tværsnit eller en kombination af flere og hvert tværsnit kan antage forskellige grader af kompression eller deformation. Fig. 3 illustrerer dette. Under simuleringen visualiseres det løbende hvordan tværsnittene med den antagne komprimering passer i forhold til de enkelte maskehuller.

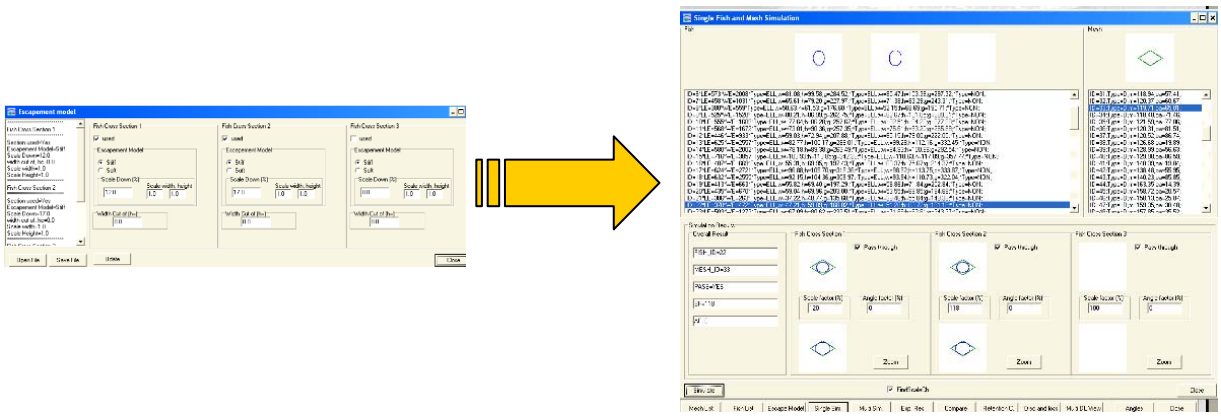

Fig. 3. Modelparameterdisplay og tværsnit/masketilpasningsdisplay under simulering.

Ved at studere sammenligningsparametrene kan det indirekte bestemmes hvilke tværsnits-informationer der skal anvendes og hvordan der skal tages højde for eventuel kompression af disse ved simulering af maskepassage. I alt benævnes disse informationer en passagemodel.

c. Dannelse af virtuel population.

På basis af regressionssammenhængene for de parametre der indgår i beskrivelsen af de tværsnit der, ifølge den identificerede passagemodel, har betydning for mulighederne for at en given art kan trænge igennem masker, kan der nu dannes en virtuel population med en vilkårlig størrelsesfordeling. Fig. 4 viser oversigtsdisplayet for en sådan population.

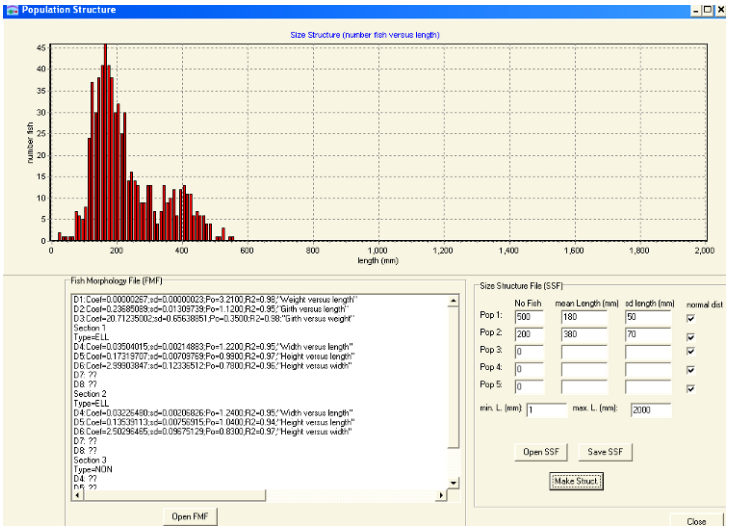

Fig. 4. Størrelsesfordeling samt datarecords og parametre for en virtuel population med to delkomponenter.

d. Simulering af basale selektionsegenskaber.

På basis af den fundne passagemodel (fra b) og en virtuel population med relevant størrelsesfordeling (fra c) foretages nu en ny serie af simuleringer i hvilke der anvendes parametre for forskellige nye maskepaneler. På denne måde er det, ved at anvende FISHSELECT-softwaren, muligt at estimere basale selektive egenskaber (selektionskurver) for nye og eksisterende netpaneler i forhold til de arter der studeres. For et specifikt design er det dermed muligt at vurdere om der er en rimelig balance mellem designets selektive egenskaber og de fastsatte mindstemål (MLS) for relevante arter. Fig. 5 illustrerer dette.

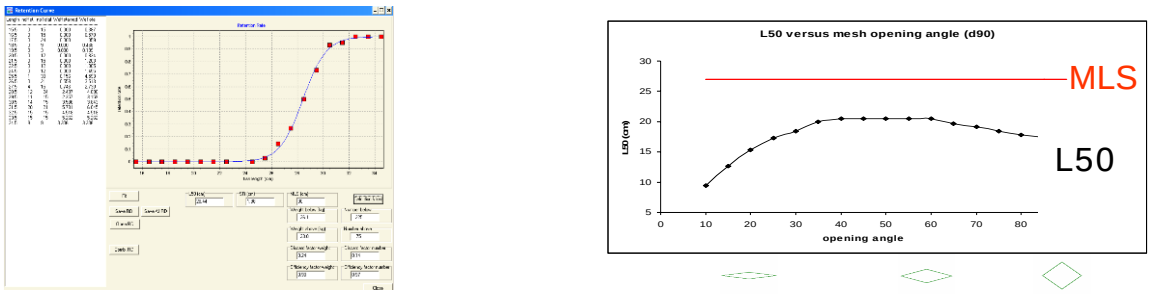

Fig. 5. Basale selektive egenskaber for en diamantmaske og mindstemål i forhold til L50 ved forskellig maskeåbning.

ICES har anbefalet at MLS svarer til L25, der er den længde hvor 25 procent af de fisk der kommer ind i redskabet tilbageholdes. Da simuleringerne af L25 har en tendens til at

være overestimerede på grund af lille SR, når det kun er en enkelt maske der tages i betragtning, har vi valgt at sammenligne MLS med L50. Dette er altså en fravigelse fra forsigtighedsprincippet, men sammenligningen giver stadig en meget tydelig indikation af mulige uoverensstemmelser mellem den del af fiskene, der tilbageholdes af redskabet og den del det er lovligt for fiskeren at bringe i land.

Det er også muligt at danne såkaldte designguides, der på tabel-form angiver de basale selektive data for en lange række beslægtede designs som f. eks for diamantmasker med forskellig maskevidde og forskellig åbningsvinkel. Denne type data kan benyttes til at konstruere plots bestående af kurver for konstant L50 som funktion af maskevidden og åbningsvinklen (isolinieplots). Et isolinieplot giver et hurtigt overblik over hvordan de selektive egenskaber kan afhænge af samspillet mellem flere parametre. Fig. 6 viser et eksempel for maskevidde og maskeåbningsvinkel.

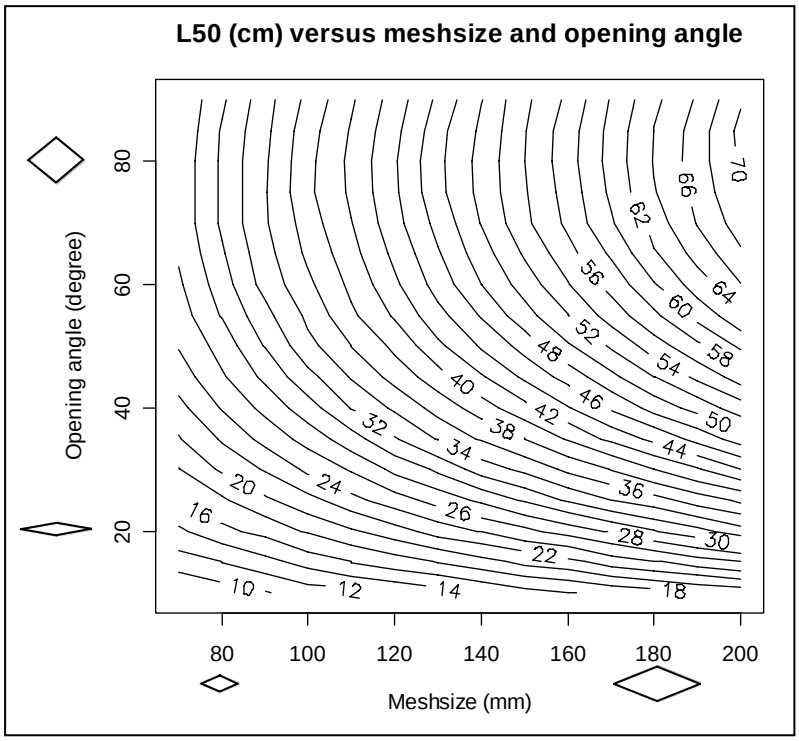

Fig. 6. Forventet variation af L50 med maskevidde og maskeåbningsvinkel for diamantmasker.

Forskellige typer af isolinieplot kan benyttes i udviklingsarbejdet med at finde frem til nye fiskeredskaber med mere optimale og veldefinerede selektionsegenskaber samt til at vurdere selektionen i eksisterende.

Anvendelser af FISHSELECT metodikken

Den udviklede FISHSELECT metode og værktøjer kan arts-specifikt anvendes til:

- udarbejdelse af design guides for netpaneler herunder for undslippelsesvinduer samt for ristsystemer.

- evaluere størrelsesselektionen I de redskaber der i dag anvendes i fiskeriet med trukne i redskaber.

- give et bedre grundlag for design af nye selektive redskaber der skal testes ved forsøgsfiskeri.

- hjælpe med at forstå resultater fra forsøgsfiskeri og placere dem i en systematisk ramme.

- give basis data for videreudvikling af simuleringsværktøjet PRESEMO (kapitel 3).

Det næste kapitel gennemgår art for art de opnåede resultater i projektet med nogle bemærkninger relateret til ovenstående.

Kapitel 2: Indsamlede FISHSELECT data og resultater

Med anvendelse af FISHSELECT metoden og de tilknyttede værktøjer, der er beskrevet i foregående kapitel, er der indsamlet og analyseret data for følgende arter af kommerciel betydning for dansk fiskeri: torsk, kuller, rødspætte, pighvar, rødtunge, gråtunge og jomfruhummer.
De efterfølgende afsnit beskriver kortfattet art for art arbejdet hermed og de opnåede resultater. En mere fyldestgørende beskrivelse kan findes i appendiks.
Fælles for alle fisk, der er blevet anvendt i forsøgene er at de er blevet aflivet med bedøvelsesmiddel umiddelbart før anvendelse.

Torsk (*Gadus morhua*).
Den mere fyldestgørende beskrivelse findes i appendiks A2, mens et overblik med tidlige foreløbige resultater fremgår af posteren for studium om torsk er i appendiks A12.
I alt 75 torsk blev anvendt i forsøgene. Til gennemfaldsforsøgene blev der anvendt 118 forskellige maskehuller hvilket resulterer i 8850 resultater til at bestemme passagemodellen udfra. Det mekaniske MorphoMeter blev benyttet til at bestemme tværsnitskonturen to steder på hvert individ: hoved (CS1) og krop (CS2) (Fig. 7).

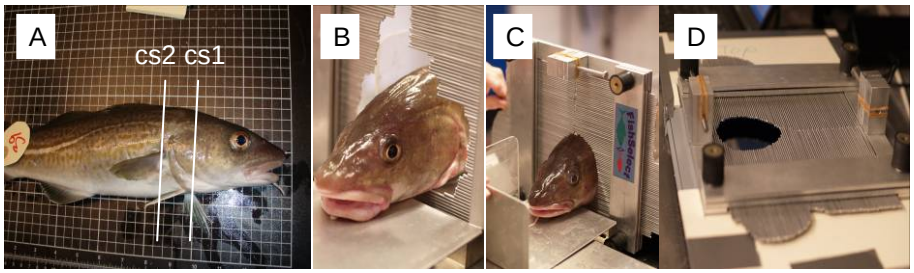

Fig. 7. A. Placering af målte tværsnit på torsk og MorphoMeter operationerne B. indlægning. C. justering af målepinde. D. scanning af kontur.

Det viste sig at en ellipse beskrev begge tværsnit tilfredsstillende for alle undersøgt størrelser af torsk (eksempel i Fig. 8).

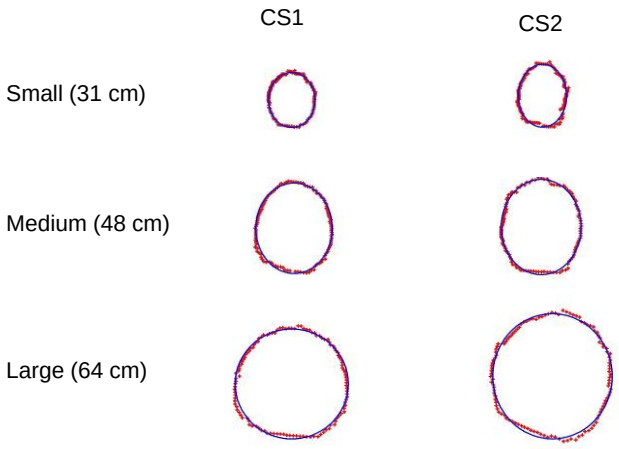

Fig. 8. Ellipser tilpassede tværsnitskonturerne på forskellige størrelser af torsk.
Det viste sig tilstrækkeligt kun at basere passagemodellen på CS1 (tværsnit på hovedet) og antage en asymmetrisk komprimering af dette. Gennemfaldsresultaterne viste indirekte så stor mulig kompression af CS2 at dets mål ikke havde praktisk betydning for maskepassage selvom både højde og bredde af dette tværsnit var større end for CS1. Med brug af passagemodellen og en virtuel torskepopulation med individmål bestemt ud fra den længdebaserede regression af tværsnitsdataene (de morfologiske database oplysninger), blev der foretaget et stort antal simuleringer med forskellige maskegeometrier. Resultaterne blev efterfølgende benyttet til at konstruere designguides for: diamant masker (Fig. 9a), rektangulære masker (Fig. 9b) samt for heksagonale masker (Fig. 9c). Det bemærkes at egenskaberne for kvadratiske masker indgår som specialtilfælde i alle tre plot.

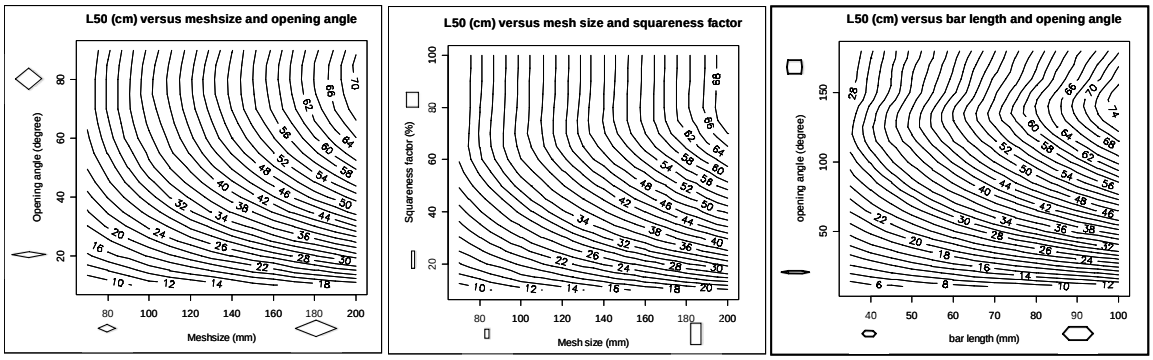

Fig. 9a-c. Isolinieplots for simulering af sammenhæng mellem maskevariabler og L50 for torsk.

I Fig. 9a ses tydeligt at for samme maskevidde vil L50 være meget afhængig af åbningsvinklen, især ved små vinkler, hvilket ofte forekommer i diamantmaskede fangstposer. Det vides at åbningsvinklen kan variere meget med fangstmængden og med positionen i posen, men også med designparametre som antallet af masker i omkredsen og trådtykkelsen. Med den kraftige afhængighed af L50 for torsk af åbningsvinklen som Fig. 9a viser betyder det at maskevidde alene ikke er egnet til at regulere størrelsesselektion af torsk i diamantmaskede fangstposer. Endvidere kan disse forhold være med til at forklare den betydelige variation der ofte forekommer i størrelsesselektion mellem træk med det samme redskab eller mellem redskaber med samme maskevidde. Dette kan meget vel også være en årsag til den store selektion range (SR: L75-L25) der ofte findes for torsk. Ifølge designguidedataene for SR (ikke vist) er SR for hver enkelt maske ret lille. I dette tilfælde bidrager kun morfologiske forskelle mellem individer af samme størrelse til SR og der må altså være andre mekanismer der bidrager til størrelsen af de eksperimentelt observerede værdier for SR.

For at opnå en mere kontrolleret og konstant størrelsesselektion af torsk ved anvendelse af diamantmaskepaneler er det på baggrund af ovenstående vigtigt med anordninger der holder åbningsvinklerne inden for nogle tilsigtede og velafgrænsede værdier. Dette vil både give en mere stabil L50 mellem forskellige træk og et mindre SR. Begge forhold vil medvirke til en mere kontrollabel størrelsesselektion.

Sammenlignes Fig 9a-b-c ses ligeledes at ændringer i maskefaconen for samme maskevidde kan resultere i meget forskellige L50. Dette er yderligere illustreret på Fig. 10.

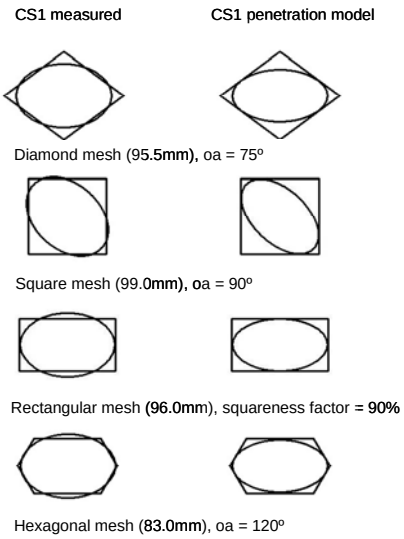

Fig. 10. Søjle 2 viser tværsnittet ved hovedet komprimeret 18% i bredden ifølge den optimale passagemodel for torsk og viser for forskellige masketyper hvilken maskevidde der netop skal til for at et tilfældigt individ på 40 cm kan trænge igennem. Åbningsvinklen er for alle masketyper den optimale. Søjle 1 viser de samme masker men her med det ukomprimerede tværsnit.

Fig. 10 viser tydeligt at en optimalt udformet heksagonal maske skal have en væsentligt mindre maskevidde end de mere traditionelle diamant- og kvadrat-formede masker for at give den samme torsk mulighed for at trænge igennem. Det bemærkes i øvrigt at den optimalt åbne diamant (åbningsvinkel 75˚) har en mindre maskevidde end kvadraten. Med FISHSELECT resultater kan man kvantificere denne forskel og give et skøn for hvilken maskefacon, som er optimal i et givent fiskeri.

Mindstemålet (MLS) for torsk i Kattegat-Skagerrak er 30 cm og for Nordsøen er det 35 cm. I Kattegat-Skagerrak foreskriver lovgivningen mindst 90 mm diamantmasker der ud fra isolinieplottet i Fig. 9a ville kræve en mindste åbningsvinkel af størrelsesorden 50 grader for at basis L50 skulle svare til MLS. I visse dele af Nordsøen foreskriver lovgivningen minimum 120 mm hvilket ville kræve en åbningsvinkel på lidt over 40 grader for at L50 svarer til MLS her.

Kuller

Den mere fyldestgørende beskrivelse findes i appendiks A4. I alt 80 kuller blev anvendt i forsøgene. Til gennemfaldsforsøgene blev der anvendt 132 forskellige maskehuller resulterende i 10560 resultater til at bestemme passagemodellen ud fra. Det mekaniske MorphoMeter blev benyttet til at bestemme tværsnitkonturen tre steder på hvert individ CS1, CS2 og CS3 (Fig. 11).

Fig. 11. Placering af målte tværsnit på kuller.

Som for torsk viste det sig at alle tre tværsnit kunne beskrives rimeligt nøjagtigt som en ellipse. Den morfologiske beskrivelse af tværsnittene for kuller kunne derfor reduceres til at beskrive højde og bredde for ellipser for hvert af de tre tværsnit. Disse morfologiske grunddata dannede herefter grundlag for regressionsanalyserne hvor tværsnitstørrelserne og -faconerne blev relateret til længden. Regressionsparametrene blev senere anvendt som grundlag for dannelse af virtuelle populationer. Fig. 12 viser plot af regressionerne.

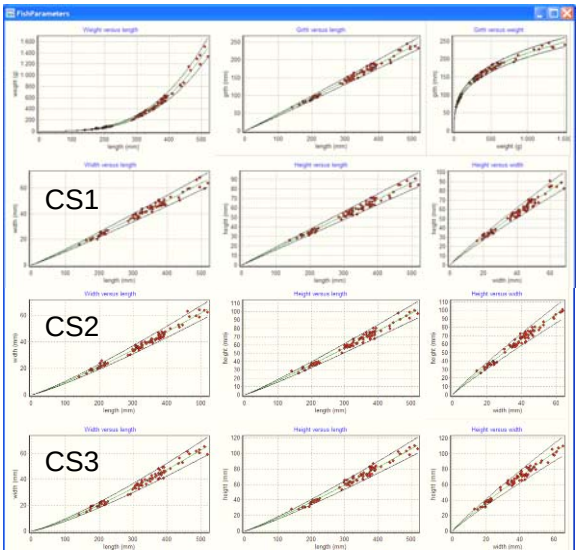

Fig. 12. Regressionsanalyse for tværsnitsparametre for kuller.

For alle tre tværsnit viser Fig. 12 en tydelig sammenhæng mellem tværsnittenes størrelse og længden af fiskene. Disse data og analyseresultater udgør de morfologiske grunddata for kuller.

Simuleringen af gennemfaldsforsøgene viste, som for torsk, at det kun er nødvendigt at tage hensyn til tværsnittet ved hovedet (CS1). Desuden skal dette tværsnit komprimeres asymmetrisk for at få en god overensstemmelse mellem simuleringer og forsøgene i laboratoriet.

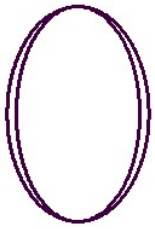

Fig. 13. Ellipse tilpasset CS1 for kuller. Ydre: ukomprimeret. Indre komprimeret 13% i bredden ifølge optimal passagemodel.

Fig. 13 viser ellipsen brugt i passagemodellen for kuller hvor der anvendes CS1. Den yderste kurve repræsenterer et typisk tværsnit for en kuller mens den inderste det samme tværsnit komprimeret ifølge passagemodellen.

På basis af regressionerne for sammenhængene mellem individlængde og tværsnitsstørrelse og passagemodellen blev der simuleret data til fremstilling af en designguide for diamantformede masker. Fig. 14 viser denne designguide.

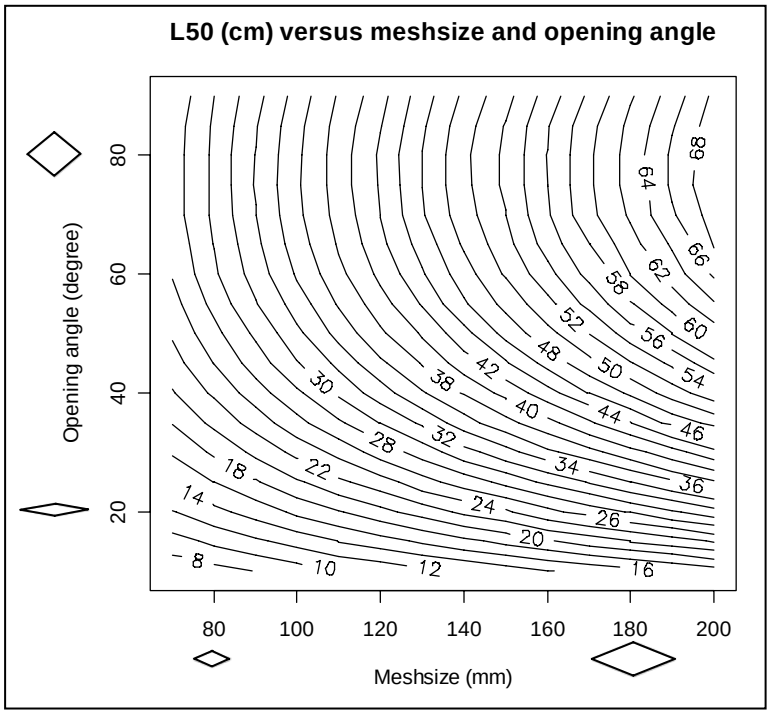

Fig. 14. Isolinieplots for simulering af sammenhæng mellem maskevariabler og L50 for kuller.

Ved at sammenligne med resultaterne for torsk i foregående afsnit, ses det at guiden for diamanter har samme tendenser hvorfor mange af de samme observationer som blev anført for torsk også vil gælde for kuller om end de præcise værdier vil være lidt anderledes. Dette indikerer derfor at det næppe i nævneværdig grad vil være muligt at selektere mellem torsk og kuller ved maskeselektion på basis af morfologiske forskelle.

For kuller er gældende mindste mål for både Nordsøen og Kattegat-Skagerrak 32 cm. Mens lovgivningen forskriver henholdsvis 120 mm og 90 mm maskevidde. Ud fra Fig. 14 forudsiges at 90 mm maskevidde vil give en L50 der altid er mindre end MLS uanset åbningsvinkel. For de 120 mm ser det bedre ud da dette kræver en åbningsvinkel der er mindst 40 grader.
Ovenstående eksempel viser, som for torsken, hvordan oplysningerne i designguiden kan anvendes i et første overordnet gennemgang af de tekniske reguleringer for fiskeriet.

Rødspætte (*Pleuronectes platessa*)
Den mere fyldestgørende beskrivelse findes i appendiks A3, mens et overblik med tidlige foreløbige resultater fremgår af posteren for studium om rødspætte i appendiks A12.
Der blev i alt anvendt 70 rødspætter i forsøgene. Tværsnittet blev registreret 3 steder på hvert individ (Fig. 15). Der blev anvendt 118 forskellige maskehuller til gennemfaldsforsøgene resulterende i 8260 resultater til at bestemme passagemodellen ud fra.

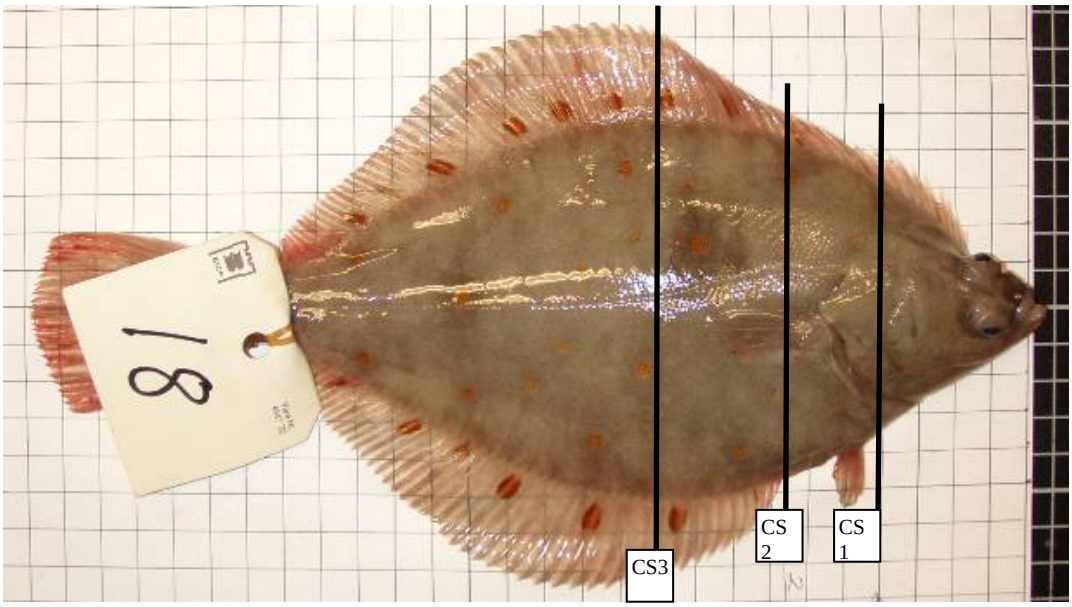

Fig. 15. Placering af målte tværsnit på rødspætte.

De tre tværsnit blev bestemt med anvendelse af MorphoMeteret og det blev undersøgt hvilken geometrisk basisfacon der bedst kunne anvendes til de tre snit. Fig. 16 viser fit af fem forskellige faconer til snittene på en typisk rødspætte.

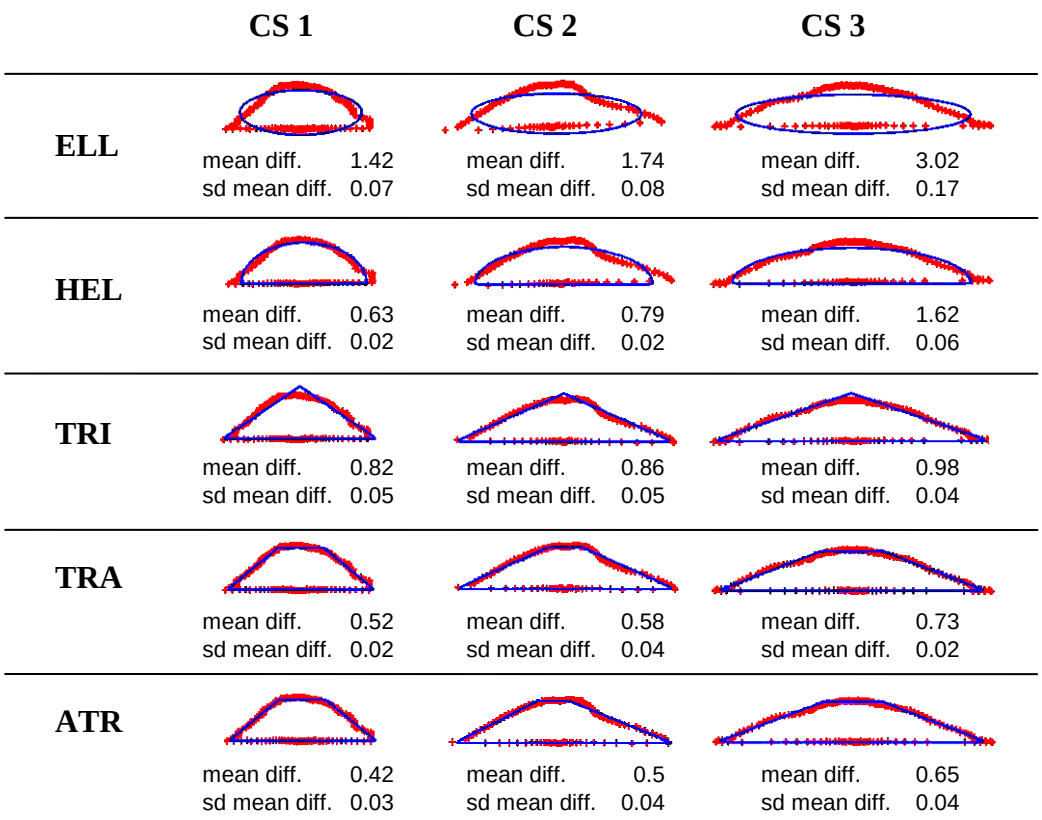

Fig. 16. Tilpasning af ellipse (ELL), halvellipse (HEL), triangel (TRI), symmetrisk trapez (TRA) eller asymmetrisk trapez (ATR) til de tre udvalgte tværsnit på en rødspætte.

Ud fra resultaterne gengivet på Fig. 16, blev det fundet at en asymmetrisk trapez (ATR) gav en god beskrivelse af alle tre snit.

Simulering af gennemfaldsforsøgene resulterede i en passagemodel der anvender en kombination af tværsnit 1 og tværsnit 3. Dette giver mening da hovedet repræsenterer den største faste (ikke komprimerbare) højde og tværsnit 3 den største bredde. Modellen blev efterfølgende anvendt i simuleringer med en virtuel population dannet på basis af de morfologiske regressioner til dannelse af designguide data for diamant masker, rektangulære masker og heksagonale masker. Fig. 17 viser designguides for rødspætter fremstillet på basis af disse simuleringer.

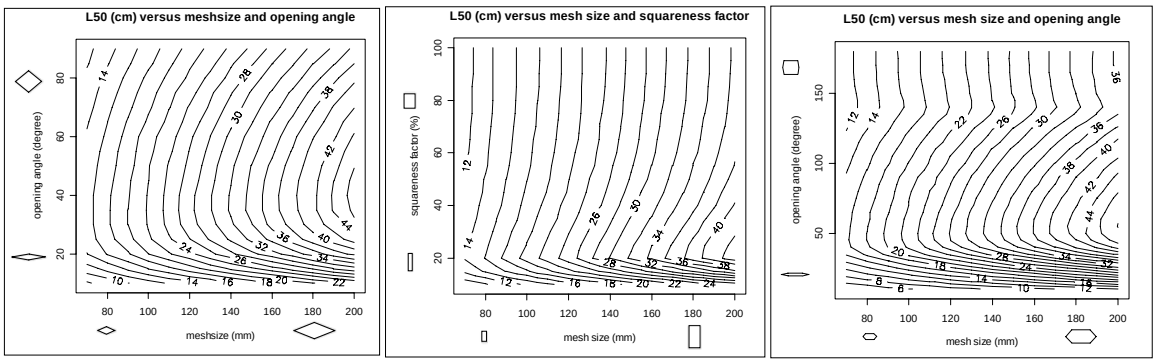

Fig. 17. Isolinieplots for simulering af sammenhæng mellem maskevariabler og L50 for rødspætte.

I Fig. 17a, der er designguiden for diamantmasker, ses at L50 afhænger af åbningsvinklen. Men for åbningsvinkler mellem 20 og 60 grader er de selektive egenskaber ret konstante og nærmest optimal for passage i fht. rødspættemorfologien. Sammenlignet med de tilsvarende resultater for torsk og for kuller, er L50 væsentligt mindre afhængig af åbningsvinklen inden for dette interval (20-60 grader). Denne mekanisme kan meget vel være årsagen den meget mindre SR-værdi der eksperimentelt er fundet for selektion af rødspætter i diamantmaskede fangstposer sammenlignet med SR for kuller og torsk. Sammenlignes L50 for forskellige masketyper (Fig. 17a-17c) for samme maskevidde ses, i modsætning til for rundfisken, at der ikke umiddelbart er nogen fordel at hente selektionsmæssigt ved den heksagonale maske i forhold til diamantmasken. For kvadratmasken (øverst i 17a-17c) ses derimod at L50 er ca. 20% lavere end for en optimalt åben diamant ved en maskevidde på 90 mm.

I Kattegat-Skagerrak er MLS 27 cm for rødspætte og mindste tilladte maskevidde i fangstposen er 90 mm mens Fig. 17a forudsiger at L50 ikke vil være højere end i bedste fald 20 cm. For at L50 skulle svare til MLS forudsiges at maskevidden bør være mindst 120 mm. Resultater fra eksperimentelt fiskeri med maskevidde 92.5 mm har indikeret en L50 på 21.9 cm, hvilket umiddelbart passer rimeligt med designguiden. Dog skal der udvises en hvis forsigtighed med forudsigelserne da vores studie også har vist at vi i nogle tilfælde med simuleringen underestimerer L50 med optil ca. 10% (se appendiks A3 for nærmere redegørelse). Under disse simuleringer antages det at åbningsvinklen for maskerne varierer jævnt mellem 20 og 50 grader under undslippelsesforsøgene og hver fisk tildeles kun én chance for at slippe gennem maskerne.

Pighvar (*Psetta maxima*)

31 pighvar blev anvendt til forsøgene. Den detaljerede gennemgang er i appendiks A5. Hvert individ fik målt tværsnittet tre steder ligesom de øvrige fladfisk. Grundet pighvarrens store bredde blev MorphoMeteret anvendt i en særlig tvillingopstilling (Fig. 18 øverst).

Fig. 18. Tvillingopstilling af MorphoMeteret for måling af pighvar.

Nederst på Fig. 18 vises et digitaliseret og konturdetekteret tværsnit ved hjælp af de indbyggede billedanalyse funktioner i FISHSELECT-softwaren.

Der blev i alt anvendt 132 forskellige maskehuller til gennemfaldsforsøgene. Dette gav i alt 4092 resultater at bestemme passagemodellen ud fra. Fig. 19 viser eksempler fra gennemfaldsforsøgene.

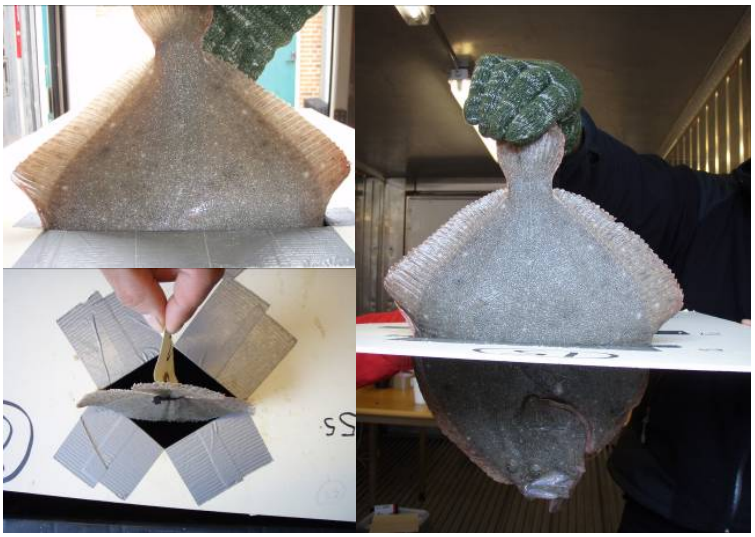

Fig. 19. Gennemfaldsforsøg med pighvar.

Det blev under gennemfaldsforsøgene med pighvar observeret at disse var meget stive og mindre deformerbare sammenlignet med andre fladfisk. Det viste sig ret let at finde frem til en passagemodel med fin overensstemmelse med gennemfaldsresultaterne. I denne model blev der kun taget højde for tværsnittet hvor kroppen er bredest. Efterfølgende simuleringer blev anvendt til at fremstille en designguide for diamantmasker (Fig. 20).

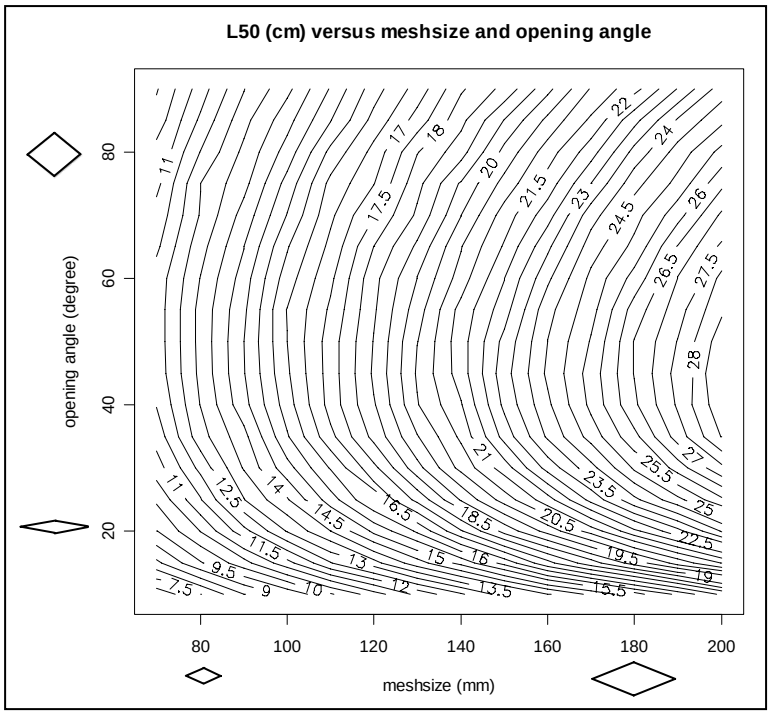

Fig. 20. Isolineplots for simulering af sammenhæng mellem maskevariabler og L50 for pighvar.

I Fig. 20 ses at L50 vil være højest og nogenlunde konstant for åbningsvinkler mellem 40 og 60 grader. For Kattegat-Skagerrak foreskrives MLS på 30 cm for pighvar. Fig. 20 viser at for at opnå en L50 svarende til dette kræves en maskevidde på mere end 200 mm. Med den gældende lovgivning med maskevidde 90 mm forudsiges at individer der er mindre end halvdelen af mindstemålet vil blive fanget.

Rødtunge (*Microstomus kitt*)
En nærmere redegørelse er i appendiks A6. Der blev anvendt 69 individer og 132 maskehuller. Dette gav 9108 resultater til at bestemme passagemodellen ud fra. Fig. 21 viser billeder fra gennemfaldsforsøgene.

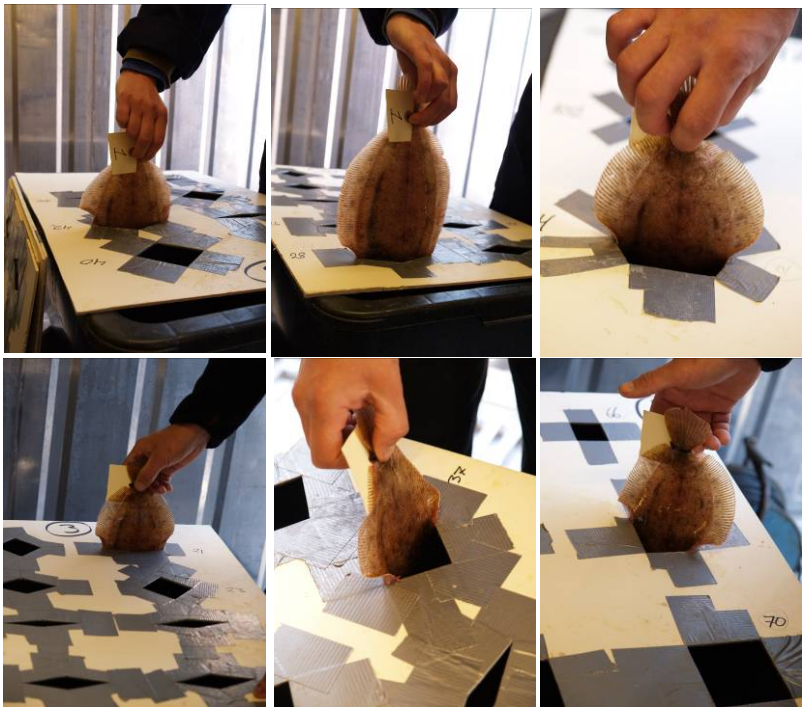

Fig. 21. Gennemfaldsforsøg med rødtunge.

På hvert individ blev tværsnittet målt tre forskellige steder. Fig. 22 viser billeder fra dette og opsamlingen af scannerdata til computer.

Fig. 22. Opmåling og scanning af tværsnitskonturer for rødtunge.

Gennemfaldsdataene og de scannede tværsnit blev brugt til at bestemme en egnet passagemodel. Tilsvarende som for rødspætte blev denne baseret på en kombination af tværsnit 1 og tværsnit 3. Efterfølgende simuleringer dannede grundlagt for at konstruere en designguide for diamantmasker. Fig. 23 viser denne.

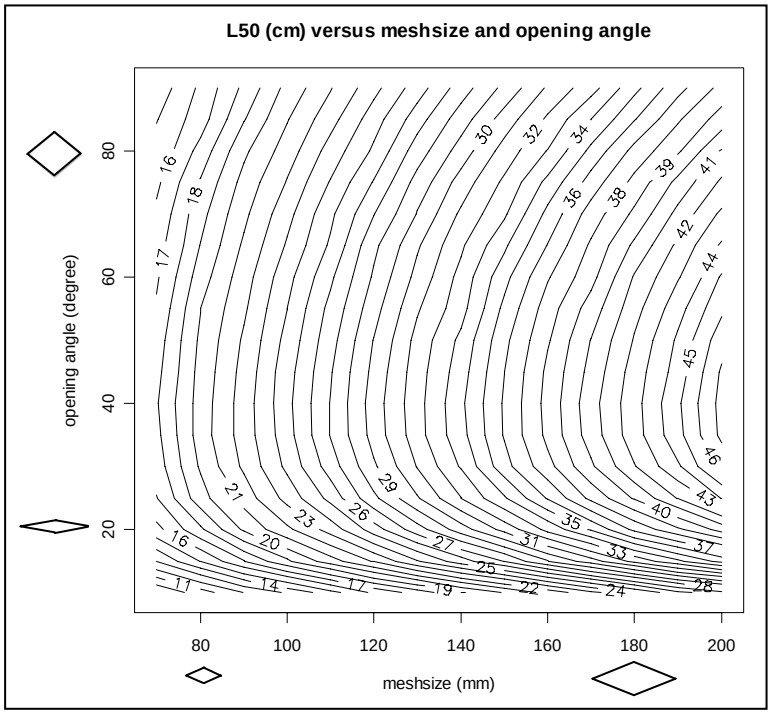

Fig. 23. Isolinieplots for simulering af sammenhæng mellem maskevariabler og L50 for rødtunge.

I Fig. 23 ses at der kræves en maskevidde på over 110 mm for at L50 skal svare til mindstemålet for Kattegat-Skagerrak på 26 cm. For den tilladte maskevidde på 90 mm forudsiges L50 til ikke at overstige 22 cm.

Gråtunge (*Solea vulgaris*)
Dette afsnit gennemgår status for gråtunge-resultaterne (en mere udførlig gennemgang findes i appendiks A7). Hvert individ fik tværsnittet målt tre steder (Fig. 24)

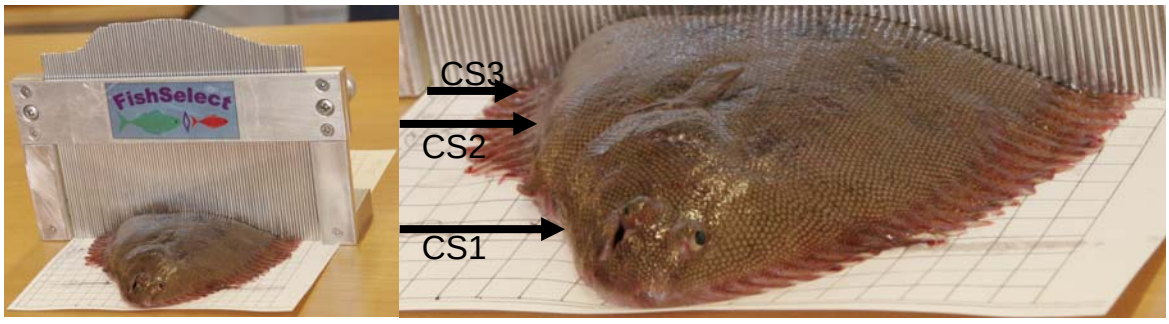

Fig. 24. Opmåling og placering af tværsnitskonturer for gråtunge.

Konturaftrykkene, der blevet registeret med MorphoMeteret, blev scannet og opsamlet i den tilsluttede laboratoriecomputer (Fig. 25).

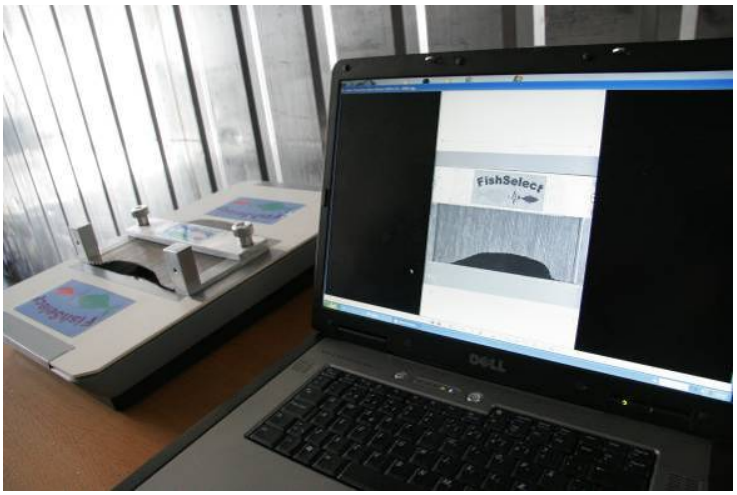

Fig. 25. Scanning af tværsnitskonturer for gråtunge.

Der blev anvendt 132 forskellige maskehuller til gennemfaldsforsøgene. Fig. 26 viser billeder fra disse. Gråtungens krop kan deformeres betydeligt (Fig. 26). Der blev i alt anvendt 74 individer hvilket gav 9768 gennemfaldsresultater til at bestemme passagemodellen ud fra.

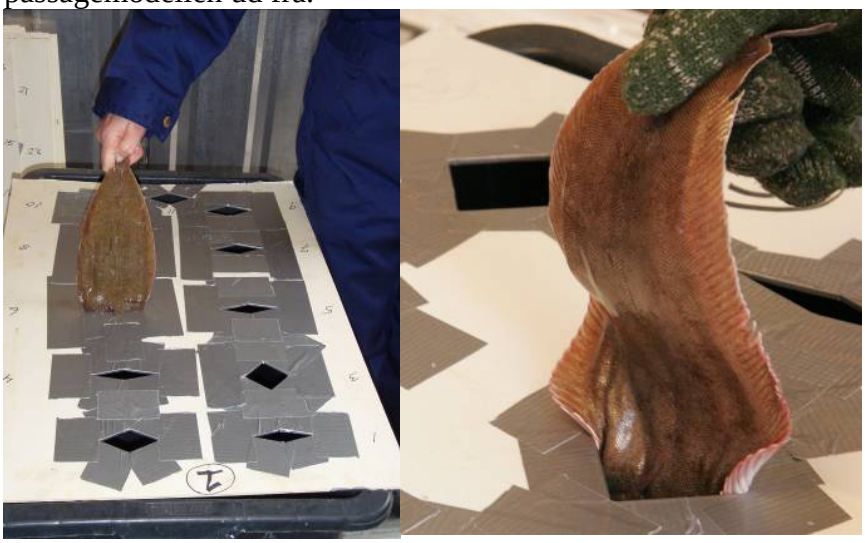
Fig. 26. Gennemfaldsforsøg med gråtunge.

Alle data er opsamlet og de morfologiske grunddata bestemt. Men det har ikke inden for projektperioden været muligt at færdiggøre dataanalysen. Derfor foreligger der ikke designguides for gråtunge som resultat i dette projekt. Men dataene til at færdiggøre dette er til stede.

Jomfruhummer (*Nephrops norwegicus*)

For jomfruhummer forventes undslippelsesforsøgene at være en mere passiv proces end for fisk hvilket betyder at dyrets orientering i forhold til maskerne i mange tilfælde vil være mindre optimal under *forsøg* på maskegennemtrængning. Derfor undersøgte vi gennemfaldsmulighederne for forskellige orienteringer af individerne. Der blev først

gennemført et pilotforsøg med kun 20 individer hvor 8 forskellige orienteringer ved maskekontakt blev undersøgt (Fig. 27).

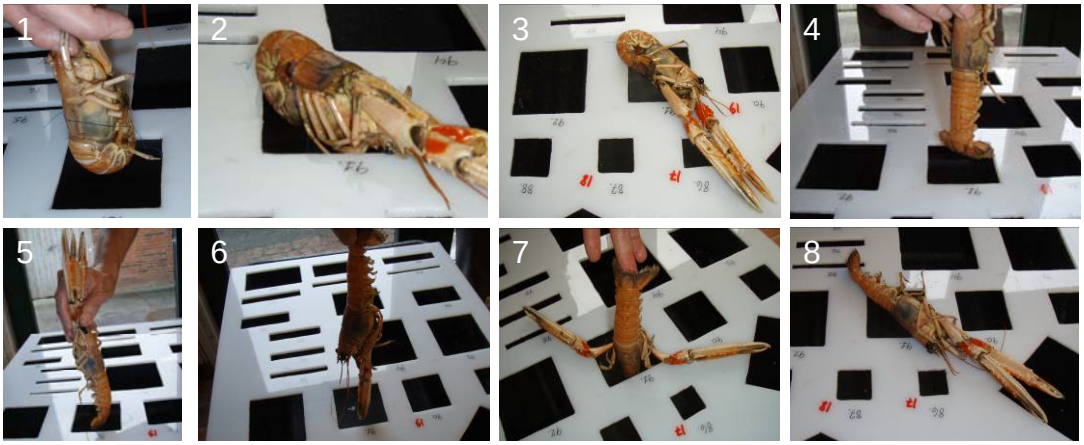

Fig. 27. Gennemfaldsforsøg med jomfruhummer ved 8 forskellige orienteringer.

En simuleringsbaseret sammenligning med eksperimentelle selektionsresultater viste at hvis vi anvendte en kombination af tre af disse kontaktorienteringer (1, 2 og 5) kunne vi forklare eksperimentelle resultater (Fig. 28).

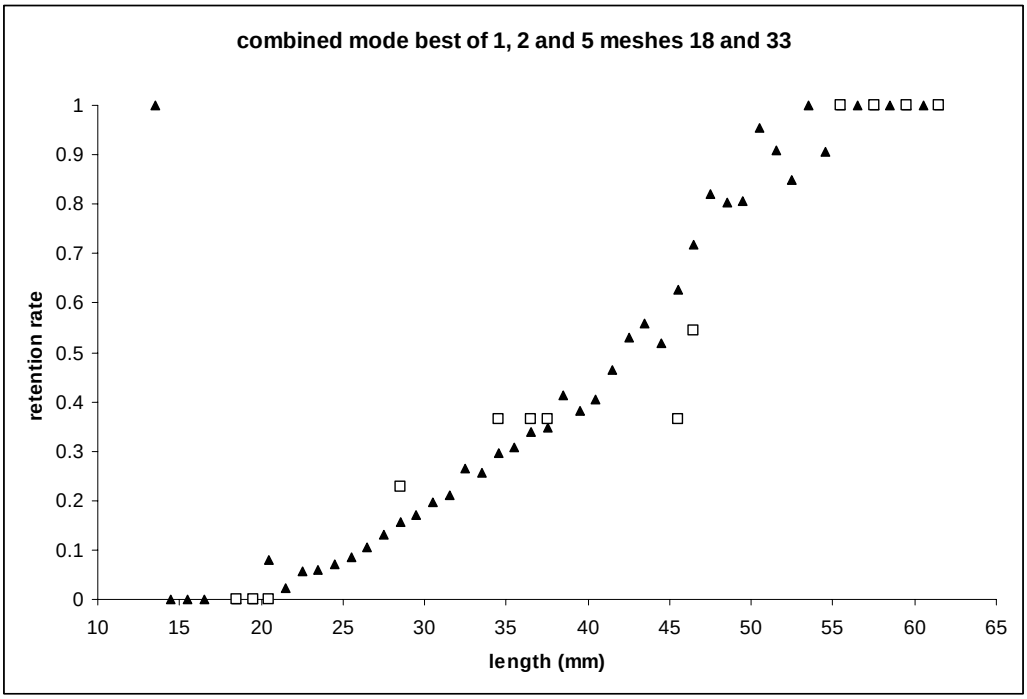

Fig. 28. Sammenligning af tilbageholdelsen af jomfruhummer i 70 mm kvadratmasket fangstpose. Trekanter er eksperimentelle resultater mens kvadrater er simulerede.

Ud fra ovenstående blev et større forsøg med 70 individer designet og gennemført. Der blev kun anvendt de tre identificerede kontaktorienteringer. Til hovedforsøget blev der

anvendt 160 forskellige maskehuller. Dette giver 3x70x160=33600 gennemfaldsresultater. I hovedforsøget blev der også foretaget scanninger af forskellige morfologiske karakteristika. Fig. 29 viser et eksempel herpå.

Det har ikke inden for projektet været muligt at analysere dataene fra hovedforsøget. Men de foreløbige resultater fra pilotforsøget har demonstreret at vi med FISHSELECT metoden kan lære noget om de fundamentale mekanismer der sandsynligvis spiller en rolle for størrelsesselektion af jomfruhummer i trukne fiskeredskaber.

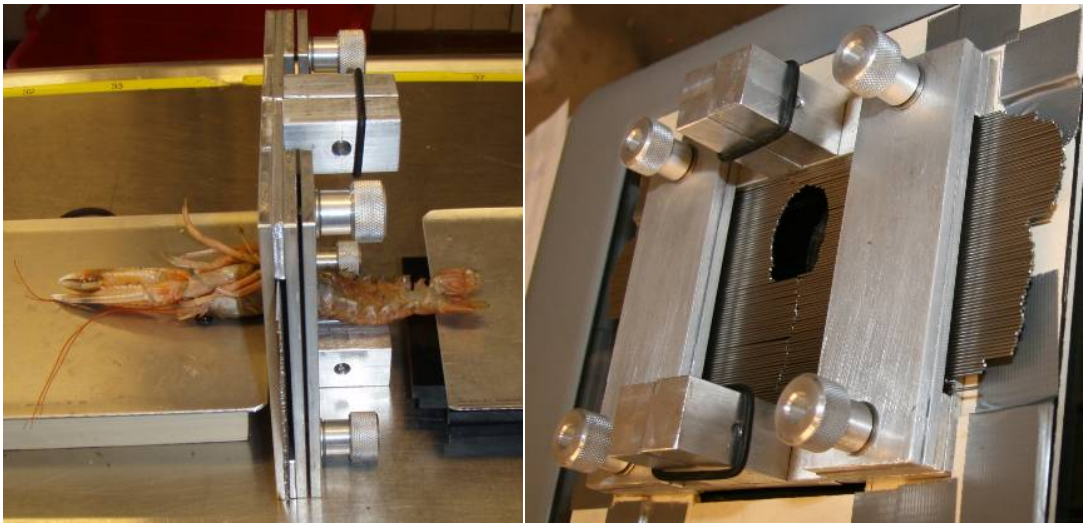

Fig. 29. Eksempel på opmåling af tværsnitskontur for jomfruhummer.

Appendiks A8 beskriver i flere detaljer resultater og arbejdet med jomfruhummer i dette projekt.

Kapitel 3: Beskrivelse af PRESEMO

I det foregående kapitel beskrev vi eksempler på hvordan FISHSELECT-metoden kan tilvejebringe kvantitativ viden om indflydelsen af; arternes tværsnits-morfologi, netpanelers maskefaconer og netpanelers maskestørrelser, på fiskens passagemuligheder gennem netpanelerne. Denne viden er nyttig og brugbar i sig selv som demonstreret både med hensyn til rådgivning om tekniske reguleringer i fiskeriet samt i forbindelse med udvikling af nye selektive redskaber. Men den kan også tjene som basis information i en mere dynamisk model, der detaljeret følger de ændringer der sker i den bagerste del af fiskeredskabet i løbet et trawltræk og som desuden inddrager en deskriptiv baseret model for fiskenes adfærd i denne del af redskabet. Simuleringsprogrammet PRESEMO (PREdictive SElective MOdel) er en realisering af en sådan model. PRESEMO muliggør simulering af selektionsprocesserne i trawls fangstposer. Der har under projektet været en omfattet anvendelse af PRESEMO til simuleringstudier af størrelsesselektionen af rundfisk i diamantmaskede fangstposer (kapitel 4). Endvidere er faciliteterne i PRESEMO er blevet udvidet i forbindelse med dette projekt. Dette kapitel indeholder derfor en kortfattet beskrivelse af PRESEMO. For en mere detaljeret beskrivelse af modellen og grundlaget for denne, henvises til artiklen (Herrmann, 2005a) samt til PhD-afhandlingen (Herrmann, 2005b). Et overblik over mulighederne med PRESEMO fremgår også posteren i appendiks A14.

PRESEMO simulering af trawl træk

PRESEMO er implementeret ud fra en individbaseret strukturel model for størrelsesselektionen i trawls fangstposer. Modellen simulerer ankomsten af forskellige populationer af fisk til fangstposen i løbet af et trawl træk. Hvert individ tildeles en vægt og tværsnitsstørrelse ud fra sin længde, og under antagelse af at tværsnittet er elliptisk. Individerne tildeles enkeltvis en tid de bruger på at passere ned gennem fangstposen, en tid mellem flugtforsøg, en tid de kan svømme i posen uden at blive udmattede og pakningstæthed når de opholder sige foran fangstopbygningen i posen. Et flugtforsøg er succesfuldt hvis individet kan trænge igennem masken det sted i fangstposen hvor forsøget finder sted. Maskens åbningsvinkel er en funktion af fangstposens geometri, der afhænger af fangstmængden. Geometrien bestemmes uden for PRESEMO og importeres til programmet. Individer som ikke undslipper inden de udmattes, falder tilbage i fangsten i posen og bliver en del af fangsten. Fangstposens geometri opdateres kontinuerligt i takt med fangstopbygningen under trækket. Under simulering visualiseres ligeledes selektionsprocesserne løbende, da indgangstidspunkt, bevægelsesmønster i posen og flugtforsøg for de enkelte individer også vises. Efter endt simulering tilpasses en logistisk funktion til de simulerede selektionsdata til bestemmelse af L50 og SR. Modellen er strukturel da den således er baseret på information om de fundamentale mekaniske, hydrodynamiske og biologiske processer, der er styrende for selektionen i fangstposer.

PRESEMO benytter information om fangstposens design, individ adfærd, passagemodeller, individernes størrelsesfordelinger og antal, og individernes morfologi. PRESEMO indeholder en lang række faciliteter til at beskrive og teste forskellige måder at modellere og simulere disse aspekter på. Fig. 30-32 illustrerer hovedsekvensen for at opsætte, gennemføre og analysere en enkel fiskeriproces med anvendelse af PRESEMO.

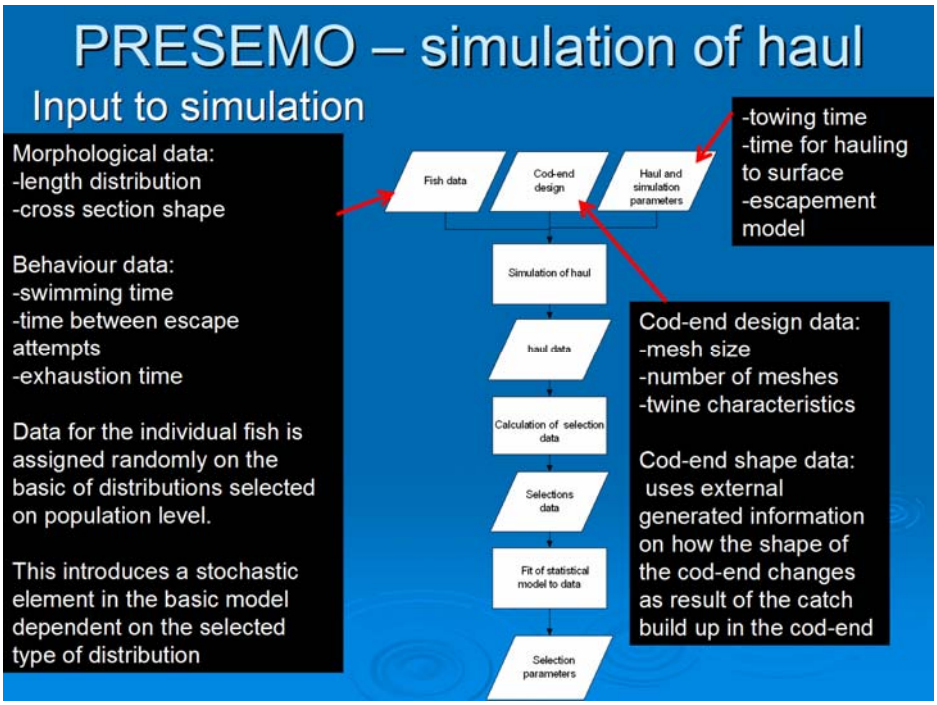

Fig. 30: input til simulering.

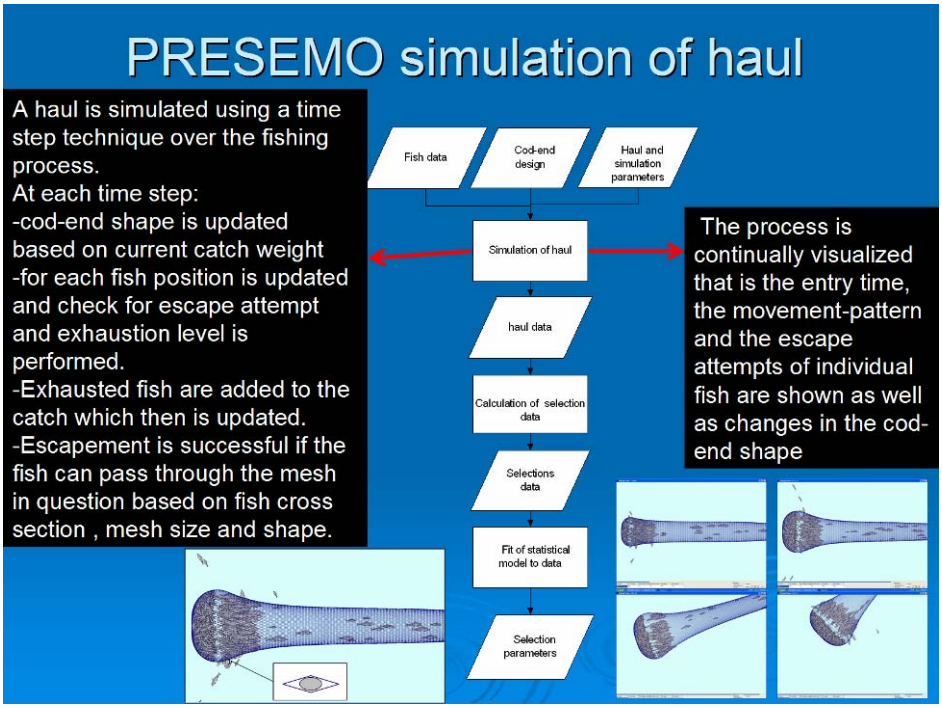

Fig. 31: simulering af trawl træk.

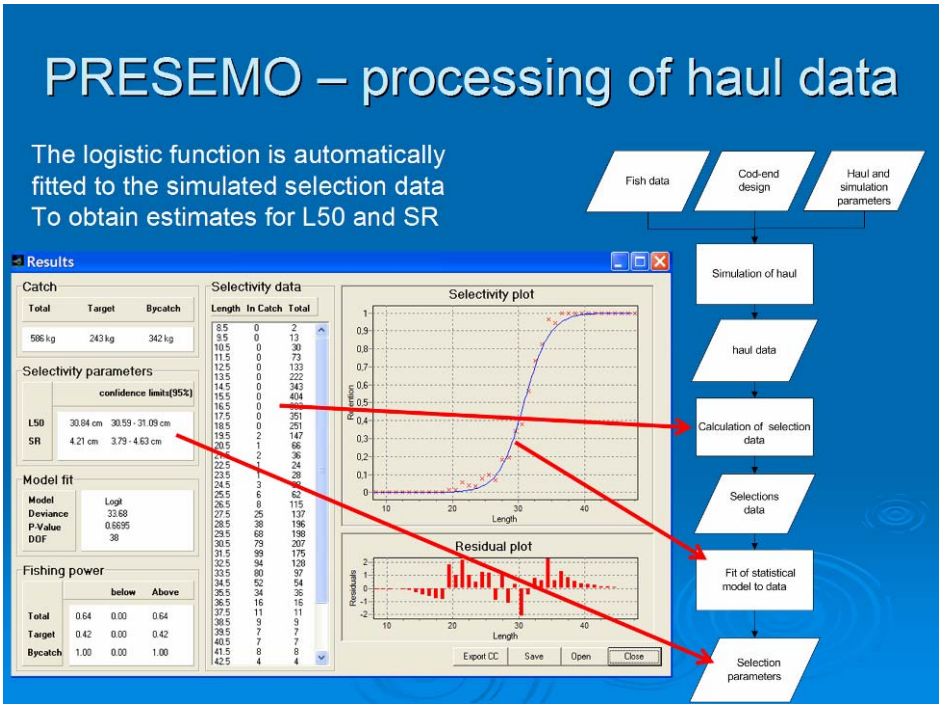

Fig. 32: analyse af trækdata.

PRESEMO stokastisk simulering af gentagne træk

En funktionalitet muliggør gentagne simuleringer med den samme fangstpose under varierende fiskeriforhold ved at randomisere de parameterværdier som har indflydelse på fangstprocesserne. Dette muliggør undersøgelse af selektion, fangsteffektivitet og discard omfang for den samme fangstpose under en lang række varierende fiskeriforhold. Fig. 33 illustrerer dette for 1000 gentagne træk. En nøjere beskrivelse af denne teknik og dens anvendelser kan findes i artiklen (Herrmann og O'Neill, 2005).

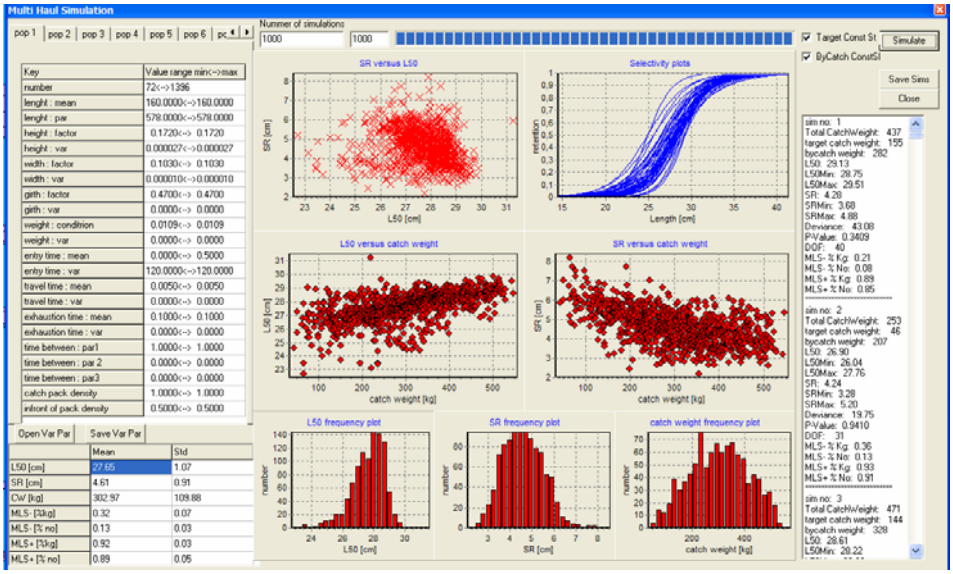

Fig. 33: simulering af gentagne træk.

PRESEMO simulering med forskellige fangstpose designs

En funktionalitet muliggør simulering og sammenligning af performance for forskellige fangstposer under de samme varierende fiskeriforhold. Dette giver en hurtig og billig måde til at vurdere konsekvenserne af at implementere forskellige fangstpose-designs.

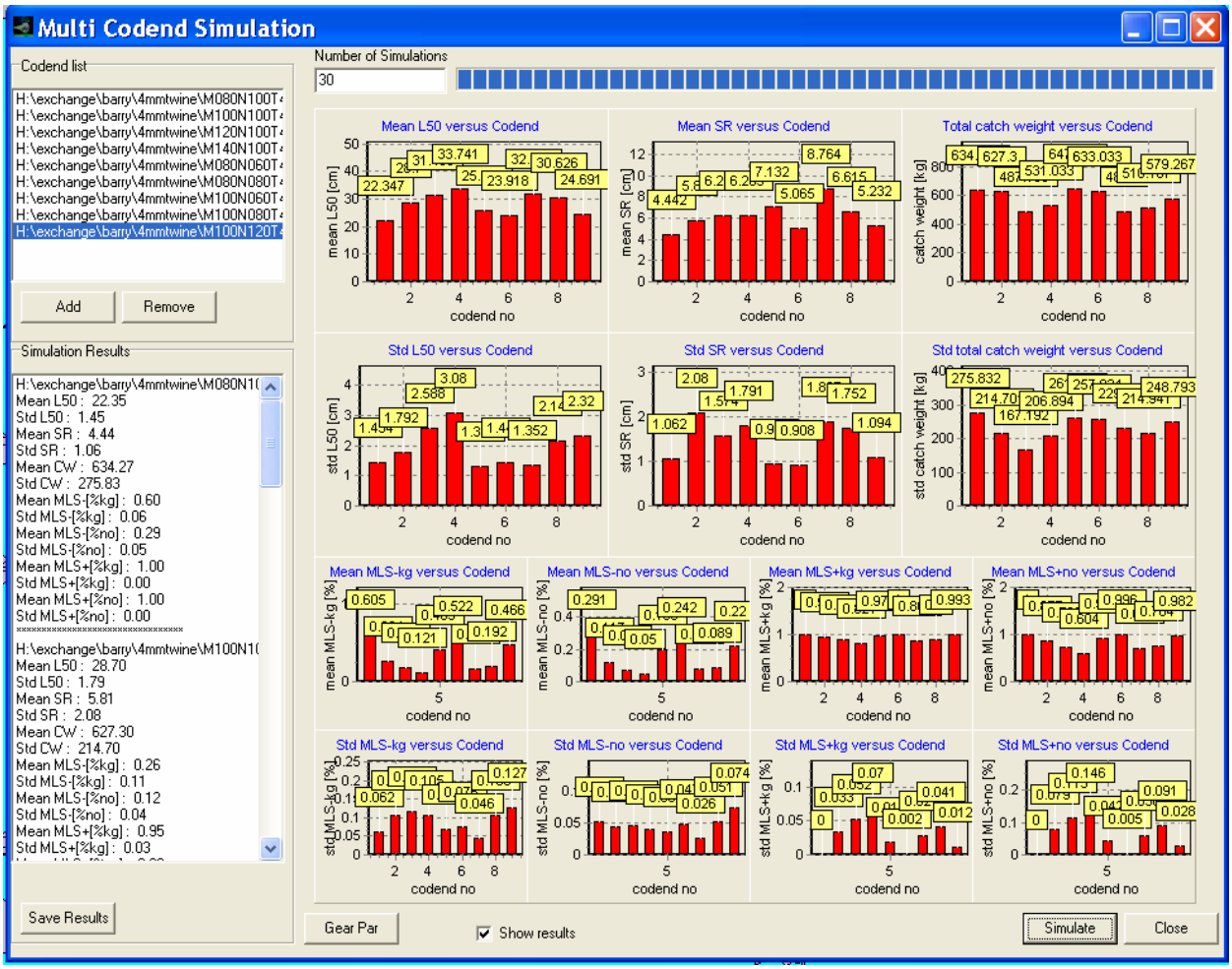

Fig. 34: simulering med forskellige fangstposedesigns og sammenligning af resultater.

I vinduet vist på Fig. 34 omhandler faciliteterne nederst sammenligning af fraktionen for fangsteffektivitet over og under MLS målt i henholdsvis vægt og individantal. Disse faciliteter, der er udviklet og implementeret i PRESEMO som en del af dette projekt, kan benyttes til konsekvensvurderinger omkring relative ændringer i fangsteffektivitet for fangst (over MLS) og for discard (under MLS) ved ændringer i de tekniske regler i et givet fiskeri.

Udvidelsesmuligheder i PRESEMO.

I dag er PRESEMO modellen begrænset til håndtering af fisk hvis tværsnit kan beskrives ved hjælp af en ellipse. Vores resultater med FISHSELECT har vist at dette er en rimelig beskrivelse for torsk og kuller. I modsætning dertil har vores FISHSELECT studier også

vist at det ikke er tilfældet for de fladfisk vi testet. Vores resultater (kapitel 2) har tilvejebragt de data og passagemodeller som muliggør en fremtidig udvidelse af PRESEMO til også at simulere størrelsesselektion af disse arter fladfisk.
En anden begrænsning i PRESEMO i dag er at det kun er muligt at simulere passagemulighederne gennem diamantformede masker. FISHSELECT resultaterne muliggør fremtidig udvidelse af PRESEMO til at håndtere simulering af selektion gennem masker med en vilkårlig facon af de arter vi har opsamlet FISHSELECT data for.

Kapitel 4: Beskrivelse af PRESEMO resultater

Beskrivelse af studiet.

Dette kapitel omfatter en kort beskrivelse af et simuleringsstudie der er gennemført i projektet. PRESEMO blev anvendt til at forudsige hvordan størrelsesselektionen af kuller i fangstposer af diamantmasker afhænger af designparametrene maskevidde, antal masker i omkredsen og trådtykkelsen. Desuden undersøgtes effekten af fangstmængden i posen. En mere detaljeret gennemgang findes i appendiks A15. Da FISHSELECT resultaterne for kuller først forelå meget sent i projektforløbet er studiet gennemført på ældre morfologi data for kuller fra litteraturen. For diskussion af eventuel effekt af anvendelse af vores nye og bedre funderede resultater henvises til Appendiks A4. Vores studie omfattede 100 forskellige fangstposedesigns, hvor der blev anvendt forskellige kombinationer af maskevidde (M=80-160 mm), antal masker i omkredsen (N=60-140) og trådtykkelse (T=3-6 mm). For hvert design blev der foretaget 1000 simuleringer under varierende fiskeriforhold for bl.a. at belyse variationen mellem træk for de forskellige designs. Således indeholdt dette studie 100.000 resultater fra simulerede enkelttræk. Fig. 35 viser screen dumps fra PRESEMO for nogle få af disse simuleringer med forskellige designs. Billederne viser fangstposens form ved forskellige mængder akkumuleret fangst.

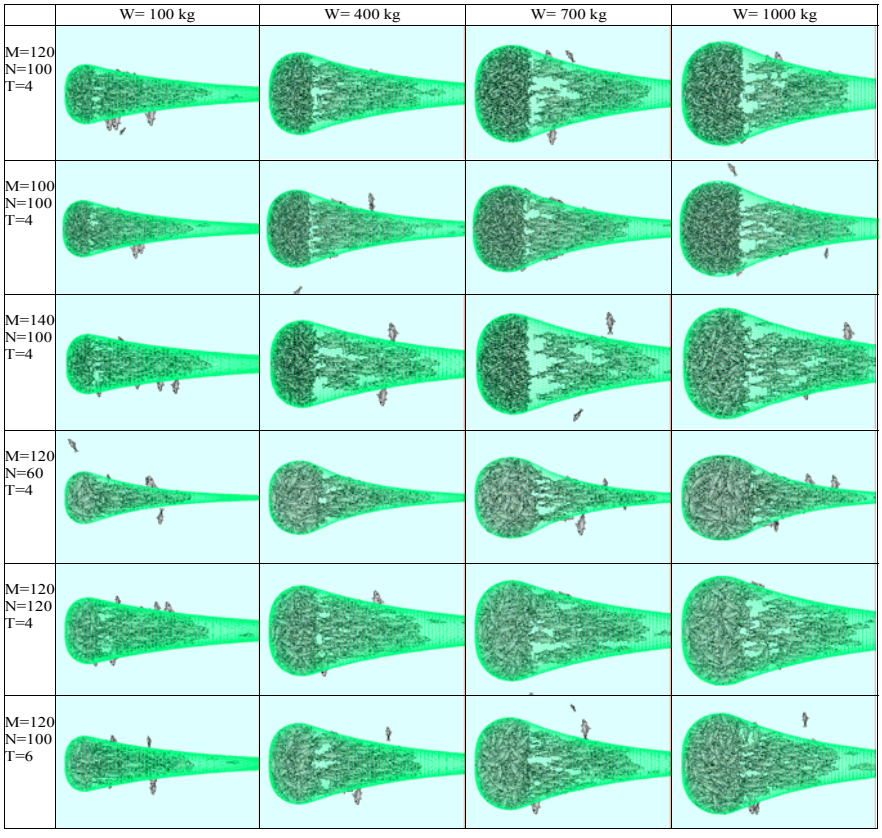

Fig. 35. Screen dump fra PRESEMO: Fangstposens form ved forskellige maskevidder i mm (M), antal masker i omkredsen (N), trådtykkelse i mm (T) og fangstvægt i kg (W).

Fordelinger af selektionsparametre

Fig. 35 viser tydeligt at fangstposernes geometri ændres betydeligt som konsekvens af den akkumulerede fangst bagerst i posen. Da maskeåbningsvinklen for diamantformede masker er direkte koblet til posens diameter vil den variere betydeligt. Det ses også i Fig. 35 at fangstposernes diameter varierer betydeligt med afstanden til den akkumulerede fangst. Dermed varierer også åbningsvinklen i maskerne med afstanden til fangsten. Sammenholdes disse observationer med FISHSELECT designguiden for kuller (Fig. 14), hvor der blev konstateret stor variation på den maximale størrelse af kuller der er i stand til at trænge igennem masker med forskellig åbningsvinkel, må det forventes at selektionen af kuller vil kunne variere betydeligt mellem de enkelte træk. PRESEMO-simuleringen i Fig. 36 viser denne variation hvor fordelingen af L50 og SR for nogle få fangstposer er afbildet på basis af 1000 simulerede træk for hver.

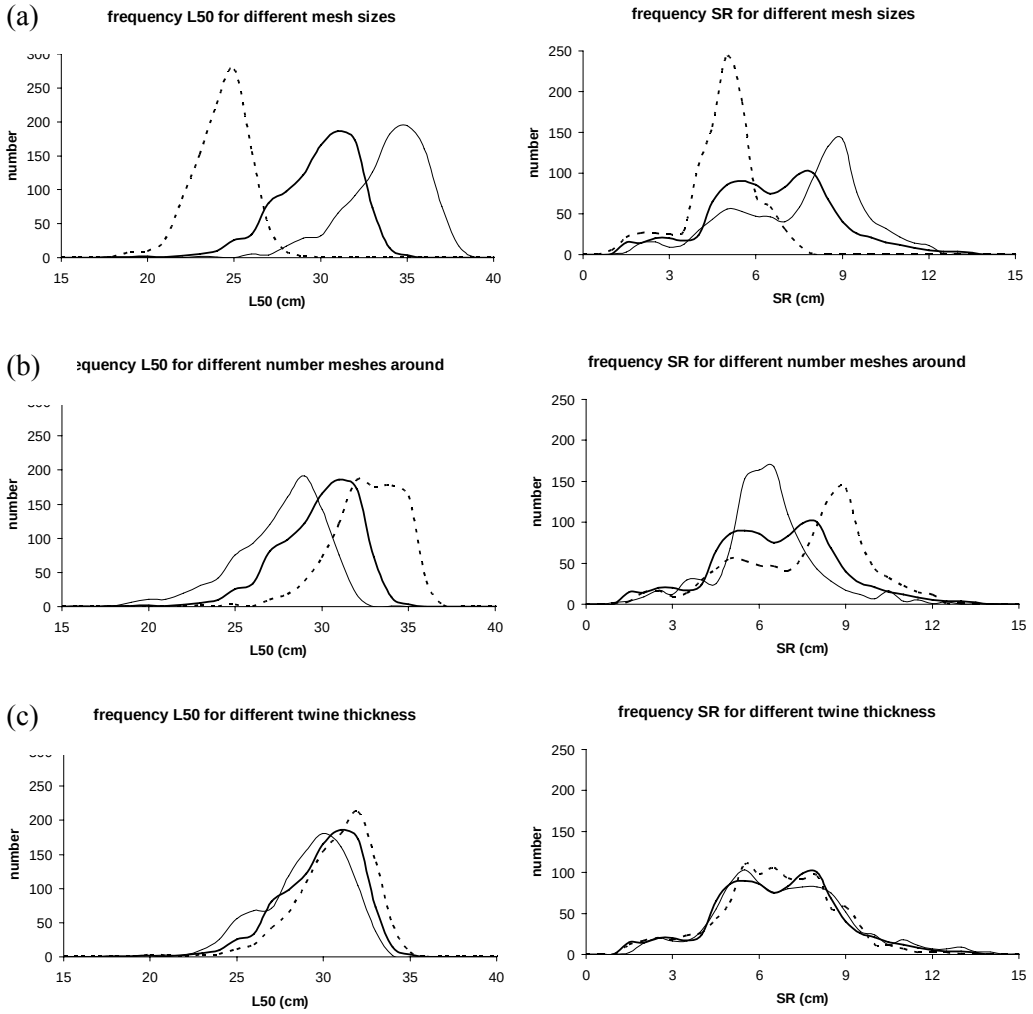

Fig. 36: Fordeling af L50 og SR for 1000 simulerede træk gennem en fiskepopulation med givne stokastiske variationer a) for tre forskellige maskevidder; b) for tre forskellige antal masker i omkredsen; c) for tre forskellige trådtykkelser. Stiplet linie svarer til den mindste værdi af den varierende parameter.

Sammenligning med eksperimentelle resultater

På Fig. 36 er det tydeligt at der kan være en betydelig variation i selektionsparametrene mellem træk for det samme redskab hvilket vi kæder sammen med parametrenes følsomhed overfor maskeåbningen ved små maskeåbninger (Fig. 14 og 35). På Fig. 36b ses f.eks. at forskelligt antal masker i omkredsen af fangstposen har en tydelig effekt i middelselektionen. Fig. 36a viser som ventet en tydelig forskel i middelselektionen for varierende maskevidde. Fig. 36c viser endvidere en tendens hvor trådens tykkelse påvirker middelselektionen dog mindre udtalt end for de to første parametre.

På basis af ovenstående resultater blev der konstrueret en kubisk polynomium-model der beskriver indflydelsen på selektion af maskevidde, antal masker i omkredsen samt en yderligere model der også inkorporerede den total fangstvægt for trækket som variabel. Disse to modelpolynomier blev fittet til de 100.000 simulerede træk-data for at afdække variablernes interaktioner og effekt på størrelsesselektionen. I Fig. 37 plottes disse to modelpolynomier (□ og Δ) sammen med diverse eksperimentelle data (♦). Desuden indeholder plottene også forudsigelser fra to eksisterende empiriske modeller (de fuldt optrukne kurver). De stiplede kurver repræsenterer grænser indenfor hvilke 95% af trækkenes selektionsværdier vil være (på basis af vores regressionsmodel hvor fangstvægten er en tilfældig faktor). Fig. 37a-c viser effekten af maskevidde for tre forskellige antal masker i omkredsen (n). Kvantitativt ser vi en rimelig overensstemmelse mellem vores data baseret på PRESEMO-simuleringerne, de eksperimentelle data samt med de empirisk baserede modellers forudsigelser. Fig. 37d viser effekten af antallet af masker i omkredsen. Tendensen er her at L50 aftager når antallet af masker øges i omkredsen. Igen finder vi en rimelig overensstemmelse mellem vores simuleringer og de eksperimentelt baserede resultater. Fig. 37e viser effekten af trådtykkelsen. Her findes en tendens til svagt faldende L50 med øget trådtykkelse. Generelt finder vi for L50 en rimelig overensstemmelse mellem resultaterne baseret på PRESEMO og de eksperimentelt baserede resultater for størrelsesselektion af kuller. De fundne tendenser viser at det at basere en lovgivning alene på maskevidde ikke er hensigtsmæssig da andre designparametre specielt antallet af masker i omkredsen kan have betydelig effekt på størrelsesselektionen af rundfisk i diamantmaskede fangstposer.

Indflydelse af designparametre og fangstvægt

For at skaffe en overskuelig måde at se interaktionen mellem designparametrene og fangstvægten har vi på basis af vores regressionsmodeller konstrueret isoplot-kurver for selektionsparametrenes middelværdi. Fig. 38 viser eksempler for hvordan middel-L50 forudsiges at afhænge af maskevidden og antallet af masker i omkredsen. Øverst vises for fangstvægt på 400 kg, midt for 600 kg og nederst for 800 kg. Det ses ved sammenligning af plottene at L50, for de samme værdier af maskevidde og antallet af masker i omkredsen, stiger med fangstvægten i det range vi har undersøgt.

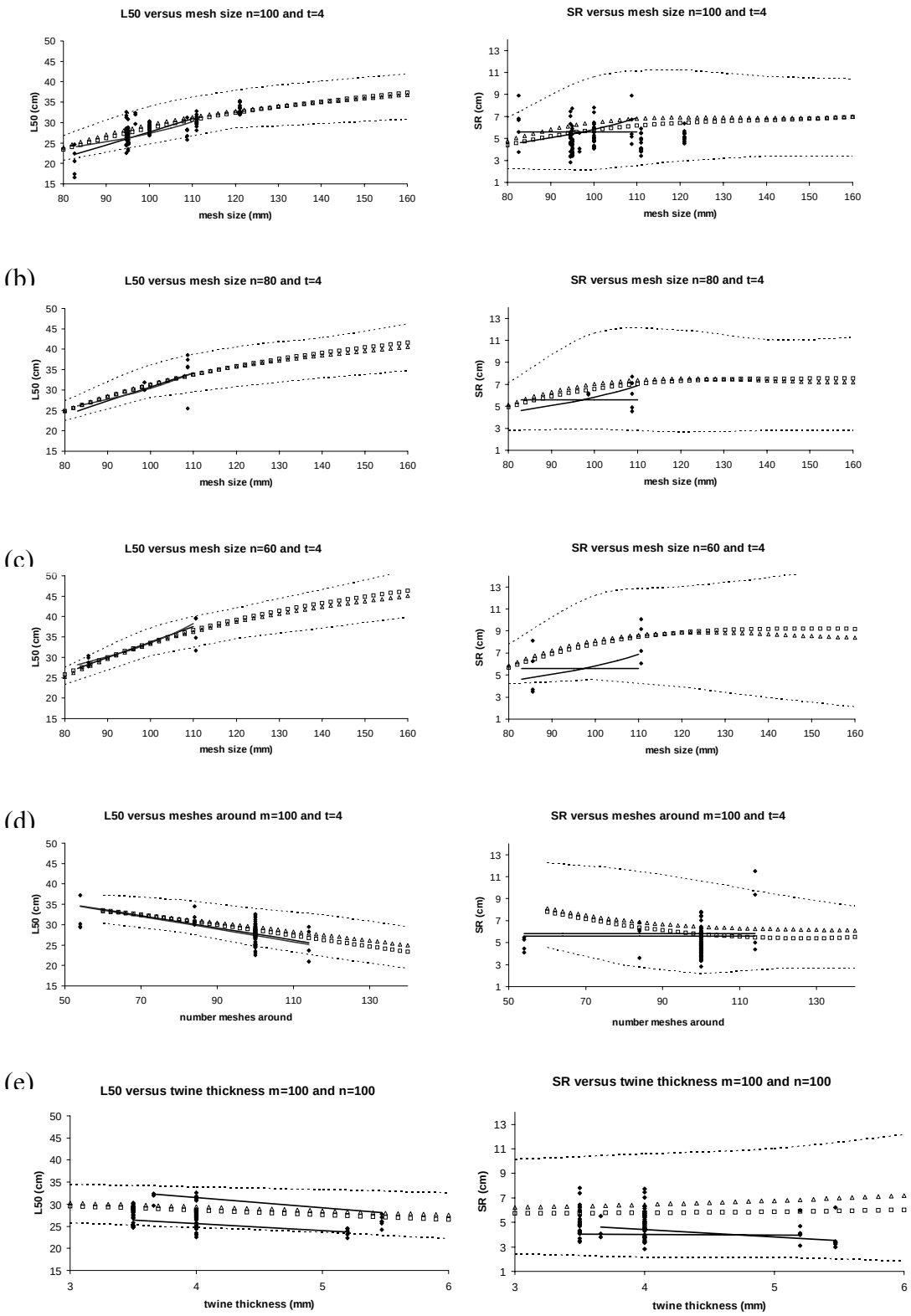

Fig. 37. Selektionsparametre (L50 og SR) for kuller i en trawlfangstpose som funktion af maskestørrelse (m), antal masker i omkredsen (n) og trådtykkelse (t) ifølge modelsimulering med PRESEMO og forsøgsfiskeri.

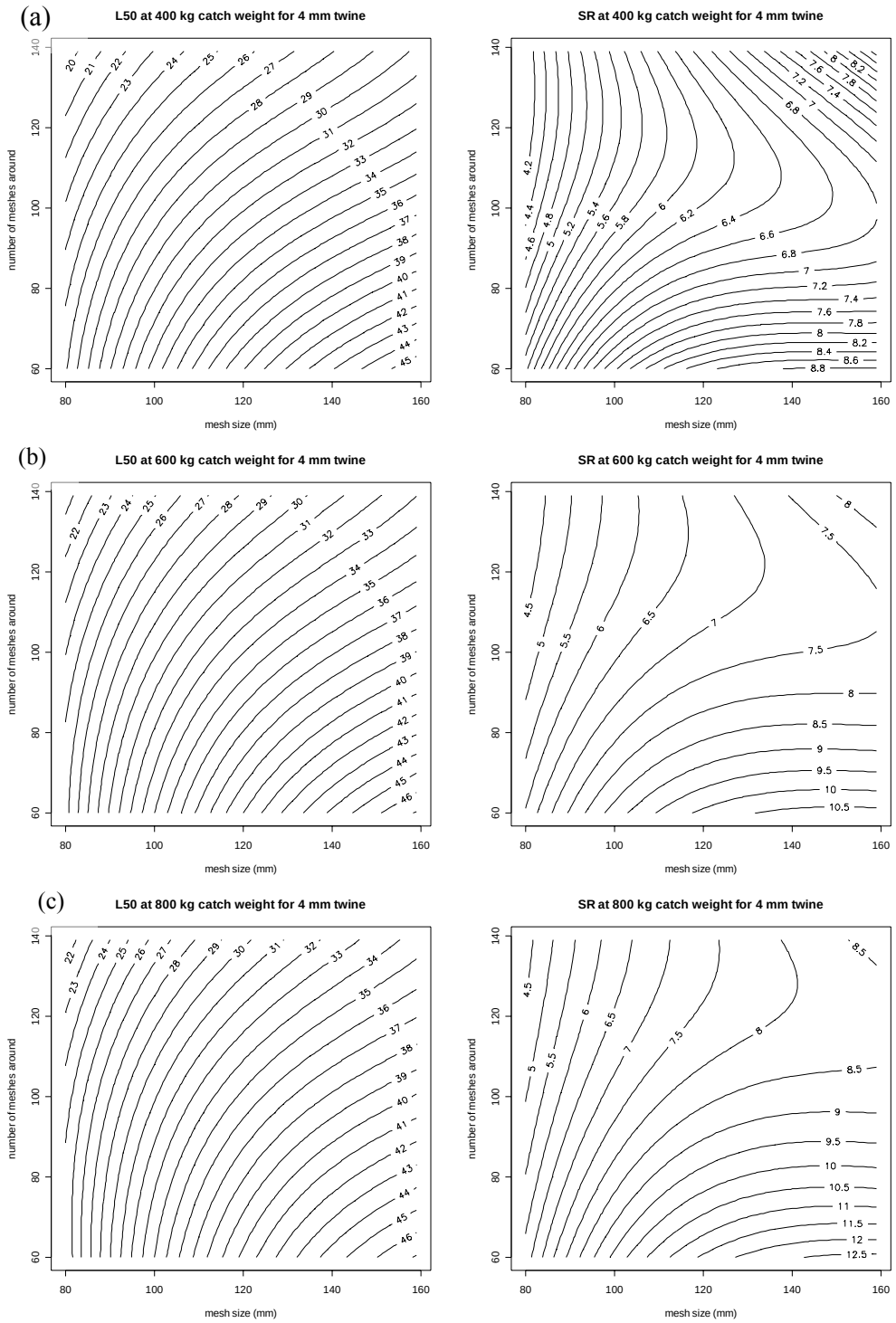

Fig. 38. Isolinieplot af selektionsparametre (L50 og SR) for kuller i en trawlfangstpose som funktion af maskestørrelse (m), antal masker i omkredsen (n) for 3 forskellige totale fangstvægte ifølge modelsimulering med PRESEMO.

Resultaterne viser at vi kan benytte PRESEMO-simuleringer til at undersøge de forventede konsekvenser af at ændre på basale designparametre for en trawls fangstpose. Resultaterne har også vist den forventede effekt af ændring i den totale fangstvægt.

For nærmere diskussion af mulighederne henvises til appendiks A15. Dette studie gælder kun for kuller. Grundet torsk og kullers morfologiske ligheder forventes lignende resultater for torsk. For fladfisk kan vi meget vel forvente en helt anden effekt af fangstvægten og antallet af masker i omkredsen ud fra hvad FISHSELECT-resultaterne har vist (Fig. 17, 20, 23). Det har dog inden for dette projekts rammer ikke været muligt at realisere en sådan analyse.

Kapitel 5: Diskussion

Evaluering af målopfyldelse

Først i denne diskussion er det formålstjenligt at vurdere om det udførte arbejde i projektet og de opnåede resultater lever op til de mål der blev sat for projektet. Resumeet i begyndelsen af denne rapport anførte tre hovedaktiviteter/mål der herunder kommenteres hver for sig.

Mål 1:
Indsamling af data. Laboratorieforsøg der identificerer de morfologiske karakteristika der er afgørende for maskepenetrering for forskellige størrelser og arter. Udvikling af effektiv måleprocedure baseret på visionsteknologiske og mekaniske metoder. Derefter gennemføres morfologimålinger på et større antal individer.
Resultat:
Med FISHSELECT-metoden og de tilhørende værktøjer beskrevet i kapitel 1 vurderes det at der er udviklet en brugbar metode og egnede værktøjer. Dataindsamling beskrevet i kapitel 2 omfatter data for 7 væsentlige arter. Det vurderes at det gennemførte arbejde og de hermed opnåede resultater lever op til hvad der med rimelighed kunne forventes.

Mål 2:
Udvikling af selektionssimuleringsværktøj. Et værktøj der kan beregne selektionen med anvendelse af morfologiske data, fiskeadfærd, redskabsdesign inklusive dettes respons på fysiske parametre som fangstmængde og relevante parametre for slæbet. Simuleringsværktøjet evalueres ved sammenligning mellem eksisterende eksperimentelle data og modelberegninger.
Resultat:
Simuleringsfaciliteterne implementeret i FISHSELECT og anvendt til at danne designguide-plottene vist i kapitel 2, vurderes delvist at opfylde målet idet de vurderes at være en nyttig og overskuelig information i forbindelse med gennemsyn af tekniske reguleringer i fiskeriet. Designguiden vurderes desuden at kunne være et nyttigt værktøj i forbindelse med udvikling af nye selektive fiskeredskaber. PRESEMO, beskrevet i kapitel 3, vurderes på det nuværende udviklingstrin at kunne opfylde resten af målet med hensyn til simulering af selektion af rundfisk i diamantmaskede fangstposer. Dette demonstreres af simuleringsstudiet i kapitel 4. Det vurderes derudover at FISHSELECT-resultaterne gennemgået i kapitel 2 har tilvejebragt grundlaget for på et senere tidspunkt at gøre det muligt at udvide PRESEMO til også at håndtere andre masketyper end diamantformede og til at håndtere fladfisk. Evalueringen af modelberegninger mod eksperimentelle data menes også opfyldt via studiet i kapitel 4 med PRESEMO. Vedrørende simuleringsfaciliteter i FISHSELECT skal det bemærkes at det også rummer muligheder for at simulere gennemsnitlig selektion for en proces gennem definering af maske-fordelinger og kontakthyppigheder. Disse faciliteter er på nuværende udviklingstrin ikke på samme niveau som faciliteterne i PRESEMO med hensyn til simulering af gentagne træk, indkorporering af adfærdskomponent, sammenligning mellem redskaber, procesvisualisering og afviklingshastighed. Men til gengæld er de langt mere generelle med hensyn simulering af selektion for komplekse redskabsdesigns bestående af paneler med forskellige masketyper og placeringer og med hensyn til

flugtmodeller og arter (se appendiks A1 og A9 for mere om simuleringsfaciliteterne i FISHSELECT). Generelt vurderes det at de to simuleringsværktøjer supplerer hinanden godt og giver forskellige muligheder for analyser og prædiktioner. Værktøjerne støtter derfor gensidigt op omkring en fortsat udvikling af begge.

Mål 3:
Prognoseberegninger. Der udvikles en prognosemodel der kan beregne et fartøjs forventede fangst og de driftsøkonomiske konsekvenser ved designændringer i fangstposen.
Resultat:
Der er i projektet udviklet og implementeret en prognosedel til PRESEMO der kan sammenligne den relative fangsteffektivitet over og under mindstemålet for forskellige fangstposedesign. Det vurderes at disse faciliteter delvist kan opfylde målet. Dog er der ikke direkte koblet en økonomidel på og den implementerede facilitet har endnu ikke været anvendt i et egentligt case-studium. På baggrund af dette vurderes det at målet kun delvist er opfyldt.

Forskellige tekniske aspekter, anvendelser og udvidelsesmuligheder
Overordnet vurderes det at de udviklede metoder og værktøjer gennem de dokumenterede anvendelser er på et niveau hvor de med fordel kan inddrages i rådgivningsarbejde om tekniske reguleringer i fiskeriet om end udviklingsarbejdet og dataindsamlingen bør fortsætte. Det vurderes også at metoderne og resultaterne fra anvendelse af dem kan være et nyttigt element i udviklingen af nye selektive redskaber. Det vurderes desuden at arbejdet i dette projekt har vist at metoderne kan være med til, gennem deres anvendelse, at tilvejebringe ny kvalitativ og kvantitativ viden om processer involveret i størrelsesselektionen i trukne redskaber og dermed bidrage til forskningen. Der vurderes at være et betydeligt potentiale på dette område specielt hvis anvendelserne kædes sammen med resultater fra eksperimentelt fiskeri og prøvetanksforsøg.

Fra udenlandske kollegaer er der udtrykt interesse for et samarbejde om metoderne og et ønske om at adoptere dem til konkrete anvendelser. Nationalt har projektet og de anvendte metoder fået en del avisomtale samt har været vist i regional -TV (appendiks A13 omhandler pressedækningen).

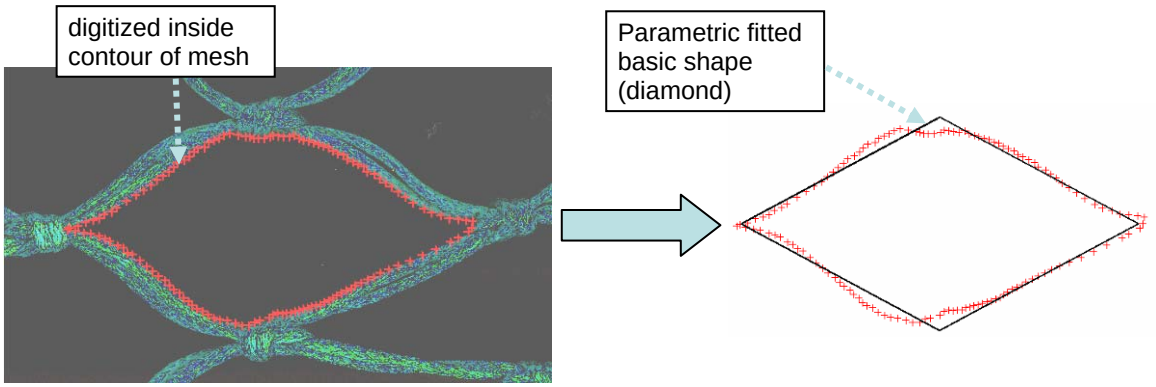

Fig. 39. Indvendig maskekontur digitaliseret med kantdetektion på scannet billede samt en idealiseret maskeform (diamant) tilpasset data.

De udviklede designguides baserer sig på forudsigelser af selektionen i idealiserede maskefaconer der kan beskrives med én af nogle få basisfaconer: diamant, kvadrat, rektangel, heksagonal. Der er kun i begrænset omfang undersøgt hvor godt disse basisformer beskriver formen i rigtige netmasker når de belastes som under fiskeri. Appendiks A10 indbefatter en mindre laboratorieundersøgelse af dette og har vist hvordan en metode til det kan implementeres på basis af scanning, digital billedbehandling og tilpasning af faconparametrene (parametrisk fitting). Fig. 39 illustrerer denne teknik.
Denne teknik kunne udvikles videre og anvendes i et systematisk studium af maskernes faktiske form og egenskaber i redskabsdesigns af relevans for danske fiskerier nu og i fremtiden. F.eks. i forbindelse undersøgelse af evt. forskelle i selektionsegenskaber for paneler når de bruges som normal net (T0) og som 90 grader drejet net (T90) kan metoden med fordel inddrages for at tilvejebringe objektiv og kvantitativ basisviden.

Bestemmelse af tværsnitsmålene (morfologien) på alle individer brugt i dette projekt er fortaget med anvendelse af det mekaniske MorphoMeter i kombination med scanningsteknik, digitalbilledbehandling og parametrisk fitting. Dette har fungeret ganske tilfredsstillende men er også tidskrævende når mange individer skal opmåles. Skal der i fremtiden rutinemæssigt og regelmæssigt foretages opmålinger på et stort antal individer kan det være formålstjenligt at færdiggøre den alternative teknologi, der er beskrevet i appendiks A11. Denne er en optisk metode baseret på digital billedanalyse af en laserlinie diffust reflekteret fra den overflade som ønskes opmålt. Metoden har været undersøgt i projektet og findes lovende, men den er ikke færdigudviklet inden for projektet. Fig. 40 illustrerer denne teknik og det pilotarbejde der er udført i projektet.

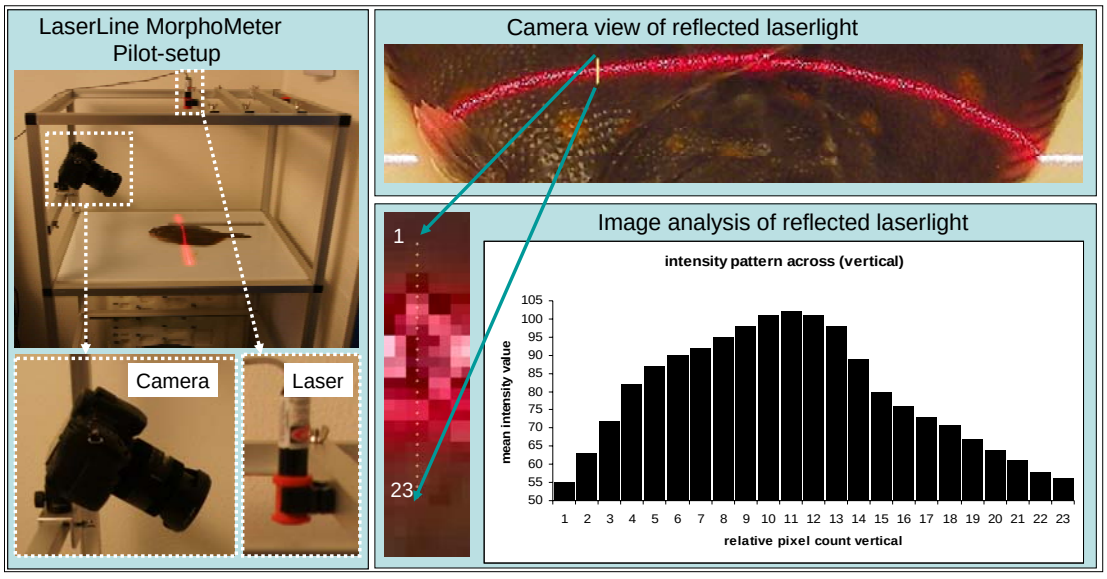

Fig. 40. Pilotforsøg med optisk opmåling (triangulering) af tværsnit på rødspætte. Højre: Centrum af laserlinien findes med bedre præcision end pixelstørrelsen ved at finde maksimum for en glat funktion (langs den gule linie) som tilpasses intensitetsmønstret på tværs af linien midlet på langs af linien.

Affødte projektideer.
Udover ovenstående teknologisk rettede aktiviteter og arbejde med at færdiggøre analyserne for de arter hvor der er indsamlet data, kunne dette projekt fremadrettet pege på anvendelser i forbindelse med forsknings- eller rådgivningsopgaver inden for emner som (på brainstorm niveau):

- Selektion af torsk i Østersøen inkl. undersøgelse af Bacoma og T90.

- Selektion for forskellige arter fladfisk i bomtrawl fiskeri.

- Indirekte adfærdsanalyse af kuller i trawl. Herunder simulering af panelkontakt sandsynligheder med her af følgende mulighed for at undersøge optimal placering af paneler i trukne redskaber.

- Analyse af blandede fiskerier i Kattegat-Skagerrak herunder af discard og relativ fangst effektivitet.

- videreudvikling af PRESEMO på basis af FISHSELECT resultater fra dette projekt.

- Udvidelse af simuleringsfaciliteter i FISHSELECT omkring discard og relativ fangst analyser herunder indbygning af optimaliseringsfaciliteter.

- Undersøgelse af nye maskefaconer til forbedring af selektion for specifikke arter inkl. afprøvning i eksperimentelt fiskeri.

- Undersøgelse af metoder til at skabe mere stabilt åbne masker i fangstposer med henblik på at nedbringe variation i selektion mellem træk og indenfor trækket.

- Inkludering af flere kommercielt eller forvaltningsmæssigt interessante arter i FISHSELECT.

Appendiksliste

Nedenfor er anført de dokumenter der er indeholdt i rapportens appendiksdel som findes i bind II til rapporten: ”Simulering af redskabsselektivitet del II: appendiks”.

A1: manuscript FISHSELECT methodology
A2: manuscript FISHSELECT study of Cod
A3: manuscript FISHSELECT study of Plaice
A4: note on FISHSELECT study of Haddock
A5: note on FISHSELECT study of Turbot
A6: note on FISHSELECT study of Lemon sole
A7: note on FISHSELECT study of Sole
A8: note on FISHSELECT study of Nephrops
A9: manual FISHSELECT software tool
A10: note on development of mesh templates and on nettings
A11: note on development of tools and methods for acquiring cross section shapes
A12: FISHSELECT FTFB posters 2007
A13: FISHSELECT newspaper articles
A14: PRESEMO ICES Boston symposium Poster 2006
A15: PRESEMO ICES journal paper

Referencer

Herrmann, B., 2005a. Effect of catch size and shape on the selectivity of diamond mesh cod-ends: I Model development. Fish. Res. 71: 1-13.

Herrmann, B., 2005b. Modelling and simulation of size selectivity in diamond mesh trawl cod-ends. PhD. afhandling, Aalborg Universitet, Dannmark. ISBN 87-91200-50-4.

Herrmann, B., O'Neill, F.G., 2005. Theoretical study of the between-haul variation of haddock selectivity in a diamond mesh cod-end. Fish. Res. 74: 243-252.

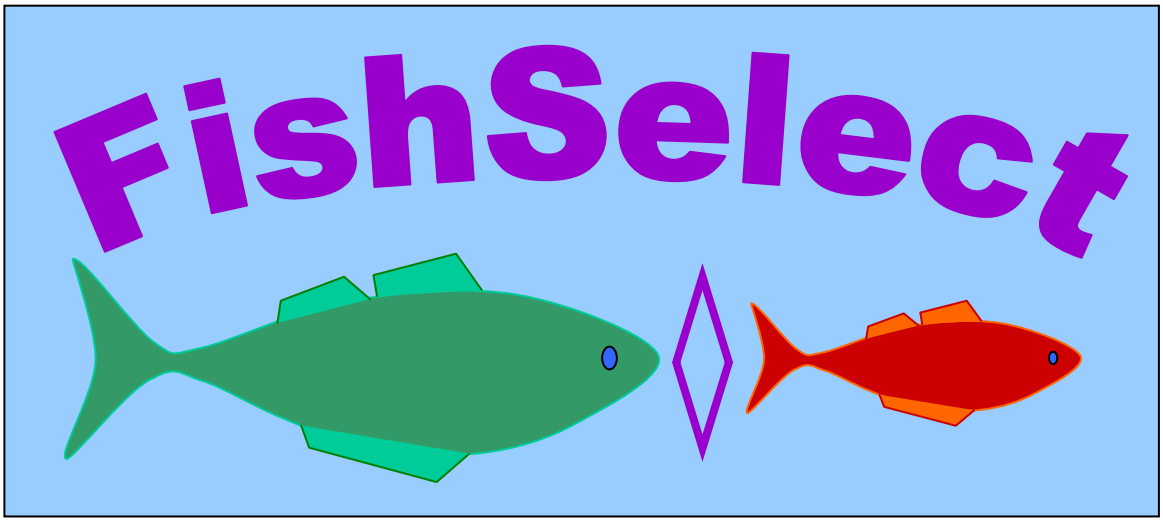

SIMULERING AF SELEKTIVITET I FISKEREDSKABER

Del 2: appendiks

Udarbejdet af: Bent Herrmann
Ludvig A. Krag
Rikke P. Frandsen
Bo Lundgren
Niels Madsen
Karl-Johan Stæhr

DTU Aqua, Sektion for Fiskeriteknologi
Nordsøen Forskerpark
Postbox 101, 9850 Hirtshals

SIMULERING AF SELEKTIVITET I FISKEREDSKABER

Dette dokument indeholder appendiksdelen for rapporten *Simulering af selektivitet i fiskeredskaber*. For beskrivelse af projektet i sammenhæng henvises til hovedrapporten.

Appendiksliste

Nedenfor er anført de dokumenter der er indeholdt i denne del.

A1: manuscript FISHSELECT methodology
A2: manuscript FISHSELECT study of Cod
A3: manuscript FISHSELECT study of Plaice
A4: note on FISHSELECT study of Haddock
A5: note on FISHSELECT study of Turbot
A6: note on FISHSELECT study of Lemon sole
A7: note on FISHSELECT study of Sole
A8: note on FISHSELECT study of Nephrops
A9: manual FISHSELECT software tool
A10: note on development of mesh templates and on nettings
A11: note on development of tools and methods for acquiring cross section shapes
A12: FISHSELECT FTFB posters 2007
A13: FISHSELECT newspaper articles
A14: PRESEMO ICES Boston symposium Poster 2006
A15: PRESEMO ICES journal paper

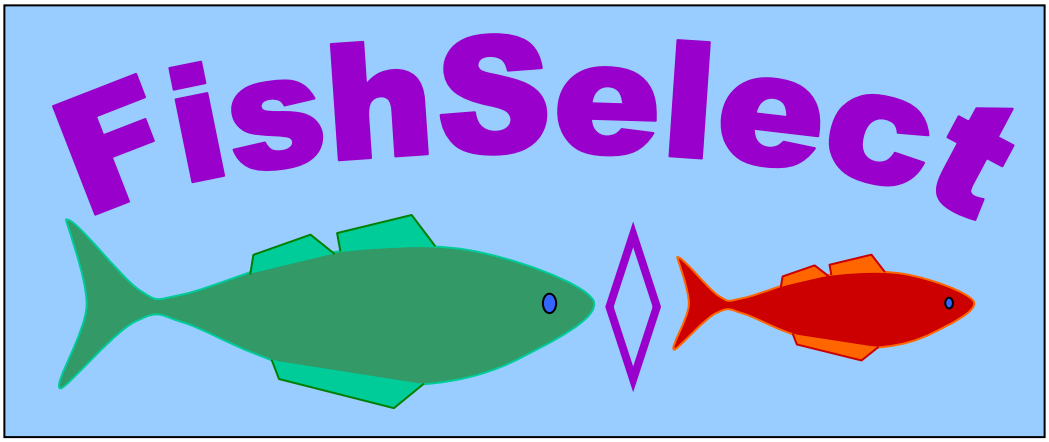

A1

Prediction of selectivity from morphological conditions: I. Development of methodology and tools

Bent Herrmann[1], Bo Lundgren, Ludvig A. Krag, Rikke P. Frandsen, Niels Madsen, Karl-Johan Stæhr

Technical University of Denmark, Institute of Aquatic Resources, North Sea Science Park, DK-9850 Hirtshals, Denmark
1: Corresponding author. Tel.: +45-3396-3204
E-mail address: bhe@difres.dk (B. Herrmann)

Abstract

A methodology (FishSelect) to estimate the morphological condition for mesh penetration by fish in towed gears and its use to simulate the basic selective properties of different nettings is presented. The output is a design guide listing predicted selection parameters of the species and nettings in question. We developed a MorphoMeter which is a mechanical tool to measure cross-section shapes of fish. The FishSelect framework can be used in fisheries management as a design tool for optimizing selectivity of fishing gears.

Keywords: Mesh penetration; Modelling; Fish morphology; FishSelect; MorphoMeter; Selectivity; Towed gear

1. Introduction

Technical measures are widely used by fisheries managers to reduce the discard and optimise the yield in a fishery. Traditionally, mesh size regulations are used to avoid capture of fish under a certain size by allowing them to penetrate through the meshes. Additionally, various selective devices have been tested and implemented in many fisheries to enhance the species or size selective performance of fishing gears. Minimum landing size (MLS) is used as an additional management measure in many fisheries to avoid that fish under a given size is targeted and landed. A particular conflict, when applying technical measures, exists in fisheries on mixed species. Differences in cross-section shapes and other morphological characteristics between species often make it difficult to find an optimal combination of mesh size and mesh shape that considers the MLS of all species. An mismatch between MLS and the selectivity of the fishing gear can either lead to a too high catch of fish under MLS or a reduced catch efficiency, due to high losses of fish of legal sizes. The former may lead to high discard rates which are observed in many fisheries. The latter may motivate an increased effort to catch the legal quota resulting in increased fishing pressure on stocks and the marine environment, extra fuel consumption or circumventing the regulations.

Thus, defining appropriate regulations for mesh sizes and mesh shapes for netting deployed in gears for mixed fisheries is an important but also a complex task. Problems are well-known in many fisheries and numerous design strategies for trawl gears have been tested in mixed fisheries as well as single species fisheries over the last decade to

improve the exploitation patterns. Implementation of these design strategies, which includes inserting square mesh escape panels and/or grids, using 90 degree turned mesh panels (T90) (EC Reg. 51/06; 2187/05; 15238/04; 850/98) and large mesh panels, has made it an even more complex task for fisheries managers to define the optimal designs.

Technical measures are often assessed through experimental fishing or by discard sampling from commercial fishing. These methods could be described as a trial and error approach which is both time consuming and costly. This is also the reason for a lack of sufficient knowledge for several species and fisheries that are nevertheless subjected to technical conservation measures. We believe that it would be a better starting point to theoretically assess the mesh sizes and shapes required to make it at least morphologically possible for unwanted species or sizes to penetrate the meshes before the gear is constructed and tested at sea. This view has also been put forward by Broadhurst et al. (2006).

The objective of our work is to develop a methodology that asses the effect of the morphological condition for mesh penetration for different species caught in towed gears. Furthermore, we outline how the methodology can be applied to construct a mathematical framework and a simulation tool for predicting the morphology-based selectivity properties. The methodology can provide managers with indicative predictions of the consequences on discard rate and catch efficiency as well as how these values are affected by selecting different mesh sizes and shapes values for a specific fishery. If it can be biologically justified, it may also be beneficial to adjust the minimum landing sizes of some of the species in question. Besides being a new approach towards providing information for both current and future gear designs and fisheries management, we expect that the use of the above methodology will provide information to validate and extend the penetration models used in the cod-end selectivity simulator PRESEMO (Herrmann, 2005a; 2005b) to enable it to work with species other than round fish and mesh shapes other than diamond shaped. This will provide fishery managers with a computer simulation tool that can provide a faster and more justified basis for decisions both on gears used in single species fisheries and in the complex multi species fisheries. In the latter case, any decision will be a trade off between discards and yields of the different species. The novel methodology presented here will aid in exposing these consequences and thus improve the foundation for the decisions.

2. Theoretical considerations

2.1. Mesh penetration

To our knowledge there does not exist any standard method to assess which morphological characteristics, that are decisive for the mesh penetration in towed gear. In previous studies, maximum girth has mainly been used as a measure to relate fish morphology to their ability to pass through meshes (Santos et al., 2006). But due to differences in deformability of muscle tissue, guts and bone structures such as the skull, we believe that max girth is inadequate in explaining the relationship between fish morphology and mesh penetration.

For each species it is relevant to investigate and define:

- Where along the length of the fish should the cross-section be measured and which parameters should be measured there?
- Is there a need to measure fish cross-section at more than one position along its length?
- Which geometrical descriptions can we use to describe the cross-section shapes of different fish species?
- Can the morphological conditions for mesh penetration be modelled similarly for different species of fish for example for round fish and flat fish?
- How can we test and validate a predictive model for the morphology-based netting panel penetration?
- Can we quantify how close a fish is from not being able to penetrate a given mesh or how far it is from being able to?
- Can we compare the predictive power of different potential models that can be constructed?

It can be appropriate to view the condition allowing a fish to actually penetrate a netting panel in a towed fishing gear as consisting of two of sub-conditions for penetration that both need to be fulfilled:

i) The morphological condition. The geometrical relation between the cross-section size and shape of the fish, and the mesh size and shape allow the fish to pass through.

ii) The behavioural condition. The fish must either actively attempt to pass through the panel or be forced mechanically towards it. An important element is that the fish is able to meet the panel oriented in an optimal way to penetrate it.

Recognizing the above, we argue that the first step in the process of designing a new selective fishing gear for a specific fishery should contain a procedure to select panel designs fulfilling at least the morphological sub-condition (i). If it is not fulfilled, then a fish trying to penetrate will end up being retained by the fishing gear, regardless of its behavioural response. An assessment of the effect of the morphological sub-condition will provide a first approximation of the selective properties of netting panels and thus provide the basis for a preliminary prediction of the consequences on discard and catch efficiency of using the investigated netting design in a specific fishery.

2.2. Stiff mesh shape assumption

When a fish tries to penetrate a mesh in a codend, both the fish cross-section shape and the mesh shape can potentially be deformed. But the tension exerted by drag forces on the mesh bars of the most commonly used diamond mesh nettings, can be assumed to exceed the muscle force of the fish in all but the very early stages of a tow (Efanov et al. 1987; Herrmann and O'Neill, 2005; 2006). The increased use of thicker and stiffer twine material in cod-end nettings in many European trawl fisheries supports this assumption. Therefore, in the methodology presented here, we will generally assume that during mesh penetration attempts, mesh deformation is negligible compared to the deformation of the fish itself. Considering the behavioural component of the penetration condition, we will assume that it is more likely that a fish will actually attempt to pass through a mesh

which looks like it can be passed. Small mesh openings represent a stronger visual barrier making escape attempts less likely. The latter assumption has many similarities with the suggestions described by Glass et al. (1993). Based on the above argumentation we will mainly use the stiff mesh shape assumption. On the other hand, when netting panels with square meshes, rectangular meshes or hexagonal meshes are considered, we will take possible deformation of the potential tensionless mesh bars perpendicular to the tow directions into account.

For the sake of completeness and comparison, we will also consider the case of "soft" meshes, where we assume that the mesh and/or the fish cross-section are fully deformable and thus take shape after each other during penetration attempts.

Based on experience with measuring the morphological parameters, we will assume though that the cross-section shape of the fish can be deformed during penetration attempts.

3. Outline of the methodology

As regulations on legal landing sizes of fish often are based on length (e.g. in form of MLS), we want to link likelihood of mesh penetration for a fish to its length. Relationships between morphological parameters of importance for mesh penetration and the length of the fish are therefore included in the methodology.

In order to make the model more efficient, the number of parameters needed to describe the cross-sections should be limited. This is obtained by explaining the shape of the cross-sections by geometrical shapes such as ellipsoids, triangles, trapezoids etc. The geometrical shape that fits the cross-section the best, therefore needs to be identified as does the extent to which the cross-section may be deformed during mesh penetration.

In order to give a balanced assessment of the potential benefit of applying new types of nettings in a given fishery, the methodology needs to be flexible and take mesh shapes other than those typically used for cod-end nettings into account. For the same reason, the aim is to be able to cover the morphology of most fish species and crustaceans relevant for the fishery in question.

The methodology consists of the following sequence of activities:

1) *Laboratory penetration experiments.*

The morphological characteristics of the fish cross-sections, that are potentially important for mesh penetration, are identified and measured on a significant number of freshly caught fish of different lengths. At the onset of the experiment, the fish is killed in a solution of anaesthetization, labelled with a unique number and its length and weight are recorded. For the penetration trials we use a large number of plates (thickness: 4-5 mm) with holes cut to simulate different types of stiff meshes. Each mesh hole gets a unique identification label. A large range of different sizes and shapes are covered, including the mesh sizes legally used in the Danish fisheries. Each mesh size is represented with the range of mesh openings typically found along the codend during catch accumulation. With the mesh plates held horizontally, it is tested and recorded which mesh holes each fish can or cannot pass through head-down and forced by gravity (Fig 1). The fish is rotated to the optimal orientation for penetration. For each new species examined, the

penetration experiment is repeated three times on a few individuals in order to assess if the experiments affect the morphology of the fish.

Fig. 1: Fall-through experiments. A cod is passing through.

2) *Simulation of experiments.*

The morphological data for the fish recorded in the laboratory penetration experiments, together with a list of descriptions of the meshes used in the experiment are loaded into FishSelect. Under varying conditions including different levels and modes of deformation of the fish cross-sections, a repetition of the penetration experiments is then simulated for the fish and meshes tested in the laboratory. FishSelect is a flexible simulation model, based on the mathematical framework described below. It has different models describing the fish cross-sections based on the morphology data and different options for both mesh geometry and for the conditions for mesh penetration based on the relations between fish morphology and mesh geometry.

3) *Comparison.*

The penetration results from the simulated experiments are now held against the results from the laboratory experiments. The resulting degree of agreement (see Section 7) over a large number of different meshes and fish for a particular set of penetration options is used both to identify the morphological features that are relevant when simulating fish penetration and to decide if the structures of the models of the morphology and the conditions for mesh penetration are reasonable for the species being investigated.

4) *Establishment of morphological relationships.*

The relationships between the morphological features identified as relevant in 3) are established and the statistical variations are estimated. If the number of fish tested in activity 1 was insufficient for establishing reliable morphological relationships, activities 1-3 are repeated on a larger number of fish. This may be the case if a pilot study is set up to ensure efficiency when measuring species that have high mortality when kept in tanks. The relationships can now be applied to simulate the morphological data for a fish population of any size structure.

5) *Predictions.*

Based on the model established in 3) and the morphological relationships established in 4) predictions about the basic selective properties for different nettings can be made for a specified populations of fish. We expect that together with information on the distribution of the fishing effort and the size structure of the fished population, these predictions can provide indicative information on the resulting discard rates and catch efficiencies when applying different netting constructions in the fishery.

The following sections outline the mathematical framework necessary for implementing the simulation model in the methodology described above.

4. Generic condition for mesh penetration

The conditions for mesh penetration should be very general with respect to mesh shape and fish cross-section shape. The inside contour of any mesh can be described by a closed curve. A convenient way to describe such a mesh curve is in polar coordinates (Kreyszig, 1979) in a local coordinate system (*xm, ym*) for the mesh (Fig. 2) using pairs of angle Θ and distance *rm*(Θ) from the origin of the coordinate system.

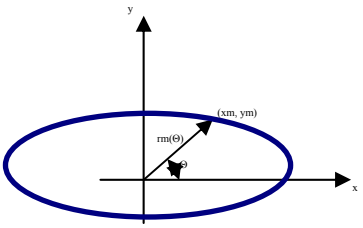

Fig. 2: Describing mesh curve in polar (Θ, rm) and Cartesian coordinates (xm, ym).

The closed curve condition means that there exists a value *rm* for all Θ (0-360 degrees) and that *rm* is the same for Θ = 0 and Θ = 360 degrees. The origin of the coordinate system (*xm, ym*) should be approximately at the centre of the mesh to ensure that *rm* has a positive value for all Θ. Similarly the outside contour of the cross-section of a fish (the fish curve) can be described in a local coordinate system (*xf, yf*) by pairs of angle Θ and distance *rf*(Θ) from origin. As for the mesh the origin should be selected to ensure that rf always has a positive value. The conversion relations from polar coordinates (Θ, *r*) to Cartesian coordinates (*x, y*) are:

$$\begin{aligned} x &= r(\Theta)\times\cos\Theta \\ y &= r(\Theta)\times\sin\Theta \end{aligned} \qquad (1)$$

and from Cartesian to polar:

$$\begin{aligned} r(\Theta) &= \sqrt{\left(x^2+y^2\right)} \\ \Theta &= \arctan 2(y,x) \end{aligned} \qquad (2)$$

where arctan2(*y, x*) calculates arctan(*y/x*) and returns an angle in the correct quadrant (0.0 to 360.0).

To evaluate whether the fish cross-section fits inside the area defined by the mesh contour, the fish curve has to be described in the mesh coordinate system. The transformation of the 2-dimensional fish coordinate system to the mesh coordinate system can be viewed as a rotation Φ to make the *x* and *y* axis of the two coordinate systems parallel followed by the translations *tx* and *ty* to give the two coordinate systems the same origin. Thus the transformation of the fish curve coordinates (*xf, yf*) can be expressed by:

$$xfm = xf \times \cos\Phi - yf \times \sin\Phi + tx$$
$$yfm = xf \times \sin\Phi + yf \times \cos\Phi + ty \qquad (3)$$

and

$$rfm(\Theta fm) = \sqrt{(xfm^2 + yfm^2)}$$
$$\Theta fm = \arctan 2(yfm, xfm)$$

where (*xfm, yfm*) are the Cartesian coordinates in the mesh coordinate system. Assuming that the functions *rm*(Θ) (the mesh curve) and *rfm*(Θ) (the fish curve of the given cross-section along the fish length) do exist, the required condition for mesh penetration is that there exists at least one set of values of the transformation parameters (Φ, *tx, ty*), for which *rm* is larger than or equal to *rfm* for all angles Θ between 0 and 360. This can be expressed as:

$$\forall \quad \Theta \in [0;360] \exists \quad (\Phi, tx, ty): \quad rm \geq rfm \qquad (4)$$

The problem of determining if (4) is fulfilled can be transformed into a minimization problem by defining the merit function:

$$merit(\Phi, tx, ty) = \frac{1}{n}\sum_{i=1}^{n} dm(\Theta_i, \Phi, tx, ty)$$

where (5)

$$dm(\Theta, \Phi, tx, ty) = \begin{cases} 0 & \forall \quad rm(\Theta) - rfm(\Theta, \Phi, tx, ty) \geq 0 \\ (rfm(\Theta, \Phi, tx, ty) - rm(\Theta)) & \forall \quad rm(\Theta) - rfm(\Theta, \Phi, tx, ty) < 0 \end{cases}$$

The summation is done over *n* discrete angles Θ_i between 0 and 359 degrees. By choosing the number *n* to be at least 360 and with points reasonably evenly distributed along the fish contour then we can assume that it is permissible to use a discrete summation in stead of a continuous integration. From (5) it is clear that merit function is non-negative for all values of (Φ, *tx, ty*). The penetration condition can be assessed by minimizing the merit function with respect to (Φ, *tx, ty*). Penetration is possible if:

$$\min(merit(\Phi, tx, ty)) = 0 \qquad (6)$$

that is, there is at least one set of values (Φ, *tx, ty*), where merit(Φ, *tx, ty*) = 0.

But besides letting the simulation procedure predict if the penetration condition given by (6) is fulfilled or not for a particular fish cross-section, we want to know how close to or how far away the condition was from being just fulfilled. To do this we introduce a scaling factor, *sf*, to scale the fish cross-section up (*sf* > 1.0) or down (*sf* < 1.0) isomorphically:

$$srfm(\Theta_i) = sf \times rfm(\Theta_i) \quad for \quad i \in [1; n] \qquad (7)$$

By varying the scaling factor and substituting *rfm* with *srfm* in (5) we find the maximum value of *sf*, for which (6) is still just fulfilled:

$$\max(sf) \quad while \quad \min(merit(\Phi, tx, ty)) = 0 \qquad (8)$$

If max(*sf*) is less than 1.0, then the fish cross-section is not able to pass through the mesh and the value of max(sf) quantifies, how far condition (6) is from being fulfilled. If max(sf) is larger than 1.0, the fish cross-section is able to pass through the mesh and the value of max(sf) quantifies, how far condition (6) is from being not fulfilled.

Formulas (1) to (8) are generic expressions for the condition telling if a fish cross-section is geometrically able to pass through a mesh. They are independent of the specific shapes of the mesh or the cross-section of the fish. To analyze a specific situation we have to define $rm(\Theta)$ and $rf(\Theta)$ for the interval Θ [0.0; 360]. Appendix A describes parametric expressions for the basic mesh shapes: diamond, square, rectangular and hexagonal. Appendix B describes parametric expressions for the basic fish cross-section shapes: ellipse, half-ellipse, triangular, symmetric trapezoid, asymmetric trapezoid.

For the soft mesh situation the condition for penetration is that the maximum circumferential length of the fish curve (*clf*) is less than the circumferential length of the mesh curve (*clm*). Appendix A contains expressions for the circumferential length for the mesh shapes and Appendix B for the fish cross-sections shapes.

5. Penetration models

The simplest possible penetration model requires applying (8) only at one position along the fish length. But if needed, the software allows evaluation of condition (8) at up to three positions along the length of the fish. The cross-section descriptions and the condition for penetration need not necessarily be the same at all positions. A model that takes the potential compression of the fish cross-section into account can be constructed in two equivalent ways: one where the parameters for the cross-section are assumed to be smaller than the uncompressed by a certain percentage; another where sf in (8) is allowed to be a certain percentage smaller than 1.0 and still assume penetration. Asymmetrical compression can be modelled by allowing different degree of compression along the vertical and horizontal axis' of the fish cross-section.

6. Estimation of cross-section shape

As mentioned in Section 4, fish cross-section shapes are approximated by parametric expressions using basic geometric shapes. In this section we present a formula both to assess how well the parametric descriptions represent the cross-section shapes of different species and to assess the parameter values. It is assumed that we have measurements defining the Cartesian coordinates of a number *n* of points (*xf, yf*) on the cross-section contour of a fish of interest obtained by experimental means, for example the MorphoMeter and the image analysis functionality built into the FishSelect software tool (see section 11). By using (2) we can transform the data to polar coordinates to

obtain a list of points on the form (Θf, $rf(\Theta f)$) for Θf in [0;360] for n points along the cross-section. Then we can select one of the basic geometrical shapes described in polar coordinates (Θb, $r(\Theta b)$) for Θb in [0;360] according to the formulas in appendix B. The formula will contain q of unknown parameter values p_1 to p_q, depending on which parametric basic description is selected. By adjusting the values for a translation (tx, ty) and a rotation Φ of the point array (Θf, $rf(\Theta f)$) to obtain the array (Θfm, $rfm(\Theta fm)$) (according to (3)) and the parameter values ($p_1,...,p_q$) of the parametric description of (Θb, $r(\Theta b)$) a best fit in the least square sense can be carried out by minimizing the function:

$$fshape(tx, ty, \Phi, p_1, .., p_q) = \frac{1}{n}\sum_{i=1}^{n}\left(rb(\Theta_i, p_1, ..., p_q) - rfm(\Theta_i, \Phi, tx, ty)\right)^2 \qquad (9)$$

If the vector (txm, tym, Φm, pm_1, ..., pm_q) minimizes (9), then the mean square difference between the fitted basic geometrical shape and the measured fish cross-section shape is:

$$md = \frac{1}{n}\sum_{i=1}^{n}\sqrt{\left(rb(\Theta_i, pm_1, ..., pm_q) - rfm(\Theta_i, \Phi m, txm, tym)\right)^2} \qquad (10)$$

The smallest value of md identifies which of the different basic geometrical shapes describes the cross-section shape best.

7. Degree of agreement with experimental results

If we use F different fish and M different meshes in the experimental setup (Activity 1 of the methodology), it produces F times M experimental penetration results PE_{ij}. The value of PE_{ij} is set to 0 if the fish (i) does not pass through the mesh (j), otherwise to 1. For the simulated penetration (Activity 2) we name the penetration results PS_{ij} for a particular escapement model and set of morphological parameters. In the same way PS_{ij} has either the value 0 or 1. We can quantify the degree of agreement (DA) between experimental and simulated results by:

$$DA = \frac{\sum_{i=1}^{F}\sum_{j=1}^{M} v(PE_{ij}, PS_{ij})}{F \times M}$$

where (11)

$$v(PE_{ij}, PS_{ij}) = \begin{cases} 0.0 & \forall \quad PE_{ij} \neq PS_{ij} \\ 1.0 & \forall \quad PE_{ij} = PS_{ij} \end{cases}$$

Thus DA is a number between 0.0 and 1.0. If the investigated penetration model is good at simulating the experimental results, DA should be close to 1.0. Thus the quality of applying different penetration models to simulate the experimental results can be compared and evaluated by applying (11).

The quality of the penetration model can not only be judged by DA, but also by looking at a plot of the number of cases where there is disagreement between the

simulated results of the fall through experiment and the experimental ones versus the scaling factor, sf, calculated in (7)-(8). If the penetration model is good, the plot should show a distribution of only few values centered around 1.0, indicating that the simulated results are not far away from agreeing with the experimental ones.

8. Virtual population data

Assume that by applying (11) we have been able to define a penetration model that produces acceptable results (DA preferably at least 0.95) (Activity 3 of the methodology) for the species being investigated.

The properties of the model are determined by q morphological parameters p_1 to p_q for one or more cross-sections along the fish. Next let assume that we have measured these morphological parameters ($p_1, \ldots, p_q$) as well as weight versus length for a considerable number of fish of a species of interest covering a relevant length range (Activity 1 and 4 in the methodology). The relationship between p_i and length, l, as well as the variance in the relationship can be modelled based on regression analysis. Demanding that the cross-section size decreases towards zero with decreasing fish length we assume a power relation of the form:

$$p_i(l) = \alpha_i \times l^{\beta_i} \qquad for \qquad i \in [1; q] \tag{12}$$

In the simplest form (12) will be linear ($\beta \approx 1.0$).

We simply find the mean value and standard deviation of α_i and use these for the description of the variation in the relationship.

In the same way we use a similar expression for the weight:

$$w(l) = \alpha_w \times l^{\beta_w} \tag{13}$$

As for p_i we estimate mean and standard deviation of α_w.

If the precision of predicting the mean morphological relationships by applying (12) and (13) is comparable to the measurement precision, they are used, otherwise more complex relationships are modelled. Assuming that the variation of the value of the α's can be modelled reasonably by normal distributions, we can model a virtual population having a specified length distribution $n(l)$. In a simulation run each of the N fish from the population is assigned morphological parameter values $p_1, \ldots, p_q$ for each cross-section and weight w, calculated in the simplest case by (12) and (13) selecting $\alpha_1, \ldots, \alpha_q$ and α_w randomly from normal distributions with the empirical means and standard deviations obtained by the regression analysis mentioned above.

9. Prediction of basic selection properties for specific mesh panel

By basic selection properties for a mesh panel we mean selection properties based on taking into account only the morphological sub-condition for mesh penetration without considering any behavioural effects, thus representing only the basic selective potential of the mesh panel.

Two measures *L50*, the 50 percent retention length, and *SR*, the selection range (*L75 – L25*), are often used to quantify the size selective properties of trawl nettings (see Wileman et al., 1996). We will use the same two measures to characterize the basic size selective properties of a mesh panel.

To estimate *L50* and *SR* for a mesh panel by the methodology represented in this paper we must first define its mesh properties, make a virtual fish population having a suitable size structure and then calculate for each fish in the population whether it is able to penetrate the mesh panel. For the sake of simplicity we will first restrict the description to the situation, in which the panel has only one type of meshes all with same size and shape. This is equivalent to simulating penetration of the selected fish population through one specific mesh. In this case the two dimensional array PS_{ij} is simply reduced to a one-dimensional vector PS_i with one penetration result for each fish in the population. To meet the criteria in the definition of the size selective properties for netting formulated in Wileman et al. (1996), we use an ideal virtual population with a uniform size distribution with predefined minimum and maximum sizes (L_{min} and L_{max}). L_{min} should be chosen so that all fish of this length can penetrate the mesh while L_{max} should be chosen so that no fish of this length can penetrate the mesh. The array of results PS_i (1 if fish i passed the mesh else 0) together with the length l_i for each fish gives the information for assessing the basic morphologically based length dependent retention of the specific mesh. Assume that we have N fish in the population making N sets of (l_i, PS_i) (i=1 to N). To calculate the length dependent retention rates data are first sorted into lengths classes each 10 mm wide. Then the total number of fish, mt_j (where $PS_i = 1$), and the number of fish not being able to pass through the mesh, mr_j (where $PS_i = 0$), are counted in each length class. This procedure is similar to the covered cod-end method for assessing trawl cod-end selection (Wileman et al., 1996). By treating the penetration results as selection data we obtain estimates of *L50* and *SR* by fitting the logistic curve (see Wileman et al., 1996) to the data:

$$r(l) = \frac{\exp\left(\frac{2\times\ln(3)}{SR}\times(l-L50)\right)}{1+\exp\left(\frac{2\times\ln(3)}{SR}\times(l-L50)\right)} \tag{14}$$

As for cod-end selection data the fitting is performed by maximizing the log-likelihood function (Wileman et al., 1996):

$$g(L50,SR) = \sum_{j=1}^{M}\left(mr_j\times\ln\left(r(l_j)\right)+\left(mt_j-mr_j\right)\times\ln\left(1-r(l_j)\right)\right) \tag{15}$$

where the summation is over M length classes. Expression (15) can be turned into a minimization problem by:

$$\min\left(-g(L50,SR)\right) \tag{16}$$

The formulas (15) for a single mesh can easily be extended to a situation dealing with more than one mesh shape and/or mesh type in the netting. Weighting each mesh j in a set of Q meshes by a relative contact factor, c_j, we simply get:

$$g(L50,SR)=\sum_{i=1}^{M}\left(\left(\sum_{j=1}^{Q}c_j\times mr_{ji}\right)\times\ln(r(l_i))+\left(\sum_{j=1}^{Q}c_j\times(mt_{ji}-mr_{ji})\right)\times\ln(1-r(l_i))\right) \qquad (17)$$

The weighting factor c_j is the relative contact likelihood between the fish and the mesh.

10. Implementation of the model

The model outlined in the previous sections is implemented in the computer program FishSelect by use of the commercially available programming tool Delphi from Borland Software Corporation. The tool allows users to develop Pascal code programs with a graphical user interface (Kerman, 2002; Wiener and Wiatrowski, 1997). The compiled code can be run on a Microsoft Windows operating system.

The minimization procedures required for formulas (6), (8), (9) and (16) have been implemented using Powell's method (Press, W.H. et al., 1986). Several technical precautions have been implemented to mitigate problems with local minima, which are often encountered in optimization algorithms.

11. MorphoMeter and extraction of cross-section contour

A mechanical sensing tool (MorphoMeter) (Fig 3) was constructed with 80 adjustable round aluminium sticks with diameter 2.5 mm and length 150 mm. The sticks are mounted close together but allowed to move with slight friction in the vertical direction between the legs of an aluminium frame. The distance between the legs is 200 mm and they are 80 mm high. The sticks can individually move up to 80 mm. Two clamping screws enable clamping the position of the sticks. By placing a flat fish like a sole on a table between the legs of the MorphoMeter in vertical position and letting the sticks sink down until the get into contact with the upper surface of the fish the MorphoMeter sticks will form a contour approximating the fish shape (Fig. 3).

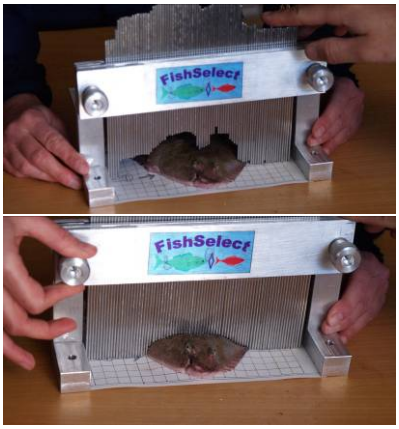

Fig. 3: Measuring cross section of a sole by use of MorphoMeter.

After clamping the position of the sticks and placing the MorphoMeter on a flatbed scanner an image of the fish cross-section contour is created (Fig. 4). Images were scanned in 24 bits colours with a resolution of 300 times 300 dpi (dots per inch).

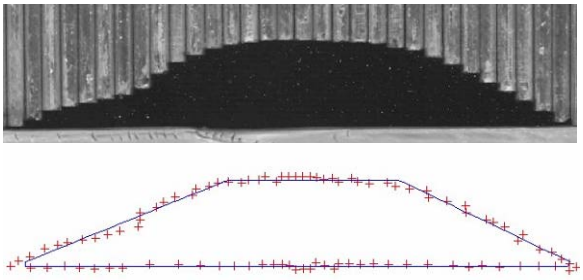

Fig. 4: Cross section of Sole. Top: scanned image of MorphoMeter. Bottom: Digitized image by FISHSELECT build in edge detection software (crosses) and fitted asymmetric trapezoid (curve).

To extract the cross-section shape from the scanned image of the MorphoMeter an image analysis functionality was built into the FishSelect software tool. It uses a thresholding technique starting from the centre of the dark object zone (the fish contour) in the image (see Fig. 4), then moving away from the centre in one direction at the time looking for stable but abrupt increase in average intensity assessed as the average of the RGB colours (Red, Green, Blue) intensity values (see Gonzales and Wintz, 1987 for details on these techniques). The parameters for the thresholding include average intensity in the object zone and the average intensity of the measuring sticks of the MorphoMeter. The sequential search for an edge in different directions typically detects between 100 and 300 points along the cross-section contour, depending on the size and shape of the fish. By use of calibration objects in the image picture coordinates in number of pixels can be transformed to measures in mm. Fig. 4 shows the scanned image of the cross-section of a sole sampled by the MorphoMeter (top) and the digitized edge points (crosses) and a fitted asymmetric trapezoid (solid line) obtained by an implementation of formula (9) (bottom).

The use of a large number of points to describe the contour increase the accuracy of the measurement and the parametric fitting smooth the contour acquired based on the position of the individual sticks. Further it makes the method more robust against single outlier points.

To assess the cross-section shape of round fish two MorphoMeters were assembled as a pair and the construction was turned 90 degrees with the sticks to moving horizontally (Fig. 5). The sticks are pushed manually into contact with the fish cross-section 360 degrees around enabling measurement of round fish cross-sections being up to 160 x 200 mm in size. Fig. 5 shows also the fit of an ellipse to the digitized edge points of the cross-section of a haddock (left).

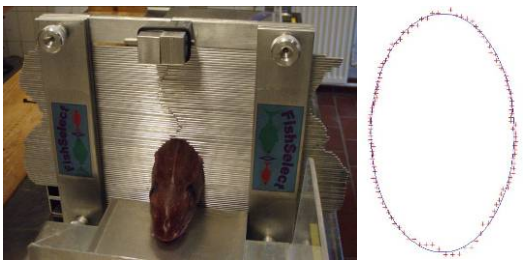

Fig. 5: Cross section of haddock. Left: haddock in assembled MorphoMeter. Right: digitized cross section (crosses) and fitted ellipse (curve).

12. Example on Cross section measurements

To evaluate the accuracy and precision of the MorphoMeter measurements and the FishSelect digitization process to assess cross-section features stiff non-deformable objects in form of a round disc of known diameter and an asymmetric trapezoid of known height were used as test objects. The process of using the MorphoMeter, the scanning technique and the image analysis to extract diameter and height was repeated 10 times for both objects. Table 1 shows the results indicating that for the features compared the precision (repetition accuracy) is within ± 0.50 and 0.32 mm) for 95% of the measurements, whereas the mean accuracy (bias with respect to the reference measurement) is 0.47 and -0.25 for the circle diameter and trapezoid height, respectively. We expect that this accuracy is sufficient for use on deformable objects like the cross-sections of many fish species.

test no\object	Disc diameter	ATR height
ref measure	120.41	17.00
1	121.28	16.78
2	120.96	16.84
3	120.73	16.62
4	121.14	16.77
5	120.71	16.77
6	120.94	16.89
7	121.07	16.74
8	120.73	16.71
9	120.82	16.78
10	120.43	16.64
mean	120.88	16.75
sd	0.25	0.08
mean bias	0.47	-0.25

Table 1: Validation of the measuring accuracy and precision by use of the MorphoMeter and FISHSELECT software tool. Test objects were a circular disc (feature compared: diameter) and an asymmetric trapezoid (feature compared: height). Reference measurements were carried out using a digital caliper. With the MorphoMeter 10 repeated measurements 10 were carried out (1-10). Mean values (mean) and standard deviation (sd) were calculated as well as bias of the mean with respect to the reference value (ref measure). All measures are in mm.

13. Discussion

The initial evaluation of the methodology indicate that FishSelect is able to provide a rough estimate on the selectivity of gear designs prior to testing them at sea (A2). The methodology does not account for the behavioural component of the selection process but its importance and influence on mesh penetration can be deducted by comparing simulated results with retention estimates from selectivity experiments. Such a comparison can also provide information on the predictive power of the FishSelect methodology and its limitations.

During a real fishing process, some individuals that do fulfill the morphological condition for successful mesh penetration will not escape because the behavioural

condition may not be fulfilled. As we do not take the behavioural aspect into account, we thus expect that the morphologically based FishSelect predictions of L50 represent upper limit estimates. For SR the situation is not so clear. However, as a rule of thump we will expect to underestimate SR because the behavioural component is expected to retain some of the fish that are simulated to escape.

The force the fish is able to produce during an attempt to penetrate a mesh is set to be equivalent to the force of gravity. How realistic this assumption is, is uncertain and lacks validation. The rationale behind the assumption is, however, that both forces are proportional to the size of the fish.

Existing simulation models like PRESEMO (Herrmann, 2005a, 2005b) are constructed to predict and study the size selection processes in cod-ends of towed gears. So far, the models have been applied to a few round fish species in diamond mesh shaped cod-ends only (Herrmann, 2005c; Herrmann and O'Neill 2005, 2006; Herrmann et al., 2006, 2007a, 2007b; O' Neill and Herrmann, 2007; Sala et al., 2006) and the aim is to predict different aspects of size selection. An important reason for the limited use has been the lack of morphological data relevant for mesh penetration for important species. Use of the methodology described in this paper will help providing this information and help identifying the most suitable models for implementation of the morphological sub-condition for mesh penetration for different types of mesh shapes and new species. Thereby it could form the basis for extending the predictive power of PRESEMO.

The tools described in this paper can be used to establish a gear design guide, which includes a database of basic size selective properties for different designs of conventional netting. Furthermore it could be a guidance for the use of selective devices like escape windows or grid systems to obtain optimum selectivity. Such a design guide can become a useful management tool that may help in the process of identifying the optimal gear types in specific fisheries. The FishSelect approach is faster and much cheaper than conducting traditionally selectivity experiments at sea. Hence it is possible to provide fishery managers with indicative information for those species, fisheries and towed fishing gears on which information is missing. FishSelect can not giving definitive conclusions about the selection in towed gear though and thus does not replace sea trials. But it will be a valuable help for fishing gear scientists as indicative selection parameters can reduce the number of gears needed to be tested.

Appendix A2 demonstrates the feasibility of the FishSelect methodology and simulation tool to study fundamental aspects of mesh selection of Cod (*Gadus Morhua*).

Acknowledgements

The research documented in this paper has been carried out with financial support from a project under the development programme for sustainable fishery financed by the Directorate for Food, Fisheries and Agri Business, Denmark. The support is acknowledged. A special acknowledgement to Gunnar Vestergaard and Svend Aage Larsen both from DIFRES for valuable help in designing and producing the MorphoMeter to assess cross-section shapes of fish.

Appendix A. Parametric expressions for basic mesh shapes

All the basic mesh types that we deal with in this paper are considered to be closed curves composed by straight-line segments. A Cartesian mesh coordinate system is defined with its origin at the centre of gravity of the mesh. The size and shape of each type is given by a few characteristic parameters, mesh bar lengths and/or an opening angle. The corresponding parametric expressions in polar coordinates referred to the origin at the centre are listed below. The following notation is used: The absolute value of x is written as $|x|$ and the half-open interval $x1 < x \le x2$ as $]x1; x2]$. Angles are in radians. Arctan2(y, x) denotes the complete arctan function where the signs of the arguments define the quadrant of the corresponding angle.

Diamond mesh

The diamond mesh is defined by the parameters mesh size *m* and opening angle *oa* (Fig. 6a)

$$rm(\Theta) = \frac{m}{2} \cdot \frac{\cos(oa/2) \cdot \sin(oa/2)}{|\sin(\Theta)| \cdot \cos(oa/2) + |\cos(\Theta)| \cdot \sin(oa/2)} \qquad (18)$$

$$clm = 2m$$

Square mesh

The square mesh (Fig. 6b) can be considered a special case of the diamond mesh with $a = m/2$ and $oa = \pi/2$.

$$rm(\Theta) = \frac{a}{\sqrt{2}} \cdot \frac{1}{|\sin(\Theta - \pi/4)| + |\cos(\Theta - \pi/4)|} \qquad (19)$$

$$clm = 4a$$

Rectangular mesh

The rectangular mesh is defined by two mesh bar lengths, *a* and *b*, at right angles (Fig. 6c.)

$$rm(\Theta) = \begin{cases} \dfrac{a}{2|\cos(\Theta)|} & \Theta \in \;]\arctan 2(-b,a); \arctan 2(b,a)] \\ & \quad \vee \;]\arctan 2(b,-a); \arctan 2(-b,-a)] \\ \dfrac{b}{2|\sin(\Theta)|} & \Theta \in \;]\arctan 2(b,a); \arctan 2(b,-a)] \\ & \quad \vee \;]\arctan 2(-b,-a); \arctan 2(-b,a)] \end{cases} \qquad (20)$$

$$clm = 2(a+b)$$

Symmetric hexagonal mesh

The hexagonal mesh is defined by two mesh bars length, *b* and *k*, and an opening angle, *oa* (Fig. 6d).

$$rm(\Theta)=\begin{cases}\dfrac{(b\cos(oa/2)+k/2)\cdot\sin(oa/2)}{|\sin(\Theta)|\cdot\cos(oa/2)+|\cos(\Theta)|\cdot\sin(oa/2)} & \Theta \in \left]\Psi_1;\Psi_2\right] \vee \left]\Psi_3;\Psi_4\right] \\ \dfrac{b\sin(oa/2)}{|\sin(\Theta)|} & \Theta \in \left]\Psi_2;\Psi_3\right] \vee \left]\Psi_4;\Psi_1\right] \end{cases}$$

where

$$\Psi_1=\arctan 2(-b\times\sin(oa/2),k/2)$$
$$\Psi_2=\arctan 2(b\times\sin(oa/2),k/2)$$
$$\Psi_3=\arctan 2(-b\times\sin(oa/2),-k/2)$$
$$\Psi_4=\arctan 2(b\times\sin(oa/2),-k/2)$$
$$clm=4b+2k$$

(21)

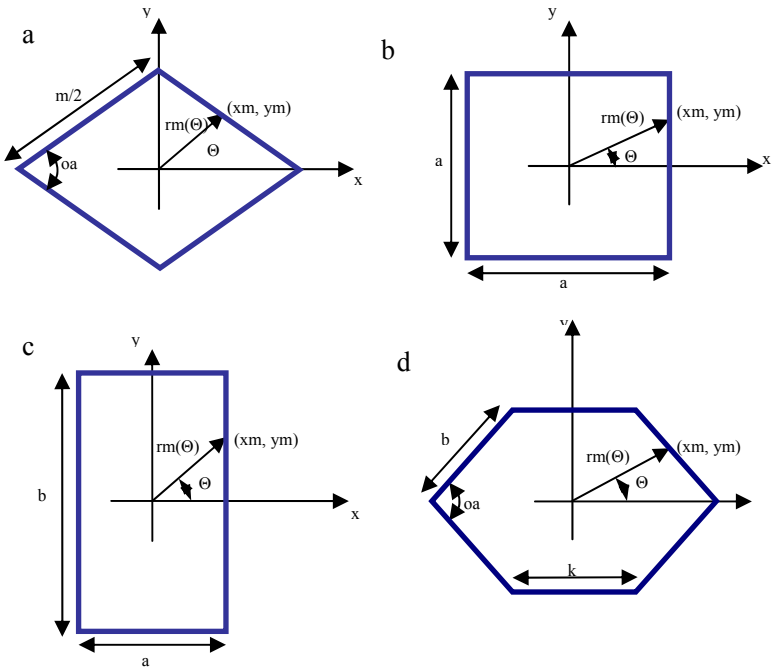

Fig. 6: Net mesh shapes.
a) Diamond mesh b) Square mesh c) Rectangular mesh d) Hexagonal mesh.

Appendix B. Parametric expressions for basic fish cross-section shapes

Elliptic cross-section

The elliptic cross-section is defined by a height, *h*, and a width, *w* (Fig. 7a).

$$rf(\Theta) = \frac{1}{2}\frac{h \times w}{\sqrt{\left(w^2 + \cos^2\Theta \times \left(h^2 - w^2\right)\right)}}$$
$$clf \approx 0.5\pi \times (h + w) \times \left(3 - \sqrt{\left(4 - \frac{(h-w)^2}{(h+w)^2}\right)}\right) \quad (22)$$

Half-ellipse cross-section

The half ellipse cross-section is composed of a half-ellipse segment and a straight-line segment and is defined by a height, *h*, and a width, *w* (Fig. 7b).

$$rf(\Theta) = \begin{cases} \dfrac{w \times h \times \left(2 \times \sqrt{\left(3h^2 \times \cos^2\Theta + w^2 \times \sin^2\Theta\right)} - w \times \sin\Theta\right)}{2 \times \left(4h^2 \times \cos^2\Theta + w^2 \times \sin^2\Theta\right)} & \Theta \in [\Psi_1; \Psi_2] \\ \dfrac{h}{2\left|\sin(\Theta)\right|} & \Theta \in]\Psi_2; \Psi_1[\end{cases}$$

where

$$\Psi_1 = \arctan 2(-h, w) \quad (23)$$
$$\Psi_2 = \arctan 2(-h, -w)$$
$$clf \approx 0.25\pi \times (2 \times h + w) \times \left(3 - \sqrt{\left(4 - \frac{(2 \times h - w)^2}{(2 \times h + w)^2}\right)}\right) + w$$

Triangular cross-section

The symmetric triangular cross-section is defined by a height, *h*, and a width, *w* (Fig.7c).

$$rf(\Theta) = \begin{cases} \dfrac{h \times w}{2w\sin(\Theta) + 4h\left|\cos(\Theta)\right|} & \Theta \in [\Psi_1; \Psi_2] \\ \dfrac{h}{2\left|\sin(\Theta)\right|} & \Theta \in]\Psi_2; \Psi_1[\end{cases}$$

where

$$\Psi_1 = \arctan 2(-h, w) \quad (24)$$
$$\Psi_2 = \arctan 2(-h, -w)$$
$$clf = 2\sqrt{\left(h^2 + 0.25 \times w^2\right)} + w$$

Symmetric trapezoid cross-section

The symmetric trapezoid cross-section is defined by a height, *h*, a bottom width, w_1, and a top width, w_2 (Fig. 7d).

$$rf(\Theta)=\begin{cases}\dfrac{h(w_1+w_2)}{2(w_1-w_2)\sin(\Theta)+4h\left|\cos(\Theta)\right|} & \Theta \in [\Psi_1;\Psi_2] \\ & \vee\ ]\Psi_3;\Psi_4] \\ \dfrac{h}{2\left|\sin(\Theta)\right|} & \Theta \in]\Psi_2;\Psi_3] \\ & \vee\ ]\Psi_4;\Psi_1[\end{cases}$$

where

$$\Psi_1=\arctan 2(-h,w_1)$$
$$\Psi_2=\arctan 2(h,w_2) \qquad (25)$$
$$\Psi_3=\arctan 2(h,-w_2)$$
$$\Psi_4=\arctan 2(-h,-w_1)$$
$$clf=2\times\sqrt{\left(h^2+0.25\times(w_1-w_2)^2\right)}+w_1+w_2$$

Asymmetric trapezoid cross-section

The asymmetric trapezoid cross-section is defined by a height, h, a bottom width, w_1, a top width, w_2 and a distance e at left(Fig. 7e).

$$rf(\Theta)=\begin{cases}\dfrac{h\times(w_2+e)}{2\times\left((w_1-w_2-e)\times\sin\Theta+h\times\cos\Theta\right)} & \Theta \in [\Psi_1;\Psi_2] \\ \dfrac{h\times(w_1-e)}{2\times(e\times\sin\Theta-h\times\cos\Theta)} & \Theta \in [\Psi_3;\Psi_4] \\ \dfrac{h}{2\left|\sin(\Theta)\right|} & \Theta \in [\Psi_2;\Psi_3] \\ & \vee\ [\Psi_4;\Psi_1]\end{cases}$$

where

$$\Psi_1=\arctan 2(-h,w_1)$$
$$\Psi_2=\arctan 2(h,2e+2w_2-w_1) \qquad (26)$$
$$\Psi_3=\arctan 2(h,-(w_1-2e))$$
$$\Psi_4=\arctan 2(-h,-w_1)$$
$$clf=w_1+w_2+\sqrt{\left(e^2+h^2\right)}+\sqrt{\left(\left(w_1-w_2\right)^2+h^2\right)}$$

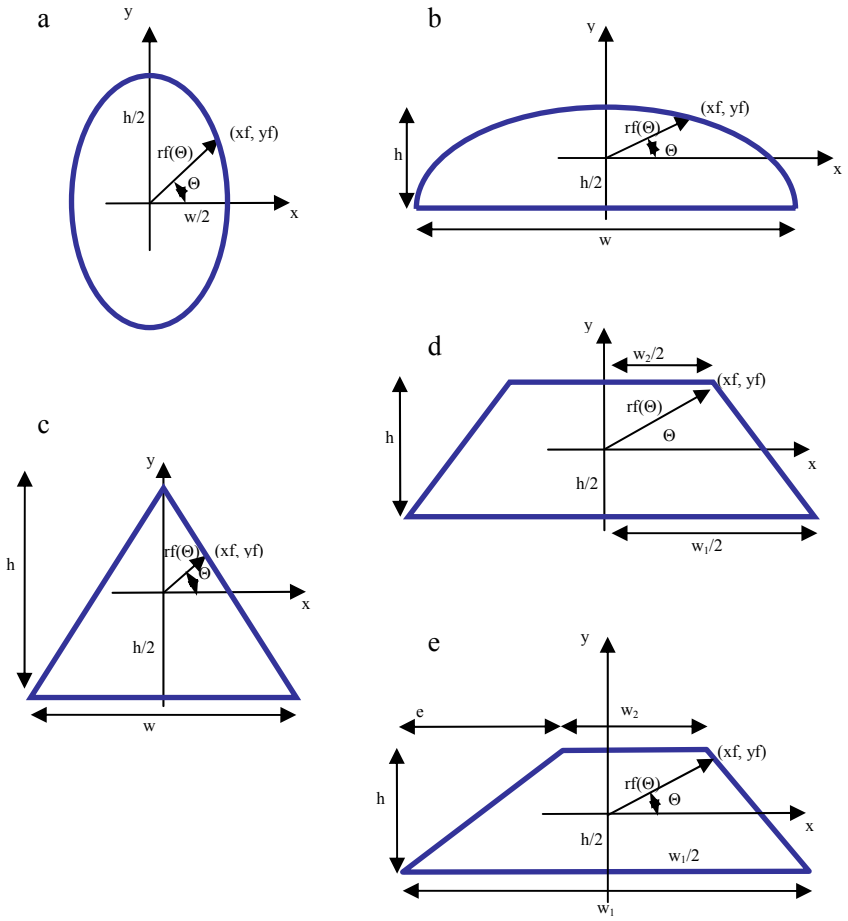

Fig. 7: Fish cross-section shapes a) Elliptic cross-section b) Half-ellipse cross-section c) Triangular cross-section d) Symmetric trapezoid cross-section e) Asymmetric trapezoid cross-section.

References

Broadhurst, M.K., Dijkstra, K.K.P., Reid, D.D, Gray, C.A., 2006. Utility of morphological data for key fish species in southeastern Australian beach-seine and otter-trawl fisheries: predicting mesh size and configuration. New Zealand Journal of Marine and Freshwater Research, Vol. 40: 259-272.

Efanov,S.F., Istomin,I.G., Dolmatov,A.A., 1987. Influence of the form of fish body and mesh on selective properties of trawls. ICES Document CM 1987/B: 13. 39pp

Glass, C.W, Wardle, C.S., Gosden, S.J., 1993. Behavioural studies of the principles underlying mesh penetration by fish. ICES Mar. Sci. Symp. 196, 92-97.

Gonzales, R.C., Wintz, P., 1987. Digital Image Processing. Addison-Wesly Publishing Company. ISBN 0-201-11026-1.

Herrmann, B., 2005a. Effect of catch size and shape on the selectivity of diamond mesh cod-ends: I Model development. Fish. Res. 71: 1-13.

Herrmann, B., 2005b. Modelling and simulation of size selectivity in diamond mesh trawl cod-ends. PhD. Thesis, Aalborg University, Denmark. ISBN 87-91200-50-4.

Herrmann, B., 2005c. Effect of catch size and shape on the selectivity of diamond mesh cod-ends: II Theoretical study of haddock selection. Fish. Res. 71: 15-26.

Herrmann, B., O'Neill, F.G., 2005. Theoretical study of the between-haul variation of haddock selectivity in a diamond mesh cod-end. Fish. Res. 74: 243-252.

Herrmann, B., O'Neill, F.G., 2006. Theoretical study of the influence of twine thickness on haddock selectivity in diamond mesh cod-ends. Fish. Res. 80: 221-229.

Herrmann, B., Priour, D., Krag, L.A., 2006. Theoretical study of the effect of round straps on the selectivity in a diamond mesh cod-end. Fish. Res. 80: 148-157.

Herrmann, B., Frandsen, R., Holst, R., O'Neill, F.G., 2007a. Simulation-based investigation of the paired-gear method in cod-end selectivity studies. Fish. Res. 83: 175-184.

Herrmann, B., Priour, D., Krag, L.A., 2007b. Simulation-based study of the combined effect on cod-end size selection of turning meshes by 90 degrees and reducing the number of meshes in the circumference for round fish. Fish. Res. 84: 222-232.

Kerman, 2002. Programming & problem solving with Delphi. Addison-Wesley, ISBN 0-201-70844-2.

Krag, L. A., Herrmann, B., Frandsen, R. P., Stæhr, K. J., Lundgren, B., Madsen, N., (Paper II). Prediction of morphological conditions for mesh penetration: II. Study of Cod (*Gadus morhua*).

Kreyszig, E., 1979. Advanced engineering mathematics. John Wiley & Sons, Inc, New York, ISBN 0-471-04271-4.

O'Neill, F.G., Herrmann, B., 2007. PRESEMO a predictive model of codend selectivity – a tool for fisheries managers. ICES journal of Marine Science, 64: 1558-1568.

Press, W.H., Flannery, B.P., Teukolsky, S.A., Vetterling, W.T., 1986. Numerical Recipes. The Art of Scientific Computing. Cambridge University Press.

Sala, A., Priour, D., Herrmann, B., 2006. Experimental and theoretical study of red mullet (Mullus barbatus) selection in codends of Mediterranean bottoms trawls. Aquatic Living Resources 19: 317-327.

Santos, M.N., Canas, A., Lino, P.G., Monteiro, C.C., 2006. Length-girth relationships for 30 marine fish species. Fish. Res. 78: 368-373.

Wiener, R.S., Wiatrowski, C., 1997. Visual object-oriented programming using Delphi. Sigs, ISBN 1-884842-60-7.

Wileman, D.A., Ferro, R.S.T., Fonteyn, R., Millar, R.B. (Editors), 1996. Manual of methods of measuring the selectivity of towed fishing gears. ICES Coop. Res. Rep. No. 215.

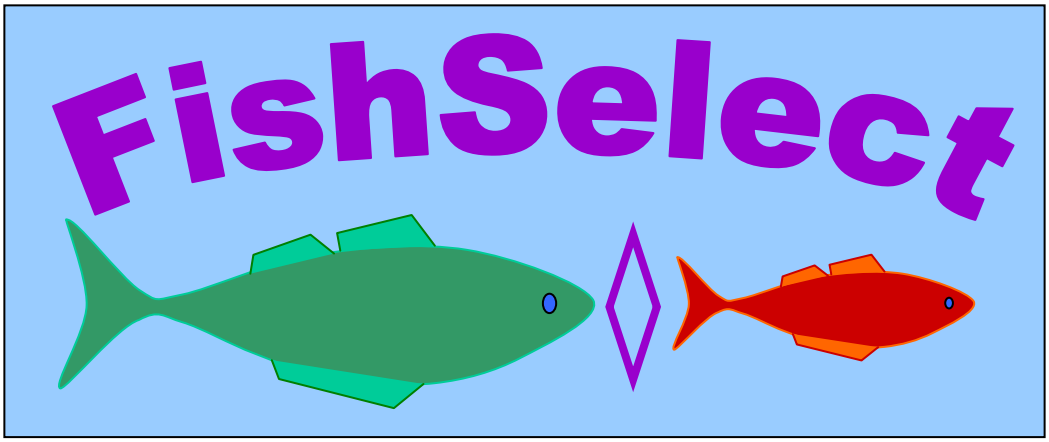

A2

Prediction of morphological conditions for mesh penetration for Cod (*Gadus morhua*)

Ludvig A. Krag, Bent Herrmann[1], Rikke P. Frandsen, Niels Madsen, Bo Lundgren, Karl-Johan Stæhr

DIFRES, Danish Institute for Fisheries Research, Technical University of Denmark, North Sea Centre, DK-9850 Hirtshals, Denmark
1: Corresponding author. Tel.: +45-3396-3204
E-mail address: bhe@difres.dk (B. Herrmann)

Abstract

Several of the cod stocks inhabiting the North East Atlantic waters are today at a critically low level. Cod is caught in most demersal fisheries both as a target species and as by-catch. We use the FISHSELECT methodology to measure the morphological parameters that determines cods ability to penetrate different mesh types and sizes. We measure and digitize selected cross-section contours along the length axis of the cod. An ellipsoid shape is fitted to the digitized cross-sections contours. The ellipsoid parameters are used in simulation software to predict mesh penetration of cod in diamond, square, rectangular and hexagonal meshes of different size. The relationship between L50 and the minimum landing sizes of cod in the North Sea and Kattegat/Skagerrak is discussed.

Keywords: Mesh penetration; Modelling; Cod; Morphology; FISHSELECT; Size selectivity

1. Introduction

The cod (*Gadus Morhua*) stocks in EC waters in the North East Atlantic have in the latest years been at a critically low level (ICES 2006). The Danish discard monitoring program has reported a considerable bycatch of undersized cod in several fisheries in Kattegat/Skagerrak and in the North Sea (unpublished data). Several technical measures have been introduced to improve the size selection (increase L50) of cod in the cod-end of towed gears.

Mesh size regulations aims at releasing undersized fish by mesh penetration and retaining marketable sizes. In a diamond mesh cod-end most fish escape through the most open meshes just in front of the catch accumulation zone and therefore escapement success is largely a function of their transverse morphology in relation to available mesh openings (Wileman et al., 1996). It is therefore important to have a mesh size and mesh opening in this part of the cod-end that will allow undersized fish to escape. An inappropriate relationship between the mesh size regulation and the minimum landing size (MLS) can lead to either an economical loss in terms of loss of marketable cod or an unwanted catch of undersized individuals, which will be discarded.

The difference in cross-section size and shape between the different species means that one mesh type may be more appropriate for some species than for other. Square mesh panels have been used to improve the selectivity of gadoids like cod (Robertson and Stewart, 1988; Tschernij et al., 1996; Madsen et al., 1999; Broadhurst, 2000; Madsen et al., 2002; Krag et al., in press), whereas diamond meshes have been found more

appropriate for flatfish species (Walsh et al., 1989; Fonteyne and M'Rabet, 1992; Tokac et al 1998; Madsen et al., 2006).

The usefulness of different mesh sizes and configurations in commercial fishing has largely been determined by trial-and-error experiments and by the commercial availability of materials and mesh sizes (A1). A better starting point for improving selection might be to first quantify the general morphological relationships for the key species and then use this information to estimate appropriate sizes, shapes, and/or configurations of meshes (Broadhurst et al., 2006). In previous studies fish morphology has been quantified by linear relationships between various morphological features, especially including girth measures, in both static gear (Stergiou and Karpouzi, 2003; Santos et al., 2006) and towed gear (Tosunoglu et al., 2003; Broadhurst et al., 2006; Tosunoglu., 2007). In the current study we have measured the morphology of cod, relevant for mesh penetration in towed fishing gear by applying the FISHSELECT methodology (A1). In EC-waters in the North East Atlantic diamond mesh netting is primarily used for the construction of towed fishing gear. Square mesh cod-ends are also used in Swedish waters in conjunction with a selection grid (Valentinson and Ulmestrand 2007), but the use of square meshes in gear design is primarily restricted to insertion of smaller square mesh netting panels in diamond mesh trawls to improve the size selection of e.g. gadoids. In this study we have investigated the selective properties of diamond and square meshes that are commercially used today. The examination has been extended to hexagonal and rectangular meshes to include others than those legally used in the North Sea and Kattegat/Skagerrak area today (EC. Reg. No. 850/98).

2. Material and methods

2.1 Fish used

Since it is live individuals that penetrate cod-end meshes during commercial fishing, we wanted to conduct our measurements on fish that are as fresh as possible. Several physiological processes, which may change the cross-section contours, start as soon as the fish dies. A total of about 150 cod were therefore caught by jigging and gillnets in Skagerrak in February, just prior to the experiment, and transferred alive to holding tanks on land. Seventy-five cod in the length range from 29-72 cm were selected and used in the experiment (Fig. 1).

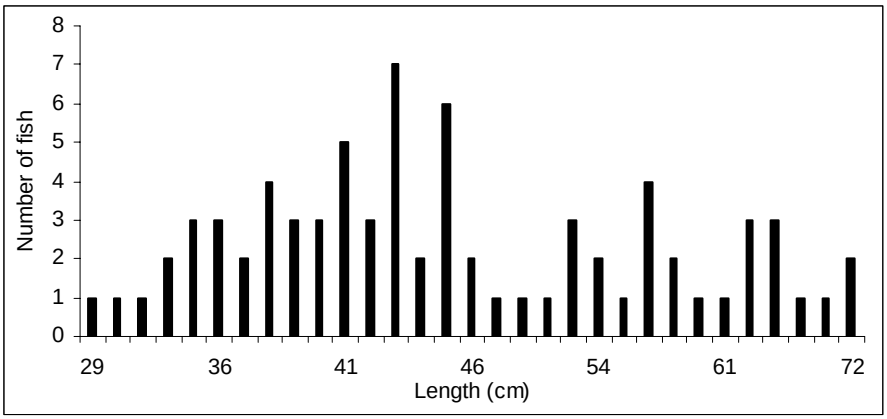

Fig 1. Length distribution of the cod used in the experiment.

Five fish at the time were taken from the holding tank and killed immediately before the measurements by a strong solution of *Ethylene-glycol-mono-phenyl-ether* ($C_6H_{10}O_2$) commonly used to anaesthetize fish. Each fish were given a unique identification number and their length and weight data was recorded. In addition to the 75 fish used in the full-scale experiment about 10 fish were used in initial experiments.

2.2 Initial experiments

Initial examination was made to identify where along the cods length axis the cross-section contour should be measured. These experiments involved both fall-through experiments and measurements of cross-sections. Both these procedures are described below. Two cross-sections (CS) were identified for cod, CS1 and CS2, where CS1 contained the maximum width and CS2 the maximum height and girth of the fish (Fig. 2A).

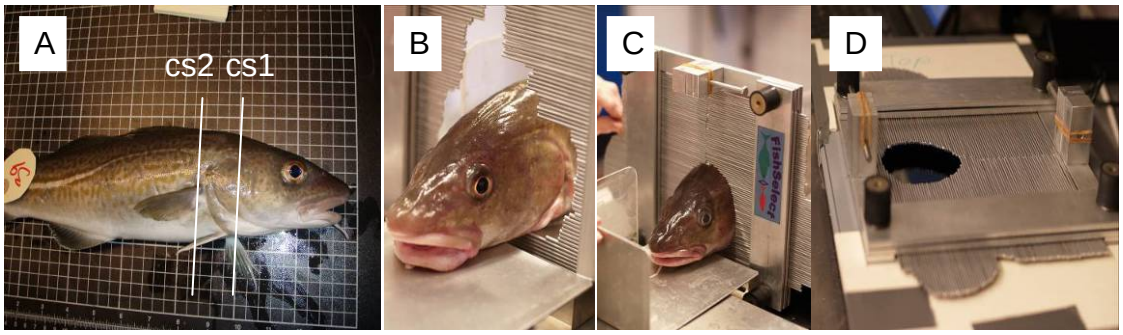

Fig 2. Position of CS1 and CS2 on cod and measurement and scanning of a cross section shape (CS1) with the mechanical sensing tool MorphoMeter.

2.3 Measurement of cross-section contours

The mechanical sensing tool (MorphoMeter) described in Herrmann et al. (A1) was used to measure cross-sections of cod with the following procedure. All the sensing sticks of the tool are moved manually into contact all the way around the circumference of the fish (Fig 2B and 2C). After that they are fixed by tightening the assembly screws (black

knobs in Fig. 2C). The whole assembly is then scanned with a flatbed scanner (Fig. 2D) and the contour extracted with the image analysis functionality in the FISHSELECT software (A1).

2.4 Estimation of cross-section shape

The edge detection software tool in FISHSELECT was used to extract and digitize the cross-sections from the MorphoMeter. Typically this resulted in a contour that was digitized at about 120 points along the perimeter. To reduce the number of parameters needed to describe the cross-sections contours, one of five different basic shapes were fitted to the points (A1). The shapes were an ellipsoid, a half ellipsoid, a triangle, a symmetric trapezoid or an asymmetric trapezoid. The selected contour shape was then fitted to the single sensing sticks measuring points based on a smoothing technique which puts less weight on points far from the mean contour. This makes the method more robust, since single point outliers will have less effect on the final shape.

Morphological relationships, describing the expected cross-section parameter values and expected variance for a fish population of the investigated species, were then established by fitting length based regression functions ($w, h = aL^b$) to the data for both CS1 and CS2, where , w = width, h = height and L = length.

2.5 Fall-through experiments

Fall-through experiments were conducted with 118 different stiff mesh templates cut out as holes in 4-5 mm thick plastic plates. Stiff mesh templates are used because we assume that the strong hydrodynamic forces acting on cod-ends in towed gear results in a high tension in the mesh bars, which makes it unlikely that a fish can distort the mesh shape, when it attempts to pass through (A1). Four different mesh types (diamond-, square-, rectangular- and hexagonal meshes) were used in the fall-through experiment (see Fig. 3 and summary of mesh types, sizes and opening angles in Table 1.).

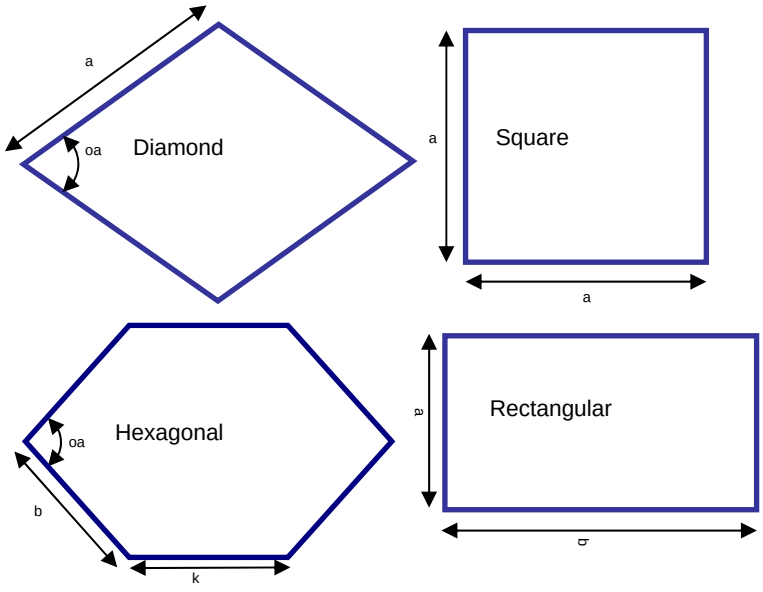

Fig 3. Mesh types used in the fall through experiments (diamond-, square-, rectangular- and hexagonal meshes).

Mesh type and OA	Size (mm)																		
	10	15	20	30	35	40	50	60	70	80	90	100	110	120	130	140	160	180	200
Diamond																			
15																	x	x	x
20												x	x	x	x	x	x		
25											x			x			x		
30										x	x			x			x		
35											x			x			x		
40											x			x			x		
45											x			x			x		
50											x			x			x		
55										x	x	x	x	x	x	x	x	x	x
60											x			x			x		
65											x			x			x		
70											x			x			x		
75											x			x			x		
80											x			x			x		
85										x	x	x	x	x	x	x	x	x	x
90											x								
Square																			
									x	x		x		x		x	x	x	x
Rectangular																			
	b	b	b	b			b		b		a			a					a
Hexagonal																			
143.6					x	x	x	x	x	x		x							
128.3					x	x	x	x	x	x		x							
106.3					x	x	x	x	x	x		x							
88.9					x	x	x	x	x	x		x							

Table 1. The 118 different mesh templates used in the fall through experiments. Mesh size and the meshes opening angle is given. For diamond and square meshes x refers to meshsize (two times a in Fig. 3). The hexagonal meshes in the table are only given by two parameters. The mesh bar (b) in this study is given as k/2 for all hexagonal meshes. For hexagonal meshes x refers to k. For rectangular meshes all combinations of a and b are made. For example for bar length b=10 mm three different meshes are made: a= 90, 120 and 200. a and b refers to bar lengths (Fig. 3).

In this experiment we used b = k/2 for all hexagonal meshes. Each fish was held by the tail and lowered to each of the 118 mesh templates head first. The template plates were kept horizontal and each fish was rotated optimally for fall-through at each mesh template. Only the force of gravity was used to pull them through (Fig 4). The result in terms of fall-through or not was recorded for each fish and template.

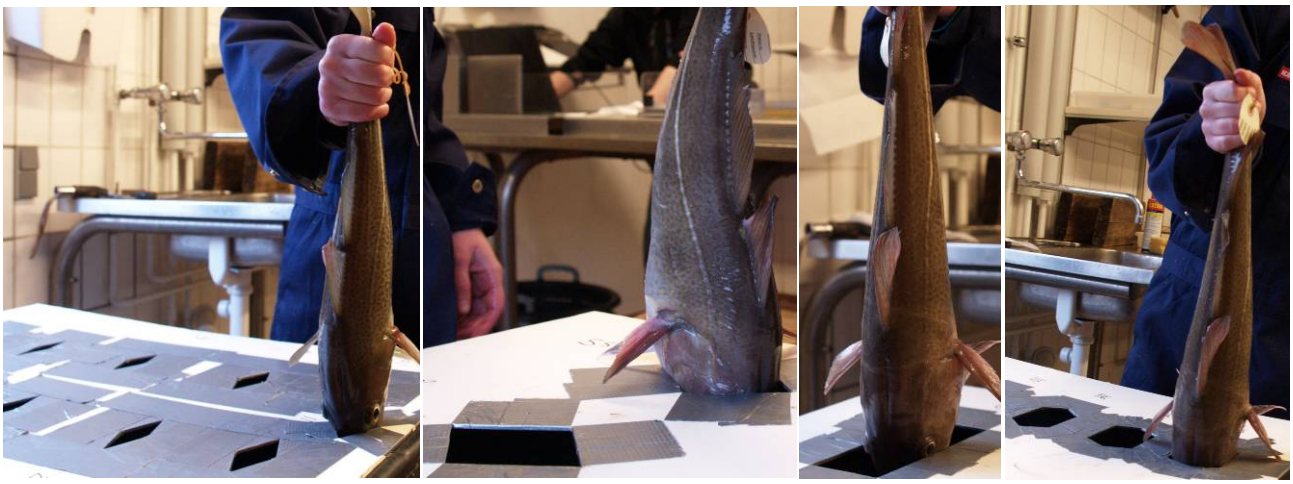
Fig 4. Fall through experiments with different mesh templates.

A total of 8850 fall-through tests were performed with the 75 cod and the 118 mesh templates used in this study.

2.6 Repeated experiments

The reliability of the results of the above experiments requires that the cross-section measures are not too much affected by the extensive handling and mechanical contact with the mesh templates. Three subsequent fall-through trials with all the 118 mesh templates were therefore conducted with two fish. The lengths of the two fish were 46.6 cm and 42.5 cm. On a third cod were the cross-sections contours of CS1 and CS2 also measured both before and after a complete fall-through trial. Cross-section measures were otherwise always done before the fall-through experiments to have the fish as fresh as possible. Finally were CS1 and CS2 measured ten subsequent times on one cod to estimate the accuracy to the MorphoMeter.

2.7 Selection of mesh penetration model

In addition to determine, which cross-sections that might be decisive for the ability of cod to penetrate different meshes, the results of the fall-through trials also indicated how much the body shape of the cod could be compressed during penetration of a stiff mesh. During the fall-through experiments it was observed that if the cod first got its head through the mesh template, then the entire fish went through with relative ease. Consequently, we began the fall-through simulations by checking only CS1, which is located on the head of the fish (Fig 2A), in the penetration criterion, when searching for the best mesh penetration model. Simulations, which checked the criterion for CS2 alone or the two cross-sections combined (CS1-CS2), were however also performed. For each simulation the degree of agreement (DA) between experimental and simulated results was calculated (A1). The DA value will vary between 0 and 100%, where 100% is full agreement between the experimental and the simulated results. The initial simulations assumed symmetric compression levels in the range from 0-25% for CS1 and 0-35% for the softer CS2. Compression is here defined as the fish ability to deform its cross-section contour during a stiff mesh penetration with the pull of gravity. Comparison with the

fall-through experiments, however, indicated that a more asymmetric compression may take place during a mesh penetration. CS1 on the head of the fish contains both soft muscle tissue and harder bony structures from the cranium which is likely to be compressed differently during a mesh penetration. Based on results from simulations with simple asymmetric (and symmetric) compression of CS1 with a compression range of 0-20% for width and height a quadratic regression model the following form was made:

$$DA = q_0 + q_1 \times CW + q_2 \times CH + q_3 \times CW^2 + q_4 \times CH^2 + q_5 \times CW \times CH \qquad (1)$$

where CW = compression width, CH = compression height and the q's are the regression constants.

The model was fitted to the DA-data using the lm-function in the statistical freeware package R (version 2.4.0). The fitted model was then used to construct iso-DA curves versus compressions in height (x-axis) and width (y-axis).
The penetration models including CS2 were only based on symmetric compression since we did not have the same basis for assuming asymmetric compression as for CS1. Finally we investigated if including criteria for a combination of the two cross-sections can improve the penetration models further in terms of increasing the DA value. Besides predicting if the mesh penetration conditions are fulfilled or not for a particular fish, the simulations also produce a scaling factor (SF), which predicts how close the conditions are from being just fulfilled for each penetration attempt. The distribution of the SF values for the cases, where the model prediction contradicts the fall-through results of the experiment, depends on how good the model is. The number of values and the symmetry of the distribution indicate if we assume too much or too little compression of the fish cross-sections during the simulations. For conflicting results SF should be close to 100%, meaning that the difference between the simulation results and the experimental fall-through results is small. The compression model that produces the highest DA value is chosen. A high DA value also indicates that we have been able to identify, which morphological features that needs to be measured.

2.8 Design guides

When the penetration model has been established, predictions about the basic selective properties, L50 and SR, for the five different mesh types (see Fig. 3) are made with varying mesh sizes and opening angles (oa). To predict the basic selective properties for different netting designs the FISHSELECT simulation software accepts an input combination including an array of properties of a virtual fish population, the parameters of the penetration model and the parameters of the mesh configurations. The established relationships between fish length, the cross-sections parameters and their random variations are used to define the properties of the fish in the virtual population, which is generated by drawing 2000 samples randomly from a uniform size distribution to ensure that we have a sufficient number of fish in the entire selective range of all the investigated meshes. The length range of this population was 2 to 80 cm. Design guides are produced that outline the selective properties of a wide range of mesh sizes of diamond, square, rectangular and hexagonal meshes.

2.9 Comparison with experimental results

For comparison with our simulations published results from two relevant single hauls using a 109 mm cod-end with 104 open meshes around the circumference have been used (Galbraith, 1994). The estimated selectivity parameters (cm) were L50 = 29.2, SR = 6.8 and L50 = 28.4, SR = 8.5 for 1500 kg and 1330 kg catch weights respectively. This gives a mean catch weight of approximately 700 kg half way through the catch build-up process. In addition the covered cod-end results presented in Dahm et al., (2002) for 43, are relevant for comparison with our simulated results. A 94.6 mm and a 95 mm cod-end, both with 100 open meshes in the circumference, were used in the two experiments, respectively.

The range of mesh openings in the cod-end were estimated based on data from the calculations in Herrmann et al. (2007). Figure 11 shows the variation of the mesh opening angles with catch weight at different distances from the catch build-up edge. We assume that cod do their last escape attempt uniformly distributed during the catch build-up process. Based on these calculations a realistic full range of mesh openness during the catch build-up is 15 to 65 degrees with a mean value of the mesh opening of approximately 35 degrees.

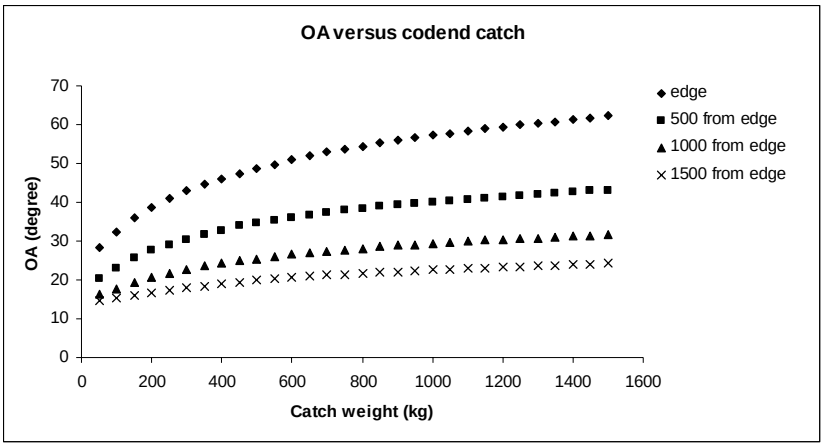

Fig. 11. Calculated opening angles (oa) from Herrmann et al., (2007) versus codend catch weights at four different distances in mm from the catch edge (edge) in the codend.

3. Results

3.1 Cross-section description

Of the five basic cross-section shapes tested the best fit statistic was obtained with the ellipsoid shape fitted to the cross-section contour of cod for both CS1 and CS2. Examples of digitized cross-sections with fitted ellipsoids are given in Fig 5.

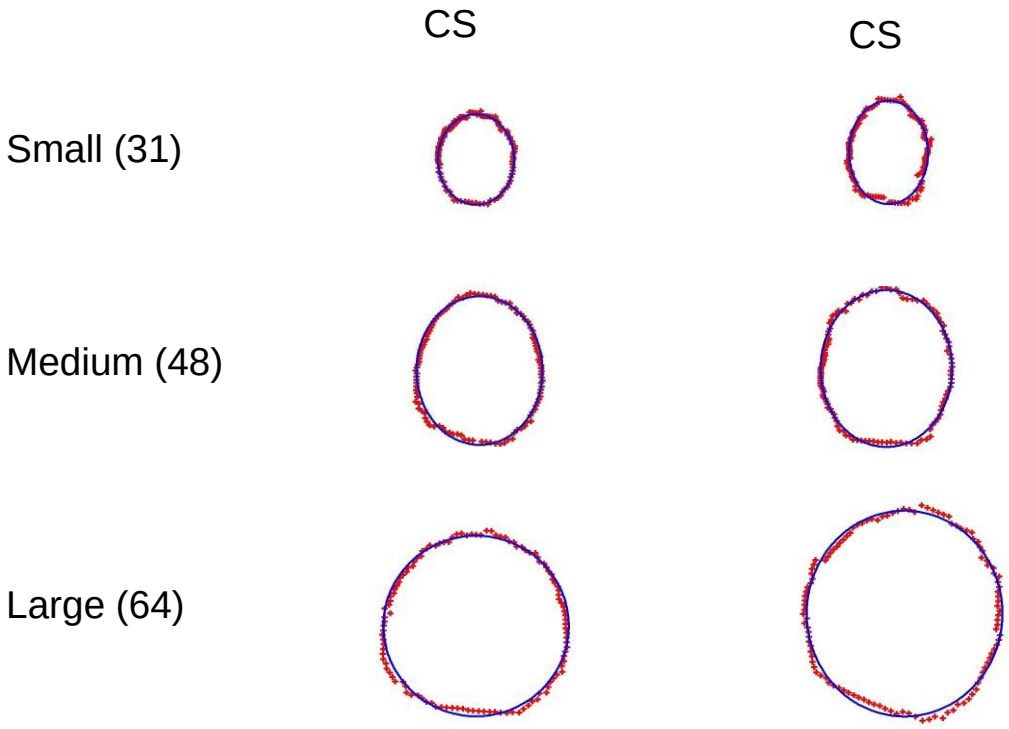

Fig 5. Examples of digitized cross sections with fitted ellipsoids for small, medium and large cods.

Length based regressions for both the width and height of the ellipsoids fitted to CS1 and CS2 are given in Fig. 6.

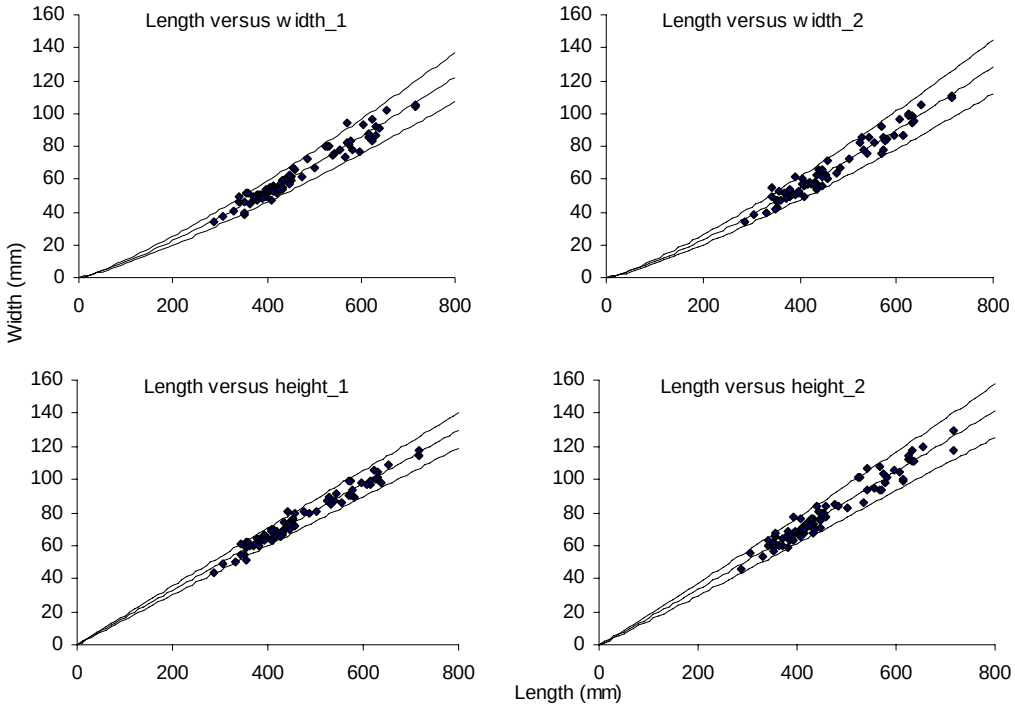

Fig 6. Length based regressions for width and height of the ellipsoids fitted to the cross section contours for CS1 (left) and CS2 (right).

3.2 Repeated measures

The variation between the ellipsoids fitted to the repeated measurements (see 2.6) obtained with the MorphoMeter was largest on the width measurement (Table 2) where 95% of the results are within ±5.3% of the mean corresponding to 2 times the standard deviation.

	CS1		CS2	
no	Width	Height	Width	Height
1	59.00	67.65	64.98	75.85
2	58.44	67.43	65.9	75.21
3	60.67	66.26	64.13	76.54
4	58.42	67.59	65.19	76.23
5	56.46	67.08	64.26	76.95
6	58.48	67.68	66.99	73.06
7	55.71	66.18	65.42	75.67
8	58.26	65.89	65.34	76.2
9	57.36	65.48	65.93	75.22
10	55.91	67.53	66.06	75.28
Mean	57.87	66.88	65.42	75.62
sd	1.53	0.84	0.86	1.07

Table 2. Width and height measures of the ellipsoids fitted to CS1 and CS2 for ten repeated measurements conducted on one fish. sd = standard deviation.

There were no deviations in the fall-through results for the first of the two examined cod in the three repeated fall-through trials. The second cod was however retained by one mesh template in the second run, while it fell through in both the first and third run. This result implies that the cod cross-sections are not affected noticeably by the extensive fall-through trials. This is further supported by the measurements of the cross-sections both before and after the fall-through trials. The dimensions of CS1 were: h = 67.84 mm and w = 57.02 mm before fall-through trials and h = 68.4 mm and w = 55.44 mm afterwards. For CS2 it was: h = 71.74 mm and w = 55.18 mm before fall-through trials and h = 71.96 and w = 57.48 after. The deviations are less than 5% and therefore within the repeated measuring accuracy as mentioned in beginning of this section.

3.3 Penetration model

All terms in the cubic DA-regression model (1) were found to be highly significant (P less than e-6). The R-square value for the model fit was 99.4%. The DA-values obtained for penetration models using only CS1 are shown as iso-DA curves in Fig 7.

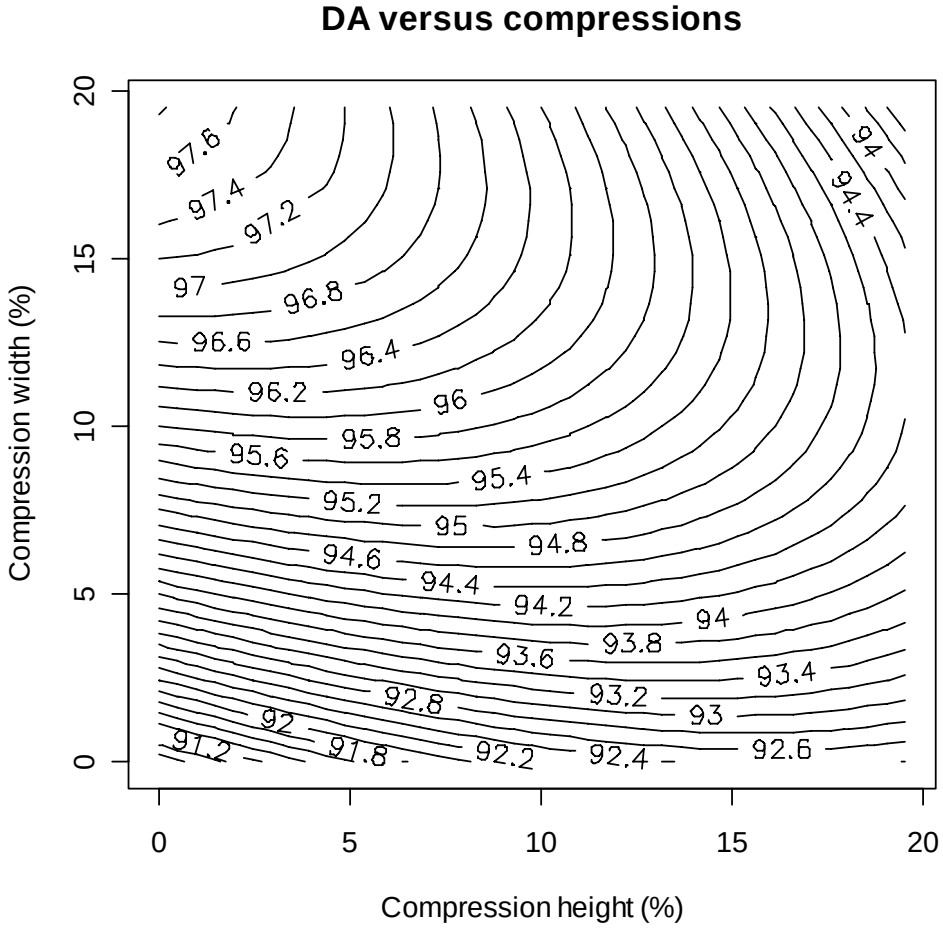

Fig. 7. Iso-DA curves versus compression of width and height of the ellipsoids fitted to CS1. The line at a 45 degrees angle from (0, 0) represents symmetrical compression.

The highest value 97.6% is obtained for a model compressing the height 0% and the width 18% (Model H0W18). The best result with penetration models using only CS2 was a DA-value of 95.7%. For the 312 tested penetration models with combinations of CS1 and CS2 the best DA-values were identical to the best found for models using CS1 alone (97.6%). This, however, required at least 32% compression of CS2, making its fitted ellipsoid become smaller than the compressed ellipsoid of CS1. CS1 will therefore alone determine the mesh penetration of cod. The ellipsoids fitted to the measured cross-section contours and those assumed for the best penetration model for both CS1 and CS2 are shown in Fig. 8.

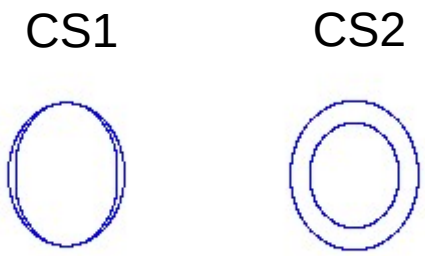

Fig. 8. Elliptical cross section of CS1 and CS2 (outer ellipsoids) fitted to the measured cross sections and cross section shape where this ellipsoid is compressed according to the optimal penetration model found for each cross section (inner ellipsoid).

The uncompressed and compressed ellipsoids fitted to CS1 are shown in different mesh types in Fig. 9.

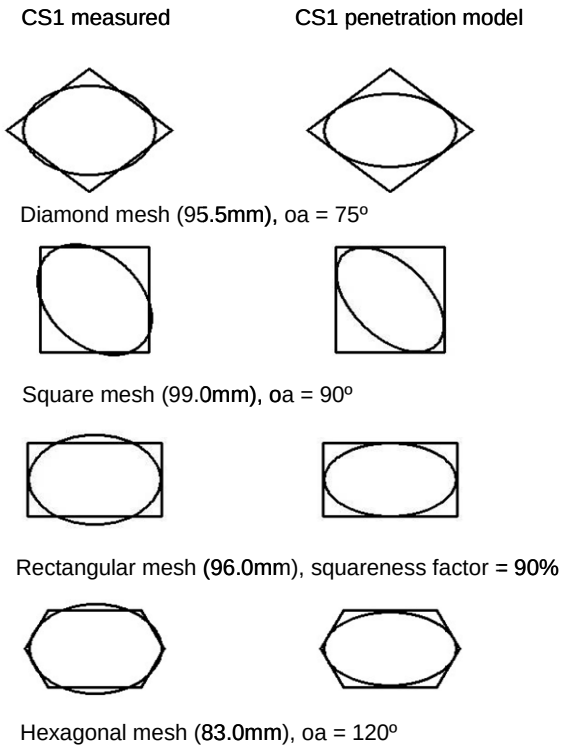

Fig. 9. The optimal mesh configurations of the four examined mesh types through which the compressed ellipsoid (W18H0) can pass through (right). The measured ellipsoid of CS1 is shown in the same meshes (left). The ellipsoid to a 40 cm cod is used.

As mentioned above the results of the fall-through experiments indicate that the width of CS2 can be compressed by more than 30% under the given conditions, becoming smaller than the width of CS1 despite the larger cross-section measures of CS2. With a model using an uncompressed approximation (stiff00) of cross-section CS2, based on the measured dimensions alone, the length of cod that can penetrate a given mesh would certainly have been underestimated. This effect is illustrated by the distributions of the SF values shown in Fig. 10.

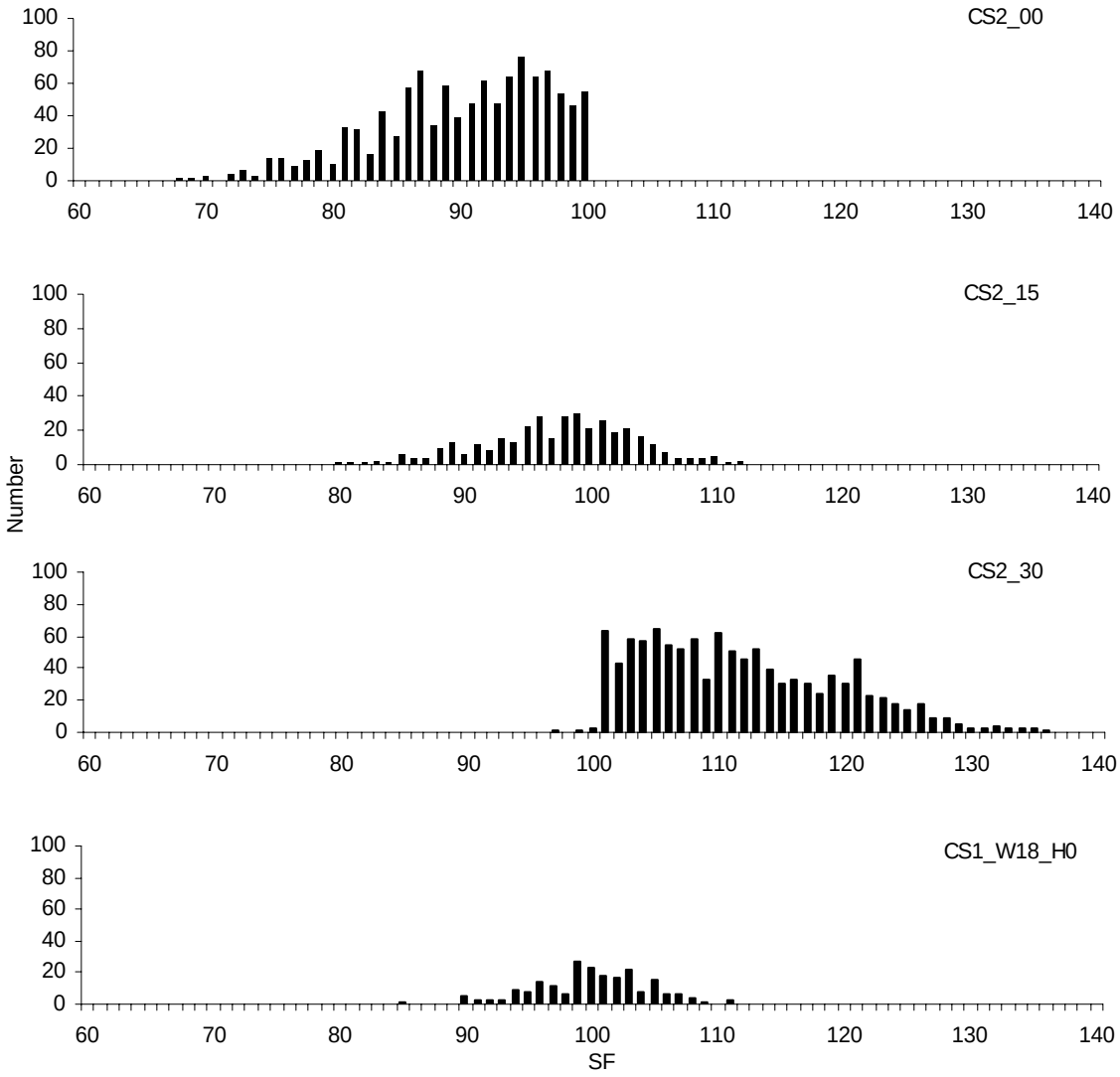

Fig 10. Distribution of scaling factor values (SF) for different penetration models of CS1 and CS2. CS2_0 = 0 compression on the ellipsoid fitted to the measurements of CS2. CS2_15 and CS2_30 correspond to 15% and 30% symmetric compression on the ellipsoid fitted to the measurements of CS2. CS1_W18_H0 = 18% compression on the width and 0% on the height on the ellipsoid fitted to the measurements of CS1. CS1_W18_H0 is the penetration model with the highest DA value.

The disagreement (1 – DA) is reduced from 12.2 % to 2.4 %, approximately a factor of 5, when changing penetration model from CS2_00 to our model with CS1 (H0W18). The above results show that the FISHSELECT method is sensitive to the quality of the approximations on the penetration model.

3.4 Comparison with experimental data

With the mean value of 35 degrees, mentioned in 2.9, as a basis point we have simulated the influence on the selectivity process of increasing the range of mesh

openness uniformly distributed in various angle intervals around 35 degrees for a preliminary prediction of the selectivity parameters for a 110 mm mesh panel (Table 3).

Range of oa distribution (degrees)	L50 (cm)	SR (cm)
35	28.85	1.49
30_40	28.92	3.23
25_45	28.79	4.95
20_50	28.43	6.85
20_55	29.55	7.38
15_60	29.03	9.06
10_65	28.40	10.83
15_55	28.03	8.71
20_65	31.31	7.95
Soft	46.46	1.74

Table 3. Morphological based predictions of L50 and SR with different distributions of the opening angle (oa) in a 110 mm codend with 100 meshes in the circumference made in double 4mm PE. The oa distribution is assumed to be uniform.

The value of SR (L75-L25) increases as a consequence of increasing the mesh oa range. The results in Table 3 (L50, SR versus mesh oa) show that realistic predictions of the selectivity parameters are obtained simply by using a reasonably wide range of values of mesh oa. The L50 value in Dahm et. al., (2002) varies between 24.61 cm and 33.47 cm in the first experiment and between 22.45 cm and 35.22 cm in the second experiment. Use of the range between 15 and 65 degrees corresponds to L50 values up to about 34 cm (Fig 13). There is a relatively large variation in the SR-values in Dahm et al., (2002) but for most of the hauls in agreement with the value of about 9, which we find for the 15_65 degree mesh opening range (Table 3). This result supports the stiff mesh assumption, which is further strengthened by the unrealistic selection parameters obtained when applying a soft mesh model (selection curve Fig 12 right). This would mean that the mesh could be fully distorted and penetration success therefore only would be restricted by the mesh perimeter. Both the number of meshes around the cod-end circumference and the mesh oa in the cod-end (correlated parameters) would have no effect on the cod-end selection contrary to experimental evidence (Reeves, 1992; Galbraith, 1994).

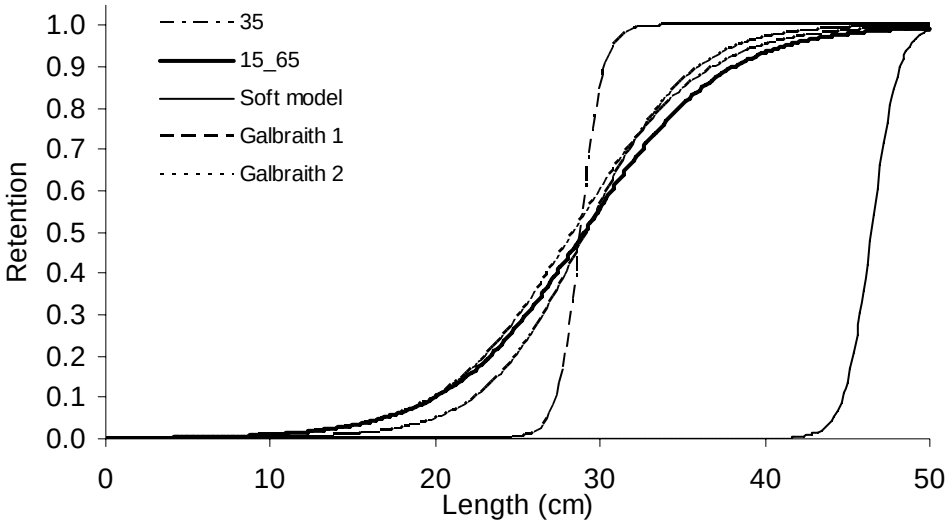

Fig 12. Simulated selections curves with different assumptions on oa (35 and 15_65) and experimental selection curve (Galbraith 1 and 2 from Galbraith et al., (1994). A soft model allowing full mesh distortion is also included.

3.5 Design guides

Design guides predicting basic selective properties for cod for each of the four mesh types have been generated based on the penetration model with CS1 W18_H0. The results for L50 are shown as iso-L50 curves of simulated L50 versus mesh size and oa for diamond mesh in Fig. 13, versus squareness and mesh size for rectangular meshes in Fig. 14 and versus oa and bar length for hexagonal meshes in Fig. 15. Since the square mesh can be considered a special case of the other types, those data are already included in the diamond mesh design guide (for oa = 90 degree), the rectangular mesh design guide (for squareness factor = 100%) and finally in the hexagonal mesh design guide (for oa = 180 degree). For a square mesh with a bar length of 100 mm across L50 has a value of about 70 cm (top right corners in Fig 13-15). Note that the L50 values in the diamond, rectangular and hexagonal design guides are much less sensitive to changes in the mesh size (x-axis) in the lower half of the oa range than in the upper range(Fig 13-15). A maximum L50 value is reached with an oa at about 75º for a diamond mesh (Fig. 13). For rectangular meshes the maximum is reached with a squareness factor of about 90% (Fig.15). Maximum L50 values are reached for hexagonal meshes with an oa at about 120º (Fig. 15). For cod this is the highest value for any mesh size of the four mesh types examined. The difference in optimum mesh size is quantified for a 40 cm cod in Fig. 9.

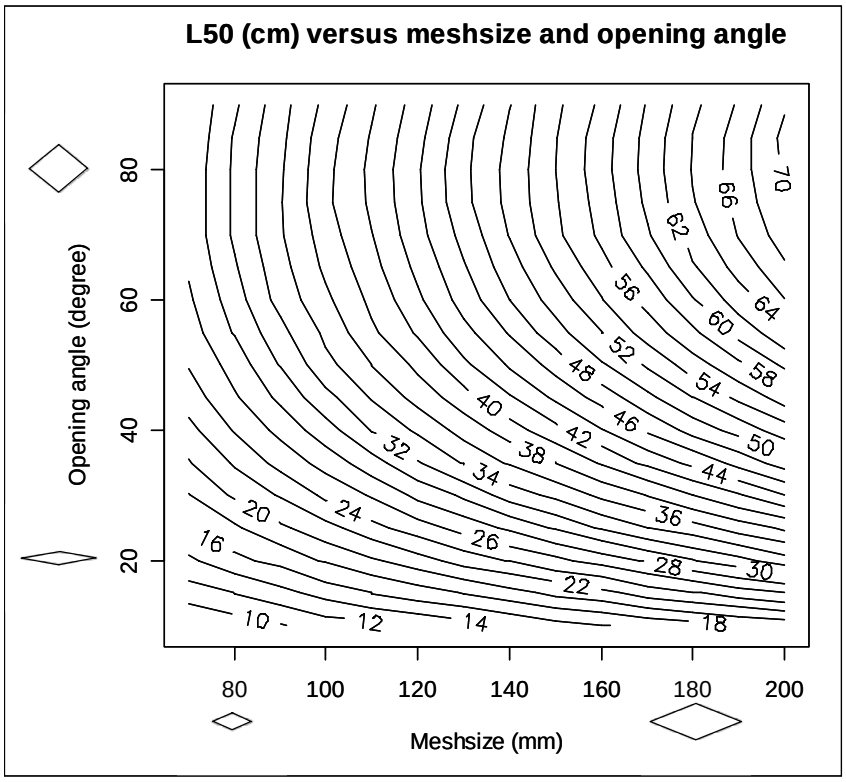

Fig 13. Iso-L50 curves as a function of mesh size (mm) and mesh opening angle (oa) in degrees. The right side of the plot (oa = 90 degree) corresponds to square meshes.

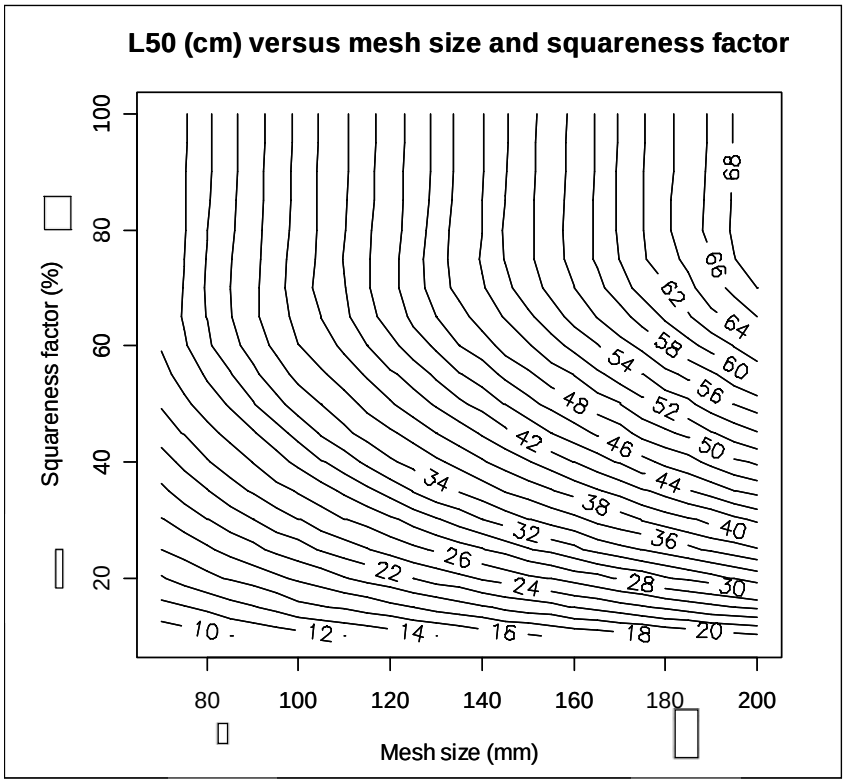

Fig 14.Iso-L50 curves as a function of bar length (mm) and squareness factor (%). The right side of the plot (squareness factor = 100%) corresponds to square meshes.

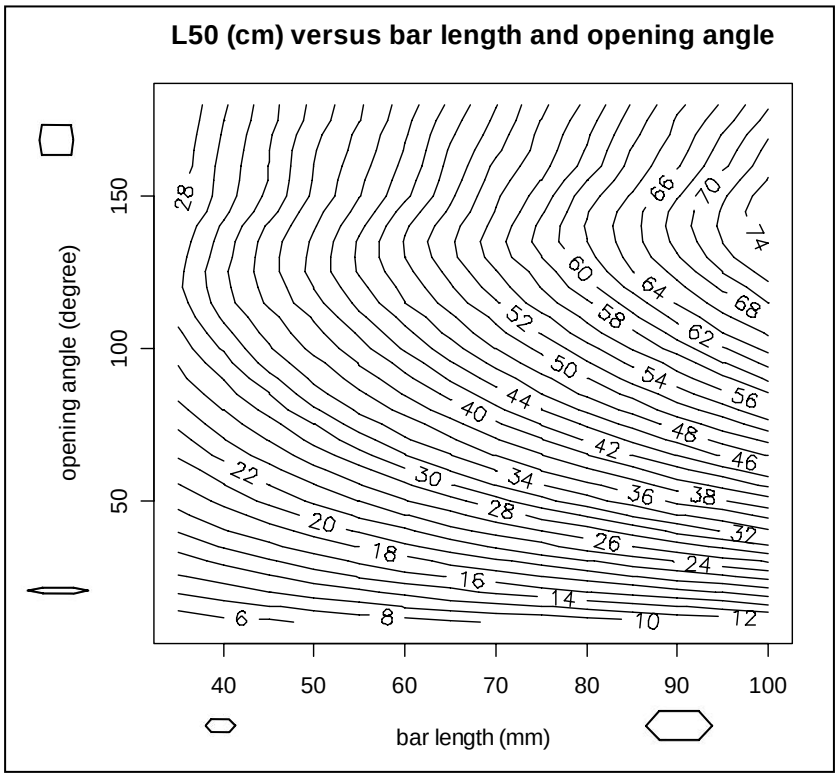

Fig 15. Iso-L50 curves as a function of bar length (mm) and opening angle (oa) in degrees. The right side of the plot (oa = 180 degree) corresponds to square meshes.

4. Discussion

With the FISHSELECT methodology we have found and measured the cross-section contours that physically will limit the ability of cod to penetrate different mesh configurations. Based on the measurements of CS1 we establish a penetration model that explains 97.6% of the results obtained during the fall-through experiments. The less explanatory (95.7%) penetration model, based on criteria using the larger measure of CS2, demonstrates that a maximum girth measure even with its associated dimensions (height and width) is an inadequate measure. In static gear as trammel nets or gill nets, where the low tension and the thin twine makes the mesh more easily distorted by the fish, the girth measure may be more relevant than in towed gear. The relatively large difference between the stiff and the soft mesh penetration model (Fig.12) demonstrates that the morphological (physical) conditions for mesh penetration is likely to be quite different between towed gear and static nets.

Of the main design features of a diamond mesh cod-end mesh size has the most significant effect upon fish size selection (Reeves et al., 1992). Using square mesh netting or shortening the selvedge ropes along a diamond cod-end has been shown to increase L50 for demersal round fish (Robertson and Stewart, 1988; Isaksen and Valdemarsen, 1990). Experiments with square mesh cod-end have resulted in narrower selection ranges

(SR) for cod and haddock (*Melanogrammus aeglefinus*) (Robertson and Stewart, 1988; Reeves et al., 1992; Halliday et al., 1999; He, 2007) which may be related to the fact that square meshes change shape less than diamond meshes during fishing operation (Robertson and Stewart, 1988; He, 2007). We observe a larger effect on the L50 estimates when increasing the mesh sizes in the upper half of the design guides (Fig. 13-15) than in the lower half. Since experimental results indicate that mesh size is the important parameter for the size selection of cod this agrees well with an assumption of relatively open meshes. Herrmann et al., (2007) theoretically found that the realistic variation in oa during a catch build-up was 15 to 65 degrees for 110mm diamond mesh cod-end. The conditions for mesh penetration will therefore vary considerably during the catch build up process. The largest retention length and the most narrow size selection for cod are obtained if the fish is exposed to a mesh configuration that resembles the contour of CS1 in the cod-end and if this configuration is kept constant during the fishing process. The design guides (Fig. 13-15) shows that there is a large potential for improving the size selection by keeping the meshes open and Fig. 9 shows the potential in using other mesh types than diamond and square meshes in cod-ends.

Mesh type alternatives to the diamond mesh should be investigated as the diamond mesh is not the optimal mesh configuration to size select cod with. The hexagonal mesh is the mesh with the greatest resemblance with the contour of CS1. Square mesh panels are widely used in Kattegat/Skagerrak and the North Sea today to improve the selection of gadoids (EC Reg. 859/98; 15238/04; 2187/05; 51/06). Panels of hexagonal mesh will according to this study improve the L50 compared to a square mesh used in the panels today.

Cod is often caught in mixed species fisheries along with several other species with different cross-section shapes. If the cod-end mesh configuration is optimized for cod alone it may result in unintentional effects on the selection of other species that contributes substantially to the total catch value in the fishery. Design guides produced with the FISHSELECT methodology predicting size selection for the major economical catch components in a fishery will allow quantitative multi-species considerations, where the consequences for each catch component can be estimated for each mesh design strategy. The possibilities and the limitations of size selection in a given fishery can be indicated.

We used gravity to simulate the force a fish uses to penetrate a mesh. This approximation acknowledges that a large fish has better swimming capabilities than smaller fish, but we do not know how closely this approximates the *in-situ* penetration force of cod. The reasonable agreement with experimental results obtained during commercial fishing (Galbraith, 1994; Dahm et al., 2002) may however justify the gravity approximation in addition to the stiff mesh approximation for cod.

We measured on cod caught in February, which is within the spawning season. The batch of cod examined contained some larger fish with relatively well developed gonads which may well affect the measured dimensions of CS2. The compression level of CS2 indicated by the fall-through experiments is however so high that CS1 still determines, whether or not the cod can pass through a given mesh and the development of gonads does not affect CS1. Seasonal morphological variation in terms of somatic or gonadal growth therefore appears to have little effect on at least the biophysical conditions for mesh penetration for cod. On the other hand, the mechanical stress inflicted on the fish,

when the fish is compressed considerably during a mesh penetration, could affect its ability to survive.

The Danish MLS for cod in the North Sea and in Kattegat/Skagerrak has with effect from the 1. January 2008 been harmonised with the EC MLS. The MLS is reduced from 40 cm to 35 cm in the North Sea, where a 120 mm cod-end is primarily used. In Kattegat/Skagerrak, where a 90 mm cod-end is used, MLS is reduced from 35 cm to 30 cm. This adjustment of the MLS is introduced to obtain a better balance between MLS and the 50 % retention length (L50) in the commonly used gears. An average oa of about 50 degrees is needed to obtain an L50 value of 30 cm for a 90 mm diamond mesh (Fig. 13). This would again require a cod-end catch weight of about 600 kg (Fig. 11). Instead of increasing the nominal cod-end mesh size or reducing the MLS an optimal and more constant oa in the cod-end meshes would provide a less variable size selection independent of the catch build-up process. Means to reduce the variation in oa during a tow could investigate the use of different mesh types like square and rectangular which only have tension in the longitudinal bars. Further could mechanisms that can control the tension in the cod-end meshes e.g. lastrigde ropes or panels in be investigated for diamond mesh codends.

The information given in the design guides will allow gear designers and managers to get a quick overview of the theoretical selectivity to various different netting designs. Designs can be optimized theoretically with relatively low cost, before they are tested practically in expensive sea trials. It is however important that gear designs are tested at sea before design parameters are fixed, e.g. by introduction into the legislation, since gear selectivity is affected by parameters like fish behaviour, vessel size, ground gear, sea state (Wileman et al., 1996), which cannot be accounted for in the FISHSELECT simulations. But use of the morphological data collected and the mesh penetration models developed during the project can be integrated into more complete predictive cod-end selection models like PRESEMO (Herrmann, 2005).

5. Acknowledgements

The research documented in this paper has been carried out with financial support from a project under the development programme for sustainable fishery financed by the Directorate for Food, Fisheries and Agri Business, Denmark.

References

Anon, 1979. Reports of the ICES Advisory Committee on Fisheries Management, 1978. ICES Coop. Res. Rep. 85, 157 pp.

Broadhurst, M.K., 2000. Modifications to reduce by-catch from prawn-trawls: a review and framework for development. Reviews in Fish Biology and Fisheries, 10, 27- 60.

Broadhurst, M.K., Dijkstra, K.K.P., Reid, D.D., Gray, C.A., 2006. Utility of morphological data for key beach-seine and otter-trawl fisheries: predicting mesh size and configuration. New Zealand Journal of Marine and Freshwater Research, 40, 259-272.

Dahm, E., Wienbeck, H., West, C.W., Valdemarsen, O'Neill, F.G., 2002. On the influence of towing speed and gear size on the selective properties of bottom trawls. Fish. Res. 55:103-119.

Fonteyne, R., M'Rabet, R., 1992. Selectivity experiments on sole with diamond and square mesh codends in the Belgian coastal beam trawl fishery. Fish. Res. 13, 221–233.

Galbraith, R.J., Fryer, R.J., Maitland, K.M.S., 1994. Demersal pair trawl cod-end selectivity models. Fish. Res. 20: 51-58.

He, P., 2007: Selectivity of large mesh trawl cod-ends in the Gulf of Maine I. Comparison of square and diamond mesh. Fish. Res. 83:44-59.

Herrmann, B. 2005. Effect of catch size and shape on the selectivity of diamond mesh cod-ends I. Model development. Fish. Res. 71:1-13.

Herrmann, B., O'Neill, F. G., 2005. Theoretical study of the between-haul variation of haddock selectivity in a diamond mesh cod-end. Fish. Res. 74, 243-252.

Herrmann, B., O'Neill, F. G., 2006. Theoretical study of the influence of twine thickness on haddock selectivity in diamond mesh cod-ends. Fish. Res. 80, 221-229.

Herrmann, B., Priour, D., Krag, L.A. 2007. Simulation-based study of the combined effect on cod-end size selection of turning meshes by 90° and reducing the number of meshes in the circumference for round fish. Fish. Res. 84, 222-232.

Herrmann, B., Lundgren, B., Krag, L.A., Frandsen, R.P., Madsen, N., Stæhr. K. A1. Prediction of morphological conditions for mesh penetration: 1. Development of methodology.

ICES, 2006. Report of the ICES Advisory Committee on fishery Management, Advisory Committee on the Marine Environmental and Advisory Committee on Ecosystems, 2006. ICES Advice. Books 1 – 10. 6, 310 pp.

ICES, 2005. ICES Advisory Committee on Fishery Management Working Group Advice for 2005, 1.4.2 cod in Subarea IV (North Sea), Division VIId (Eastern Channel), and Division IIIa (Skagerrak).

Isaksen, B., Valdemarsen, W, J., 1990. Selectivity in codends with short lastrigde ropes. ICES CM 1990/B:46.

Krag, L. A., Frandsen, R. P., Madsen, N., In press. Evaluation of a simple means to reduce discard in the Kattegat-Skagerrak Nephrops (Nephrops norvegicus) fishery: Commercial testing of different codends and square-mesh panels. Fish. Res.

Madsen, N., Moth-Poulsen, T., Holst, R., Wileman, D., 1999. Selectivity experiments with escape windows in the North Sea *Nephrops* (*Nephrops norvegicus*) trawl fishery. Fish. Res. 42, 167–181.

Madsen, N., Holst, R., Foldager, L., 2002. Escape windows to improve the size selectivity in the Baltic cod trawl fishery. Fish. Res. 57, 223–235.

Reeves, S.A., Armstrong, D.W., Fryer, R.J., Coull, K.A., 1992. The effect of mesh size, cod-end extension length and cod-end diameter on the selectivity of Scottish trawls and seines. ICES J. Mar. Sci. 49, 279-288.

Robertson, J.H.B., Stewart, P.A.M., 1988. A comparison of size selection of haddock and whiting by square and diamond mesh codends. J. Cons. Explor. Mer. 44, 148–161.

Santos, M.N., Canas, A., Lino, P.G., Monteiro., 2006. Length-grith relationship for 30 marine fish species. Fish. Res. 78, 368-373.

Stergiou, K.I., Karpouzi, V.S., 2003. Length-grith relationships for several marine fishes. Fish. Res. 60, 161-168.

Tokac, A., Lok, A., Tosunoglu, Z., Metin, C. Ferro, R.S.T., 1998. Cod-end selectivities of a modified bottom trawl for three species in the Aegean Sea. Fish. Res. 39, 17–31.

Tosunoglu, Z., Ozbligin, Y,D., Ozbilgin, H., 2003. Determination of the Appropriate Hanging Ratio to Ease the Escape of Juvenile Red Mullet (*Mullus barbatus* L., 1758) and Annular Sea Bream (*Diplodus annularis* L., 1758) from a Trawl Codend. Turk. J. Vet. Anim. Sci. 27, 1193-1199.

Tschernij, V., Larsson, P.-O., Suuronen, P., Holst, R., 1996. Swedish trials to improve selectivity in demersal trawls in the Baltic cod fishery, 1994–1995. ICES-CM-1996/B:21.

Valentinson, D., Ulmestrand, M., 2007. Species selective Nephrops trawling: Swedish grid experiments. Fish. Res. In Press.

Walsh, S.J., Cooper, C., Hickey, W., 1989. Size selection of plaice by square and diamond mesh cod-ends. ICES CM 1989/B.22.

Wileman, D.A., Ferro, R.S.T.., Fonteyne, R and Millar, R.B., 1996. Manual of methods of measuring the selectivity of towed fishing gears. ICES Cooperative Research Report, no. 215, 126p.

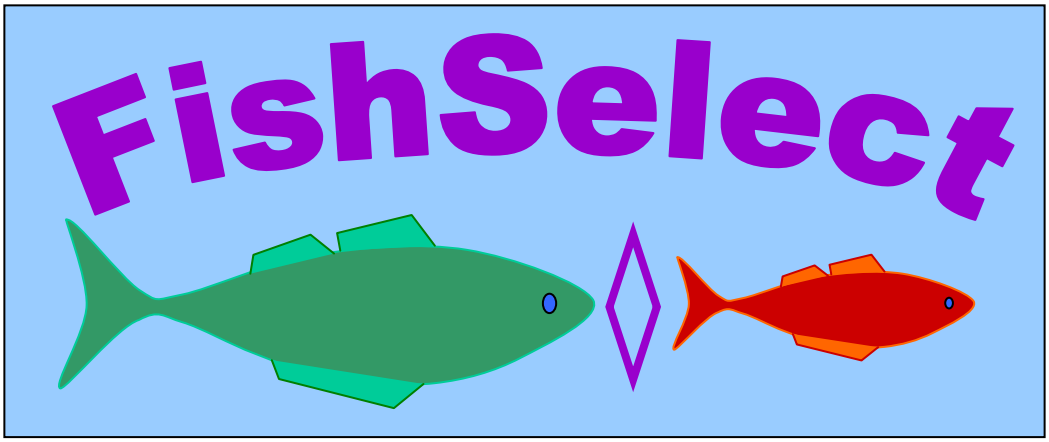

A3

Prediction of codend selectivity based on the interaction between mesh configuration and fish morphology: III. Study of Plaice (*Pleuronectes platessa*)

Rikke P. Frandsen[1], Bent Herrmann, Ludvig A. Krag, Bo Lundgren, Niels Madsen, Karl-Johan Stæhr

DTU aqua, Institute for aquatic resources, North Sea Science Park, DK-9850 Hirtshals, Denmark
1: Corresponding author. Tel.: +45-3396-3270
E-mail address: rif@difres.dk (R. P. Frandsen)

Abstract
Plaice is caught in demersal fisheries both as target species and as by-catch. For a sustainable exploitation of a resource like plaice, choice of netting that optimizes catches and minimizes discards is important. In mixed species fisheries, this is a complex process resulting in a trade off between catches and discards of the different species. FISHSELECT is a simulation tool that makes it possible to predict the selective properties of a netting panel prior to testing at sea. In the present study we use the FISHSELECT methodology to identify the morphological characteristics and corresponding cross-sections of plaice that are expected to affect the selective properties in different mesh sizes and types. The simulations are validated against selective parameters obtained in field experiments.

Keywords: mesh penetration; modeling; Plaice; *Pleuronectes platessa*; fish morphology; FISHSELECT; selectivity

1. Introduction

It is well established that the interaction between shape of the mesh and cross section shape of the fish is a main factor in determining the selective properties of a codend. During the last decades, the consequences of this interaction have been investigated in experiments comparing the selective properties of diamond mesh codends versus square mesh codends. These studies find that square mesh codends are more selective for round fish species but less selective for flat fish species. The reason for the difference in selective properties of diamond and square meshes is argued to be linked to the morphology of the fish (e.g. Clark, 1963; Efanov et al., 1987; Fonteyne and M'Rabet, 1992; Madsen et al., 2006).
When compared to diamond mesh codends with the same mesh size, a square mesh codend is thus found to have a larger length at 50% retention (L50) and lower selection range (SR) for several species of round fish e.g. cod (*Gadus morhua*) and haddock (*Melanogrammus aeglefinnus*) (e.g. Cooper and Hickey, 1989; Halliday et al., 1999). This effect was also observed by Thorsteinsson (, 1992) who, in a catch comparison experiment, found square mesh codends to reduce by-catch of small herring (*Clupea harengus*), capelin (*Mallotus villosus*) and whiting (*Merlangius merlangus*). For flatfish however, L50 is found to be lower in a square mesh codend than in a diamond mesh codend with the same mesh size. This effect has been documented for: yellowtail flounder (*Limanda ferruginea*), American plaice (*Hippoglossoides platessoides*), witch flounder (*Glyptocephalus cynoglossus*) and winter flounder (*Pseudopleuronectes americanus*) (He, 2007; Simpson, 1989; Walsh et al., 1992). While the effect of mesh shape on L50 of flatfish is unambiguous, there is no clear tendency for the effect on SR (He, 2007; Simpson, 1989; Walsh et al., 1992).
FISHSELECT is a novel methodology where morphological features relevant for mesh penetration are identified and linked to the selectivity of different mesh configurations (Herrmann et al (A1)). The method improves the understanding of the interaction between the fish and the netting panels

and it provides estimates on the selective properties of codends prior to testing at sea. The present study focus on plaice (*Pleuronectes platessa*) on which published selectivity data are sparse.
We use the FISHSELECT to theoretically estimate selectivity of plaice in codends made up of mesh shapes used today (diamond and square) as well as alternative mesh designs in order to identify the most advantageous nettings for this species.

2. Materials and methods

2.1 Laboratory experiments

In February 2007, plaice were collected by use of gill nets in Skagerrak. During the following laboratory experiments, the plaice were kept in tanks where mortality was low. Only live, undamaged fish were used in the experiments. When they were removed from the tanks, they were killed in a solution of *ethylene-glycol-mono-phenyl-ether* commonly used for anaesthetization of fish.

Templates, plates with holes simulating 118 different mesh types, were used in the penetration experiments (see Herrmann et al. (A1)). The mesh shapes examined were diamond, square, rectangular and hexagonal and for each shape and size, they were laid out with a series of different openings in order to reflect the mesh configurations expected to be found in a codend (Table 1). The templates used, follow the descriptions in Krag et al. (A2). Note that a square mesh is considered the same as diamond mesh with 90 degree opening angle.

Table 1. Mesh sizes and opening angles investigated. Definition of opening angle is outlined in Herrmann et al (A1)

	Diamond	Hexagonal	Rectangle
Number of meshes	64	36	18
Min mesh size	77.7	69.8	100.4
Max mesh size	200.4	200.6	273.0
Min opening angle	14.4	86.1	90.0
Max opening angle	90.0	180.0	90.0

Besides length, weight and gender, three cross-sections (CS1, CS2 and CS3) were measured on each fish with the MorphoMeter (see Fig 2 and description in Herrmann et al. (A1)). The position of each of the cross sections was based on experience from initial experiments, where the parts of the fish, that might prevent mesh penetration, were identified. CS1 is positioned on the highest point of the head. CS2 by the anal spine and CS3 at position with the maximum width of the body excluding the fins (Fig. 1). The length of the fish was measured to the nearest millimeter below.

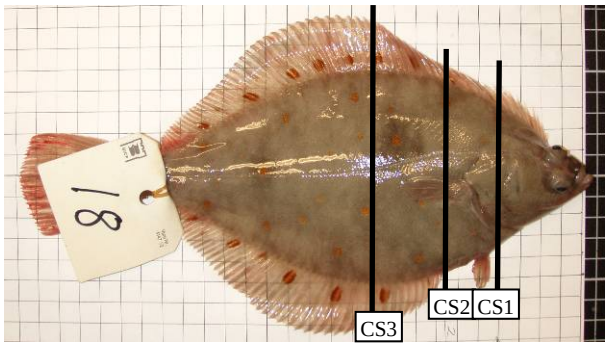

Fig. 1. Picture of plaice with position of the three cross sections shown.

Fig. 2. Plaice in MorphoMeter. CS1 is being measured.

In the penetration experiments, the templates were placed horizontally and it was tested whether the fish, could pass through a given mesh or not under the force of gravity. Fish were oriented head down and turned to the optimal orientation with the highest chance of penetration (Fig. 3). The pass through experiments complies with the methodology outlined by Herrmann et al. (A1).


Fig. 3. Penetration experiment. Plaice in a hexagonal mesh. Note the deforming fins.

2.2 Data analysis

Each cross section outlined by the MorphoMeter was scanned and the contour extracted with the image analysis function in the FISHSELECT software tool. To reduce the number of parameters needed to describe the shape of the cross-section, five geometric shapes were fitted to the contour data; an ellipsoid, a half ellipsoid, a triangle, a symmetrical trapezoid and an asymmetrical trapezoid. Each CS was fitted to all geometric shapes and the mean difference between each geometric shape and the outline in question was averaged over all fish. Depending on the geometric shape, the outlines of the cross-sections are thus described by a limited number of parameters, and we establish a relationship between these parameters and the length of the fish.

As outlined in the FISHSELECT protocol (Herrmann et al. (A1)), a series of penetration models with different degrees of compression of the different cross-sections, possible exclusion of fins as well as inclusion and exclusion of cross-sections, were tested. The models are used to simulate whether fish from the experiment will be able to pass through the meshes in the templates or not. In order to identify the best model, simulated results are held against the experimental results and the degree of agreement (DA) is established. DA ranges from 0 - 100% agreement between the model and the experimental results.

2.3 Validation of the penetration model

Selection parameters from field experiments were used to validate the chosen penetration model and to justify its use for predicting selectivity of a real codend. Unfortunately, selection data are sparse on plaice and to our knowledge data from just two studies are accessible (Allan, 2006 (bottom trawl experiment); van Beek et al., 1981 (beam trawl experiment)). Besides these data, we have unpublished otter trawl data on selection of plaice in a nominal 70 mm square mesh codend and a nominal 90 mm diamond mesh codend. To validate the penetration model we simulate the selective properties of these codends and compare the output with the estimates obtained in the field. With regards to fish, we use the relationships between fish length and cross-section parameters to produce a virtual population of 2000 plaice with stochastically varying cross-section shapes as outlined in Herrmann et al. (A1).

2.4 Production of a design guide

To predict the basic selective properties for different netting designs, we used the virtual population of fish created in section 2.3. In the FISHSELECT software, simulations were carried out for a series of mesh configurations by using the properties of these fish combined with the penetration model. The output of this exercise is a design guide that contains expected basic selective properties both of the nettings used today and of other designs that might have a potential in future fisheries.

3. Results

A total of 70 plaice measuring 18-46 cm were investigated (see size distribution in Fig. 4). Of these, 56 were females and 4 were roe fish.

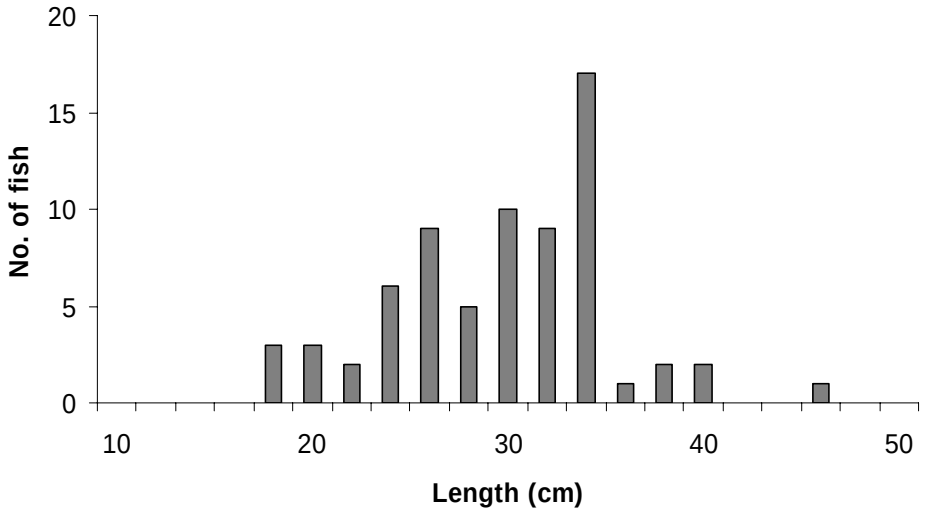

Fig. 4. Length distibution of fish used in the penetration experiment

3.1 Cross-section shape

Mean difference between the outlines of the cross-sections and the 5 geometric shapes ranged from 0.42 to 3.02 mm (Table 2). CS1, CS2 and CS3 all had the highest resemblance (mean difference at 0.42, 0.50 and 0.65 mm respectively) with an asymmetric trapezoid. The asymmetric trapezoid is therefore used to describe the shape of the cross-sections in the following analyses.

	CS 1	CS 2	CS 3
ELL	 mean diff. 1.42 sd mean diff. 0.07	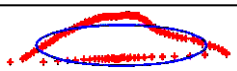 mean diff. 1.74 sd mean diff. 0.08	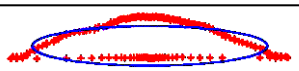 mean diff. 3.02 sd mean diff. 0.17
HEL	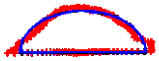 mean diff. 0.63 sd mean diff. 0.02	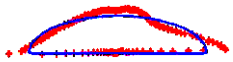 mean diff. 0.79 sd mean diff. 0.02	 mean diff. 1.62 sd mean diff. 0.06
TRI	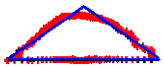 mean diff. 0.82 sd mean diff. 0.05	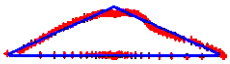 mean diff. 0.86 sd mean diff. 0.05	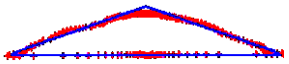 mean diff. 0.98 sd mean diff. 0.04
TRA	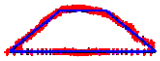 mean diff. 0.52 sd mean diff. 0.02	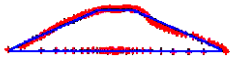 mean diff. 0.58 sd mean diff. 0.04	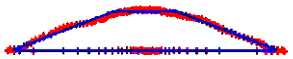 mean diff. 0.73 sd mean diff. 0.02
ATR	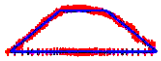 mean diff. 0.42 sd mean diff. 0.03	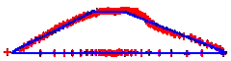 mean diff. 0.5 sd mean diff. 0.04	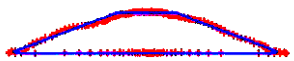 mean diff. 0.65 sd mean diff. 0.04

Table 2. The three cross-sections (CS1, CS2 and CS3) fitted to five geometric shapes; ellipsoid (ELL), half ellipsoid (HEL), triangle (TRI), symmetrical trapezoid (TRA) and asymmetric trapezoid (ATR). Mean difference (mm) between the geometric shape and the outline in question, averaged over all fish is shown together with the standard deviation (sd)(mm) of the estimate.

3.2 Morphological relationships

The asymmetric trapezoid can be described by four parameters: *W1*, *W2*, *h* and *e* (Fig. 5). Parameter data were plotted versus fish length (*l*), and for each cross section a power function of fish length was fitted to parameter data (Fig. 6). For the relationships between length and parameters *W1* and *h*, the power function fitted data well with R^2 above 0.75. Parameters *W2* and *e* are sensitive to actual shape and more variable and values of R^2 are therefore lower.

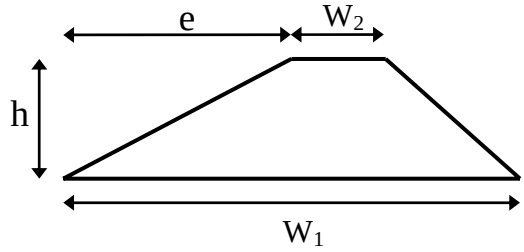

Fig 5. Parameters describing the assymetric trapezoid

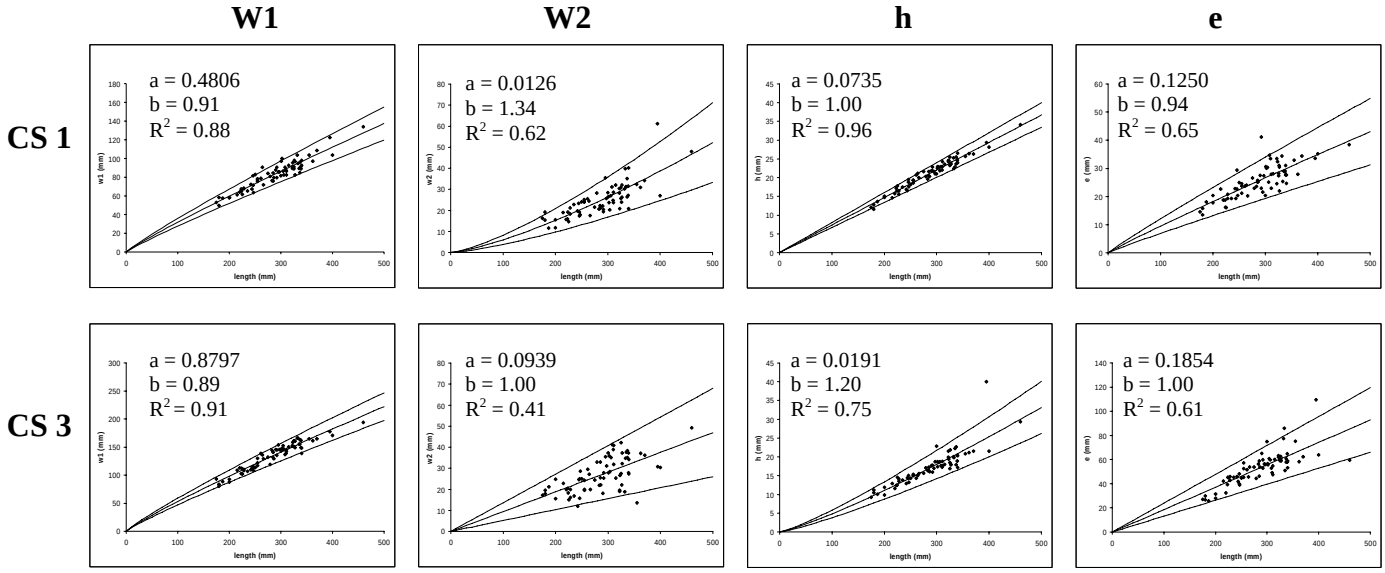

Fig. 6. Morphological relationships between length (l) of fish and cross-section parameters assuming an assymetric trapezoid shape. A power function ($x = a \bullet l^b$) was fitted to data. The functions are plotted (solid lines) and the 95% confidence limits are indicated (dotted lines).

3.3 Penetration experiment

Results from the penetration experiment make up a matrix of 8260 cells, each indicating success or failure for a given fish to penetrate a given mesh. Data was checked and 8 obviously erroneous results were replaced by question marks. They were handled as missing values in the data matrix in the following analysis.

During the penetration experiment, it was experienced that, depending on the opening angle and shape of the mesh, the height of the head was the limiting factor in some cases, whereas the width and height of the body was limiting in other cases. Furthermore, the fins were found to be highly deformable and the fish body tended to curve slightly perpendicularly to the spine. Information on height and width can be extracted directly from the three cross-sections while different modes of compression of the cross-sections can be used to simulate features like body curving and deformable fins.

3.4 Identification of the best penetration model

An initial screening of a broad range of compression modes was performed as a first step in the search for the best penetration model. Each fish from the experiment is described by three asymmetric trapezoids representing the three cross sections. In the penetration models, each of the three cross sections were assigned one of four levels of compression along the width axis (w-axis) ranging from 0% to 60%. The same levels were used for compression along the height axis (h-axis)

and finally areas of the trapezoids were cut away, where the nominal height (*h*) was below one of four levels from 0% to 75%. This cropping of the pointed parts of the trapezoid is equivalent to ignoring the fins or other soft parts.
The FISHSELECT fall-through simulation program was then run in order to test various models including one to three cross-sections, all subjected to the levels of compression and cropping described above. The results of the simulations for each model were compared to the experimental results and DA was quantified (Table 3). When using only one cross-section to predict, whether a fish will penetrate a mesh or not, the highest DA (94.4%) is found for CS3. This indicates that in most cases, mesh penetration is determined by the maximum width of the fish. Combining CS3 with CS1 increases DA to 96.2% indicating that in some cases, the height of the head is limiting mesh penetration. Including all three cross-sections, only increases DA with 0.07 %. It is therefore concluded that most of the information relevant for mesh penetration that can be extracted from the cross sections CS1 and CS3.

DA	CS1	CS2	CS3
CS1	78.2 %	-	-
CS2	93.1 %	92.1 %	-
CS3	96.2 %	95.9 %	94.4 %

Table 3. Degree of agreement (DA) between simulation of mesh penetration and results from the penetration experiment. The simulations include information on CS1, CS2 and CS3 alone or in combination obtained in the initial screening.

The penetration models that take both CS1 and CS3 into account were sorted with regard to DA. This revealed that highest DA's were obtained with no compression along the h-axis of CS1 and no compression along the w-axis of CS3. In order to find the best penetration model, the levels of compression and cropping of both CS1 and CS3, were increased. The best penetration model had a DA of 96.8% and was obtained with the following combination:
CS1: 40% compression on the w-axis, zero compression on the h-axis and cropping areas of the trapezoid where height is less than 70% of h (Fig. 8A).
CS3: Zero compression on the w-axis, 25% compression on the h-axis and cropping areas where height is less than 22% of h (Fig. 8B).
The robustness of this model was supported by the fact that small changes in degree of cropping and compression of either CS1 or CS3 only resulted in minor changes in DA. An investigation of DA's obtained with the different mesh shapes further confirms the robustness of the model since variation in DA between the shapes is low (diamond: DA=96.5%, hexagonal: DA=97.0% and rectangle: DA=96.9%).

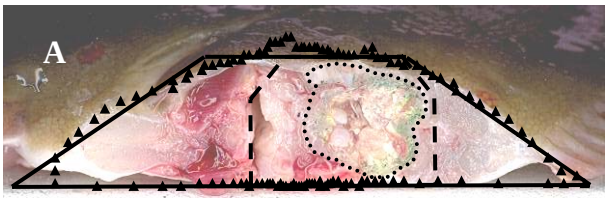

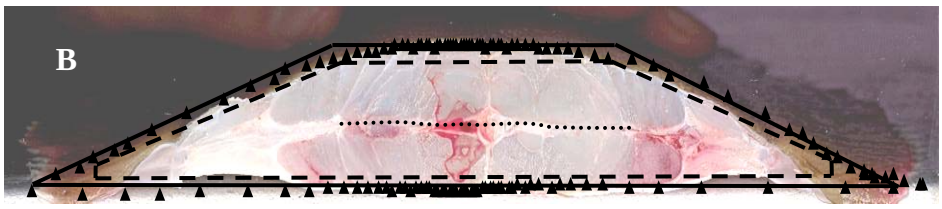

Fig. 8. CS1 (A) and CS3 (B). Backgrounds are scanning pictures of plaice cut over at the position of the cross section and underformable bonestructures indicated (dotted line). The cross section was captured by use of the morphometre prior to cutting (triangles) and the assymmetric trapezoids were fitted (solid line). The best penetration model results in reductions of the cross sections (dashed line).

3.5 Validation of penetration model

The penetration model found to have the highest DA was used to predict the selective properties of codends, on which we have data from field experiments (Table 4).

	van Beek et al. 1981	van Beek et al. 1981	van Beek et al. 1981	van Beek et al. 1981	Allan, 2006	Allan, 2006	Unpubl.	Unpubl.
Codend								
Mesh shape	diamond	diamond	diamond	diamond	diamond	diamond	diamond	square
Mesh size (mm)	90.4	109.1	122.3	137.2	119.64	129.42	92.5	68.5
Material	Nylon	Nylon	Nylon	Nylon	Brezline® PE	Brezline® PE	PE	Nylon
Twine thickness (mm)	n.a.	n.a.	n.a.	n.a.	5	5	5	3
No. of twines	1	1	1	1	2	2	2	1
No. of hauls	24	26	24	20	5	9	18	6
No. of meshes around	n.a.	n.a.	n.a.	n.a.	100	100	92	92
Catchweight (kg)	276	212	192	84	517-636	267-652	33-1488	180-420
Experiment								
L50 (cm)	19.0	22.9	25.4	30.0	29.09	31.94	21.91	13.93
SR (cm)	3.2	3.5	5.6	5.4	2.1	2.22	2.49	2.27
SF (L50 / Meshsize)	2.10	2.10	2.07	2.19	2.43	2.47	2.37	2.03
Simulation								
OA (degree)	n.a.	n.a.	n.a.	n.a.	20-50	20-50	20-50	80-130
L50 (cm)	n.a.	n.a.	n.a.	n.a.	26.25	28.65	20.05	12.74
SR (cm)	n.a.	n.a.	n.a.	n.a.	2.36	2.51	1.64	1.64

Table 4. Properties of the experiementally tested codends, their estimated selective parameters and the corresponding simulated selective parameters. Mesh sizes were measured with an ICES gauge with a 4 kg spring load.

The virtual population of 2000 fish was created and to ensure that the entire selective range of all investigated meshes is covered, the length distribution of the virtual population was constructed as a uniform distribution ranging from 20 to 600 mm (fig 9).

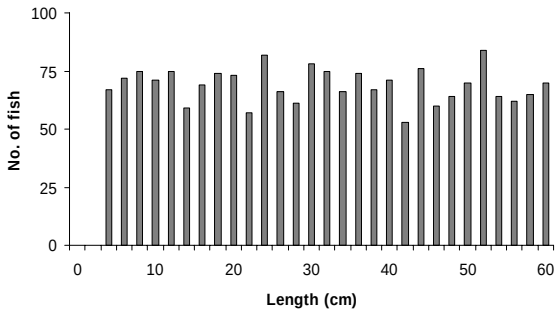

Fig. 9 Length distribution of fish in the virtual population.

This fish population was used as input in the model in combination with the mesh sizes from the tested codends. Depending on the mesh shape and the codend geometry each mesh size will take on a range of different mesh configurations, either by different opening angles (diamond meshes) or by different distances between the tension bars (square and rectangular meshes). The model output is a range of L50's illustrating the effect of mesh configuration on L50 (Fig. 10).

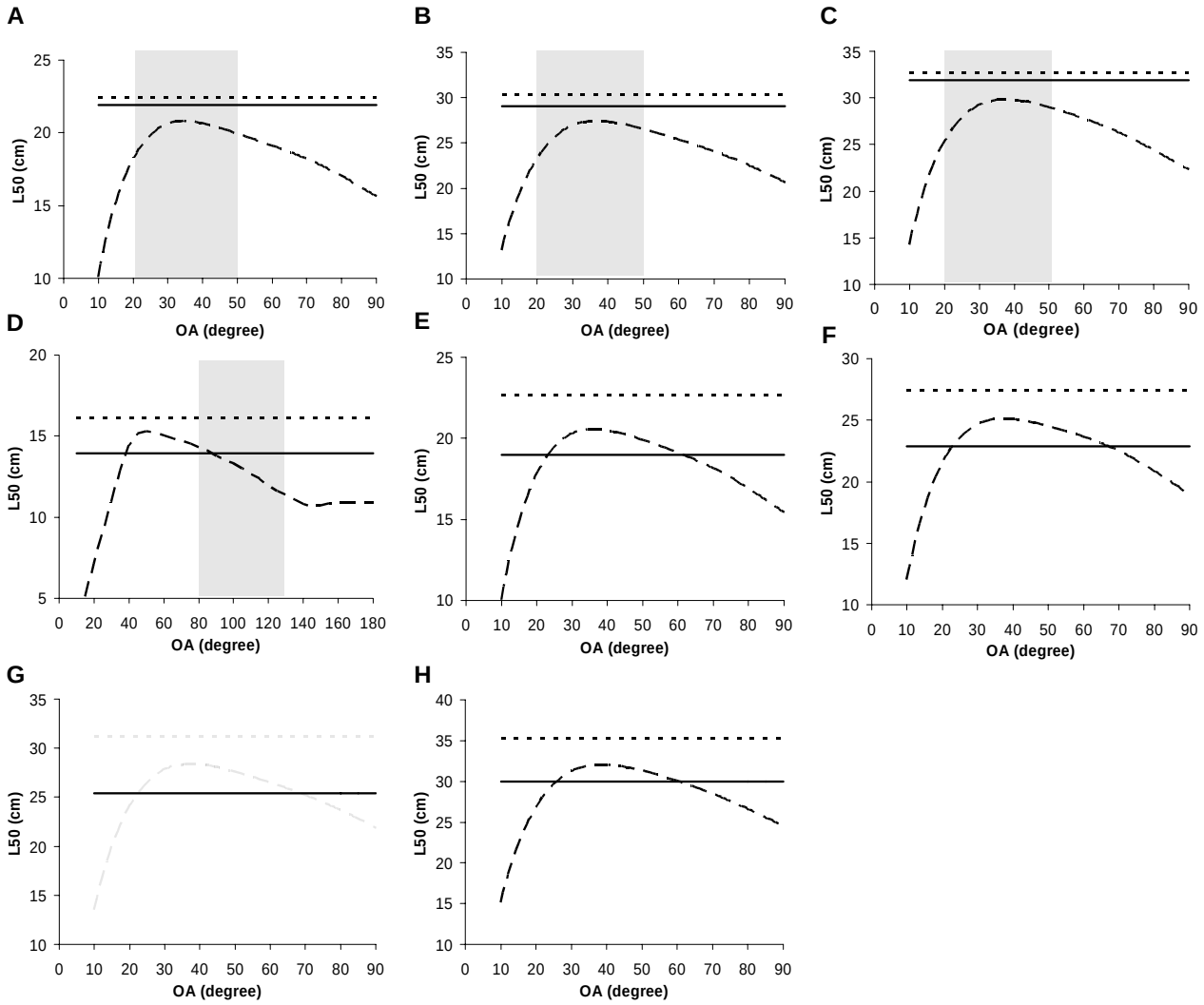

Fig. 10. Comparison of the L50 values obtained from field experiements (solid line) with simulated L50 values (hatched line) for a range of opening angles (OA)l. Stretched mesh sizes are: A.92.5 mm (Unpublished diamond mesh data), B. 119.6 mm (Allan 2006, diamond mesh), C. 129.4 mm (Allan 2006, diamond mesh), D. 68.5 mm (Unpublished square mesh data), E. 90.4 mm (Beek et al. 1991, diamond mesh), F. 109.1 mm (van Beek et al. 1991, diamond mesh), G. 122.3 mm (van Beek et al. 1991, diamond mesh) and H. 137.2 (van Beek et al. 1991, diamond mesh). Further details about the codends are listed in table 4. Dotted line indicates the L50 value obtained, when assuming a fully deformable mesh. Grey area indicates the expected mesh openings in the tested gears.

For diamond meshes, the highest L50's are found for opening angles ranging from 30 to 50 degrees (Fig. 10A-C and 10E-H)). In square meshes, the low tension bars perpendicular to the towing direction may transform the mesh into the shape of a hexagon. The highest L50 for square mesh

netting is found when the opening angle of a corresponding hexagonal mesh is 40 to 80 degrees (Fig. 10D).
In FISHSELECT simulations, the bars of the meshes are assumed to be undeformable. In order to justify this assumption, contrasting case is illustrated by making the shape of the mesh identical to the shape of the cross-section of the fish. L50 of such a deformable netting depends only on the mesh size, but is independent of the opening angle and initial mesh shape (Fig. 10A-10H).

When fishing, the mesh opening angles of a diamond mesh codend are determined by the number of meshes around, the distance from the accumulated catch and the catch size (Herrmann et al. 2007). The number of meshes around is unknown for the beam trawl experiment (van Beek et al., 1981) and opening angles can therefore not be estimated. Without knowledge of the actual mesh configurations in the codends it is not possible to estimate values of SR and L50. For all four beam trawl codends, the experimentally obtained L50 lies within the range of simulated L50 (Fig. 10E-H).
The range of opening angles to be expected in the rear end of the trawl in the other diamond mesh experiments referred to in this study have been estimated by methods outlined in (A2). Starting at the edge of the accumulated catch to 1.7 m in front of this, the opening angles will range from 20 – 50 degrees. In this range, the simulated L50 values (hatched line) are lower by 5 to 20% than the experimental value (solid line) (Fig. 10A-C).
With the deformable netting assumption,L50 is overestimated in the diamond mesh codends by 2 to 4 % in the otter trawl experiment and by 17-23% in the beam trawl experiments (Fig. 10A-C and 10E-H).

Mesh geometry is expected to be less variable in square mesh netting than in diamond mesh netting and square meshes often assumed to be fully open (e.g. Robertson and Stewart, 1988). Though less pronounced than for diamond meshes, the geometry of meshes in a square mesh codend do vary. Based on underwater photos (Robertson, 1986) and photos from flume tank testing, the square mesh act similar to hexagonal meshes with opening angles estimated to be between 80 and 130 degrees. An undeformed square mesh corresponds to an opening angle of 180 degrees. Simulated L50 values for this range of mesh openings varies from 2 % above the experimentally estimated L50 value to 19 % below (Fig. 10D). If the meshes are assumed fully deformable, they take shape after the cross section of the fish. This would result in a L50 value, which is higher than any of the L50 values simulated for undeformable meshes, and it also exceeds the experimentally estimated L50 value, by 14 %.
Based on the estimates of mesh geometry in the tested otter trawl codends, and the assumption that all opening angles of the codend netting are present in equal frequency, we are able to simulate the selective properties for the tested codends (Table 4). For the diamond mesh codends the result is an underestimation of L50 by 8.5 to 10.3% while estimates of SR ranged from being 34.1% below to 13.1% above the experimental value. Simulations for the square mesh codend underestimate L50 by 8.5% and SR by 27.8% (Table 4).

3.6 Design guide

The penetration model was used to generate selection parameters for a series of mesh configurations based on three basic mesh shapes; diamond, rectangle and hexagonal. For diamond and hexagonal, each mesh size was investigated with different opening angles (fig 11A and 11B). For rectangles, each mesh size was investigated with different proportion between the bar lengths (Fig 11C).

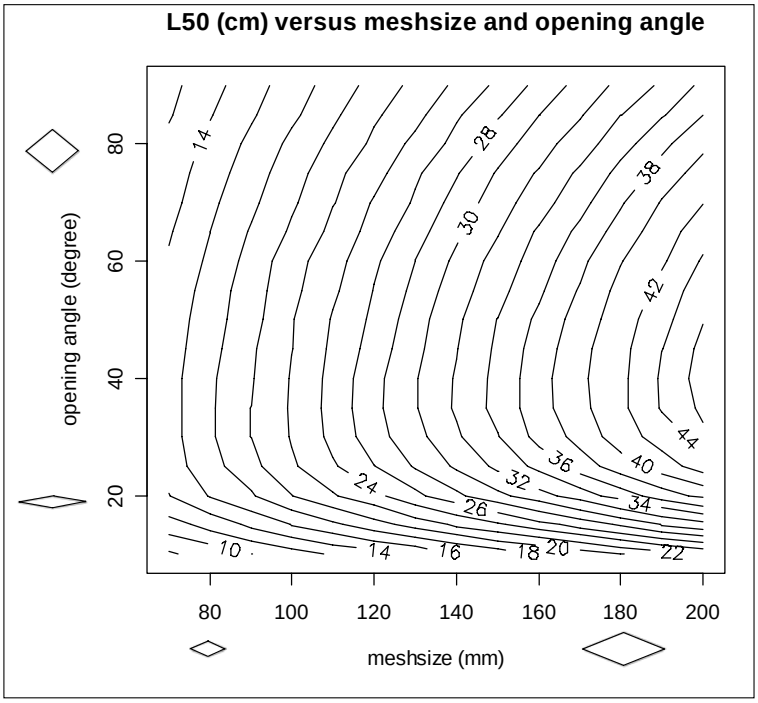

Fig. 11A. Isoline plot showing L50s in diamond meshes as a result of variation in mesh size (bar lenght) and opening angle. Stretched mesh size equals 2 times bar length and an opening angle of 90 degrees results in a square mesh.

For diamond mesh (Fig. 11A), the retention of plaice is high until an opening angle around 20 degrees, but then L50 rises steeply. Max L50 is reached around an opening angle of 35-40 degrees where after it slowly decreases concurrently with the largest diagonal of the mesh.

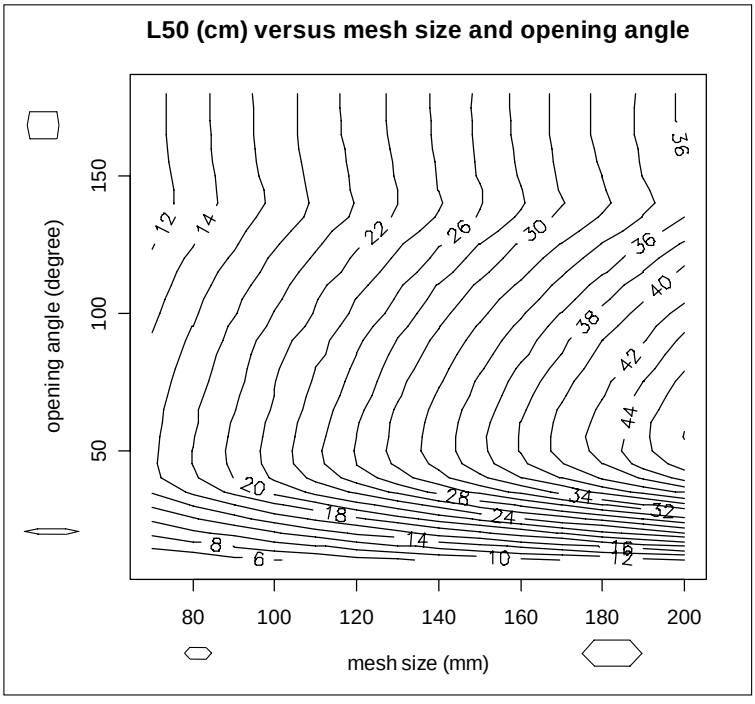

Fig. 11B. Isoline plot showing L50s in hexagonal meshes as a result of variation in mesh size (bar lenght) and opening angle. An opening angle of 180 degrees results in a square mesh.

For hexagonal meshes, L50 is very low at small opening angles (Fig. 11B). At small opening angles, the height of the head (CS1) is limiting mesh penetration, but L50 increases steeply as the opening angle increases and peaks around an opening angle of 50 degrees. At this opening angle, width of the body (CS3) becomes the limiting factor for mesh penetration. When increasing the opening angle of a hexagonal mesh, the longest diagonal shortens until an opening angle of 140 degree. At a further increase in the opening angle another diagonal becomes the longest and it increases slightly, which is reflected in the value of L50.

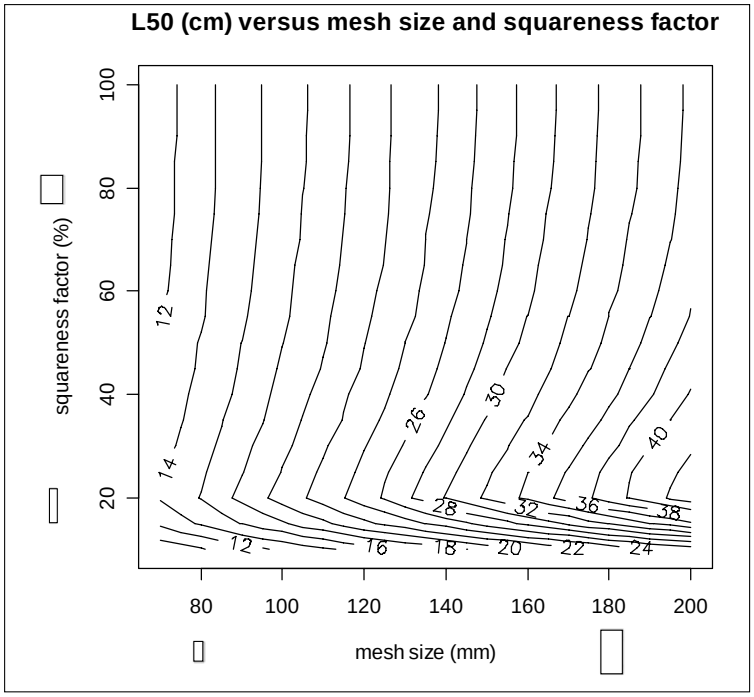

Fig. 11C. Isoline plot showing L50s in rectangular meshes as a result of variation in mesh size (bar length) and shape (squareness). A squareness factor of 100% results in a square mesh.

In rectangular meshes, mesh opening is determined by the squareness factor, which is defined as the ratio between the short and the long mesh bars. At high values of the squareness factor, the optimal orientation of plaice is with its width along the mesh diagonal and at small values, optimal orientation is parallel to the long mesh bar. L50 increases rapidly with mesh opening (Fig. 11C) at small values of squareness factor, when the height of the head is the limiting factor in mesh penetration. From a value of the squareness factor of approximately 20% the width of the body and thus the diagonal of the mesh becomes the limiting factor. The diagonal decreases to a squareness factor value of 50% after which it levels off.
Selective parameters of plaice in a grid is estimated by use of rectangular meshes where the long bar is held constant (400 mm) and the short bar corresponds to the bar distance. With bar distances from 20-40 mm, L50 / bar distance equals 14.

For meshes with the same stretched size, rectangular meshes have the lowest value of L50 of the mesh shapes investigated here, while maximum L50 for diamond and hexagonal meshes are similar.

4. Discussion

The morphological measurements of CS1 and CS3 could explain 96.8 % of the results obtained by laboratory experiments on mesh penetration of plaice. Furthermore, these cross-sections could be approximated with the geometric shape of an asymmetric trapezoid with good accuracy. It was also found that for both cross-sections the associated cross-section parameters that determine mesh penetration are well-correlated with the length of the fish. Based on the above, it is concluded that these cross-sections are adequate in the analysis of mesh penetration.
Cropping away parts of the cross-sections as well as deforming them along one of the axes, is a method to modify the trapezoids to make them better fit the real shape of the fish during penetration. The actual compression of the soft parts is limited, but they are deformable and may alter the cross-section shape when forced through a mesh as well as when they are placed on the table for measuring. The compression and cropping used in the best penetration model may thus appear to be crude, but it does preserve the non-deformable properties of the bone structures (Fig. 8).

The virtual fish population we have created consists of fish ranging from 20 to 600 mm. Their morphological measures are based on the relationships obtained from the fish examined in the present experiment, where fish lengths ranged from 180 to 460 mm. The shapes of both the smallest and largest fish are thus based on extrapolations. For the small fish, this is justified by the fact that metamorphosis, where plaice takes on the shape of a flatfish, is completed at a length of 13-14 mm (Russell, 1976) and we thus assume the relationships to be valid from this stage. Variation in all parameters between individuals increase with fish size but since variation in the parameters is incorporated in the creation of the virtual fish population, the extrapolation to large fish is assumed to be justified.

Whether a fish penetrates the codend or not depends both on the morphology and the behaviour of the fish. In this study we focused exclusively on the influence of morphology, since regardless of the behaviour of a fish, it will only be able to penetrate a mesh, if it is large enough. The selection parameters predicted by FISHSELECT are therefore expected to be maximum values for a corresponding codend.
The values of L50 simulated for the beam trawl experiments are approximately equal to the values obtained in the field experiments. This indicates that under the given conditions, plaice fully exploit the chance of escape, and L50 can be predicted from the morphology alone. But in the case of the otter trawl experiments, the predicted values of L50 are consistently 8.5-10.3 % lower than the values obtained by field experiments. An underestimate of L50 values challenges the very concept of FISHSELECT and we therefore need to confront the basic assumptions of the methodology. The crudest assumption must be that we set the muscle force of the fish to be comparable to the pull of gravity. Both forces increase with the size of the fish, but whether they are comparable is likely to be species-specific and in particular determined by the swimming mode of the fish. If the actual muscle force of the fish is larger than the pull of gravity, the consequence will be that FISHSELECT consistently underestimates the L50. The use of dead fish in the penetration experiments also induces the risk of missing a change in cross section shape caused by the muscle contraction. In the case of flatfish such as plaice, an increased flexion of the body affects the cross section shape. In combination with scales, such a change in shape is likely to aid the fish through the mesh to an extent that cannot be predicted by FISHSELECT alone. In the present study, fish are simulated to attempt escape once. If the actual number of attempts is higher, the chance that a fish meets a mesh having the optimal configuration increases as does L50 as shown by Herrmann and O'Neill (, 2005).

The difference in results between the beam trawl and the otter trawl experiment is uncertain. One otter trawl experiment was performed as a twin trawl experiment (Unpubl. diamond) while all the rest were covered codend experiments. The selectivity ogives in the beam trawl experiments are drawn by eye on pooled data while the SELECT method (Millar, 1992) in combination with Fryer's model (Fryer, 1991) has been used on two of the otter trawl experiments (Allan, 2006). Both unpublished data sets have been analyzed using the SELECT method one on stacked data (Unpubl. diamond) and one on pooled data (Unpubl. square). These differences can not systematically explain the differences found in the selective parameters. Remaining is the factor of fishing gear and towing speed. Previous experiments have shown that length distribution of plaice caught in beam trawls is comparable to that of otter trawls. But the same experiments showed that the proportion of undersized plaice in otter trawls were somewhat though not substantially smaller than in beam trawls (Dahm et al., 1996). Towing speed in the beam trawl experiment was 5 knots while towing speed in the otter trawl experiments was 3.5 knots (Allan, 2006) and 2.5 knots (Unpubl.). At high towing speed, the relative swimming speed of the fish and thus its ability to actively navigate to the panels of the codend is reduced. Furthermore, the number of attempts is potentially higher when the travel time of the fish through the codend is longer. The effect of towing speed on codend selectivity has previously been investigated for haddock, but not proven (Dahm et al., 2002).

The assumption of undeformable meshes is based on the belief that stiffness of the mesh bars under tension in a codend is so large that fish cannot deform the bars with muscle power. This assumption is supported by Allan (, 2006) who, for plaice, finds no connection between selection parameters and twine tenacity.
With regard to SR, the differences between FISHSELECT estimates and results obtained in the otter trawl experiments vary. In general though, plaice has a relatively low SR compared to round fish. Among other things, SR is determined by variation within the fish population, variation in mesh configurations within the codend, contact frequency between fish and netting and the handling of between haul variation in L50. In the FISHSELECT simulations, the range of opening angles most likely to occur in a trawl codend have little variation in L50 (Fig. 10 & 11). This offers an explanation to why SR in general is low for plaice. SR in the beam trawl experiments is substantially higher than those in the otter trawl experiments.

The disagreement between the experimentally estimated selective properties of the beam trawl and the otter trawl makes the justification of the use of FISHSELECT in predicting mesh penetration of plaice uncertain.
For all mesh shapes, highest L50 was obtained for mesh configurations that had highest resemblance with the cross section of a plaice. The corresponding mesh opening was approximately 30 and 50 degrees for diamond mesh and hexagonal mesh respectively and for rectangular meshes, squareness factor of the optimal mesh was 20%. This supports previous findings indicating that square mesh codends have a poor size selectivity of flat fish compared to diamond meshes.

The fish used in the present experiment were caught in February in the North Sea and previous experiments have shown that some spatial and temporal variation should be expected (Özbilgin et al., 2006). In the present experiment, 6% of the fish were roe fish and if these are excluded from the analysis, DA increases by 0.1% to 96.9%. This indicates that the found penetration model is relatively robust to small changes in population structure.
Different fisheries are characterized by different types of vessels as well as different types and sizes of trawls and footgear and all these factors have been shown to influence the selective properties of the gear (e.g. Engås and Godø, 1989; Özbilgin et al., 2006; Tschernij and Suuronen, 2002). The

selectivity parameters obtained for mesh configurations listed in the design guide should therefore be regarded as a guidelines only and before introducing new gear types into any fishery, their selective properties should be tested by a vessel from the fleet in question.

5. Acknowledgements

The research documented in this paper has been carried out with financial support from a project under the development programme for sustainable fishery financed by the Directorate for Food, Fisheries and Agri Business, Denmark. The support is acknowledged.

6. References

Allan, L., 2006. The effect of mesh size and twine tenacity on the selectivity of cod-ends in a Scottish whitefish fishery. Dissertation University of Aberdeen, Fisheries Research Services. 1-53.

Clark, J. R., 1963, Size selection of fish by otter trawls. In: The selectivity of fishing gear. Int. Comm. Northwest Atl. Fish Spec. Publ. 5, 24-96

Cooper, C., Hickey, W., 1989. Selectivity experiments with square mesh codends of 130, 140 and 155mm. Newfoundland and Labrador Inst. of Fisheries and Marine Technology, St. John's, NF, Canada. World Symp. on Fishing Gear and Fishing Vessel Design, 1988, 52-56.

Dahm, E., Weber, W., Damm, U., and Lange, K., 1996. The Place box - effects of different fishing gear and area on the catch composition. ICES C.M. 1996/B:21, 1-17.

Dahm, E., Wienbeck, H., West, C. W., Valdemarsen, J. W., and O'Neill, F. G., 2002. On the influence of towing speed and gear size on the selective properties of bottom trawls. Fisheries Research 55, 103-119.

Efanov, S. F., Istomin, I. G., and Dolmatov, A. A., 1987. Influence of the form of fish body and mesh on selective properties of trawls. ICES C.M. Fish Capture Committee 1987/B:13, 1-39.

Engås, A. and Godø, O. R., 1989. Escape of fish under the fishing line of a Norwegian sampling trawl and its influence on survey results. J.Cons.int.Explor.Mer. 45, 269-276.

Fonteyne, R. and M'Rabet, R., 1992. Selectivity experiments on sole with diamond and square mesh codends in the Belgian coastal beam trawl fishery. Fisheries Research 13, 221-233.

Fryer, R. J., 1991. A model of the between-haul variation in selectivity. ICES Journal of Marine Science 48, 281-290.

Halliday, R. G., Cooper, C. G., Fanning, P., Hickey, W. M., and Gagnong, P., 1999. Size selection of Atlantic cod, haddock and Pollock (saithe) by otter trawls with square and diamond mesh codends of 130-155 mm mesh size. Fisheries Research 41, 255-271.

He, P., 2007. Selectivity of large mesh trawl codends in the Gulf of Maine, I, Comparison of square and diamond mesh. Fisheries Research 83, 44-59.

Herrmann, B. and O'Neill, F. G., 2005. Theoretical study of the between-haul variation of haddock selectivity in a diamond mesh cod-end. Fisheries Research 74, 243-252.

Herrmann, B., Priour, D., Krag, L.A., 2007b. Simulation-based study of the combined effect on cod-end size selection of turning meshes by 90 degrees and reducing the number of meshes in the circumference for round fish. Fish. Res. 84: 222-232.

Madsen, N., Tschernij, V., Hansen, K., and Larsson, P. O., 2006. Development and testing of a species-selective flatfish ottertrawl to reduce cod bycatches. Fisheries Research 78, 298-308.

Millar, R. B., 1992. Estimating the size-selectivity of fishing gear by conditioning on the total catch. J.Am.Stat.Assoc. 87, 962-968.

Özbilgin, H., Ferro, R. S. T., Robertson, J. H. B., Holtrop, G., and Kynoch, R. J., 2006. Seasonal variation in trawl codend selection of northern North Sea haddock. ICES Journal of Marine Science 63, 737-748.

Robertson, J.H.B., 1986. Design and construction of square mesh cod-ends. Scottish Fisheries Information Pamphlet, no. 12: 1-10. Marine Laboratory, Aberdeen Department of Agriculture and Fisheries for Scotland

Robertson, J. H. B. and Stewart, P. A. M., 1988. A comparison of size selection of haddock and whiting by square and diamond mesh codends. ICES Journal of Marine Science 44, 148-161.

Russell, F. R., 1976, The eggs and Planktonic stages of British marine fishes. 1-524. London, Academic Press

Simpson, D.G., 1989. Codend selection of Winter flounder (*Pseudopleuronectes americanus*). NOAA Technical Report NMFS, no. 75: 1-10 US Department of Commerce, National Marine Fisheries Service

Thorsteinsson, G., 1992. The use of square mesh codends in the Icelandic shrimp (*Pandalus borealis*) fishery. Fisheries Research 13, 255-266.

Tschernij, V. and Suuronen, P., 2002. Improving trawl selectivity in the Baltic. TemaNord, no. 512: 1-56. Copenhagen Nordic Counsil of Ministers

van Beek, F. A., Rijnsdorp, A. D., and van Leeuwen, P. I., 1981. Results of mesh selection experiments on North Sea Plaice with a commercial beam trawler in 1981. ICES C.M. 1981/B:12, 1-12.

Walsh, S. J., Millar, R. B., Cooper, C. G., and Hilbish, T. J., 1992. Codend selection in American plaice: diamond versus square mesh. Fisheries Research 13, 235-254.

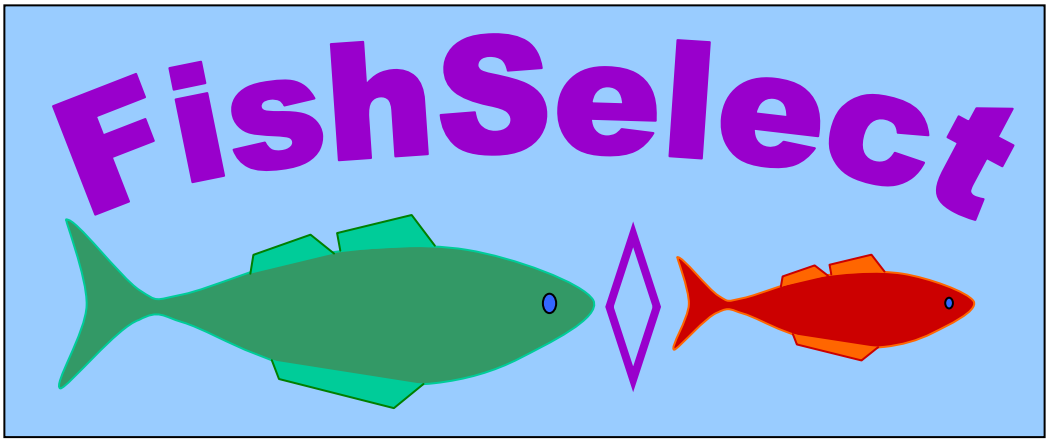

A4

A note on the FISHSELECT results for haddock

Haddock were caught by chartering a commercial trawler in November 2007. Approximately 200 live individuals were brought to tanks in the laboratory. Of these individuals 80 were used in the FISHSELECT experiments. Fig. 1 shows the size structure of these individuals.

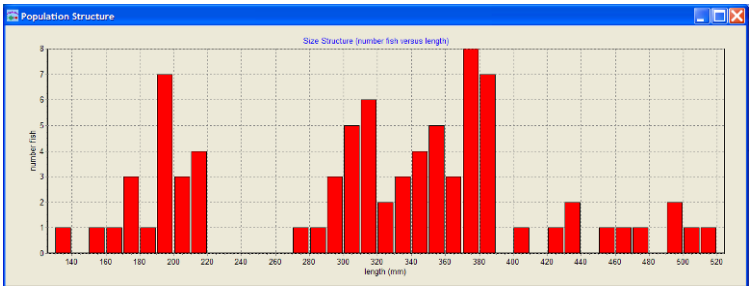

Fig. 1.

Because the body of haddock is very deformable (see Fig 6) we decided to hang the individuals vertically when measuring two of the three cross-sections CS2 and CS3 (fig 2).

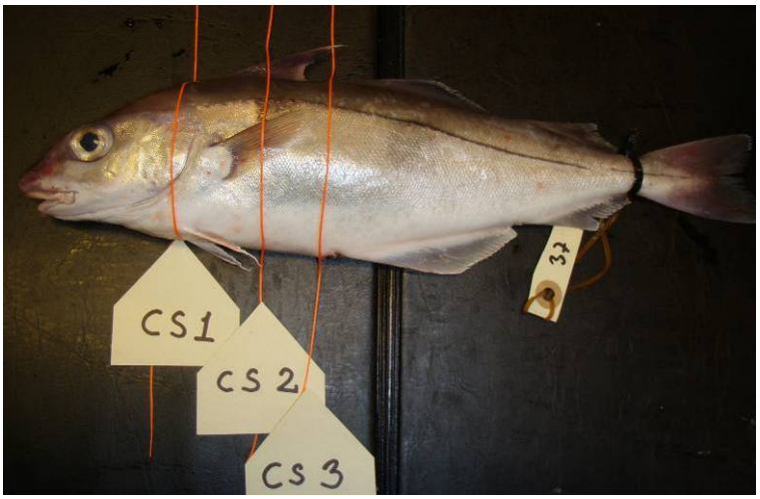

Fig. 2.

To do this a special fixture from which the fish could be hung with a hook in the mouth was produced (fig. 3) and the mechanical MorphoMeter was mounted horizontally.

Fig. 3.

For cross-section 1 at the head we had to place the haddocks horizontally and the MorphoMeter vertically to avoid that the gill lids (operculum) bend out and bias the measurement (Fig. 4).

Fig. 4.

Fig. 5 shows the work in the laboratory with scanning of the cross-section replica using the flatbed scanner and acquiring the data in a laptop computer.

Fig. 5.

Fig. 6 shows details of the fall-through experiments, when the fish pass through the meshes in the mesh template plates and the data are entered into the FISHSELECT software installed in a laptop computer.

Fig. 6.

21 different mesh template plates were used in the fall-through experiments with a total of 132 different mesh hole shapes: diamond (type=D), square (type=S), rectangle (type=R) and hexagonal (type=H)). With 80 haddock in the experiment this makes 10560 fall through results. Table 1 shows the parametric data (mesh number/ID, meshsize, opening angle) for all the 132 mesh template holes used in the experiment with the syntax developed for the FISHSELECT software tool. The data listed are not nominal measures but obtained by scanning each mesh hole, digitizing the contour using the built-in image analysis functionality in the FISHSELECT software tool. The parametric description is obtained by fitting one of the shape types listed above to the contour using the built-in functionality.

Table 1.

ID=1;Type=D;m=77.69;oa=30.54;ID=2;Type=D;m=78.01;oa=55.58;ID=3;Type=D;m=80.27;oa=87.01;
ID=4;Type=D;m=88.20;oa=25.8;ID=5;Type=D;m=88.47;oa=30.92;ID=6;Type=D;m=88.80;oa=37.32;
ID=7;Type=D;m=88.35;oa=39.69;ID=8;Type=D;m=88.71;oa=45.85;ID=9;Type=D;m=89.75;oa=50.1;
ID=10;Type=D;m=89.26;oa=57.29;ID=11;Type=D;m=90.05;oa=60.08;ID=12;Type=D;m=89.76;oa=61.79;
ID=13;Type=D;m=90.59;oa=69.79;ID=14;Type=D;m=89.26;oa=76.33;ID=15;Type=D;m=90.38;oa=81.45;
ID=16;Type=D;m=89.70;oa=85.36;ID=17;Type=D;m=91.16;oa=89.99;ID=18;Type=D;m=100.78;oa=19.87;
ID=19;Type=D;m=98.31;oa=56.16;ID=20;Type=D;m=99.84;oa=86.21;ID=21;Type=D;m=109.42;oa=20.31;
ID=22;Type=D;m=109.56;oa=55.22;ID=23;Type=D;m=109.18;oa=86.48;ID=24;Type=D;m=118.27;oa=19.67;
ID=25;Type=D;m=114.16;oa=26.49;ID=26;Type=D;m=118.83;oa=31.73;ID=27;Type=D;m=117.90;oa=35.61;
ID=28;Type=D;m=118.35;oa=41.37;ID=29;Type=D;m=118.23;oa=46.22;ID=30;Type=D;m=119.86;oa=50.09;
ID=31;Type=D;m=118.94;oa=57.41;ID=32;Type=D;m=120.37;oa=60.67;ID=33;Type=D;m=119.71;oa=65.01;
ID=34;Type=D;m=118.48;oa=71.46;ID=35;Type=D;m=121.59;oa=77.86;ID=36;Type=D;m=120.31;oa=81.51;
ID=37;Type=D;m=120.52;oa=86.74;ID=38;Type=D;m=126.68;oa=19.89;ID=39;Type=D;m=128.99;oa=56.63;
ID=40;Type=D;m=129.98;oa=86.59;ID=41;Type=D;m=140.39;oa=19.84;ID=42;Type=D;m=138.48;oa=55.95;
ID=43;Type=D;m=140.23;oa=85.85;ID=44;Type=D;m=163.35;oa=14.39;ID=45;Type=D;m=158.72;oa=20.57;
ID=46;Type=D;m=158.13;oa=25.07;ID=47;Type=D;m=159.35;oa=30.48;ID=48;Type=D;m=157.85;oa=35.52;

ID=49;Type=D;m=159.03;oa=40.22;ID=50;Type=D;m=160.04;oa=46.09;ID=51;Type=D;m=159.03;oa=51.43;
ID=52;Type=D;m=160.76;oa=56.13;ID=53;Type=D;m=160.54;oa=60.74;ID=54;Type=D;m=160.56;oa=66.13;
ID=55;Type=D;m=161.10;oa=71.33;ID=56;Type=D;m=160.77;oa=76.62;ID=57;Type=D;m=159.68;oa=80.65;
ID=58;Type=D;m=160.97;oa=85.57;ID=59;Type=D;m=177.19;oa=15.68;ID=60;Type=D;m=180.96;oa=56.47;
ID=61;Type=D;m=182.90;oa=86.00;ID=62;Type=D;m=195.97;oa=15.85;ID=63;Type=D;m=200.40;oa=55.71;
ID=64;Type=D;m=200.30;oa=86.89;ID=65;Type=S;b=34.67;ID=66;Type=S;b=40.07;ID=67;Type=S;b=50.14;
ID=68;Type=S;b=60.23;ID=69;Type=S;b=69.69;ID=70;Type=S;b=80.08;ID=71;Type=S;b=89.95;
ID=72;Type=S;b=100.27;ID=73;Type=R;b=90.59;a=9.81;ID=74;Type=R;b=90.96;a=14.49;
ID=75;Type=R;b=91.35;a=19.33;ID=76;Type=R;b=91.05;a=29.19;ID=77;Type=R;b=91.23;a=49.01;
ID=78;Type=R;b=91.79;a=68.83;ID=79;Type=R;b=120.42;a=8.99;ID=80;Type=R;b=121.67;a=14.85;
ID=81;Type=R;b=122.15;a=19.38;ID=82;Type=R;b=121.61;a=29.57;ID=83;Type=R;b=122.40;a=48.84;
ID=84;Type=R;b=121.93;a=69.02;ID=85;Type=R;b=202.66;a=9.89;ID=86;Type=R;b=203.93;a=14.28;
ID=87;Type=R;b=203.45;a=19.02;ID=88;Type=R;b=200.19;a=29.96;ID=89;Type=R;b=203.26;a=49.13;
ID=90;Type=R;b=203.62;a=69.37;ID=91;Type=H;b=17.49;k=35.25;oa=142.05;ID=92;Type=H;b=17.61;k=36.17;oa=130.44;
ID=93;Type=H;b=18.06;k=36.51;oa=103.65;ID=94;Type=H;b=17.02;k=35.71;oa=86.08;
ID=95;Type=H;b=20.25;k=39.95;oa=147.81;ID=96;Type=H;b=20.35;k=39.75;oa=126.92;
ID=97;Type=H;b=19.96;k=39.31;oa=107.59;ID=98;Type=H;b=19.98;k=40.81;oa=91.84;
ID=99;Type=H;b=25.37;k=50.15;oa=143.40;ID=100;Type=H;b=24.91;k=49.24;oa=126.33;
ID=101;Type=H;b=26.22;k=48.60;oa=102.92;ID=102;Type=H;b=26.04;k=48.05;oa=89.54;
ID=103;Type=H;b=29.74;k=59.42;oa=143.88;ID=104;Type=H;b=30.53;k=60.21;oa=128.98;
ID=105;Type=H;b=29.86;k=59.42;oa=105.49;ID=106;Type=H;b=29.94;k=59.80;oa=88.85;
ID=107;Type=H;b=35.15;k=68.93;oa=142.28;ID=108;Type=H;b=34.18;k=70.03;oa=128.34;
ID=109;Type=H;b=35.29;k=69.42;oa=106.33;ID=110;Type=H;b=35.62;k=69.47;oa=89.76;
ID=111;Type=H;b=40.78;k=80.51;oa=145.98;ID=112;Type=H;b=40.66;k=79.42;oa=129.65;
ID=113;Type=H;b=40.34;k=80.04;oa=105.87;ID=114;Type=H;b=41.03;k=80.19;oa=88.19;
ID=115;Type=H;b=49.89;k=99.69;oa=141.66;ID=116;Type=H;b=50.59;k=99.35;oa=127.28;
ID=117;Type=H;b=50.47;k=99.31;oa=106.32;ID=118;Type=H;b=50.97;k=98.67;oa=88.05;
ID=119;Type=D;m=66.38;oa=26.86;ID=120;Type=D;m=67.25;oa=29.74;ID=121;Type=D;m=67.66;oa=37.95;
ID=122;Type=D;m=67.59;oa=41.83;ID=123;Type=D;m=67.81;oa=44.22;ID=124;Type=D;m=67.61;oa=51.56;
ID=125;Type=D;m=68.85;oa=55.10;ID=126;Type=D;m=69.35;oa=63.60;ID=127;Type=D;m=70.11;oa=64.87;
ID=128;Type=D;m=68.44;oa=69.86;ID=129;Type=D;m=69.33;oa=74.24;ID=130;Type=D;m=68.80;oa=79.65;
ID=131;Type=D;m=70.12;oa=85.60;ID=132;Type=D;m=69.69;oa=89.67;

For each haddock the three cross-section contours on the images, of the Morphometer were digitized and it was found that an ellipse provided a reasonable description of the shapes. Fig. 7 shows the digitized contour for the cross-section at the head of one haddock. Left: the contour obtained by edge detection in the scanned image of the mechanical Morphometer. Right: The ellipse fitted to the digitized shape.

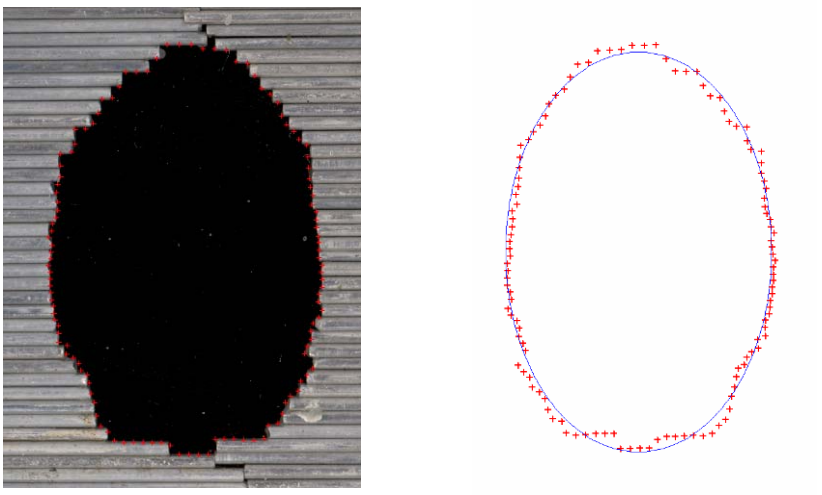

Fig. 7.

The relationships between the fish length and the parameters of the ellipse (height and width) for each cross-section were obtained by regression analysis according to the

FISHSELECT methodology. For the 80 individuals we found the following overall fit statistics (Table 2).

Table 2.

Cross-section No.	Mean deviation (mm)	sd mean deviation (mm)	Maximum deviation (mm)	sd Maximum deviation (mm)
1	0.39	0.03	1.53	0.13
2	0.40	0.02	1.53	0.10
3	0.39	0.01	1.50	0.03

The data and the regression lines for the length to width and height are shown in Fig. 8 and Table 3.

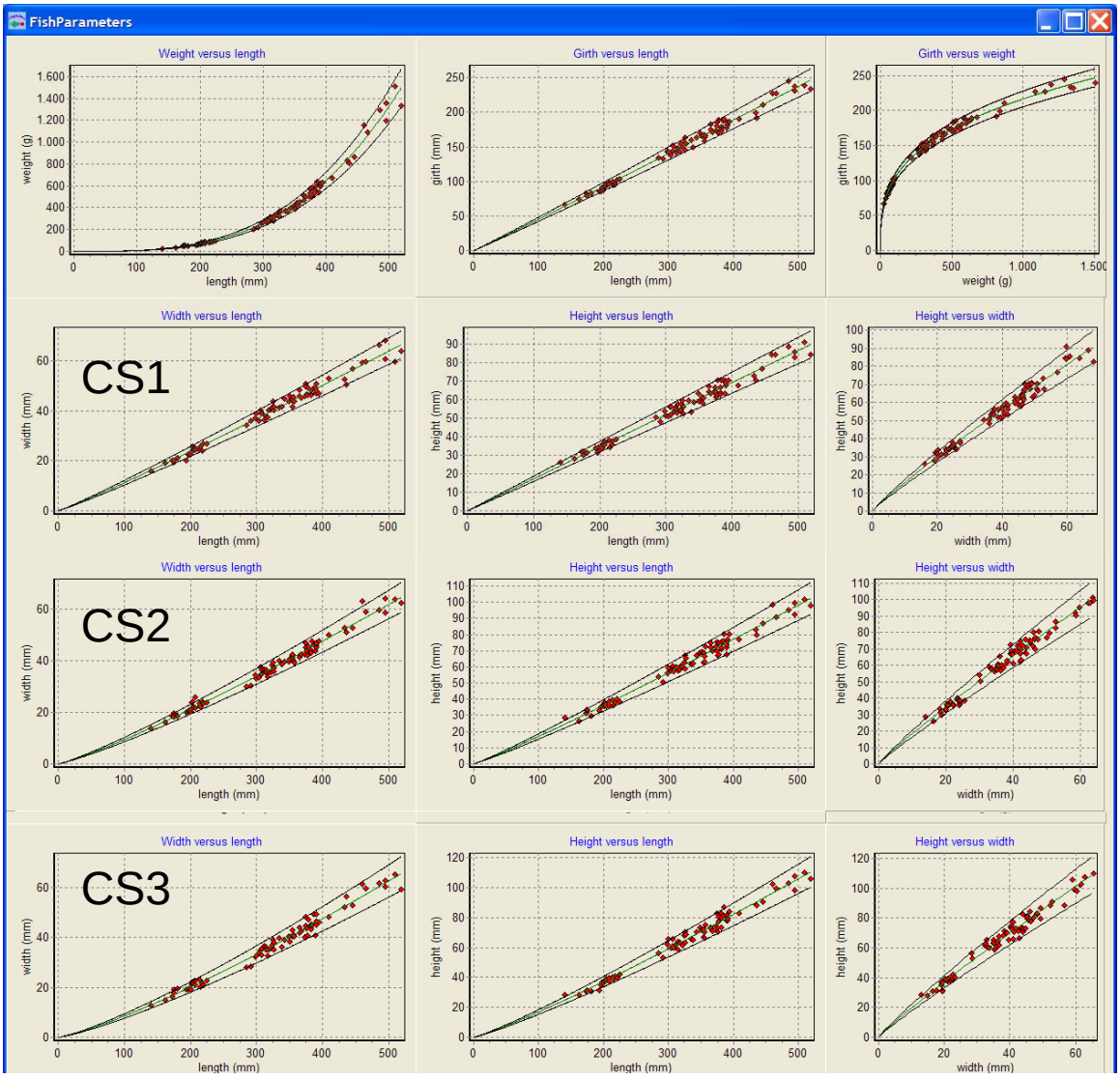

Fig. 8.

Table 3.

D1:Coef=0.00000307;sd=0.00000018;Po=3.2000;R2=0.99;"Weight versus length"
D2:Coef=0.25660519;sd=0.01003369;Po=1.1100;R2=0.98;"Girth versus length"
D3:Coef=20.57947177;sd=0.57427209;Po=0.3500;R2=0.99;"Girth versus weight"
Section 1
Type=ELL
D4:Coef=0.07786109;sd=0.00321705;Po=1.0800;R2=0.98;"Width versus length"
D5:Coef=0.17277102;sd=0.00711065;Po=1.0000;R2=0.98;"Height versus length"
D6:Coef=1.94938520;sd=0.09554160;Po=0.9100;R2=0.97;"Height versus width"
Section 2
Type=ELL
D4:Coef=0.04289129;sd=0.00191786;Po=1.1700;R2=0.98;"Width versus length"
D5:Coef=0.11238330;sd=0.00541593;Po=1.0900;R2=0.98;"Height versus length"
D6:Coef=2.20524949;sd=0.11951399;Po=0.9200;R2=0.98;"Height versus width"
Section 3
Type=ELL
D4:Coef=0.02819856;sd=0.00145803;Po=1.2400;R2=0.98;"Width versus length"
D5:Coef=0.08871715;sd=0.00409883;Po=1.1400;R2=0.98;"Height versus length"
D6:Coef=2.44087015;sd=0.13811091;Po=0.9100;R2=0.98;"Height versus width"

Fig. 8 shows that the FISHSELECT regression models can describe the relationships well, including the between-individual-variation. This is further confirmed the very high R2 values (minimum 0.98) in Table 3.

The next step was to find a penetration model that with single cross-sections alone or more than one in combination could describe the ability of cod to penetrate meshes of different size and shape. This included defining to which extent the cross-sections can be compressed. To identify the best model we simulate the experimental 10 560 fall-through results obtained for the 80 haddock used in the experiment. Models assuming different levels of symmetrical and asymmetrical compression for the cross-sections 1-3 alone were first applied to simulate the experimental results. More than 60 000 different models were tested requiring simulation of more than 630 000 000 fall-through results to be compared with the experimental results. This required large amounts of computer power to carry this work out in a few weeks. Therefore the work was split up in blocks that could be run simultaneously in parallel on several computers, which were procured to the project. The best results were obtained with a model assuming a stiff mesh and using cross-section 1 (CS1 at the head) alone with 13% compression in the width and 0% compression in the height. For this model 97.9% of the simulated fall-through trials were in agreement with the experimental ones. Using this model extended with conditions including CS2 and/or CS3 did not lead to a better degree of agreement (DA)-values. The best results for these combinations were found when using large compression values for both CS2 and particular CS3 (the cross-section having maximal girth). Thus it was concluded that it would still be the less deformable and less compressible, but smaller, cross-section CS1 that was decisive for penetration through a non-deformable mesh. Since a DA=97.9% without taking any measurement uncertainty into account is considered a very fine, the model based on CS1 alone is used for predicting the basic selective properties of different mesh shapes, mesh sizes and grids for haddock. Fig. 9 illustrates the asymmetrical compression used for cross-section 1 on a typical haddock. The outer curve represents ellipse fitted to the measured cross–section, while the inner curve represents the ellipse used in the optimal penetration model in which the width can be compressed 13%.

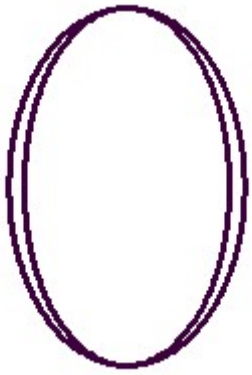

Fig. 9

The regression results for CS1 (Table 3) show that the power (po) for both width and height is very close to 1.0 making it easy to compare this model approximately with the one used by in PRESEMO (Herrmann 2005a; O'Neill and Herrmann 2007) based on Jones (1963) not taking compression in to account.

Our model taking the 13% compression of width into account and approximating the power relation by a linear relation (power = 1.0) gives length to height and width relation factor-values of hf=0.1728 and wf=0.0677 whereas Jones (1963) had values for an elliptical shape at hf=0.172 and wf=0.103. The uncompressible height factors were thus nearly identical whereas the compressible width factor is much smaller than the value found by Jones and used by Herrmann (2005) and O'Neill and Herrmann (2005b) in PRESEMO. It will especially be interesting to find out how our new and improved estimates, of which morphological features of haddock are decisive for mesh penetration, will affect the predictions made especially in O'Neill and Herrmann (2007). But we can conclude that assuming an elliptical cross-section shape for haddock (see Table 2) and taking only one cross-section into account for haddock as assumed in Herrmann (2005b) seems to be a reasonable approximation.

We have also done simulations using our penetration model for haddock and the regression relationships between length and width and height for cross-section 1 and the between-individual-variations of those relationships to estimate the basic selection parameters of diamond meshes of different mesh size and openness for haddock. With the morphological relationships we created a virtual population of haddock of 2000 individuals uniformly distributed in length between 30 mm to 800 mm to insure that there were individuals in the selective range for all diamond meshes of various mesh sizes in range 70 to 200 mm with opening angles from 10 to 90 degree. Fig. 10 shows an isoline-plot for the 50% retention length, L50, for this variable range.

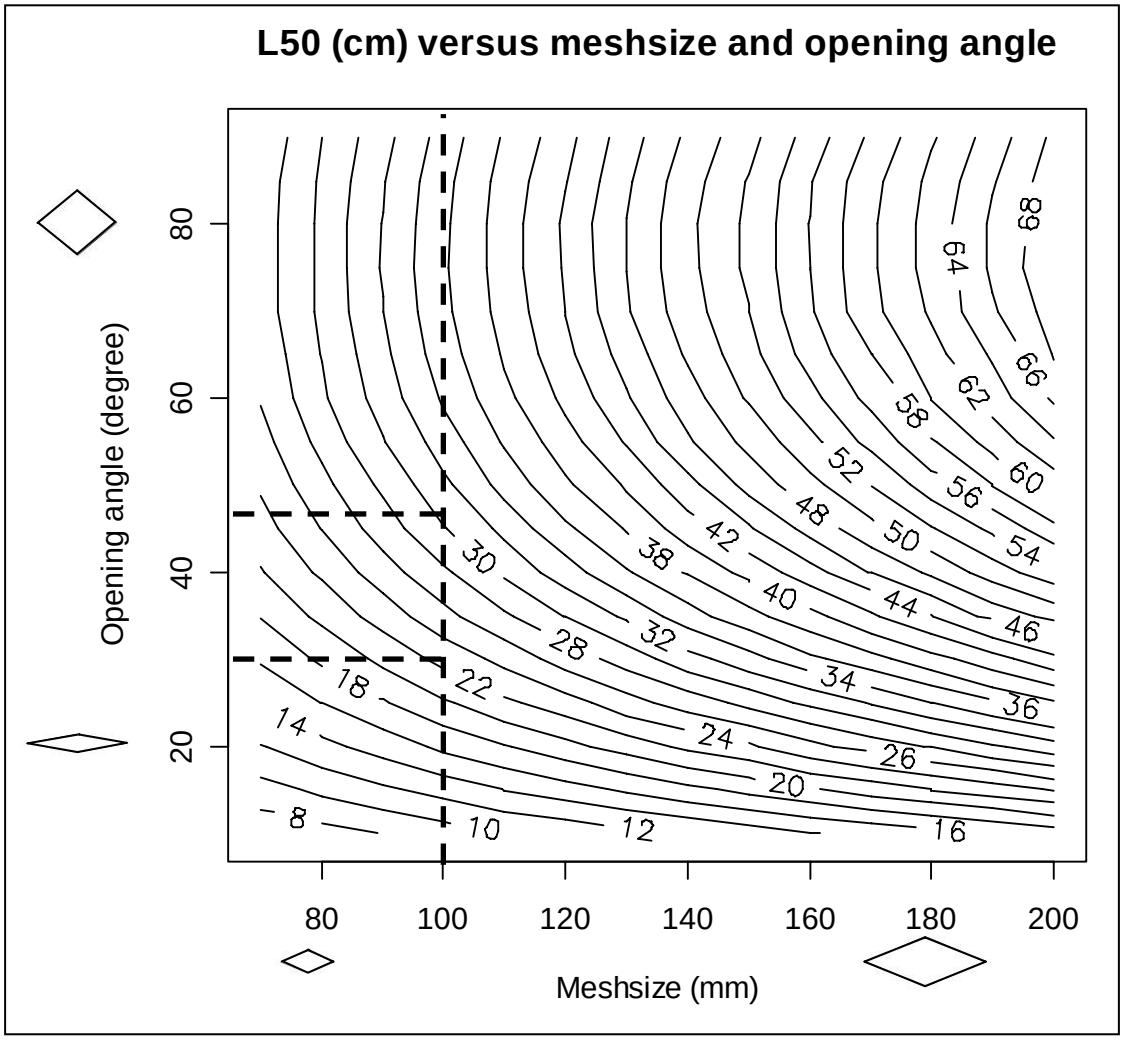

Fig. 10.

The simulated basic L50 values along the dashed thick vertical line in Fig. 10 corresponds to those of a mesh size of 100 mm for different mesh openness angles, oa. Experimental results by Lowry and Robertson (1996) and O'Neill and Kynoch (1996) showed values for individual hauls of L50 in the range from 22.3 to 30.3 cm. In Fig. 10 this range is marked by horizontal dashed lines. Thus the range in L50 corresponds to a range in mean opening angle from approximately 30 to 47 degrees. This is not unrealistic for mesh openness just ahead of the catch accumulation line based on data from Herrmann et al. 2007. This area in a cod-end is where most escape attempts is observed to take place (Wileman et al. 1996). Further the dependency of basic L50 on mesh openness can explain the huge between-hauls-variation in selectivity often observed experimentally for diamond mesh cod-ends and the relatively large selection range SR compared to what could be expected from the between-individuals-variation in the morphological parameters. Thus Fig. 10 illustrates the importance of controlling the mesh openness for diamond mesh cod-ends in order to get a well defined selectivity.

Similar plots as in Fig. 10 can be created for other mesh types like squares, rectangles and hexagonal shaped using the penetration model and the virtual population for example to investigate if other mesh type could have more beneficial selective properties with regard to haddock. But it has not been possible within the timeframe of this project to conduct such an analysis.

References

Herrmann, B., 2005a. Effect of catch size and shape on the selectivity of diamond mesh cod-ends: I Model development. Fish. Res. 71: 1-13.

Herrmann, B., O'Neill, F.G., 2005b. Theoretical study of the between-haul variation of haddock selectivity in a diamond mesh cod-end. Fish. Res. 74: 243-252.

Jones, 1963. Some theoretical observations on the escape of haddock from a codend. ICNAF spec. Publ., No. 5.

Lowry, N., Robertson, J.H.B., 1996. The effect of twine thichness on cod-end selectivity of trawls for haddock in the North Sea. Fish. Res. 26, 353-363.

O'Neill, F.G., Kynoch, R.J., 1996. The effect of cover mesh size and codend catch size on codend selectivity. Fish. Res. 28: 291-303.

O'Neill, F.G., Herrmann, B., 2007. PRESEMO a predictive model of codend selectivity – a tool for fisheries managers. ICES journal of Marine Science, 64: 1558-1568.

Wileman, D.A., Ferro, R.S.T., Fonteyne, R., Millar, R.B. (Editors), 1996. Manual of methods of measuring the selectivity of towed fishing gears. ICES Coop. Res. Rep. No. 215.

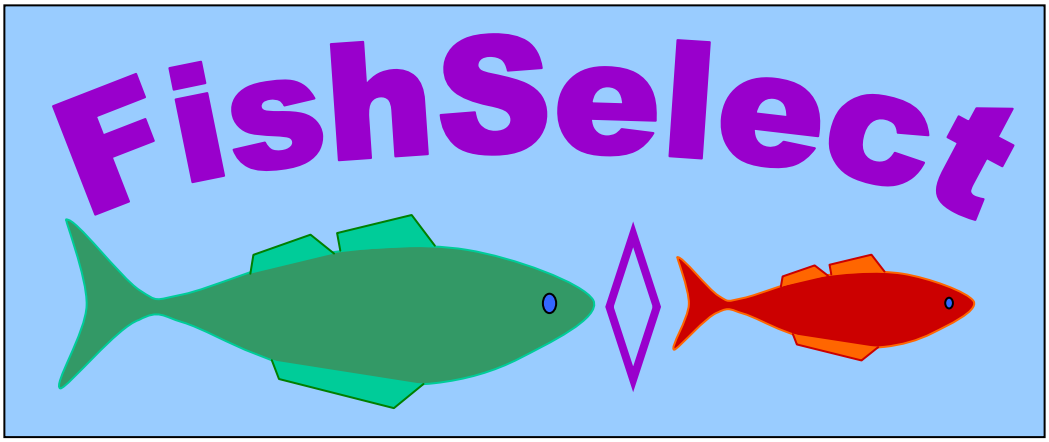

A5

A note on the FISHSELECT results for turbot

Turbot where caught in May 2007 by gillnets and by trawl using a research vessels ("Havfisken"). 31 living individuals were brought to tanks in the laboratory and used in the FISHSELECT experiments. Fig. 1 shows the size structure for these individuals.

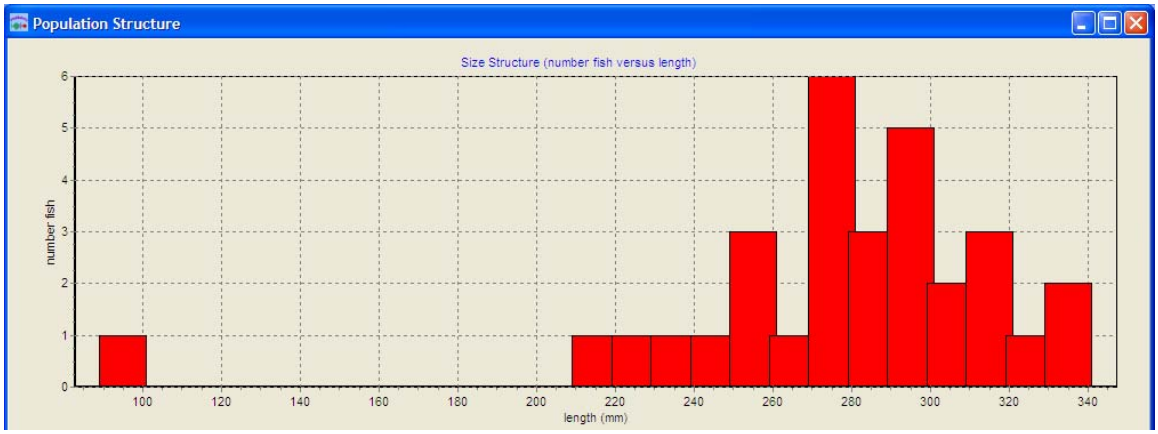

Fig. 1.

The cross section of the sole was measured three places alone the length: on the head representing the maximal stiff height (CS1), on the body representing the maximal width (CS3) and just behind the gill between CS1 and CS3. The measurements were carried out on a table using a single mechanical Morphometer due to the large width of turbots (Fig. 2).

Fig. 2.

Due to the width of large turbots special wide mechanical Morphometer was used for some individuals. It was assembled using two single morphometers. Fig. 3 shows the work in the laboratory with this including the scanning of the cross sections.

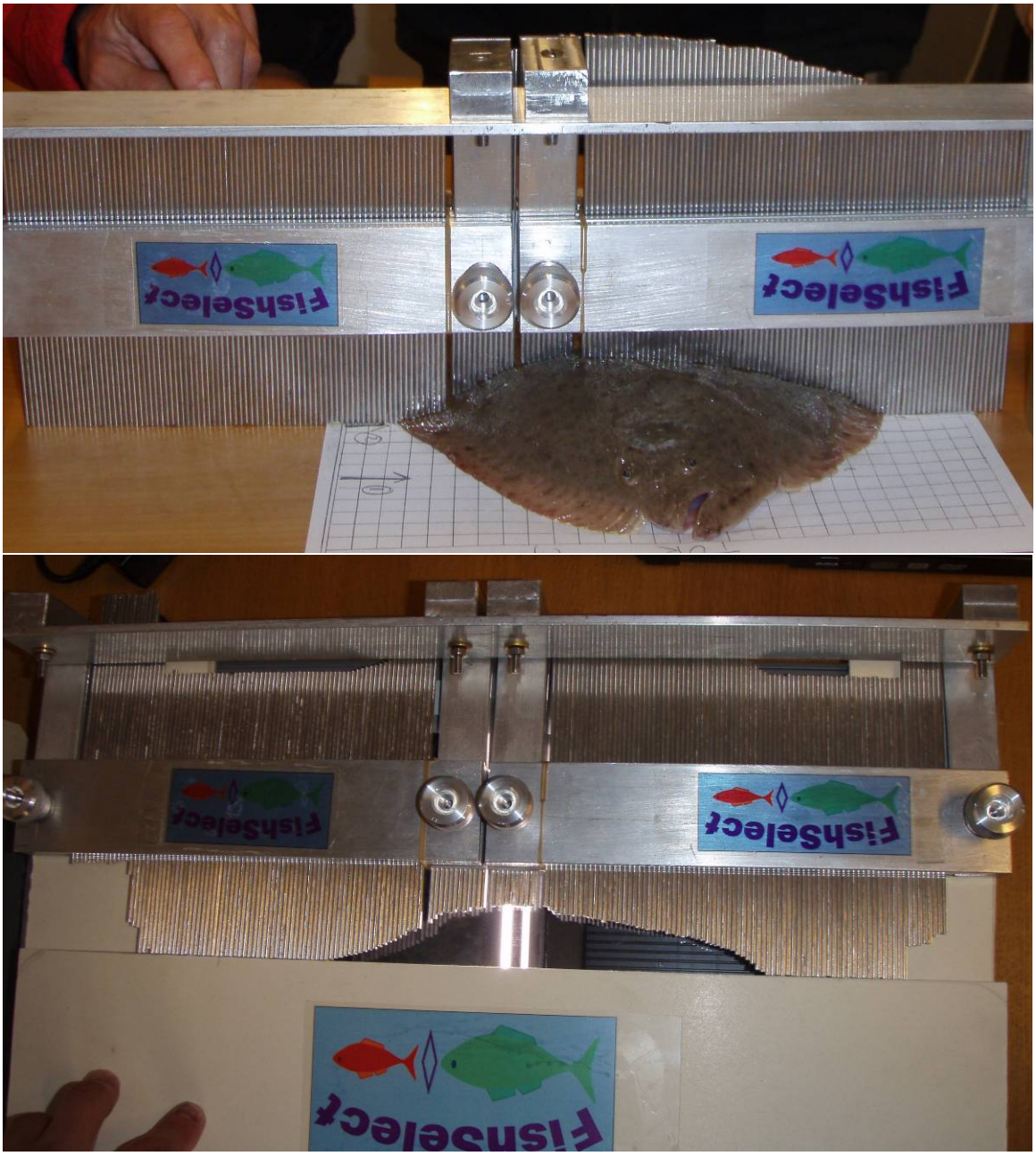

Fig. 3.

Fig. 4 shows the work in the laboratory with fall through experiments of the fish through the meshes in the mesh plates. The right hand picture illustrate that the turbot cross sections are very stiff compared to other species of flat fish maybe leading to a simple penetration model without much deformation to account for.

Fig. 4.

21 different mesh plates were used in the fall through experiments with a total of 132 different mesh holes (shapes: diamond (type=D), square (type=S), rectangle (type=R) and hexagonal (type=H)). With 31 sole in the experiment this makes 4092 fall through results. Table 1 summarizes the data for the individual 132 meshes used in the experiment using the developed syntax in the FISHSELECT software tool. The data listed is not nominal measures but is actual measures obtained by scanning each mesh hole, digitizing the contour using build in image analysis functionality in the FISHSELECT software tool as well as obtaining a parametric description using build in functionality for this.

Table 1.

ID=1;Type=D;m=77.69;oa=30.54;ID=2;Type=D;m=78.01;oa=55.58;ID=3;Type=D;m=80.27;oa=87.01;
ID=4;Type=D;m=88.20;oa=25.8;ID=5;Type=D;m=88.47;oa=30.92;ID=6;Type=D;m=88.80;oa=37.32;
ID=7;Type=D;m=88.35;oa=39.69;ID=8;Type=D;m=88.71;oa=45.85;ID=9;Type=D;m=89.75;oa=50.1;
ID=10;Type=D;m=89.26;oa=57.29;ID=11;Type=D;m=90.05;oa=60.08;ID=12;Type=D;m=89.76;oa=61.79;
ID=13;Type=D;m=90.59;oa=69.79;ID=14;Type=D;m=89.26;oa=76.33;ID=15;Type=D;m=90.38;oa=81.45;
ID=16;Type=D;m=89.70;oa=85.36;ID=17;Type=D;m=91.16;oa=89.99;ID=18;Type=D;m=100.78;oa=19.87;
ID=19;Type=D;m=98.31;oa=56.16;ID=20;Type=D;m=99.84;oa=86.21;ID=21;Type=D;m=109.42;oa=20.31;
ID=22;Type=D;m=109.56;oa=55.22;ID=23;Type=D;m=109.18;oa=86.48;ID=24;Type=D;m=118.27;oa=19.67;
ID=25;Type=D;m=114.16;oa=26.49;ID=26;Type=D;m=118.83;oa=31.73;ID=27;Type=D;m=117.90;oa=35.61;
ID=28;Type=D;m=118.35;oa=41.37;ID=29;Type=D;m=118.23;oa=46.22;ID=30;Type=D;m=119.86;oa=50.09;
ID=31;Type=D;m=118.94;oa=57.41;ID=32;Type=D;m=120.37;oa=60.67;ID=33;Type=D;m=119.71;oa=65.01;
ID=34;Type=D;m=118.48;oa=71.46;ID=35;Type=D;m=121.59;oa=77.86;ID=36;Type=D;m=120.31;oa=81.51;
ID=37;Type=D;m=120.52;oa=86.74;ID=38;Type=D;m=126.68;oa=19.89;ID=39;Type=D;m=128.99;oa=56.63;
ID=40;Type=D;m=129.98;oa=86.59;ID=41;Type=D;m=140.39;oa=19.84;ID=42;Type=D;m=138.48;oa=55.95;
ID=43;Type=D;m=140.23;oa=85.85;ID=44;Type=D;m=163.35;oa=14.39;ID=45;Type=D;m=158.72;oa=20.57;
ID=46;Type=D;m=158.13;oa=25.07;ID=47;Type=D;m=159.35;oa=30.48;ID=48;Type=D;m=157.85;oa=35.52;
ID=49;Type=D;m=159.03;oa=40.22;ID=50;Type=D;m=160.04;oa=46.09;ID=51;Type=D;m=159.03;oa=51.43;
ID=52;Type=D;m=160.76;oa=56.13;ID=53;Type=D;m=160.54;oa=60.74;ID=54;Type=D;m=160.56;oa=66.13;
ID=55;Type=D;m=161.10;oa=71.33;ID=56;Type=D;m=160.77;oa=76.62;ID=57;Type=D;m=159.68;oa=80.65;
ID=58;Type=D;m=160.97;oa=85.57;ID=59;Type=D;m=177.19;oa=15.68;ID=60;Type=D;m=180.96;oa=56.47;
ID=61;Type=D;m=182.90;oa=86.00;ID=62;Type=D;m=195.97;oa=15.85;ID=63;Type=D;m=200.40;oa=55.71;
ID=64;Type=D;m=200.30;oa=86.89;ID=65;Type=S;b=34.67;ID=66;Type=S;b=40.07;ID=67;Type=S;b=50.14;
ID=68;Type=S;b=60.23;ID=69;Type=S;b=69.69;ID=70;Type=S;b=80.08;ID=71;Type=S;b=89.95;
ID=72;Type=S;b=100.27;ID=73;Type=R;b=90.59;a=9.81;ID=74;Type=R;b=90.96;a=14.49;
ID=75;Type=R;b=91.35;a=19.33;ID=76;Type=R;b=91.05;a=29.19;ID=77;Type=R;b=91.23;a=49.01;
ID=78;Type=R;b=91.79;a=68.83;ID=79;Type=R;b=120.42;a=8.99;ID=80;Type=R;b=121.67;a=14.85;
ID=81;Type=R;b=122.15;a=19.38;ID=82;Type=R;b=121.61;a=29.57;ID=83;Type=R;b=122.40;a=48.84;

ID=84;Type=R;b=121.93;a=69.02;ID=85;Type=R;b=202.66;a=9.89;ID=86;Type=R;b=203.93;a=14.28;
ID=87;Type=R;b=203.45;a=19.02;ID=88;Type=R;b=200.19;a=29.96;ID=89;Type=R;b=203.26;a=49.13;
ID=90;Type=R;b=203.62;a=69.37;ID=91;Type=H;b=17.49;k=35.25;oa=142.05;ID=92;Type=H;b=17.61;k=36.17;oa=130.44;
ID=93;Type=H;b=18.06;k=36.51;oa=103.65;ID=94;Type=H;b=17.02;k=35.71;oa=86.08;
ID=95;Type=H;b=20.25;k=39.95;oa=147.81;ID=96;Type=H;b=20.35;k=39.75;oa=126.92;
ID=97;Type=H;b=19.96;k=39.31;oa=107.59;ID=98;Type=H;b=19.98;k=40.81;oa=91.84;
ID=99;Type=H;b=25.37;k=50.15;oa=143.40;ID=100;Type=H;b=24.91;k=49.24;oa=126.33;
ID=101;Type=H;b=26.22;k=48.60;oa=102.92;ID=102;Type=H;b=26.04;k=48.05;oa=89.54;
ID=103;Type=H;b=29.74;k=59.42;oa=143.88;ID=104;Type=H;b=30.53;k=60.21;oa=128.98;
ID=105;Type=H;b=29.86;k=59.42;oa=105.49;ID=106;Type=H;b=29.94;k=59.80;oa=88.85;
ID=107;Type=H;b=35.15;k=68.93;oa=142.28;ID=108;Type=H;b=34.18;k=70.03;oa=128.34;
ID=109;Type=H;b=35.29;k=69.42;oa=106.33;ID=110;Type=H;b=35.62;k=69.47;oa=89.76;
ID=111;Type=H;b=40.78;k=80.51;oa=145.98;ID=112;Type=H;b=40.66;k=79.42;oa=129.65;
ID=113;Type=H;b=40.34;k=80.04;oa=105.87;ID=114;Type=H;b=41.03;k=80.19;oa=88.19;
ID=115;Type=H;b=49.89;k=99.69;oa=141.66;ID=116;Type=H;b=50.59;k=99.35;oa=127.28;
ID=117;Type=H;b=50.47;k=99.31;oa=106.32;ID=118;Type=H;b=50.97;k=98.67;oa=88.05;
ID=119;Type=D;m=66.38;oa=26.86;ID=120;Type=D;m=67.25;oa=29.74;ID=121;Type=D;m=67.66;oa=37.95;
ID=122;Type=D;m=67.59;oa=41.83;ID=123;Type=D;m=67.81;oa=44.22;ID=124;Type=D;m=67.61;oa=51.56;
ID=125;Type=D;m=68.85;oa=55.10;ID=126;Type=D;m=69.35;oa=63.60;ID=127;Type=D;m=70.11;oa=64.87;
ID=128;Type=D;m=68.44;oa=69.86;ID=129;Type=D;m=69.33;oa=74.24;ID=130;Type=D;m=68.80;oa=79.65;
ID=131;Type=D;m=70.12;oa=85.60;ID=132;Type=D;m=69.69;oa=89.67;

For each sole the three cross sections were digitized and it was found that an asymmetrical trapezoid provided the best description of the shapes. Fig. 5 shows the detection of contour in the scanned image of the mechanical MorphoMeter of the body of one turbot. While Fig. 6 show the fits of an asymmetrical trapezoid to the digitized contours of the three cross sections.

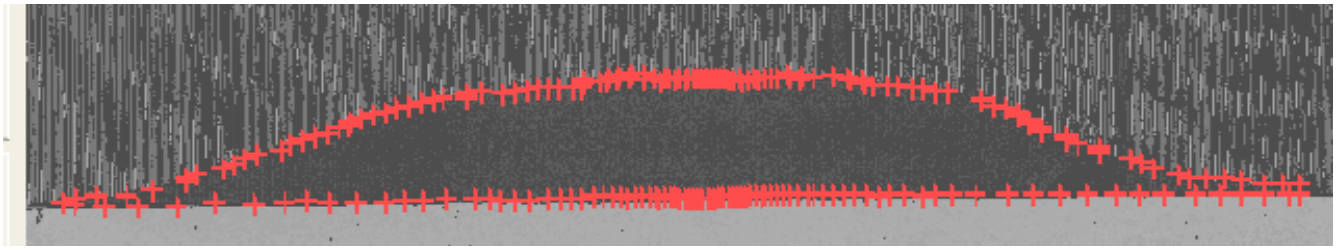

Fig. 5

Fig. 6.

This procedure was carried out for each individual and regression describing the relationships between the length and the parameters the asymmetrical trapezoid (bottom width, top width, height and top translation) for each cross section were obtained according to the FISHSELECT methodology. For the 31 individuals fitting an asymmetrical trapezoid to the cross section we found the following overall fit statistics (Table 2).

Table 2

Cross section No.	Mean deviation (mm)	sd mean deviation (mm)	Maximum deviation (mm)	sd Maximum deviation (mm)
1	0.68	0.08	2.80	0.27
2	0.94	0.06	4.54	0.33
3	0.92	0.07	4.05	0.27

Making the regressions for the length to parameter values leads to the results shown in Fig. 7-9 and Table 3.

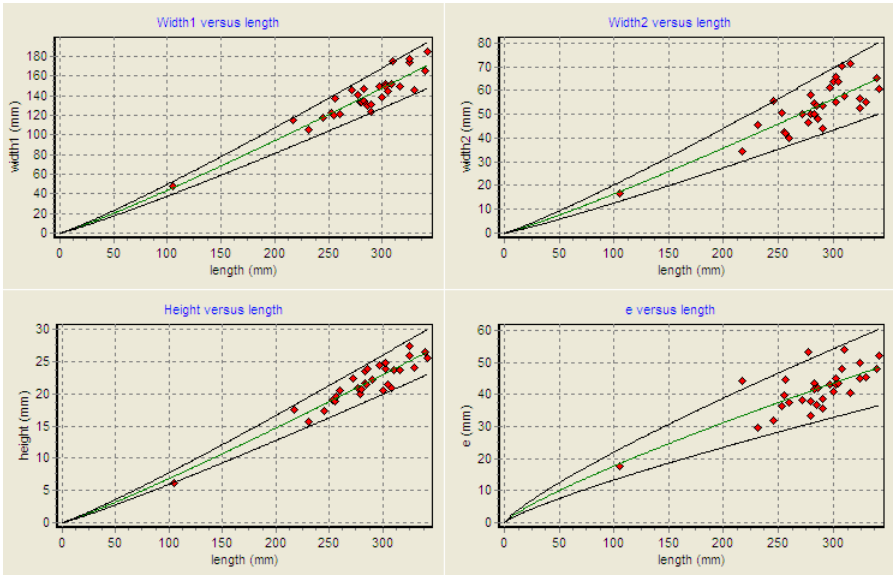

Fig. 7. CS1

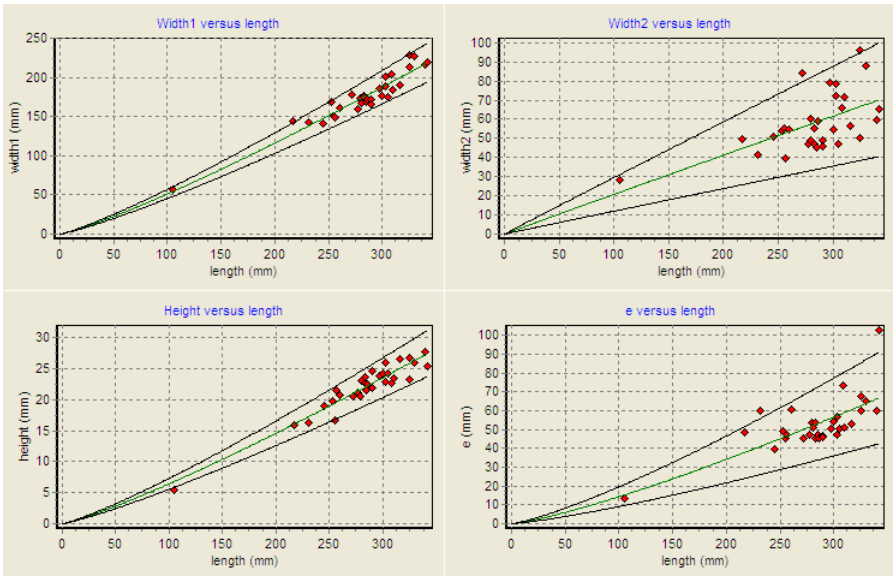

Fig. 8. CS2

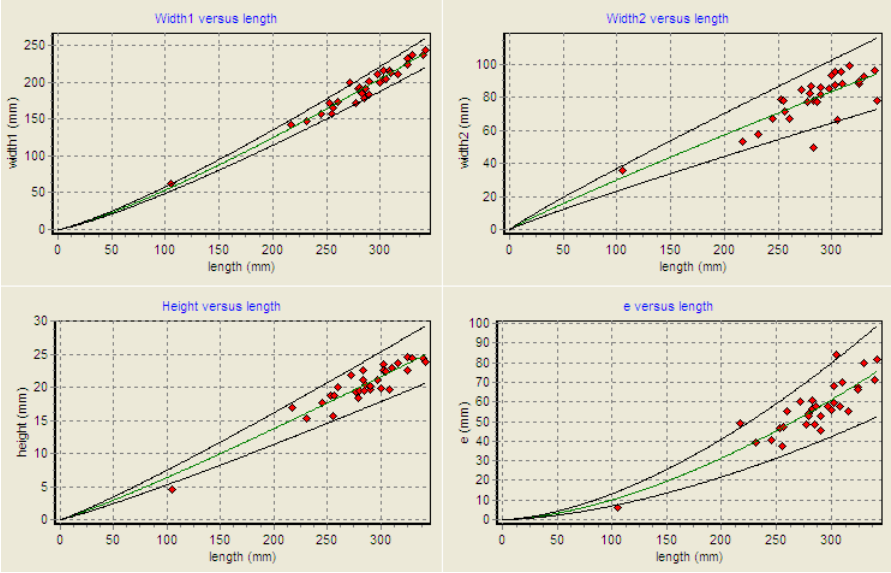

Fig. 9. CS3

Table 3.

D1:Coef=0.00000971;sd=0.00000087;Po=3.1200;R2=0.96;"Weight versus length"
D2:Coef=0.34010986;sd=0.01455621;Po=1.2700;R2=0.96;"Girth versus length"
D3:Coef=39.02153109;sd=1.74532492;Po=0.4000;R2=0.97;"Girth versus weight"
Section 1
Type=ATR
D4:Coef=0.26295767;sd=0.01818224;Po=1.1100;R2=0.85;"Width1 versus length"
D5:Coef=0.09484399;sd=0.01099674;Po=1.1200;R2=0.69;"Width2 versus length"
D6:Coef=1.19084706;sd=0.17480314;Po=0.7700;R2=0.55;"Width2 versus width1"
D7:Coef=0.04323858;sd=0.00285988;Po=1.1000;R2=0.88;"Height versus length"
D8:Coef=0.40568664;sd=0.04984409;Po=0.8200;R2=0.57;"e versus length"
Section 2
Type=ATR
D4:Coef=0.22421273;sd=0.01274989;Po=1.1800;R2=0.91;"Width1 versus length"
D5:Coef=0.21741873;sd=0.04599627;Po=0.9900;R2=0.33;"Width2 versus length"
D6:Coef=0.36675934;sd=0.07290400;Po=0.9800;R2=0.44;"Width2 versus width1"
D7:Coef=0.02813538;sd=0.00191477;Po=1.1800;R2=0.91;"Height versus length"
D8:Coef=0.04546273;sd=0.00828235;Po=1.2500;R2=0.49;"e versus length"
Section 3
Type=ATR
D4:Coef=0.19444402;sd=0.00802288;Po=1.2200;R2=0.96;"Width1 versus length"
D5:Coef=0.41525501;sd=0.04731338;Po=0.9300;R2=0.63;"Width2 versus length"
D6:Coef=1.38920992;sd=0.15382754;Po=0.7700;R2=0.65;"Width2 versus width1"
D7:Coef=0.03841474;sd=0.00334379;Po=1.1100;R2=0.88;"Height versus length"
D8:Coef=0.00528345;sd=0.00081122;Po=1.6400;R2=0.76;"e versus length"

Fig. 7-9 shows that the FISHSELECT regression models can describe the relationships reasonable including the between individuals variation. The R2-values are in general on an acceptable level for all parameters and very good for widths at the bottom of the cross sections and for the heights (see Table 3).

Several penetration model building on CS1, CS2 and CS3 alone and in combinations assuming different levels of symmetrical or asymmetrical compression as well as cutting of height being below a certain percentage of the maximal height was tested against the experimental fall through results. More than 200 000 models were tested. Based on comparing the degree of agreement for these models it became clear that for turbot it was sufficient only to take CS3 into account. Further it was found that no compression in the

height did lead to the best results which complied well with the observations make during the fall through experiments. Therefore, to fine tune the model a series of penetration models for only CS3 assuming zero compression in width and height and only differing by assuming different percentage of width cut. In Fig. 10 we plot the number of disagreements width the experimental fall through experiments for the different CS3 models only taking cut into account. In the Fig. 10 it is seen that the lowest number of disagreements 44 is found assuming 21% cut while a model based on zero cut would lead to 105 disagreements. Thus a model based on only the morphological parameters without cross section deformation as would be the case without using the FISHSELECT methodology to identify the most appropriate model would have 2.4 times (105/44) as many disagreements. This illustrates the power of using the FISHSELECT methodology. Thus we base predictions on the best on these models. The 44 disagreements correspond to a level of agreement at 98.9% based a total of 4092 experimental fall through results. We consider this level of agreement to be very fine.

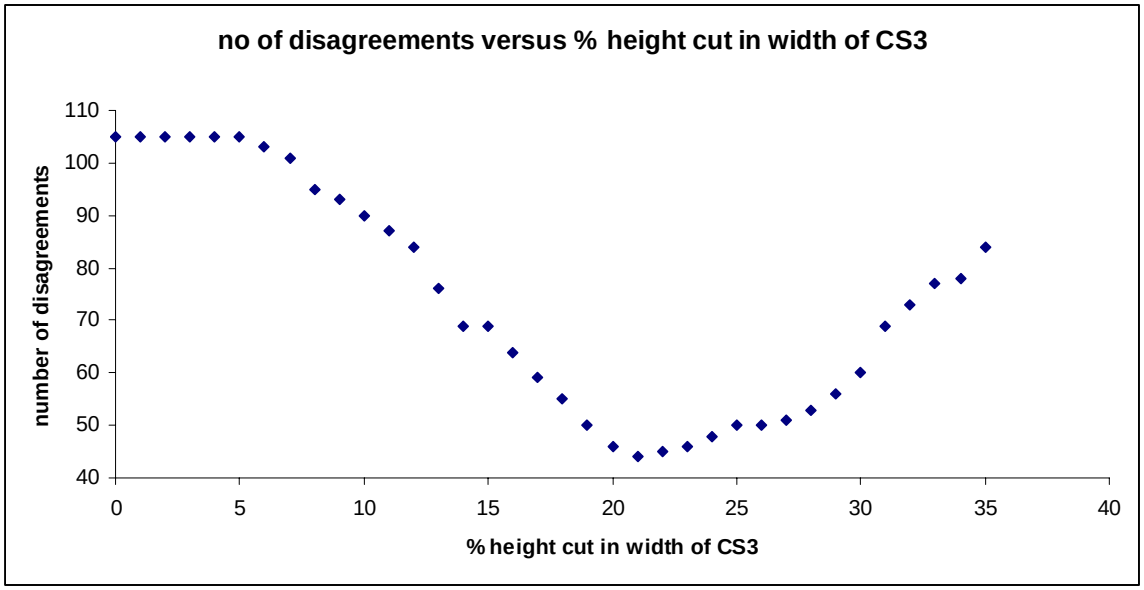

Fig. 10

Fig. 11 illustrates the use of different levels of cut on a typical turbot cross section 3. Top without cut, in centre the model selected for prediction and at bottom cut increased by 10% relative to the model selected.

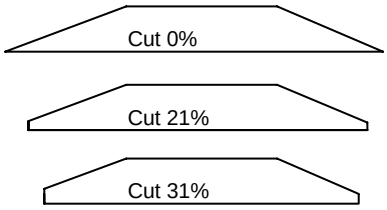

Fig. 11

Based on the regression models for the relationship for the parametric description of the

cross section sizes and shapes versus length including the between individuals variation a virtual population of 2000 turbots was created with lengths being uniformly distributed between 30 mm and 600 mm. Together with the selected penetration model this virtual population was applied to predict the basic selective properties for stiff diamond shaped meshes through simulations using the FISHSELECT software tool. Mesh sizes were in the range 70 mm to 200 mm in steps of 10 mm thus making a total of 14 different mesh sizes. For each mesh size mesh openness angles from 10 degrees to 90 degrees in steps of 5 degrees were simulated. This makes 17 different opening angles (OA) for each mesh size. This makes a total of 238 different diamond meshes. For each of these meshes it was then simulated weather or not each of the 2000 virtual turbots could pass through the mesh. In total this makes 476 000 simulated penetration attempt results. This takes 2-4 days to run on a desktop computer depending on its processor. By processing these results using the design guide functionality in the FISHSELECT software tool the 2000 results for each mesh is automatically applied to create a retention data file similar to the file format obtained for cod-end selecting by experimental fishing using the covered cod-end method. This involves sorting the penetration results into length classes 10 mm width each containing the results for the number of the fish in the virtual population width length ± 5 mm of the middle point in the length class. Table 4 shows a part one (up to length 25.5 cm) of one of these retention data files. In the Table *noRet.* represents the number of fish in the length class that was simulated to be able to pass through the mesh. While *noTotal* is the total number of fish of the 2000 with length within that specific length class.

Table 4.

Length	**noRet.**	**noTotal**
3.5	0	38
4.5	0	31
5.5	0	40
6.5	0	51
7.5	0	48
8.5	0	31
9.5	0	19
10.5	0	36
11.5	0	36
12.5	0	31
13.5	0	35
14.5	0	37
15.5	0	43
16.5	0	34
17.5	0	24
18.5	5	35
19.5	14	34
20.5	24	26
21.5	35	35
22.5	42	42
23.5	27	27
24.5	38	38
25.5	50	50

The tool then automatically fit a logistic function to the retention data for each mesh applying a maximum likelihood estimator build into the software tool. The result of this process is a file containing estimates of the basic 50% retention length L50 and the selection range SR for each mesh according to the FISHSELECT methodology. Table 5 contains the first part of this file.

Table 5.

M	oa	L50	SR
70	10	6.67	0.46
70	15	8.38	0.71
70	20	9.49	0.07
70	25	10.09	0.81
70	30	10.76	0.89
70	35	11.2	0.74
70	40	11.53	0.62
70	45	11.72	0.66
70	50	11.74	0.57
70	55	11.74	0.57
70	60	11.69	0.6
70	65	11.41	0.51
70	70	11.18	0.66
70	75	10.87	0.56
70	80	10.67	0.6
70	85	10.23	0.63
70	90	9.95	0.56
80	10	7.47	0.66
80	15	9.44	0.17
80	20	10.52	0.87
80	25	11.45	0.82
80	30	12.15	0.64
80	35	12.79	0.67
80	40	13.02	0.57
80	45	13.12	0.57

The data in the of which Table 5 is a part of represents the design guide for diamond shaped stiff meshes with respect to Turbot. m is the mesh size in mm and oa the full mesh opening angle in degrees. L50 and SR are in units cm. The design guide data can be presented by a so called iso plot for L50 which consists of curves with equal L50 estimates for combinations of mesh size and opening angle. Fig. 12 shows this.

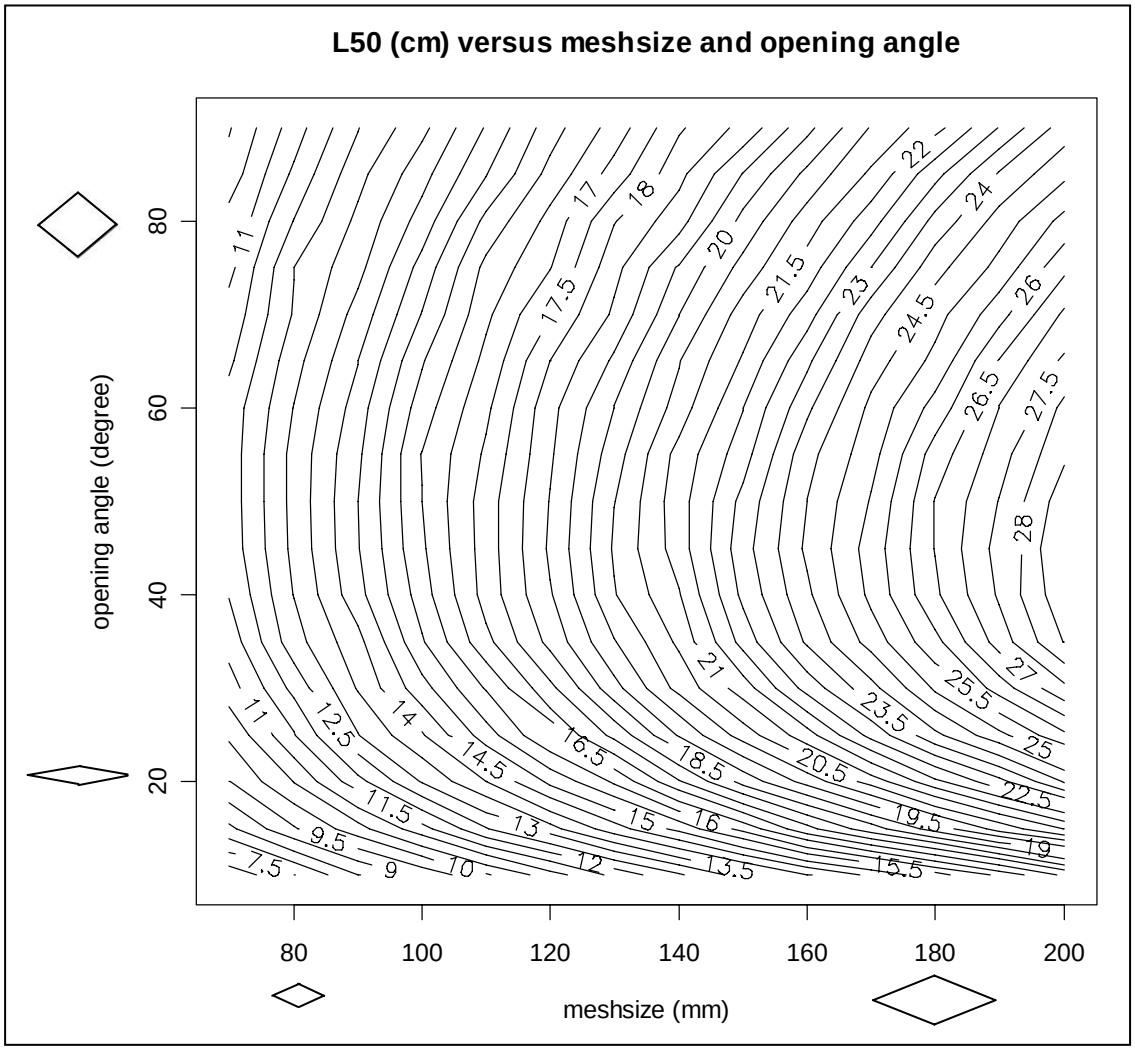

Fig. 12.

Inspecting Fig. 12 is evident that the legal 90 mm mesh size for Kattegat-Skagerak is not in balance with the minimum landing size MLS at 30 cm for Turbot in the trawl fishery as this would require a mesh size of more than 200 mm. From Fig. 12 thus it is seen that we predict that the legal mesh size would at best lead to retention of approximately 50% of the individuals being sized 47% of MLS. From Fig. 12 it is also seen that the retention properties depend on the opening angle thus the maximum is between 40 to 55 degrees openness.

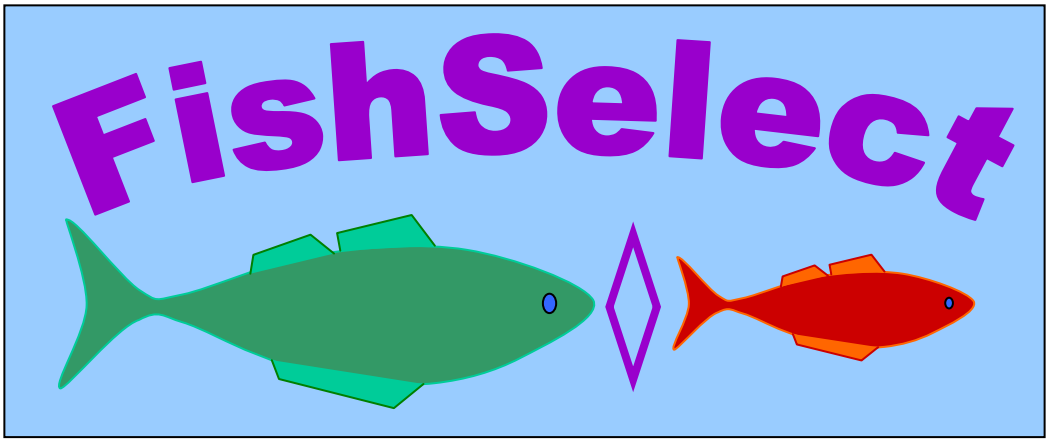

A6

A note on the FISHSELECT results for Lemon Sole

Lemon Soles where caught by gillnets and by trawl fishing from a research vessels ("Havfisken") and from a commercial vessel in May 2007. 69 living individuals were brought to tanks in the laboratory and used in the FISHSELECT experiments. Fig. 1 shows the size structure for these individuals.

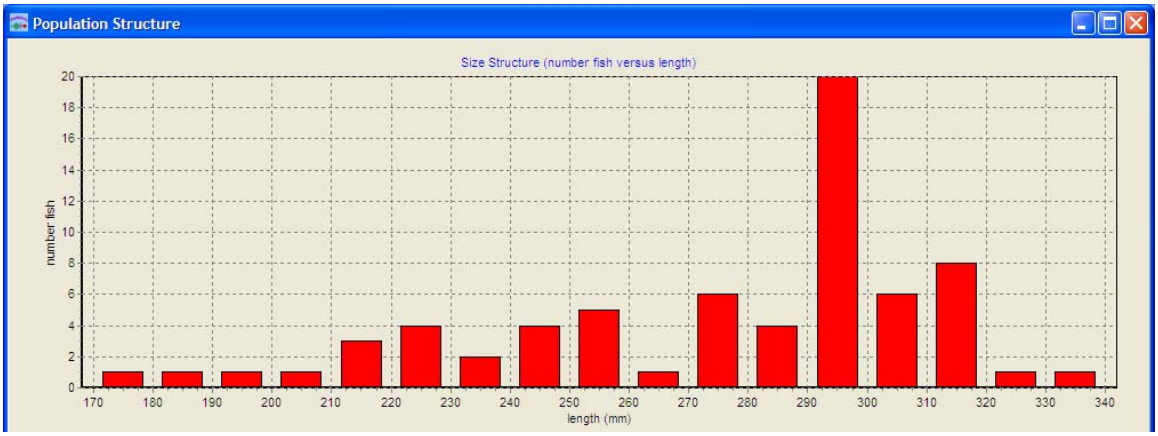

Fig. 1.

The cross section of the lemon sole was measured three places alone the length: on the head representing the maximal stiff height (CS1), on the body representing the maximal width (CS3) and just behind the gill between CS1 and CS3. The measurements were carried out on a table using a single mechanical Morphometer. Fig. 2 shows the position of the cross sections.

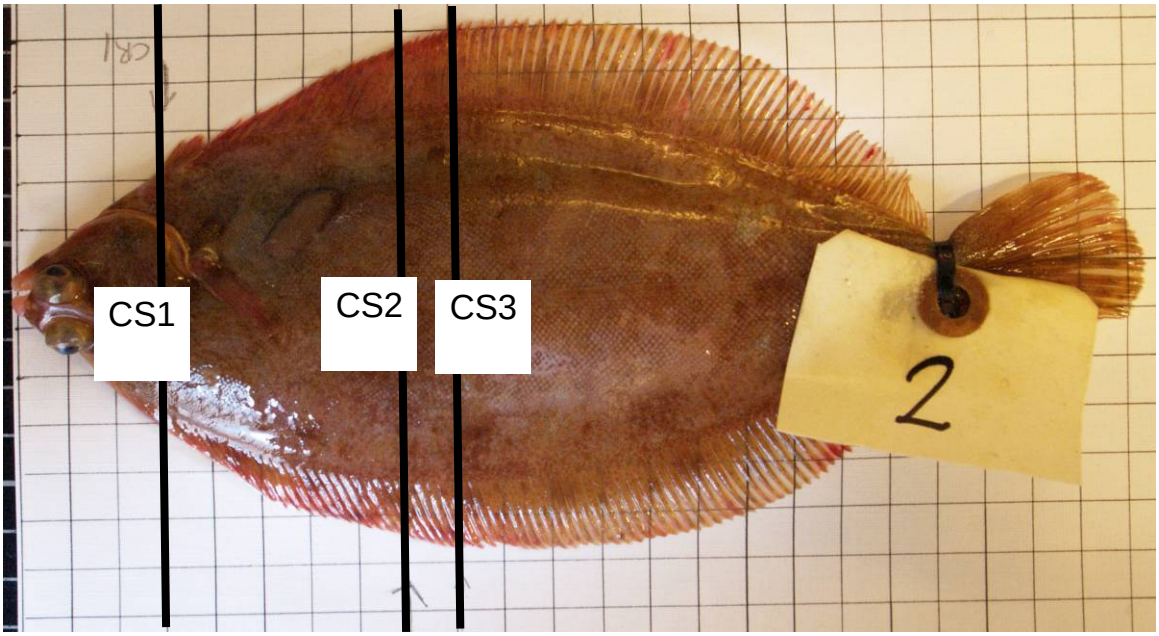

Fig. 2.

Fig. 3 shows the work in the laboratory with acquiring the cross sections including scanning of the Morphometer using the flatbed scanner and saving the data in a laptop computer.

Fig. 3.

Fig. 4 shows the work in the laboratory with fall through experiments of the fish through the meshes in the mesh plates. The right hand picture illustrate that the lemon sole cross sections are flexible which maybe necessary to take into account when defining a suitable penetration model.

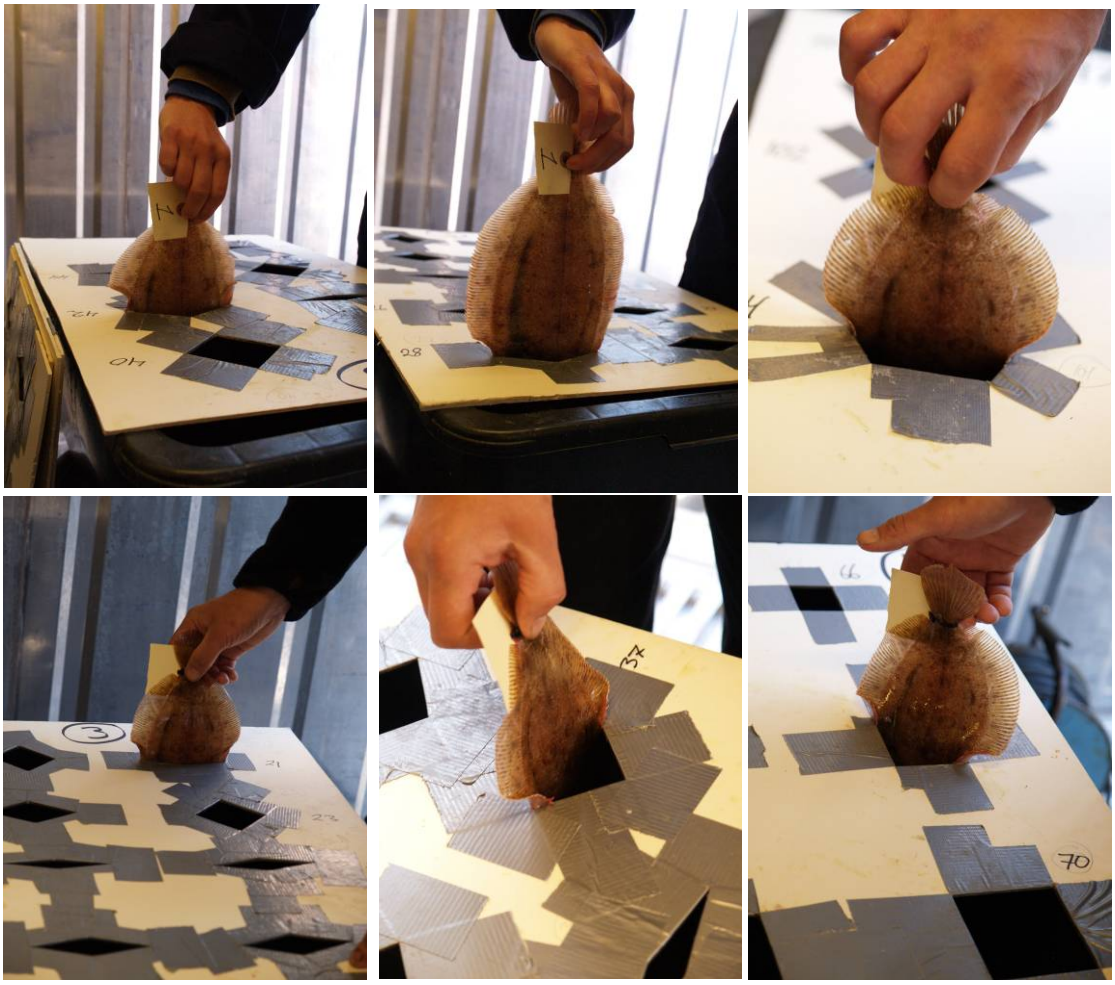
Fig. 4.

21 different mesh plates were used in the fall through experiments with a total of 132 different mesh holes (shapes: diamond (type=D), square (type=S), rectangle (type=R) and hexagonal (type=H)). With 31 sole in the experiment this makes 4092 fall through results. Table 1 summarizes the data for the individual 132 meshes used in the experiment using the developed syntax in the FISHSELECT software tool. The data listed is not nominal measures but is actual measures obtained by scanning each mesh hole, digitizing the contour using build in image analysis functionality in the FISHSELECT software tool as well as obtaining a parametric description using build in functionality for this.

Table 1.

ID=1;Type=D;m=77.69;oa=30.54;ID=2;Type=D;m=78.01;oa=55.58;ID=3;Type=D;m=80.27;oa=87.01;
ID=4;Type=D;m=88.20;oa=25.8;ID=5;Type=D;m=88.47;oa=30.92;ID=6;Type=D;m=88.80;oa=37.32;
ID=7;Type=D;m=88.35;oa=39.69;ID=8;Type=D;m=88.71;oa=45.85;ID=9;Type=D;m=89.75;oa=50.1;
ID=10;Type=D;m=89.26;oa=57.29;ID=11;Type=D;m=90.05;oa=60.08;ID=12;Type=D;m=89.76;oa=61.79;
ID=13;Type=D;m=90.59;oa=69.79;ID=14;Type=D;m=89.26;oa=76.33;ID=15;Type=D;m=90.38;oa=81.45;
ID=16;Type=D;m=89.70;oa=85.36;ID=17;Type=D;m=91.16;oa=89.99;ID=18;Type=D;m=100.78;oa=19.87;
ID=19;Type=D;m=98.31;oa=56.16;ID=20;Type=D;m=99.84;oa=86.21;ID=21;Type=D;m=109.42;oa=20.31;
ID=22;Type=D;m=109.56;oa=55.22;ID=23;Type=D;m=109.18;oa=86.48;ID=24;Type=D;m=118.27;oa=19.67;
ID=25;Type=D;m=114.16;oa=26.49;ID=26;Type=D;m=118.83;oa=31.73;ID=27;Type=D;m=117.90;oa=35.61;
ID=28;Type=D;m=118.35;oa=41.37;ID=29;Type=D;m=118.23;oa=46.22;ID=30;Type=D;m=119.86;oa=50.09;
ID=31;Type=D;m=118.94;oa=57.41;ID=32;Type=D;m=120.37;oa=60.67;ID=33;Type=D;m=119.71;oa=65.01;
ID=34;Type=D;m=118.48;oa=71.46;ID=35;Type=D;m=121.59;oa=77.86;ID=36;Type=D;m=120.31;oa=81.51;
ID=37;Type=D;m=120.52;oa=86.74;ID=38;Type=D;m=126.68;oa=19.89;ID=39;Type=D;m=128.99;oa=56.63;
ID=40;Type=D;m=129.98;oa=86.59;ID=41;Type=D;m=140.39;oa=19.84;ID=42;Type=D;m=138.48;oa=55.95;
ID=43;Type=D;m=140.23;oa=85.85;ID=44;Type=D;m=163.35;oa=14.39;ID=45;Type=D;m=158.72;oa=20.57;
ID=46;Type=D;m=158.13;oa=25.07;ID=47;Type=D;m=159.35;oa=30.48;ID=48;Type=D;m=157.85;oa=35.52;
ID=49;Type=D;m=159.03;oa=40.22;ID=50;Type=D;m=160.04;oa=46.09;ID=51;Type=D;m=159.03;oa=51.43;
ID=52;Type=D;m=160.76;oa=56.13;ID=53;Type=D;m=160.54;oa=60.74;ID=54;Type=D;m=160.56;oa=66.13;
ID=55;Type=D;m=161.10;oa=71.33;ID=56;Type=D;m=160.77;oa=76.62;ID=57;Type=D;m=159.68;oa=80.65;
ID=58;Type=D;m=160.97;oa=85.57;ID=59;Type=D;m=177.19;oa=15.68;ID=60;Type=D;m=180.96;oa=56.47;
ID=61;Type=D;m=182.90;oa=86.00;ID=62;Type=D;m=195.97;oa=15.85;ID=63;Type=D;m=200.40;oa=55.71;
ID=64;Type=D;m=200.30;oa=86.89;ID=65;Type=S;b=34.67;ID=66;Type=S;b=40.07;ID=67;Type=S;b=50.14;
ID=68;Type=S;b=60.23;ID=69;Type=S;b=69.69;ID=70;Type=S;b=80.08;ID=71;Type=S;b=89.95;
ID=72;Type=S;b=100.27;ID=73;Type=R;b=90.59;a=9.81;ID=74;Type=R;b=90.96;a=14.49;
ID=75;Type=R;b=91.35;a=19.33;ID=76;Type=R;b=91.05;a=29.19;ID=77;Type=R;b=91.23;a=49.01;
ID=78;Type=R;b=91.79;a=68.83;ID=79;Type=R;b=120.42;a=8.99;ID=80;Type=R;b=121.67;a=14.85;
ID=81;Type=R;b=122.15;a=19.38;ID=82;Type=R;b=121.61;a=29.57;ID=83;Type=R;b=122.40;a=48.84;
ID=84;Type=R;b=121.93;a=69.02;ID=85;Type=R;b=202.66;a=9.89;ID=86;Type=R;b=203.93;a=14.28;
ID=87;Type=R;b=203.45;a=19.02;ID=88;Type=R;b=200.19;a=29.96;ID=89;Type=R;b=203.26;a=49.13;
ID=90;Type=R;b=203.62;a=69.37;ID=91;Type=H;b=17.49;k=35.25;oa=142.05;ID=92;Type=H;b=17.61;k=36.17;oa=130.44;
ID=93;Type=H;b=18.06;k=36.51;oa=103.65;ID=94;Type=H;b=17.02;k=35.71;oa=86.08;
ID=95;Type=H;b=20.25;k=39.95;oa=147.81;ID=96;Type=H;b=20.35;k=39.75;oa=126.92;
ID=97;Type=H;b=19.96;k=39.31;oa=107.59;ID=98;Type=H;b=19.98;k=40.81;oa=91.84;
ID=99;Type=H;b=25.37;k=50.15;oa=143.40;ID=100;Type=H;b=24.91;k=49.24;oa=126.33;
ID=101;Type=H;b=26.22;k=48.60;oa=102.92;ID=102;Type=H;b=26.04;k=48.05;oa=89.54;
ID=103;Type=H;b=29.74;k=59.42;oa=143.88;ID=104;Type=H;b=30.53;k=60.21;oa=128.98;
ID=105;Type=H;b=29.86;k=59.42;oa=105.49;ID=106;Type=H;b=29.94;k=59.80;oa=88.85;
ID=107;Type=H;b=35.15;k=68.93;oa=142.28;ID=108;Type=H;b=34.18;k=70.03;oa=128.34;
ID=109;Type=H;b=35.29;k=69.42;oa=106.33;ID=110;Type=H;b=35.62;k=69.47;oa=89.76;
ID=111;Type=H;b=40.78;k=80.51;oa=145.98;ID=112;Type=H;b=40.66;k=79.42;oa=129.65;
ID=113;Type=H;b=40.34;k=80.04;oa=105.87;ID=114;Type=H;b=41.03;k=80.19;oa=88.19;
ID=115;Type=H;b=49.89;k=99.69;oa=141.66;ID=116;Type=H;b=50.59;k=99.35;oa=127.28;
ID=117;Type=H;b=50.47;k=99.31;oa=106.32;ID=118;Type=H;b=50.97;k=98.67;oa=88.05;
ID=119;Type=D;m=66.38;oa=26.86;ID=120;Type=D;m=67.25;oa=29.74;ID=121;Type=D;m=67.66;oa=37.95;
ID=122;Type=D;m=67.59;oa=41.83;ID=123;Type=D;m=67.81;oa=44.22;ID=124;Type=D;m=67.61;oa=51.56;
ID=125;Type=D;m=68.85;oa=55.10;ID=126;Type=D;m=69.35;oa=63.60;ID=127;Type=D;m=70.11;oa=64.87;
ID=128;Type=D;m=68.44;oa=69.86;ID=129;Type=D;m=69.33;oa=74.24;ID=130;Type=D;m=68.80;oa=79.65;
ID=131;Type=D;m=70.12;oa=85.60;ID=132;Type=D;m=69.69;oa=89.67;

For each lemon sole the three cross sections were digitized and it was investigated how well the basic shapes ELL (ellipse), HEL (half ellipse), TRI (triangle), TRA (symmetrical trapezoid) and ATR (asymmetrical trapezoid). Table 2 (CS1), 3 (CS2) and 4 (CS3) list the main fit statistic from this based on all 69 lemon soles in this study. It was found that an asymmetrical trapezoid provided the best description of the shapes giving the smallest max mean deviation between digitized shapes and the parametric fitted basic shapes. Fig. 5 shows the detection of contour in the scanned image of the mechanical Morphometer of the body of one lemon sole. While Fig. 6 Show the fits of an asymmetrical trapezoid to the digitized contours of the three cross sections for one individual.

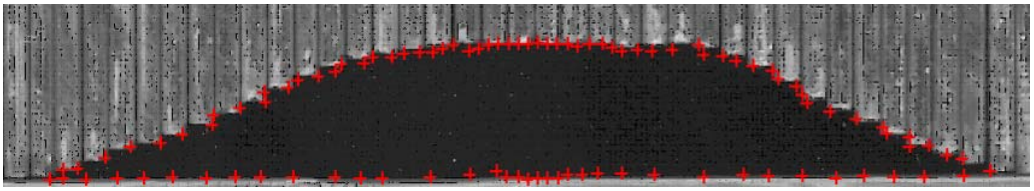

Fig. 5

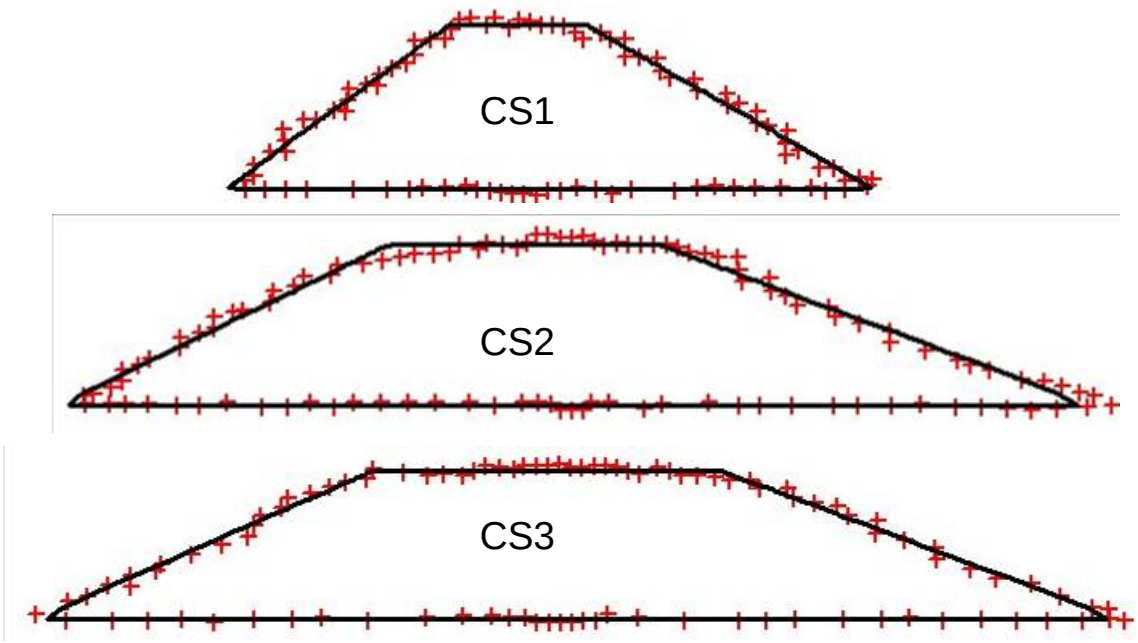

Fig. 6.

Traditionally ellipses are used for cross section descriptions for use in models predicting mesh penetration. Fig. 7 compared with Fig. 6 together with the mean fit statistics in Tables 2-4 highlights that this is a much poorer description than using the asymmetrical trapezoid to describe cross section shapes on lemon sole.

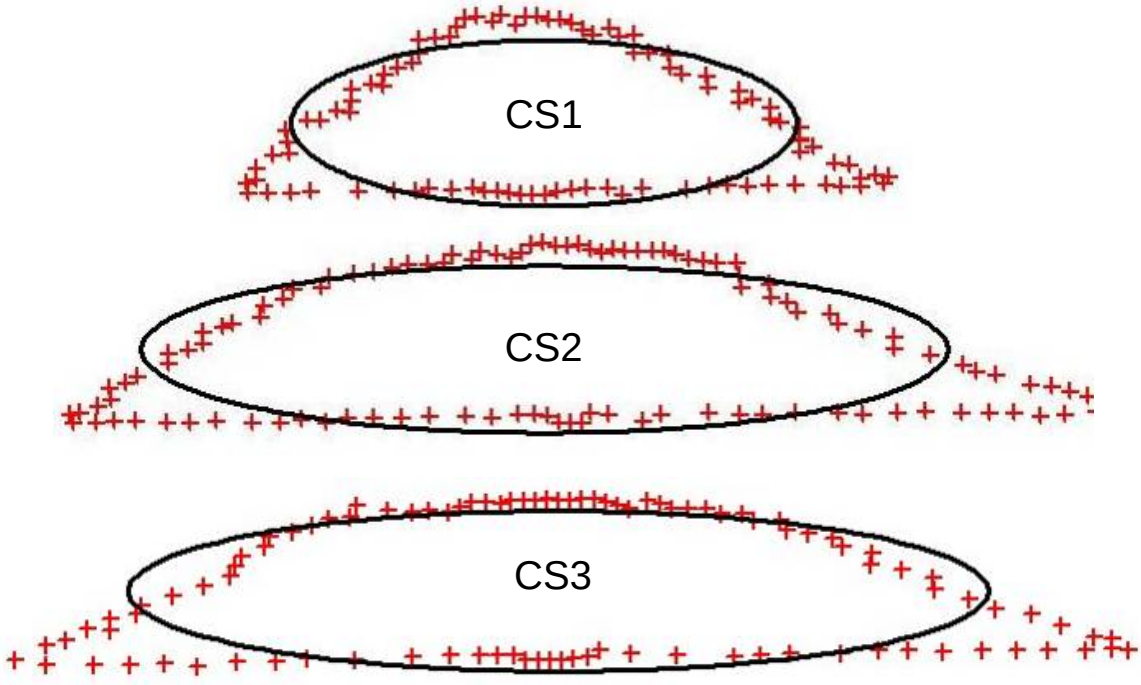

Fig. 7

Table 2: CS1

SHAPE MODEL	mean dif. (mm)	sd mean dif (mm)	max dif (mm)	sd max dif. (mm)
ELL	1.38	0.09	4.25	0.39
HEL	0.6	0.03	2.68	0.16
TRI	0.63	0.07	2.61	0.27
TRA	0.4	0.04	1.96	0.21
ATR	0.4	0.06	1.76	0.19

Table 3: CS2

SHAPE MODEL	mean dif. (mm)	sd mean dif (mm)	max dif (mm)	sd max dif. (mm)
ELL	2.82	0.2	8.42	0.53
HEL	1.45	0.09	5.8	0.46
TRI	0.95	0.04	3.92	0.08
TRA	0.68	0.02	3.67	0.04
ATR	0.79	0.02	3.19	0.08

Table 4: CS3

SHAPE MODEL	mean dif. (mm)	sd mean dif (mm)	max dif (mm)	sd max dif. (mm)
ELL	3	0.27	8.93	0.72
HEL	1.62	0.16	6.51	0.65
TRI	1.07	0.12	4.78	0.51
TRA	0.79	0.09	4.45	0.48
ATR	0.96	0.11	3.84	0.43

This procedure was carried out for each individual and regression describing the relationships between the length and the parameters the asymmetrical trapezoid (bottom width, top width, height and top asymmetry) for each cross section were obtained

according to the FISHSELECT methodology. This gives the results shown in Fig. 8-10 and Table 5.

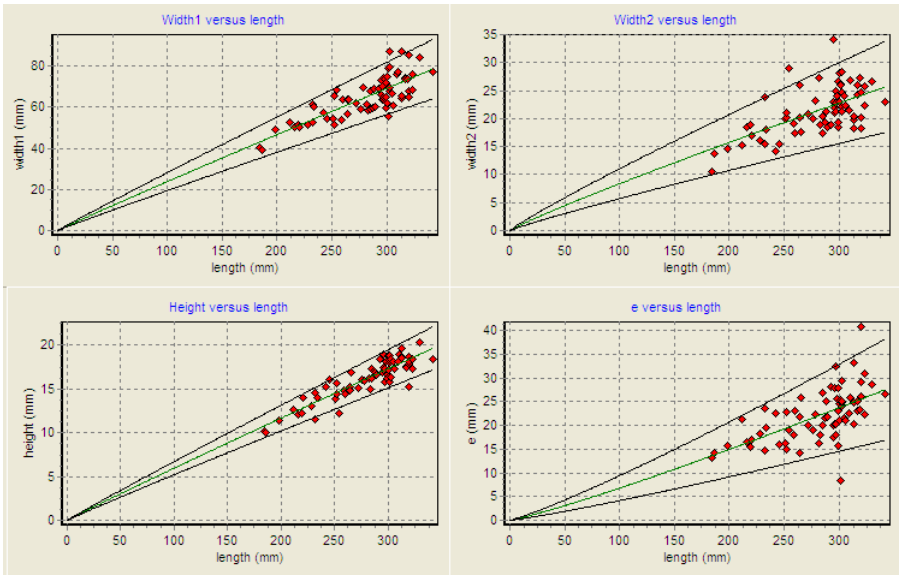

Fig. 8. CS1

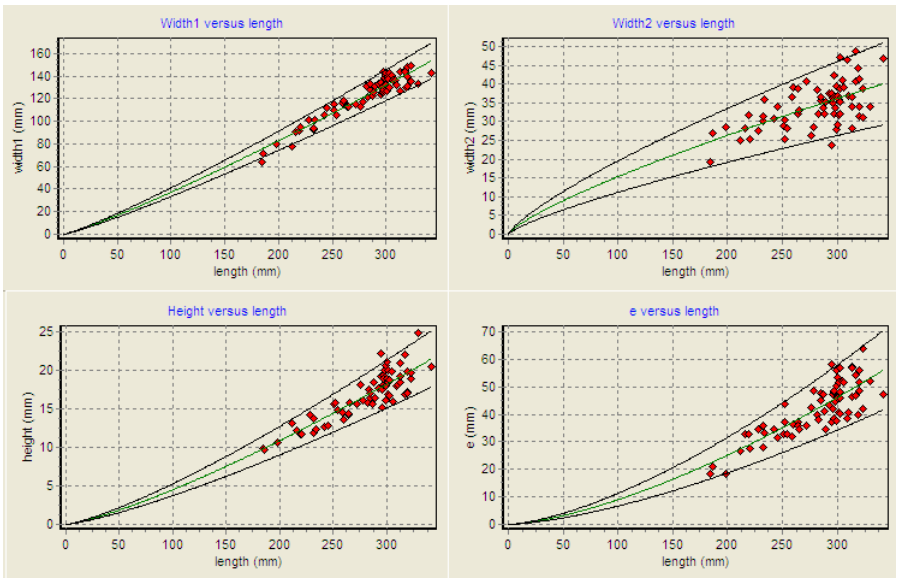

Fig. 9. CS2

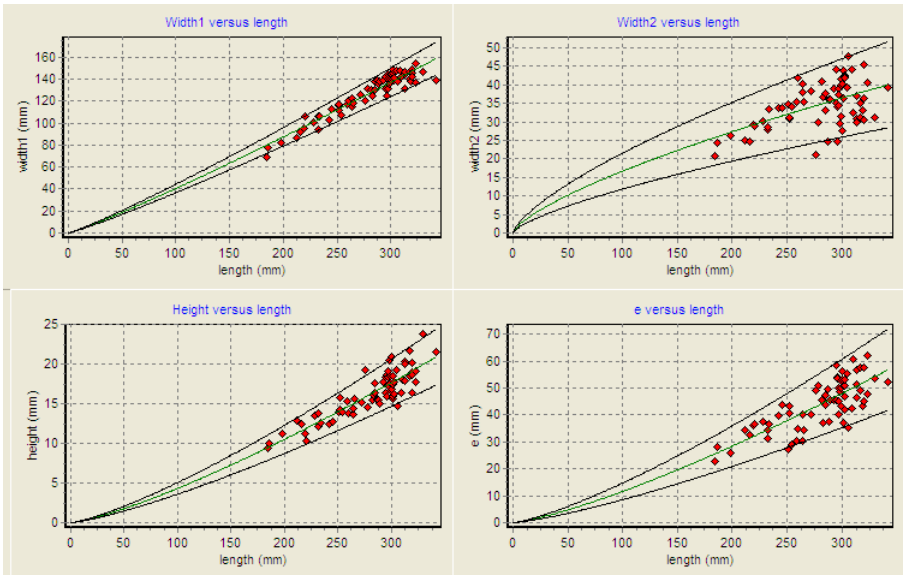

Fig. 10. CS3

Table 5.

D1:Coef=0.00000346;sd=0.00000023;Po=3.2000;R2=0.96;"Weight versus length"
D2:Coef=0.49047194;sd=0.02357244;Po=1.1400;R2=0.91;"Girth versus length"
D3:Coef=47.41672523;sd=2.06283801;Po=0.3400;R2=0.92;"Girth versus weight"
Section 1
Type=ATR
D4:Coef=0.27325530;sd=0.02508555;Po=0.9700;R2=0.64;"Width1 versus length"
D5:Coef=0.12686085;sd=0.02012733;Po=0.9100;R2=0.37;"Width2 versus length"
D6:Coef=0.73229375;sd=0.10861488;Po=0.8100;R2=0.44;"Width2 versus width1"
D7:Coef=0.06838360;sd=0.00429731;Po=0.9700;R2=0.81;"Height versus length"
D8:Coef=0.03554790;sd=0.00688111;Po=1.1400;R2=0.34;"e versus length"
Section 2
Type=ATR
D4:Coef=0.18725930;sd=0.00967605;Po=1.1500;R2=0.90;"Width1 versus length"
D5:Coef=0.42251624;sd=0.05756452;Po=0.7800;R2=0.36;"Width2 versus length"
D6:Coef=1.43779781;sd=0.19067206;Po=0.6600;R2=0.39;"Width2 versus width1"
D7:Coef=0.01299451;sd=0.00110928;Po=1.2700;R2=0.76;"Height versus length"
D8:Coef=0.00939051;sd=0.00120658;Po=1.4900;R2=0.67;"e versus length"
Section 3
Type=ATR
D4:Coef=0.24409267;sd=0.01167987;Po=1.1100;R2=0.90;"Width1 versus length"
D5:Coef=0.63539813;sd=0.09215714;Po=0.7100;R2=0.30;"Width2 versus length"
D6:Coef=1.41941765;sd=0.19713565;Po=0.6600;R2=0.36;"Width2 versus width1"
D7:Coef=0.01191480;sd=0.00100657;Po=1.2800;R2=0.77;"Height versus length"
D8:Coef=0.03056311;sd=0.00405550;Po=1.2900;R2=0.60;"e versus length"

Fig. 8-10 shows that the FISHSELECT regression models can describe the relationships reasonable including the between individuals variation. The R2-values are in general not very high but a reason for that could well be the relative small range for length compared to the between individual variation in the relationships (see Table 5).

Several penetration models build on CS1, CS2 and CS3 alone and in combinations assuming different levels of symmetrical or asymmetrical compression as well as cutting of height being below a certain percentage of the maximal height was tested against the experimental fall through results. More than 200000 models were tested. Based on comparing the degree of agreement for these models it if was found that the best agreement was found for the following model (Table 6):

Table 6.

```
*****************************
Fish Cross Section 1
*****************************
Section used=Yes
Escapement Model=Stiff
Scale Down=0.0
width cut of, hc=0.0
Scale width=0.52
Scale Height=1.0
*****************************
Fish Cross Section 2
*****************************
Section used=No
Escapement Model=Stiff
Scale Down=0.0
width cut of, hc=0.0
Scale width=1.0
Scale Height=1.0
*****************************
Fish Cross Section 3
*****************************
Section used=Yes
Escapement Model=Stiff
Scale Down=0.0
width cut of, hc=32.0
Scale width=1.0
Scale Height=0.7
*****************************
```

For this model which is combining CS3 with CS1 the number of disagreements are 338 of the 9108 experimental fall through results. This corresponds to a DA at 96.3%. This model uses the head (CS1) height stating that it should not be compressible while the head width is scaled largely down (down to 52%). Further it uses the widest cross section (CS3) stating that it should be cut in width for height below 32% and that the height should be scaled down to 70%. Fig. 11 illustrates this model.

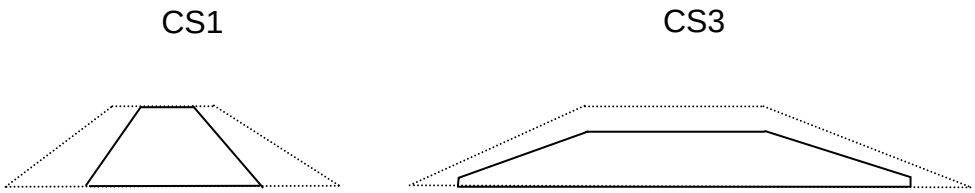

Fig. 11

For the three cross sections alone the smallest number of disagreements for the models tested was: 2510~DA= 72.4% for CS1; 493~DA= 94.6% for CS2; 478~DA=94.8%. Thus compared to the combined model the best based on CS3 alone would result in 41.4% more disagreements for the fall through experiments carried out. As DA at 96.3% was considered to be acceptable we could continue to make predictions based on this model. Based on the regression models for the relationship for the parametric description of the cross section sizes and shapes versus length including the between individuals variation a virtual population of 2000 lemon soles was created with lengths being uniformly distributed between 30 mm and 600 mm. Together with the selected penetration model

this virtual population was applied to predict the basic selective properties for stiff diamond shaped meshes through simulations using the FISHSELECT software tool.

Mesh sizes were in the range 70 mm to 200 mm in steps of 10 mm thus making a total of 14 different mesh sizes. For each mesh size mesh openness angles from 10 degrees to 90 degrees in steps of 5 degrees were simulated. This makes 17 different opening angles for each mesh size. This makes a total of 238 different diamond meshes. For each of these meshes it was then simulated weather or not each of the 2000 virtual lemon soles could pass through the mesh. In total this makes 476000 simulated penetration attempt results.

Processing these results using the design guide functionality in the FISHSELECT software tool a table containing estimates of the basic 50% retention length L50 and the selection range SR for each of the 238 different meshes was created. Based on the information in this table an isoplot for L50 was created (Fig. 12).

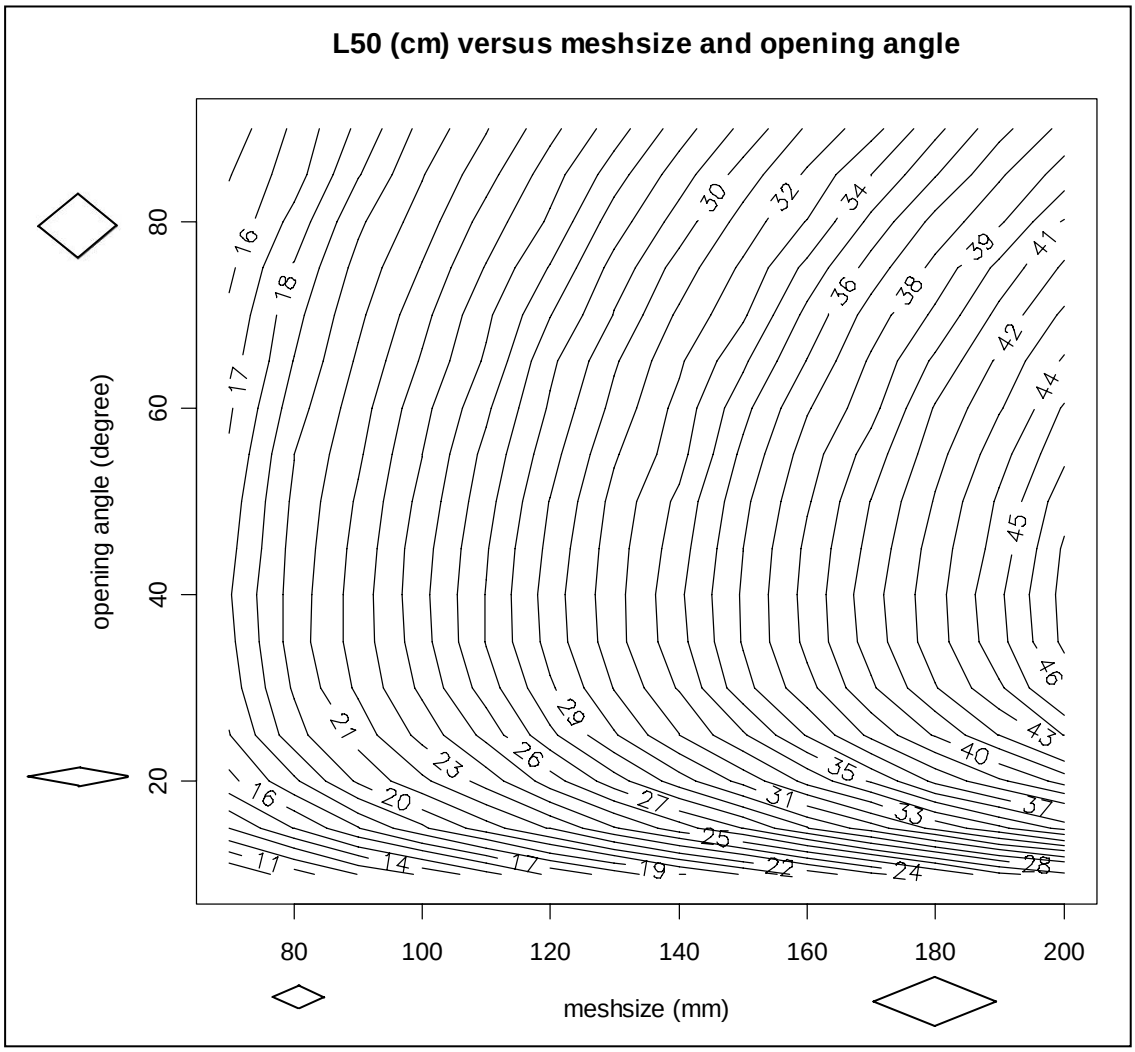

Fig. 12.

Inspecting Fig. 12 is evident that the legal 90 mm mesh size for Kattegat-Skagerak is not in balance with the minimum landing size MLS at 26 cm for Lemon sole in the trawl fishery as L50 is predicted to be below 22 cm depending on the opening angle. To release at least 50% of the individuals through penetration would at least require a mesh size between 110 and 120 mm according to our predictions. From Fig. 12 it is also that the retention properties depend on the opening angle thus the maximum for lemon sole is found for approximately 40 degrees openness.

The same procedure can be carried out for other mesh types based on the results presented here. But it has not been possible to carry out this within the limits of this project.

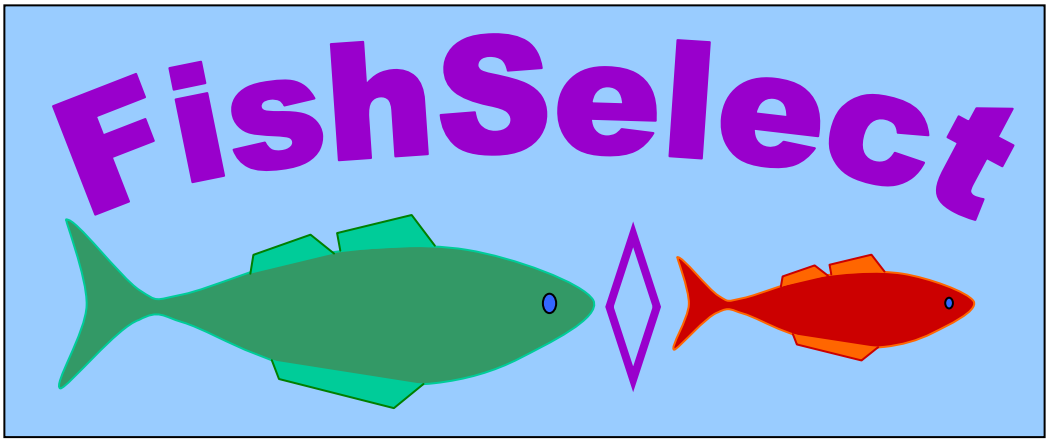

A7

A note on the FISHSELECT results for sole

In May 2007, soles were caught by gillnets and by trawl fishing from a research vessels ("Havfisken"). Approximately 100 live soles were brought to tanks in the laboratory where they were kept. The fish were anaesthetized when removed from the tanks. Of this batch of fish, 74 were used in the FISHSELECT experiments. Fig. 1 shows the size structure for these individuals.

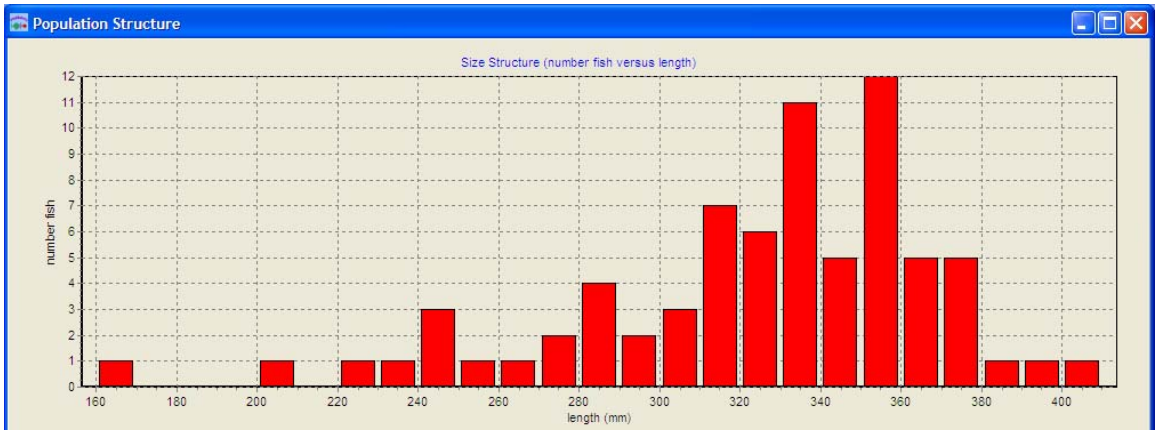

Fig. 1. Size distribution of the soles investigated in the experiment.

Three cross sections were measured at fixed positions along the length of the sole (Fig 2).
Cross section 1 (CS1): On the head representing the maximal non-deformable height
Cross section 2 (CS2): On the body representing the maximal width
Cross section 3 (CS3): Just behind the gill between CS1 and CS3.

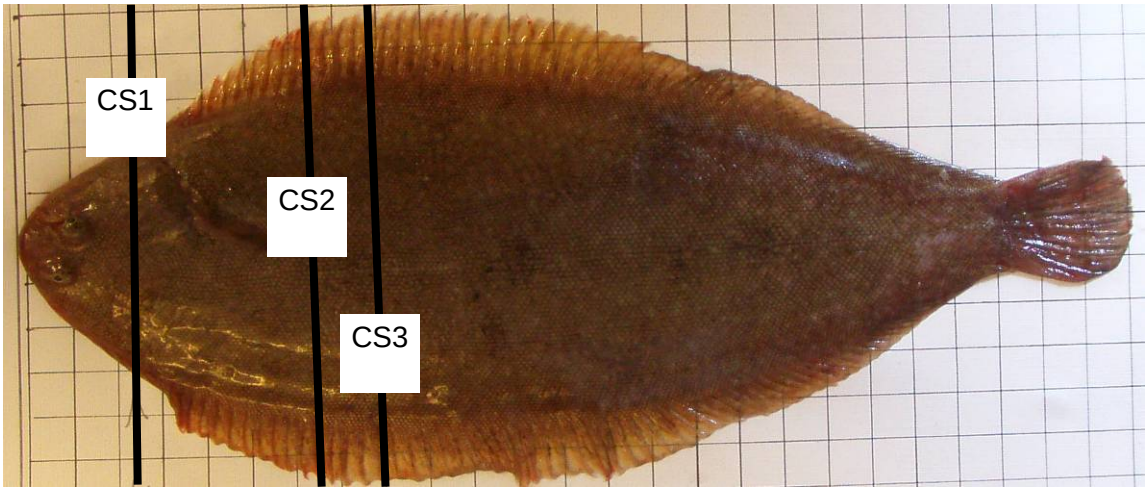

Fig. 2. Position of the 3 cross sections.

The measurements were carried out on a table using a single mechanical MorphoMeter (Fig. 3). Each cross section was digitized by use of a flat bed scanner and the FISHSELECT software which transfers the outlines of the cross section to a system of co-ordinates (Fig 4+6).

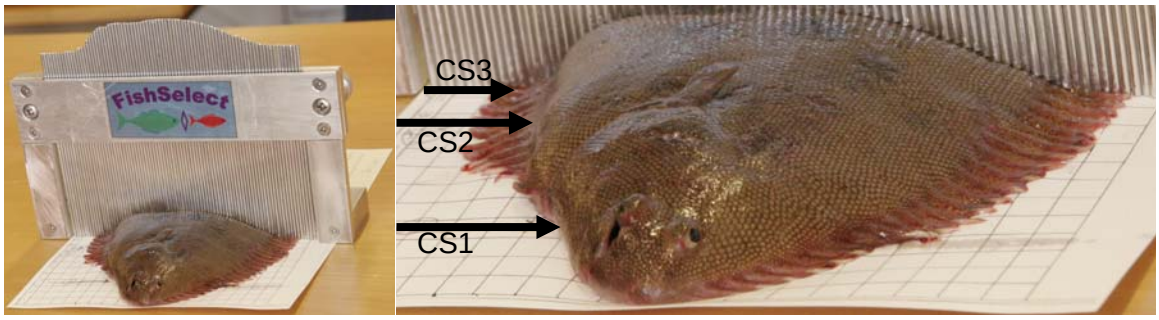

Fig. 3. Experimental setup for use of the MorphoMeter when measuring the cross sections of sole. In this case cross section 3 is being measured and on the close-up, the position of the other cross sections is indicated by arrows.

Fig. 4. Experimental setup of the process of scanning the MorphoMeter with the outline of the cross section and acquiring the data in a laptop computer.

Templates with 132 holes of different shape and size were used in the penetration experiments. The holes illustrates meshes and the shapes investigated were diamond, square, rectangle and hexagonal. For each shape and size, a series of different openings were laid out in order to reflect the mesh configurations found in a codend.
Table 1 summarizes the data for the 132 meshes investigated by use of syntax developed as part of the FISHSELECT software tool. The data listed is not nominal measures but is actual measures obtained by scanning each mesh hole, digitizing the contour using build in image analysis functionality in the FISHSELECT software tool as well as obtaining a parametric description using build in functionality for this.

Table 1. Data on the 132 meshes investigated. ID: unique mesh id, Type: mesh shape (diamond=D, square=S, rectangular=R, hexagonal=H), m: stretched mesh size, oa: opening angle, b and k: bar length, a: 2nd bar length when the bars are unequal. A detailed description of mesh configurations is given in the paper describing the methodology of FISHSELECT.

ID=1;Type=D;m=77.69;oa=30.54;ID=2;Type=D;m=78.01;oa=55.58;ID=3;Type=D;m=80.27;oa=87.01;
ID=4;Type=D;m=88.20;oa=25.8;ID=5;Type=D;m=88.47;oa=30.92;ID=6;Type=D;m=88.80;oa=37.32;
ID=7;Type=D;m=88.35;oa=39.69;ID=8;Type=D;m=88.71;oa=45.85;ID=9;Type=D;m=89.75;oa=50.1;
ID=10;Type=D;m=89.26;oa=57.29;ID=11;Type=D;m=90.05;oa=60.08;ID=12;Type=D;m=89.76;oa=61.79;
ID=13;Type=D;m=90.59;oa=69.79;ID=14;Type=D;m=89.26;oa=76.33;ID=15;Type=D;m=90.38;oa=81.45;
ID=16;Type=D;m=89.70;oa=85.36;ID=17;Type=D;m=91.16;oa=89.99;ID=18;Type=D;m=100.78;oa=19.87;
ID=19;Type=D;m=98.31;oa=56.16;ID=20;Type=D;m=99.84;oa=86.21;ID=21;Type=D;m=109.42;oa=20.31;
ID=22;Type=D;m=109.56;oa=55.22;ID=23;Type=D;m=109.18;oa=86.48;ID=24;Type=D;m=118.27;oa=19.67;
ID=25;Type=D;m=114.16;oa=26.49;ID=26;Type=D;m=118.83;oa=31.73;ID=27;Type=D;m=117.90;oa=35.61;
ID=28;Type=D;m=118.35;oa=41.37;ID=29;Type=D;m=118.23;oa=46.22;ID=30;Type=D;m=119.86;oa=50.09;
ID=31;Type=D;m=118.94;oa=57.41;ID=32;Type=D;m=120.37;oa=60.67;ID=33;Type=D;m=119.71;oa=65.01;
ID=34;Type=D;m=118.48;oa=71.46;ID=35;Type=D;m=121.59;oa=77.86;ID=36;Type=D;m=120.31;oa=81.51;
ID=37;Type=D;m=120.52;oa=86.74;ID=38;Type=D;m=126.68;oa=19.89;ID=39;Type=D;m=128.99;oa=56.63;
ID=40;Type=D;m=129.98;oa=86.59;ID=41;Type=D;m=140.39;oa=19.84;ID=42;Type=D;m=138.48;oa=55.95;
ID=43;Type=D;m=140.23;oa=85.85;ID=44;Type=D;m=163.35;oa=14.39;ID=45;Type=D;m=158.72;oa=20.57;
ID=46;Type=D;m=158.13;oa=25.07;ID=47;Type=D;m=159.35;oa=30.48;ID=48;Type=D;m=157.85;oa=35.52;
ID=49;Type=D;m=159.03;oa=40.22;ID=50;Type=D;m=160.04;oa=46.09;ID=51;Type=D;m=159.03;oa=51.43;
ID=52;Type=D;m=160.76;oa=56.13;ID=53;Type=D;m=160.54;oa=60.74;ID=54;Type=D;m=160.56;oa=66.13;
ID=55;Type=D;m=161.10;oa=71.33;ID=56;Type=D;m=160.77;oa=76.62;ID=57;Type=D;m=159.68;oa=80.65;
ID=58;Type=D;m=160.97;oa=85.57;ID=59;Type=D;m=177.19;oa=15.68;ID=60;Type=D;m=180.96;oa=56.47;
ID=61;Type=D;m=182.90;oa=86.00;ID=62;Type=D;m=195.97;oa=15.85;ID=63;Type=D;m=200.40;oa=55.71;
ID=64;Type=D;m=200.30;oa=86.89;ID=65;Type=S;b=34.67;ID=66;Type=S;b=40.07;ID=67;Type=S;b=50.14;
ID=68;Type=S;b=60.23;ID=69;Type=S;b=69.69;ID=70;Type=S;b=80.08;ID=71;Type=S;b=89.95;
ID=72;Type=S;b=100.27;ID=73;Type=R;b=90.59;a=9.81;ID=74;Type=R;b=90.96;a=14.49;
ID=75;Type=R;b=91.35;a=19.33;ID=76;Type=R;b=91.05;a=29.19;ID=77;Type=R;b=91.23;a=49.01;
ID=78;Type=R;b=91.79;a=68.83;ID=79;Type=R;b=120.42;a=8.99;ID=80;Type=R;b=121.67;a=14.85;
ID=81;Type=R;b=122.15;a=19.38;ID=82;Type=R;b=121.61;a=29.57;ID=83;Type=R;b=122.40;a=48.84;
ID=84;Type=R;b=121.93;a=69.02;ID=85;Type=R;b=202.66;a=9.89;ID=86;Type=R;b=203.93;a=14.28;
ID=87;Type=R;b=203.45;a=19.02;ID=88;Type=R;b=200.19;a=29.96;ID=89;Type=R;b=203.26;a=49.13;
ID=90;Type=R;b=203.62;a=69.37;ID=91;Type=H;b=17.49;k=35.25;oa=142.05;ID=92;Type=H;b=17.61;k=36.17;oa=130.44;
ID=93;Type=H;b=18.06;k=36.51;oa=103.65;ID=94;Type=H;b=17.02;k=35.71;oa=86.08;
ID=95;Type=H;b=20.25;k=39.95;oa=147.81;ID=96;Type=H;b=20.35;k=39.75;oa=126.92;
ID=97;Type=H;b=19.96;k=39.31;oa=107.59;ID=98;Type=H;b=19.98;k=40.81;oa=91.84;
ID=99;Type=H;b=25.37;k=50.15;oa=143.40;ID=100;Type=H;b=24.91;k=49.24;oa=126.33;
ID=101;Type=H;b=26.22;k=48.60;oa=102.92;ID=102;Type=H;b=26.04;k=48.05;oa=89.54;
ID=103;Type=H;b=29.74;k=59.42;oa=143.88;ID=104;Type=H;b=30.53;k=60.21;oa=128.98;
ID=105;Type=H;b=29.86;k=59.42;oa=105.49;ID=106;Type=H;b=29.94;k=59.80;oa=88.85;
ID=107;Type=H;b=35.15;k=68.93;oa=142.28;ID=108;Type=H;b=34.18;k=70.03;oa=128.34;
ID=109;Type=H;b=35.29;k=69.42;oa=106.33;ID=110;Type=H;b=35.62;k=69.47;oa=89.76;
ID=111;Type=H;b=40.78;k=80.51;oa=145.98;ID=112;Type=H;b=40.66;k=79.42;oa=129.65;
ID=113;Type=H;b=40.34;k=80.04;oa=105.87;ID=114;Type=H;b=41.03;k=80.19;oa=88.19;
ID=115;Type=H;b=49.89;k=99.69;oa=141.66;ID=116;Type=H;b=50.59;k=99.35;oa=127.28;
ID=117;Type=H;b=50.47;k=99.31;oa=106.32;ID=118;Type=H;b=50.97;k=98.67;oa=88.05;
ID=119;Type=D;m=66.38;oa=26.86;ID=120;Type=D;m=67.25;oa=29.74;ID=121;Type=D;m=67.66;oa=37.95;
ID=122;Type=D;m=67.59;oa=41.83;ID=123;Type=D;m=67.81;oa=44.22;ID=124;Type=D;m=67.61;oa=51.56;
ID=125;Type=D;m=68.85;oa=55.10;ID=126;Type=D;m=69.35;oa=63.60;ID=127;Type=D;m=70.11;oa=64.87;
ID=128;Type=D;m=68.44;oa=69.86;ID=129;Type=D;m=69.33;oa=74.24;ID=130;Type=D;m=68.80;oa=79.65;
ID=131;Type=D;m=70.12;oa=85.60;ID=132;Type=D;m=69.69;oa=89.67;

Head first and under the force of gravity, each fish was guided through all the meshes and success or failure of penetration was recorded (Fig 5). This resulted in a total of 9768 penetration results.

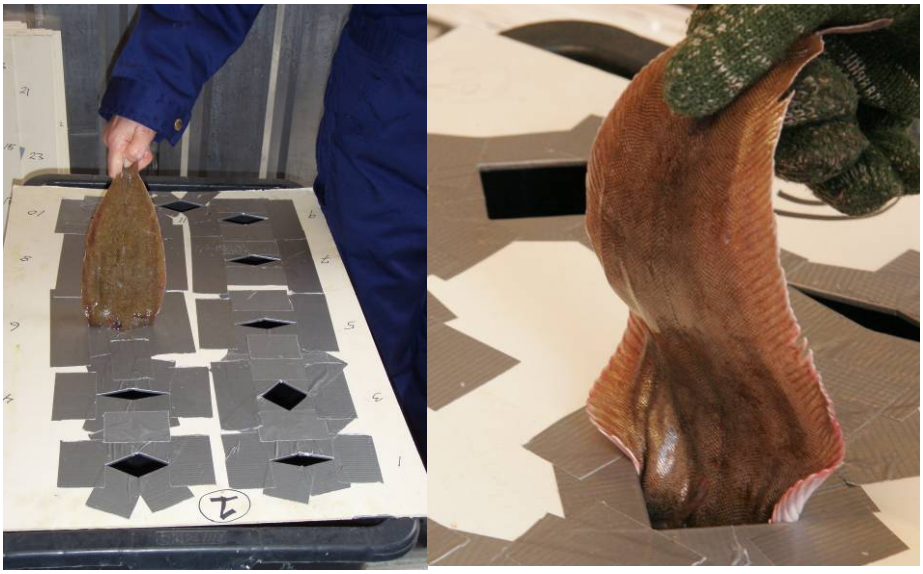

Fig. 5. Images from the penetration experiment testing whether a given fish is able to penetrate a given mesh in the templates. The right hand picture illustrate that the fins and some part of the body of the sole is very flexible and it should be expected that a suitable penetration model needs to account for this.

For each sole the three cross sections were digitized (Fig. 6) and it was found that an asymmetrical trapezoid provided the best description of the shapes (Fig. 7). An image analysis tool in FISHSELECT extracts the contour in the scanned image of the mechanical Morphometer and translates the contour into a system of co-ordinates (Fig. 6). Subsequently a number of different geometrical shapes are fitted to the outline of the cross section and for all three cross sections, an asymmetrical trapezoid fitted best (Fig. 7)

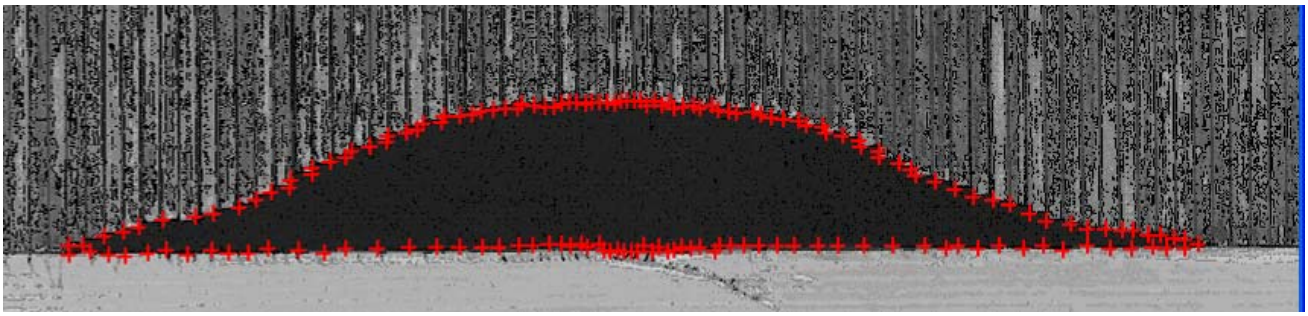

Fig. 6. Digitized outline of one of the cross sections measured by the MorphoMeter

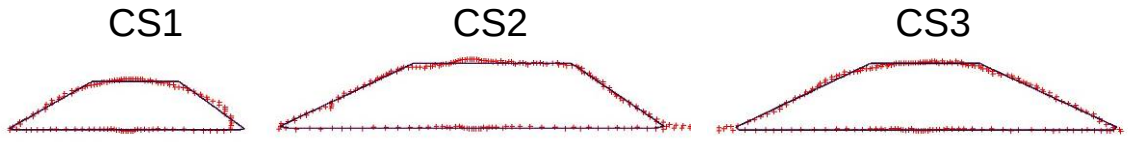

Fig. 7. Asymmetrical trapezoids fitted to the outlines of all three cross sections.

This procedure was carried out for each individual and for the 74 individuals fitting an asymmetrical trapezoid to the cross section we found the following overall fit statistics (Table 2).

Table 2. Overall fit statistics of fitting an asymmetrical trapezoid to cross section outlines.

Cross section No.	Mean deviation (mm)	sd mean deviation (mm)	Maximum deviation (mm)	sd Maximum deviation (mm)
1	0.49	0.01	2.10	<0.01
2	0.63	0.01	2.65	0.04
3	0.68	<0.01	2.77	0.04

Regression describing the relationships between the fish length and the parameters of the asymmetrical trapezoid (bottom width, top width, height and top asymmetry) for each cross section were obtained according to the FISHSELECT methodology.
Making the regressions for the length to width and height leads to the results shown in Fig. 8-10 and Table 3.

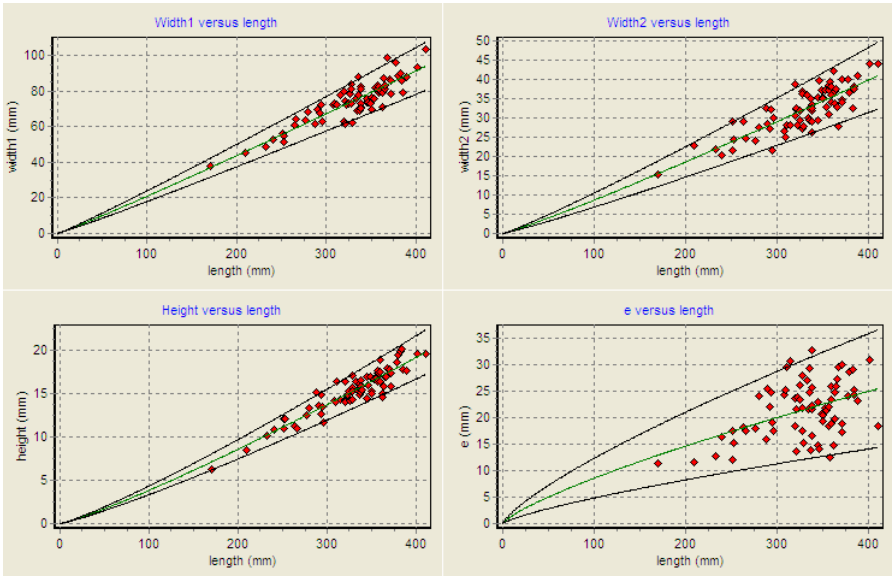

Fig. 8. CS1

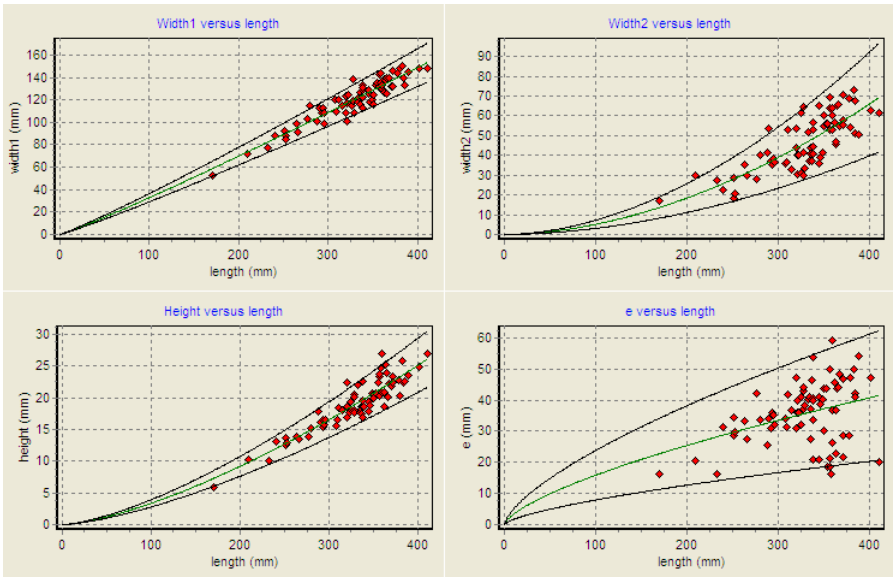

Fig. 9. CS2

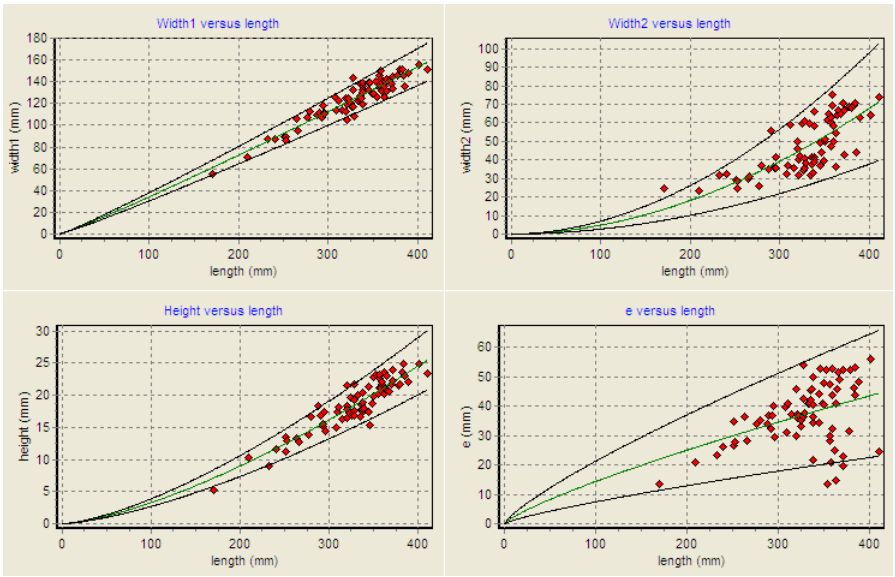

Fig. 10. CS3

Table 3.

D1:Coef=0.00000047;sd=0.00000006;Po=3.5200;R2=0.91;"Weight versus length"
D2:Coef=0.59323483;sd=0.03579144;Po=1.0700;R2=0.86;"Girth versus length"
D3:Coef=54.08053886;sd=2.70676533;Po=0.2900;R2=0.91;"Girth versus weight"
Section 1
Type=ATR
D4:Coef=0.15919327;sd=0.01146446;Po=1.0600;R2=0.79;"Width1 versus length"
D5:Coef=0.05465890;sd=0.00579444;Po=1.1000;R2=0.67;"Width2 versus length"
D6:Coef=1.16970908;sd=0.14759143;Po=0.7700;R2=0.51;"Width2 versus width1"
D7:Coef=0.01833819;sd=0.00119357;Po=1.1600;R2=0.86;"Height versus length"
D8:Coef=0.24803478;sd=0.05407921;Po=0.7700;R2=0.20;"e versus length"
Section 2
Type=ATR
D4:Coef=0.21705087;sd=0.01224145;Po=1.0900;R2=0.88;"Width1 versus length"
D5:Coef=0.00107347;sd=0.00021336;Po=1.8400;R2=0.60;"Width2 versus length"
D6:Coef=0.01398639;sd=0.00267729;Po=1.6900;R2=0.68;"Width2 versus width1"
D7:Coef=0.00423337;sd=0.00036033;Po=1.4500;R2=0.83;"Height versus length"
D8:Coef=0.69219883;sd=0.17354220;Po=0.6800;R2=0.13;"e versus length"

Section 3
Type=ATR
D4:Coef=0.23779199;sd=0.01312788;Po=1.0800;R2=0.88;"Width1 versus length"
D5:Coef=0.00077241;sd=0.00017106;Po=1.9000;R2=0.57;"Width2 versus length"
D6:Coef=0.01285822;sd=0.00294252;Po=1.7000;R2=0.60;"Width2 versus width1"
D7:Coef=0.00413309;sd=0.00037569;Po=1.4500;R2=0.84;"Height versus length"
D8:Coef=0.35995251;sd=0.08678130;Po=0.8000;R2=0.18;"e versus length"

Fig. 8-10 shows that the FISHSELECT regression models can be used to reasonably describe the relationships between fish length and cross section parameters including the between individuals variation. The R2-values however could be better (see Table 3). Especially e versus has a low R2 value indicating that there is no clear relationship between the two. As e contains the skewness of the trapezoid, the lack of relationship between this parameter and fish length may indicate that it could be sufficient to use a symmetrical trapezoid for the shape descriptions. But within the time period of the project it has not been possible to analyze this in sufficient detail.

Without a final decision on whether the cross section description could be simplified to a symmetrical trapezoid in stead of an asymmetrical, initial analysis to find a suitable penetration model was started using the latter description. Using more than 200 single cross section models cut based on fin cut algorithms implemented in the FISHSELECT software tool and based on asymmetrical compressions in height and width it is a very computer resource demanding task to identify the best penetration model.
At the time of reporting, the preliminary models had a DA (degree of agreement) above 95.1% and there are still a couple of weeks of computing time left before all initial models have been run.
95.1% is relatively high and is very likely that the final model will have a higher DA. We are therefore confident that we will succeed in finding a sufficiently accurate model when the data analysis is complete. In the future, this model will allow making predictions for sole based on this study.

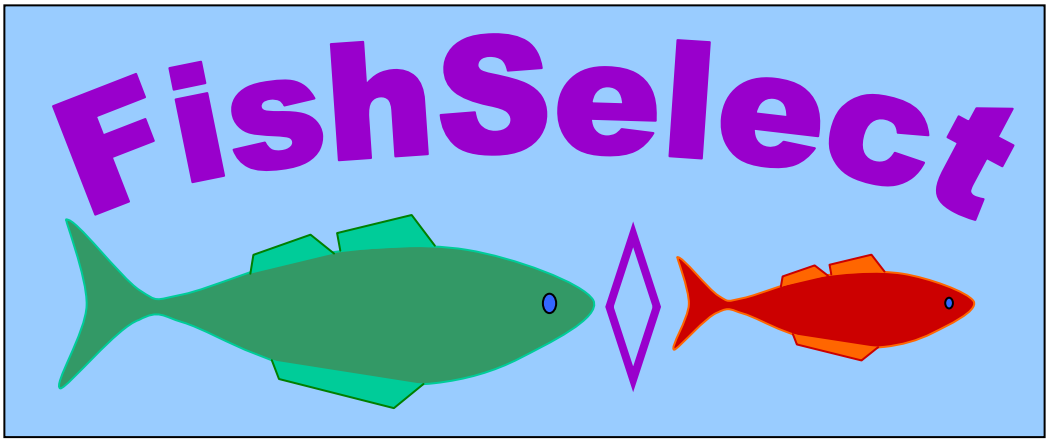

A8

Note on Nephrops (*Nephrops Norvegicus*)

A study of size selection of Nephrops using the FISHSELECT methodology has been initiated as part of the project. The study is carried in corporation with another project (SELTRA). In the current project the data collection and laboratory work has been carried out as well as initial analysis of data from a pilot experiment in the laboratory with the purpose to specify the main laboratory work. The analysis of the data from the main laboratory work is expected to be carried out in SELTRA and reported there.

Method.

Experimental fishing has provided parameter estimates for size selection of Nephrops. For example, it has been estimated for a full square mesh cod-end with mesh size 70 mm for pooled data that L50 ≈ 42.0 mm and SR ≈ 15.5 mm (≈ 47.0 – 32.5) (see Fig. 1). We use this information as basis for the initial part of the study. Compared to the relatively active escapement process of the fish investigated in this project, we expect that Nephrops size selection through the meshes in towed gears is a more random process. A fish attempting to penetrate a mesh in a towed fishing gear is thus assumed to be able to orientate itself optimal for penetration. For Nephrops we expect that this will not necessary be the situation. Our hypothesis is that the average size selection process of Nephrops in towed gears is controlled by contact with the meshes at different orientations. This means that in order to predict size selection of Nephrops by the FISHSELECT methodology we need to identify the different orientations (contact modes) for the Nephrops and estimate to which level each of these modes contribute to the average size selection. Assuming that the contributions of the different contact modes are approximately the same for different netting gear designs we can use results for a limited number of designs to estimate the relative contributions of the different contact modes in all gear types. This may include eliminating modes found not to contribute significantly to the overall process. The contact modes found to be contributing to the selective process are run in the "standard" FISHSELECT methodology to establish the basic selective properties for a large number of different mesh designs and grids.
A subsequent analysis combine these results and based on a comparison with field data, the program provides each contact mode with a level of importance ranging form zero to one. The higher the level, the more important is the specific contact mode estimated to be in the selective process in a trawl. These information enables prediction of the basic size selective properties for different mesh designs and grids with respect to Nephrops. Even if it's not be possible to establish very precise predictions on the level of importance, the basic selective properties for the separate contact modes, should provide useful information about the upper and lower limits for the size selective properties of different gear designs with respect to Nephrops. It should also provide useful knowledge about basic mechanisms likely to be involved in size selection of Nephrops.

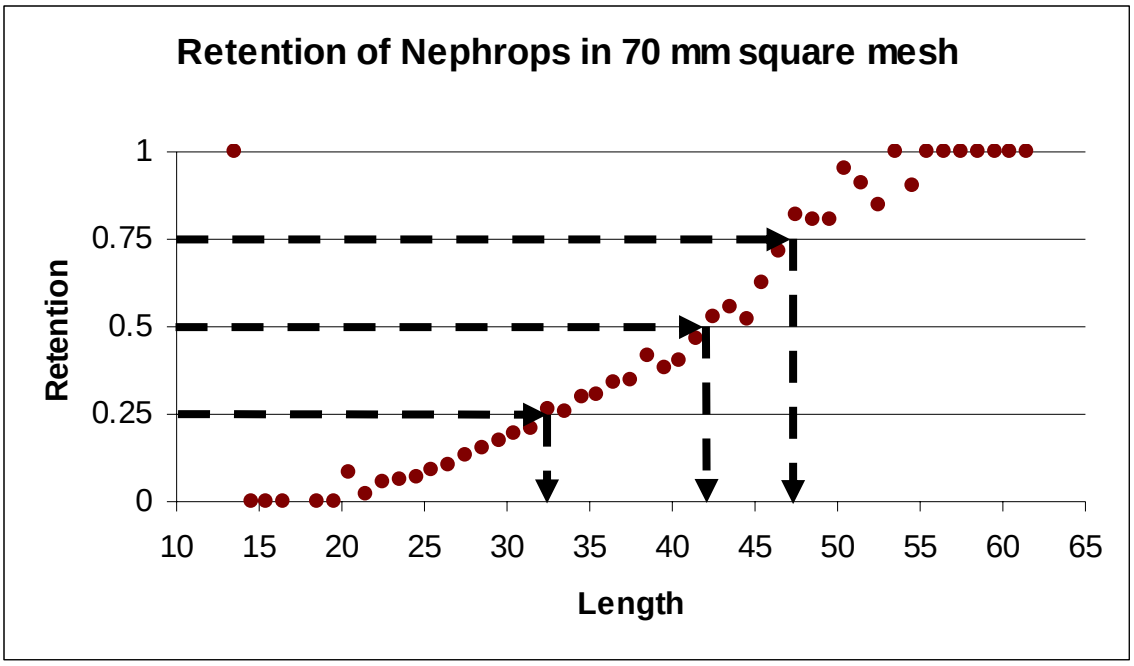

Fig. 1

Pilot experiment.

For the FISHSELECT pilot experiment we used the following 8 contact modes (Fig. 2):

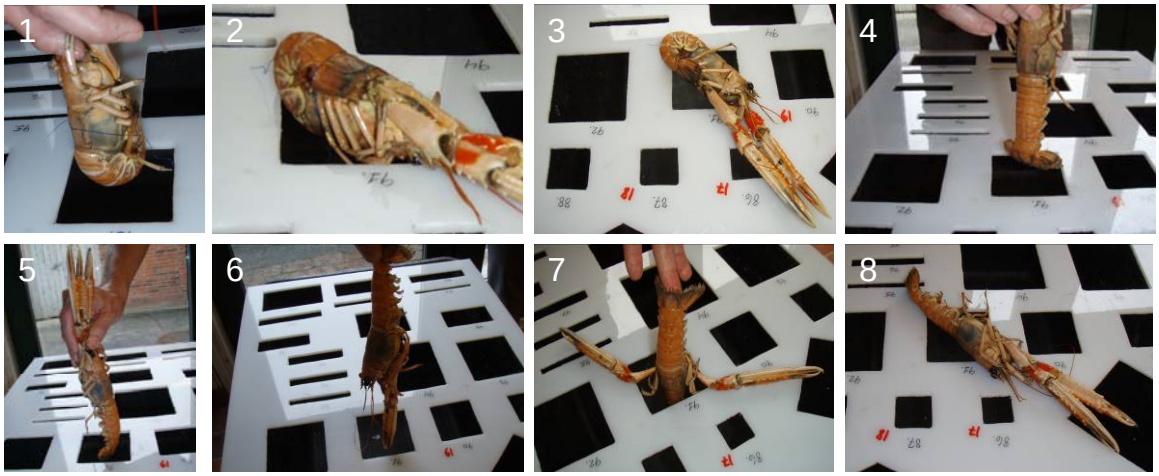

Fig. 2

In the pilot experiment, a subset of only 43 meshes was used. These meshes reflected the mesh configurations relevant for the codends on which we had field data. For the square mesh codend (70mm), we had retention data in the entire selective range and these data were therefore used as reference data when estimating the level on importance for the different contact modes. This square mesh codend is made of very soft material with tensionless mesh bars easy to distort (Fig. 3). The mesh designs therefore also included hexagonal shapes emulating squares distorted in tensionless mesh bars perpendicular to the towing direction.

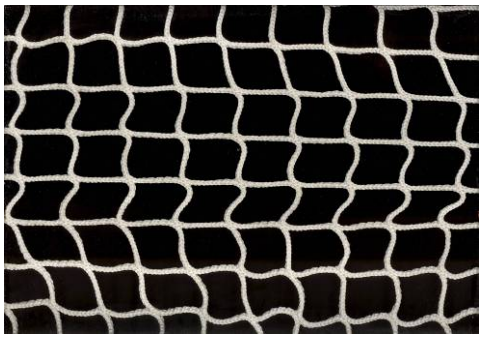

Fig. 3

Table 1 lists the mesh designs used for the penetration experiments in the pilot experiment.

Table 1

ID=1;Type=D;m=90;oa=15;ID=2;Type=D;m=90;oa=20;ID=3;Type=D;m=90;oa=25;
ID=4;Type=D;m=90;oa=30;ID=5;Type=D;m=90;oa=35;ID=6;Type=D;m=90;oa=40;
ID=7;Type=D;m=90;oa=45;ID=8;Type=D;m=90;oa=50;ID=9;Type=D;m=90;oa=55;
ID=10;Type=D;m=90;oa=60;ID=11;Type=D;m=90;oa=65;ID=12;Type=D;m=90;oa=70;
ID=13;Type=D;m=90;oa=75;ID=14;Type=D;m=90;oa=80;ID=15;Type=D;m=90;oa=85;
ID=16;Type=D;m=90;oa=90;ID=17;Type=S;b=30;ID=18;Type=S;b=35;ID=19;Type=S;b=60;
ID=20;Type=R;b=200;a=35;ID=21;Type=R;b=200;a=40;ID=22;Type=H;b=15;k=30;oa=145;
ID=23;Type=H;b=15;k=30;oa=130;ID=24;Type=H;b=15;k=30;oa=105;
ID=25;Type=H;b=15;k=30;oa=90;ID=26;Type=H;b=15;k=30;oa=80;ID=27;Type=H;b=15;k=30;oa=60;
ID=28;Type=H;b=15;k=30;oa=40;ID=29;Type=H;b=17.5;k=35;oa=145;ID=30;Type=H;b=17.5;k=35;oa=130;
ID=31;Type=H;b=17.5;k=35;oa=105;ID=32;Type=H;b=17.5;k=35;oa=90;ID=33;Type=H;b=17.5;k=35;oa=80;
ID=34;Type=H;b=17.5;k=35;oa=60;ID=35;Type=H;b=17.5;k=35;oa=40;ID=36;Type=H;b=30;k=60;oa=145;
ID=37;Type=H;b=30;k=60;oa=130;ID=38;Type=H;b=30;k=60;oa=105;ID=39;Type=H;b=30;k=60;oa=90;
ID=40;Type=H;b=30;k=60;oa=80;ID=41;Type=H;b=30;k=60;oa=70;ID=42;Type=H;b=30;k=60;oa=60;
ID=43;Type=H;b=30;k=60;oa=40;

We used 20 individual in the pilot experiment ranging from 18 mm to 61 mm in carapace length. Fig. 4 shows the length structure for the individuals used in the pilot experiment.

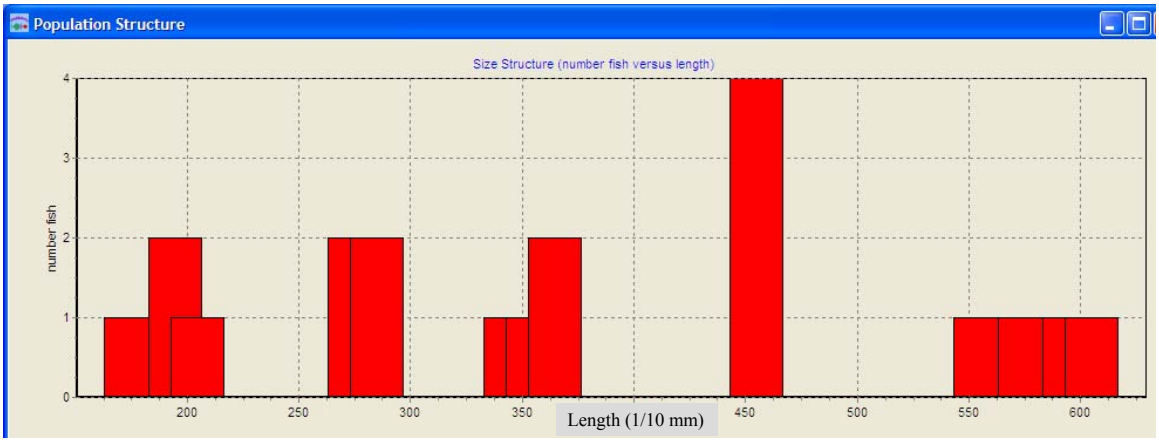

Fig. 4

With 20 individuals, 43 meshes and 8 different contact modes the penetration experiment for the pilot study yielded of 20x43x8= 6880 results.

A facility in the FISHSELECT software tool enabled us to link results from the penetration experiments to information on carapax length. This enabled us to use the penetration results to create retention data for each mesh and each of the contact modes 1 to 8. The resulting retention data could then be used to estimate the basic selective properties either separately or by combining results from different meshes, modes or both. Table 2 shows the retention data for the different modes based on the penetration results for the 20 Nephrops for a full open 70 mm square mesh (mesh id 18 in Table 1).

Table 2

Length	no total	retention 1	retention 2	retention 3	retention 4	retention 5	retention 6	retention 7	retention 8
18.5	1	0	0	0	0	0	0	missing v.	1
19.5	1	0	0	0	0	0	0	missing v.	1
20.5	2	0	0	0	0	0	0	1*	2
28.5	4	0	4	4	0	0	0	4	4
34.5	1	0	1	1	0	0	0	1	1
36.5	1	0	1	1	0	0	0	1	1
37.5	2	0	2	2	0	0	0	2	2
45.5	2	0	2	2	2	0	0	2	2
46.5	2	1	2	2	1	0	0	1*	2
55.5	1	1	1	1	1	1	1	1	1
57.5	1	1	1	1	1	1	1	1	1
59.5	1	1	1	1	1	1	1	1	1
61.5	1	1	1	1	1	1	1	1	1

* only one individual the is other missing value. Retention in % can be obtained by division of the retention with “no total”.

For comparative purposes, fig. 5 plots the retention curves for the data in table 2 (squares) together with the field data shown in Fig. 1 (triangles).

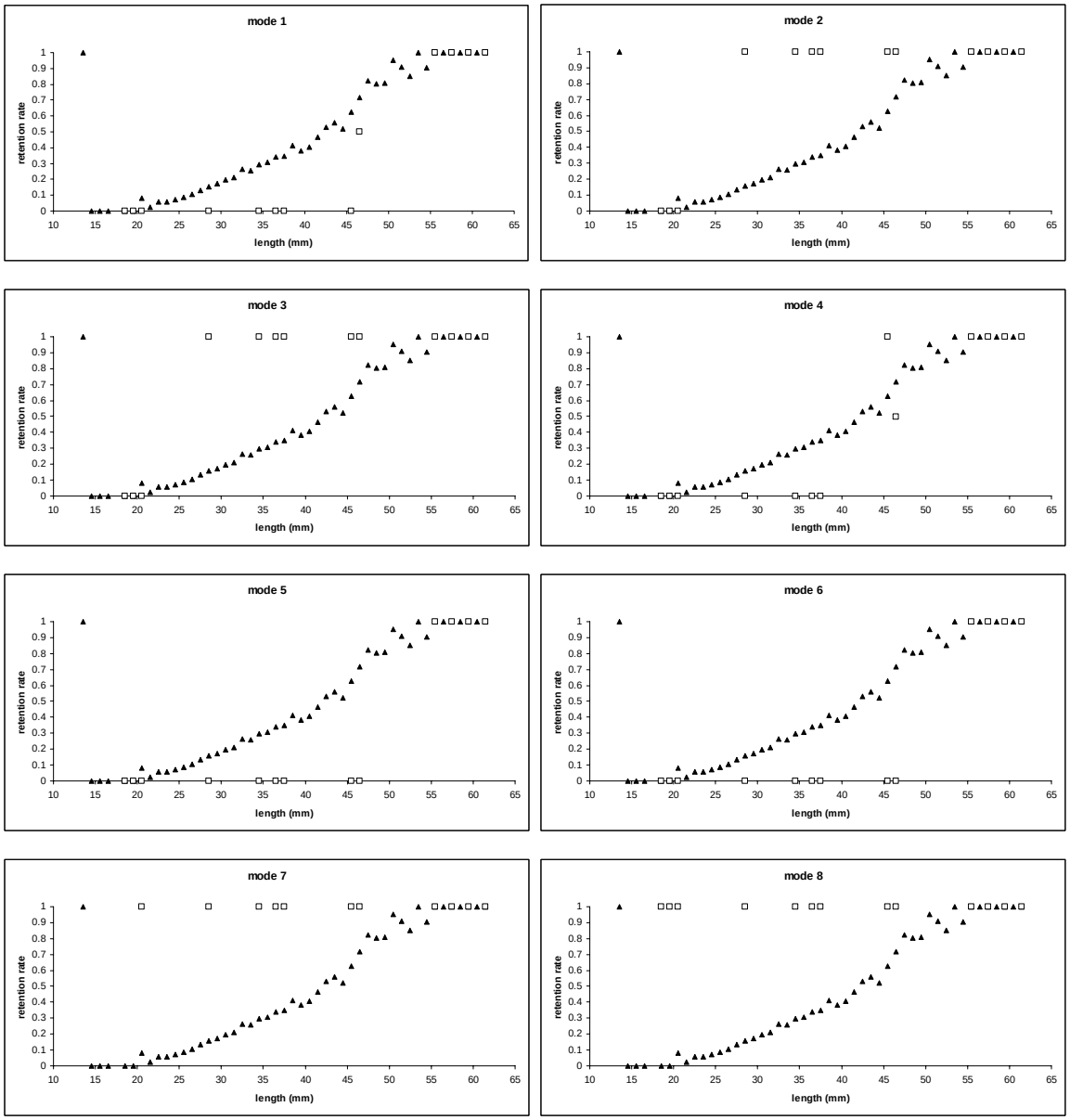

Fig. 5. The black triangles represent the experimental data from Fig. 1 while the white squares represent the penetration results for the individual modes 1 to 8.

To get an idea of the level of importance of the different contact modes, we subsequently compared the estimated L50 and SR with the experimentally obtained estimates. Even for a minor study like this, contact modes, meshes and different levels of importance quickly adds up to a large number of combinations that turned out to be impossible to analyze by means of the functionalities already implemented in the FISHSELECT software tool. We therefore developed and implemented functionalities to carry out this analysis automatically.

The core of this analysis was to define a function to rank the quality of the results for all combinations investigated. The reference was the parameter values obtained in the field and the combinations resulting in high resemblance with these parameters should be ranked first. We used the following function:

$$Cri = \sqrt{\left(\left(\frac{simL_{50} - refL_{50}}{refL_{50}}\right)^2 + \left(\frac{simSR - refSR}{refSR}\right)^2\right)} \quad (1)$$

In (1) refL50 and refSR represent the experimentally obtained results and simL50 and simSR represent the simulated parameters estimated for the combination being evaluated. For a perfect match with the experimental results (simL50 = refL50 and simSR = refSR), the value will be zero. For a poorer match, the function will undertake increasing values. The *Cri*-value is thus used to rank the quality of the different combination of modes and meshes.

Initially we investigated the situation assuming that all codend meshes were full open (perfect square) while all 8 contact modes were tested at three levels of importance (0, 3, 6). This makes 3^8 = 6561 combinations. Table 3 shows the top 17 match from this initial investigation.

Table 3

w1=0.00;w2=28.57;w3=0.00;w4=28.57;w5=28.57;w6=14.29;w7=0.00;w8=0.00;Cri=0.017933;L50=41.62;SR=15.74
w1=0.00;w2=14.29;w3=14.29;w4=28.57;w5=28.57;w6=14.29;w7=0.00;w8=0.00;Cri=0.017933;L50=41.62;SR=15.74
w1=0.00;w2=0.00;w3=28.57;w4=28.57;w5=28.57;w6=14.29;w7=0.00;w8=0.00;Cri=0.017933;L50=41.62;SR=15.74
w1=0.00;w2=28.57;w3=0.00;w4=28.57;w5=14.29;w6=28.57;w7=0.00;w8=0.00;Cri=0.017933;L50=41.62;SR=15.74
w1=0.00;w2=14.29;w3=14.29;w4=28.57;w5=14.29;w6=28.57;w7=0.00;w8=0.00;Cri=0.017933;L50=41.62;SR=15.74
w1=0.00;w2=0.00;w3=28.57;w4=28.57;w5=14.29;w6=28.57;w7=0.00;w8=0.00;Cri=0.017933;L50=41.62;SR=15.74
w1=14.29;w2=0.00;w3=28.57;w4=28.57;w5=0.00;w6=28.57;w7=0.00;w8=0.00;Cri=0.020866;L50=41.21;SR=15.36
w1=14.29;w2=14.29;w3=14.29;w4=28.57;w5=0.00;w6=28.57;w7=0.00;w8=0.00;Cri=0.020866;L50=41.21;SR=15.36
w1=14.29;w2=28.57;w3=0.00;w4=28.57;w5=0.00;w6=28.57;w7=0.00;w8=0.00;Cri=0.020866;L50=41.21;SR=15.36
w1=14.29;w2=0.00;w3=28.57;w4=28.57;w5=14.29;w6=14.29;w7=0.00;w8=0.00;Cri=0.020866;L50=41.21;SR=15.36
w1=14.29;w2=14.29;w3=14.29;w4=28.57;w5=14.29;w6=14.29;w7=0.00;w8=0.00;Cri=0.020866;L50=41.21;SR=15.36
w1=14.29;w2=28.57;w3=0.00;w4=28.57;w5=14.29;w6=14.29;w7=0.00;w8=0.00;Cri=0.020866;L50=41.21;SR=15.36
w1=14.29;w2=0.00;w3=28.57;w4=28.57;w5=28.57;w6=0.00;w7=0.00;w8=0.00;Cri=0.020866;L50=41.21;SR=15.36
w1=14.29;w2=14.29;w3=14.29;w4=28.57;w5=28.57;w6=0.00;w7=0.00;w8=0.00;Cri=0.020866;L50=41.21;SR=15.36
w1=14.29;w2=28.57;w3=0.00;w4=28.57;w5=28.57;w6=0.00;w7=0.00;w8=0.00;Cri=0.020866;L50=41.21;SR=15.36
w1=18.18;w2=18.18;w3=9.09;w4=18.18;w5=18.18;w6=18.18;w7=0.00;w8=0.00;Cri=0.021854;L50=42.37;SR=15.81
w1=18.18;w2=9.09;w3=18.18;w4=18.18;w5=18.18;w6=18.18;w7=0.00;w8=0.00;Cri=0.021854;L50=42.37;SR=15.81

w1 to w8 is the relative level of importance for contact mode 1 to 8 in the specific run. The sum of w1 to w8 is thus 100% and as the number of levels was set to 3, the maximum number of different values within that run will also be 3.
L50 and SR are the simulated selection estimates – the reference data from the field were: L50=42 mm and SR = 15.5 mm. Inspecting the results for the top matches show that the modes investigated, when weight appropriately, make it possible to obtain estimates on selectivity that are relatively close to those obtained in the field. And keep in mind that this initial analysis was based on one mesh (full open) and 3 levels of importance only. Inspecting the relative levels of importance show that mode 7 and 8 are attributed with zero in the combinations that have the highest rank indicating that they explain no or very little of the process of selection. For mode 7 and 8 the first contribution (11.11 %) is found at rank no. 53 and 250 respectively.

When investigating at the combinations giving the poorest parameter estimates, it is seen that mode 7 and mode 8 are attributed with high levels of importance (Table 4):

Table 4

w1=0.00;w2=0.00;w3=0.00;w4=0.00;w5=16.67;w6=16.67;w7=33.33;w8=33.33;Cri=1.768735;L50=19.35;SR=41.61
w1=0.00;w2=0.00;w3=0.00;w4=0.00;w5=0.00;w6=33.33;w7=33.33;w8=33.33;Cri=1.768735;L50=19.35;SR=41.61
w1=20.00;w2=0.00;w3=0.00;w4=0.00;w5=0.00;w6=0.00;w7=40.00;w8=40.00;Cri=1.779267;L50=6.21;SR=39.71
w1=0.00;w2=0.00;w3=0.00;w4=0.00;w5=0.00;w6=40.00;w7=20.00;w8=40.00;Cri=1.782853;L50=23.42;SR=42.27
w1=0.00;w2=0.00;w3=0.00;w4=0.00;w5=20.00;w6=20.00;w7=20.00;w8=40.00;Cri=1.782853;L50=23.42;SR=42.27
w1=0.00;w2=0.00;w3=0.00;w4=0.00;w5=40.00;w6=0.00;w7=20.00;w8=40.00;Cri=1.782853;L50=23.42;SR=42.27
w1=0.00;w2=0.00;w3=0.00;w4=0.00;w5=50.00;w6=0.00;w7=0.00;w8=50.00;Cri=1.800089;L50=28.91;SR=42.98
w1=0.00;w2=0.00;w3=0.00;w4=0.00;w5=0.00;w6=50.00;w7=0.00;w8=50.00;Cri=1.800089;L50=28.91;SR=42.98
w1=0.00;w2=0.00;w3=0.00;w4=0.00;w5=50.00;w6=0.00;w7=0.00;w8=50.00;Cri=1.800089;L50=28.91;SR=42.98
w1=0.00;w2=0.00;w3=0.00;w4=0.00;w5=25.00;w6=25.00;w7=0.00;w8=50.00;Cri=1.800089;L50=28.91;SR=42.98
w1=0.00;w2=0.00;w3=0.00;w4=0.00;w5=0.00;w6=50.00;w7=0.00;w8=50.00;Cri=1.800089;L50=28.91;SR=42.98
w1=25.00;w2=0.00;w3=0.00;w4=0.00;w5=0.00;w6=0.00;w7=25.00;w8=50.00;Cri=1.861638;L50=9.12;SR=41.68
w1=33.33;w2=0.00;w3=0.00;w4=0.00;w5=0.00;w6=0.00;w7=0.00;w8=66.67;Cri=2.007938;L50=13.26;SR=44.76
w1=0.00;w2=0.00;w3=0.00;w4=0.00;w5=0.00;w6=20.00;w7=40.00;w8=40.00;Cri=2.191681;L50=3.40;SR=46.34
w1=0.00;w2=0.00;w3=0.00;w4=0.00;w5=20.00;w6=0.00;w7=40.00;w8=40.00;Cri=2.191681;L50=3.40;SR=46.34
w1=0.00;w2=0.00;w3=0.00;w4=0.00;w5=25.00;w6=0.00;w7=25.00;w8=50.00;Cri=2.308304;L50=6.82;SR=48.84
w1=0.00;w2=0.00;w3=0.00;w4=0.00;w5=0.00;w6=25.00;w7=25.00;w8=50.00;Cri=2.308304;L50=6.82;SR=48.84
w1=0.00;w2=0.00;w3=0.00;w4=0.00;w5=33.33;w6=0.00;w7=0.00;w8=66.67;Cri=2.331343;L50=12.96;SR=50.01
w1=0.00;w2=0.00;w3=0.00;w4=0.00;w5=0.00;w6=33.33;w7=0.00;w8=66.67;Cri=2.331343;L50=12.96;SR=50.01

Based on these results we conclude that it is unlikely that mode 7 and 8 play any major contribution in size selection of Nephrops in real fishery.
The plots in fig. 5 also back up this conclusion as modes 7 and 8 show full retention down to at least 20 mm. At this carapax length, field data have zero retention (Fig. 2).

We therefore chose to eliminate mode 7 and 8 from further analysis. In order to simplify the model, we aim at reducing the number of modes as far as possible without loosing vital information. We therefore look into more detail at the effect of model 1 to 6. In table 3 we observe that each of these modes contribute to the results in the highest ranked combinations. Based on this alone, it is therefore not possible to eliminate any of these modes. It is likely though, that the selective effects of some of these modes are similar, and for predictive purposes it is therefore not necessary to distinct between them. Such similarities are investigated by looking into the penetration results for the 6 modes across the 43 meshes applied in this pilot experiment. Having tested 20 individuals on 43 meshes the amount of penetration results for each mode is 860. Table 5 summarizes the percentages difference in penetration results for mode 1 to 6.

Table 5

mode\mode	**1**	**2**	**3**	**4**	**5**	**6**
1	-	32%	42%	5%	5%	5%
2	-	-	10%	32%	37%	37%
3	-	-	-	41%	47%	47%
4	-	-	-	-	6%	5%
5	-	-	-	-	-	0%
6	-	-	-	-	-	-

From Table 5 it is evident that mode 5 and 6 have similar properties with regards to their ability to penetrate the 43 meshes. We assume that it is more likely for Nephrops to meet

the meshes of a towed gear in mode 5 than mode 6. Furthermore the results of mode 5 are evaluated to be more independent of the person performing the experiment as the legs of the *Nephrops* automatically orient correctly, we choose to eliminate mode 6. Mode 5 is now the most optimal mode for mesh penetration and data for this mode will provide useful information for size selection of Nephrops as it provides an upper limit for penetration. This comply with the field data as can be seen by investigating Fig. 5 for mode 5. For mode 5 we have data indicating full retention at length around 55 mm which fits well with full retention in the field data.
The deviation of results for mode 4 compared to mode 5 is small (6%). Therefore we also eliminate mode 4 also because we find the mode tail spread out to be unlikely and also difficult to handle experimentally. Thus now we are down to modes 1, 2, 3 and 5. In modes 1 to 3, the tail is flexed up which we find to be very likely. Based on the results in Table 5, we could choose to eliminate mode 1 for mode 5 as the deviation in results is only 5%. But inspection of the simulated L50's of the two modes reveals high deviation for some meshes. Table 6 list the difference between estimates of L50 between modes 1 and 5 using 5 as basis.

Table 6

mesh id	deviation L50 (%)	mesh id	deviation L50 (%)
1	0	23	1
2	0	24	0
3	17	25	0
4	-1	26	22
5	16	27	0
6	2	28	2
7	0	29	19
8	20	30	19
9	22	31	0
10	24	32	17
11	6	33	0
12	3	34	17
13	6	35	0
14	6	36	0
15	6	37	0
16	6	38	0
17	16	39	0
18	1	40	0
19	missing value	41	3
20	0	42	0
21	0	43	-1
22	19		

Table 6 shows that L50 for several of the meshes investigated in the pilot experiment is more than 15% larger for mode 5 than for mode 1. Looking at Fig. 2 to inspect the morphology being involved in the penetration attempts this makes sense. For two meshes, it is predicted that L50% is 1% smaller for mode 1 than for mode 5. We expect this to be due to the experimental uncertainty by only using 20 individuals in the pilot experiment which highlights the importance of using more individuals in the main experiment. Based

on the findings described above, we conclude that we cannot represent mode 1 by mode 5.
From Table 5 it is clear that we cannot represent mode 2 or 3 by mode 1 or 5 (deviations between 32 and 47%). Looking at Fig. 5 for mode 2 and 3 indicates that they could well play a role in the size selection process because their upper limit for zero retention seem to fit well with the field data. Combining mode 1 and mode 5 with either mode 2 or mode 3 would thus provide explanation for the selection process in the entire selective range. The only way to reduce the number of modes further is to replace one of modes 2 or 3 by the other. Based on Table 5, deviation between the two is 10% and this does not support such a reduction.
Based on experiences from the laboratory it is evaluated that mode 2 is the more stable of the two as *Nephrops* in mode 3 tended to roll into mode 2. Therefore we choose to drop mode 3. We thus end up with three modes (1, 2 and 5) on which we will base further studies of the size selection of *Nephrops*. Of these, mode 5 will be representing the upper morphological limit for the size selection of *Nephrops*.

After having selected the modes expected to be fully explanatory for the process of selection, the next step is to estimate their individual level of importance. We therefore rerun the simulations for the full open square based on modes 1, 2 and 5 but now with 10 different levels of importance making 10^3=1000 combinations. Table 7 shows the results for the 20 best matches:

Table 7

w1=72.73;w2=27.27;w5=0.00;Cri=0.013267;L50=42.35;SR=15.66
w1=71.43;w2=28.57;w5=0.00;Cri=0.025162;L50=42.01;SR=15.89
w1=75.00;w2=25.00;w5=0.00;Cri=0.028947;L50=42.95;SR=15.22
w1=66.67;w2=25.00;w5=8.33;Cri=0.029155;L50=43.20;SR=15.41
w1=63.64;w2=27.27;w5=9.09;Cri=0.029172;L50=42.62;SR=15.89
w1=62.50;w2=25.00;w5=12.50;Cri=0.031429;L50=43.32;SR=15.50
w1=60.00;w2=26.67;w5=13.33;Cri=0.032238;L50=42.91;SR=15.87
w1=58.33;w2=25.00;w5=16.67;Cri=0.034774;L50=43.44;SR=15.59
w1=56.25;w2=25.00;w5=18.75;Cri=0.037070;L50=43.51;SR=15.64
w1=64.29;w2=28.57;w5=7.14;Cri=0.037784;L50=42.22;SR=16.08
w1=70.00;w2=30.00;w5=0.00;Cri=0.041589;L50=41.63;SR=16.13
w1=53.33;w2=26.67;w5=20.00;Cri=0.042708;L50=43.11;SR=16.02
w1=50.00;w2=25.00;w5=25.00;Cri=0.043847;L50=43.69;SR=15.77
w1=54.55;w2=27.27;w5=18.18;Cri=0.044130;L50=42.89;SR=16.10
w1=52.94;w2=23.53;w5=23.53;Cri=0.048762;L50=44.03;SR=15.40
w1=69.23;w2=30.77;w5=0.00;Cri=0.049699;L50=41.42;SR=16.24
w1=57.14;w2=28.57;w5=14.29;Cri=0.050090;L50=42.43;SR=16.26
w1=45.00;w2=25.00;w5=30.00;Cri=0.050203;L50=43.84;SR=15.88
w1=47.37;w2=26.32;w5=26.32;Cri=0.050440;L50=43.39;SR=16.09
w1=61.54;w2=23.08;w5=15.38;Cri=0.051150;L50=43.90;SR=15.13

Inspecting Table 7 support the thesis that combining just modes 1, 2 and 5 when simulating selectivity of *Nephrops.* Interestingly we observe that mode 1 seem to contribute most while the mode with the most optimal orientation (mode 5) contribute the least. For several results on the top 20 list mode 5 does not contribute at all (w5=0.0) including all results in top 3. This indicates that a major part of the *Nephrops* does not meet the mesh panel in optimal orientation for mesh penetration. Rather it seems like the dominant mode will be the one with the tail flexed (mode 1) or modes with similar selective properties. Fig. 6 plots combination with the highest rank in Table 7.

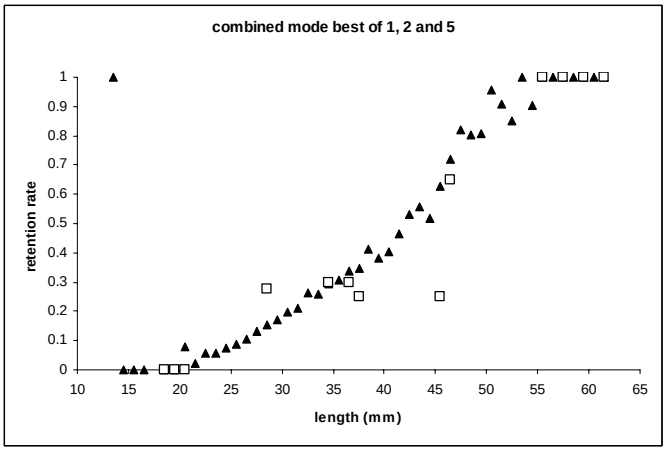

Fig. 6

From 6 it seems that by combination of mode 1, 2 and 5 we can simulate the selection observed in the field.

When looking at the three modes separately i.e. 100% contribution from one mode, it is evident that none of the modes can stand alone in explaining the selective process. The value of the function *Cri* are thus 33 to 75 times higher than the values of the best combination of the three modes (Table 7) which illustrates the much poorer representation of the field data. Results for this are shown in Table 8.

Table 8

w1=100.00;w2=0.00;w5=0.00;Cri=1.005082;L50=46.50;SR=0.01
w1=0.00;w2=100.00;w5=0.00;Cri=1.117350;L50=21.01;SR=0.01
w1=0.00;w2=0.00;w5=100.00;Cri=1.006449;L50=47.01;SR=0.01

From Table 8 it is clear that selection range (SR) for the "clean" modes is very low compared to what is observed in the field. Results shown in Table 7 and 8 indicate that a likely explanation for the relatively large SR usually observed in field experiments testing selectivity of *Nephrops* is likely to be that different contact modes coming in to play.
For the full open square mesh, the simulated L50 (mode 1 and mode 5) is not very different from the one obtained in the field. These simulations are based on the 20 individuals only and prior to using the model to predict the selective properties of nettings for which we have no reference data, a main experiment using more individuals needs to be conducted.
Before we close the analysis of the pilot data we take a brief look at the effect of square meshes not being fully open. Flume tank observation on the mesh openings for the codend in question, has indicated that it the meshes can be closed down to a corresponding hexagonal shape with opening angle at 80 degrees. The justification for using the hexagonal shape is, that the soft material used for the netting is easily distorted in the tensionless bars by individuals trying to pass through the mesh. To make an initial test of this effect, we conducted an extra run of simulations combining selection of modes 1, 2 and 5 in both of the extreme mesh openings; the full open square and the 80 degrees corresponding hexagonal shaped (mesh id 18 and mesh id 33). This results in 6 "modes"

(2 meshes times the contact modes). To limit computing time, we reduced the number of levels to 5 making 5^6=15625 combinations. Table 9 shows the best 20 matches for this.

Table 9

w1=36.36;w2=9.09;w3=27.27;w4=0.00;w5=27.27;w6=0.00;Cri=0.006276;L50=41.85;SR=15.42
w1=50.00;w2=16.67;w3=16.67;w4=0.00;w5=16.67;w6=0.00;Cri=0.006798;L50=41.91;SR=15.60
w1=25.00;w2=16.67;w3=33.33;w4=0.00;w5=16.67;w6=8.33;Cri=0.008274;L50=41.68;SR=15.45
w1=25.00;w2=16.67;w3=33.33;w4=8.33;w5=16.67;w6=0.00;Cri=0.008274;L50=41.68;SR=15.45
w1=20.00;w2=20.00;w3=40.00;w4=10.00;w5=10.00;w6=0.00;Cri=0.008714;L50=42.34;SR=15.55
w1=20.00;w2=20.00;w3=40.00;w4=0.00;w5=10.00;w6=10.00;Cri=0.008714;L50=42.34;SR=15.55
w1=27.27;w2=9.09;w3=36.36;w4=0.00;w5=27.27;w6=0.00;Cri=0.010090;L50=42.12;SR=15.65
w1=18.18;w2=27.27;w3=36.36;w4=18.18;w5=0.00;w6=0.00;Cri=0.010400;L50=41.84;SR=15.35
w1=18.18;w2=27.27;w3=36.36;w4=9.09;w5=0.00;w6=9.09;Cri=0.010400;L50=41.84;SR=15.35
w1=18.18;w2=27.27;w3=36.36;w4=0.00;w5=0.00;w6=18.18;Cri=0.010400;L50=41.84;SR=15.35
w1=30.77;w2=7.69;w3=30.77;w4=0.00;w5=30.77;w6=0.00;Cri=0.011252;L50=41.54;SR=15.54
w1=28.57;w2=28.57;w3=28.57;w4=7.14;w5=0.00;w6=7.14;Cri=0.012513;L50=41.61;SR=15.63
w1=28.57;w2=28.57;w3=28.57;w4=0.00;w5=0.00;w6=14.29;Cri=0.012513;L50=41.61;SR=15.63
w1=28.57;w2=28.57;w3=28.57;w4=14.29;w5=0.00;w6=0.00;Cri=0.012513;L50=41.61;SR=15.63
w1=30.00;w2=20.00;w3=30.00;w4=10.00;w5=10.00;w6=0.00;Cri=0.012958;L50=42.05;SR=15.30
w1=30.00;w2=20.00;w3=30.00;w4=0.00;w5=10.00;w6=10.00;Cri=0.012958;L50=42.05;SR=15.30
w1=33.33;w2=11.11;w3=33.33;w4=0.00;w5=22.22;w6=0.00;Cri=0.014762;L50=42.62;SR=15.50
w1=0.00;w2=0.00;w3=60.00;w4=0.00;w5=40.00;w6=0.00;Cri=0.016032;L50=42.36;SR=15.71
w1=36.36;w2=27.27;w3=27.27;w4=9.09;w5=0.00;w6=0.00;Cri=0.017698;L50=42.36;SR=15.74
w1=36.36;w2=27.27;w3=27.27;w4=0.00;w5=0.00;w6=9.09;Cri=0.017698;L50=42.36;SR=15.74

In Table 9 the contact mode factors w1 to w6 is sequenced to represent: (mesh id18 in mode 1), (mesh id18 in mode 2), (mesh id18 in mode 5), (mesh id33 in mode 1), (mesh id33 in mode 2), (mesh id33 in mode 5). The inclusion of the another mesh configuration further reduced the value of *Cri* indicating that the simulated parameters are very close to the parameters obtained in the field (Table 8). When plotting retention data (Fig. 7) the similarity between simulated results (squares) and field data (triangles) is evident.

Fig. 7 plots the best ranked combination of Table 9 against the experimental dataset.

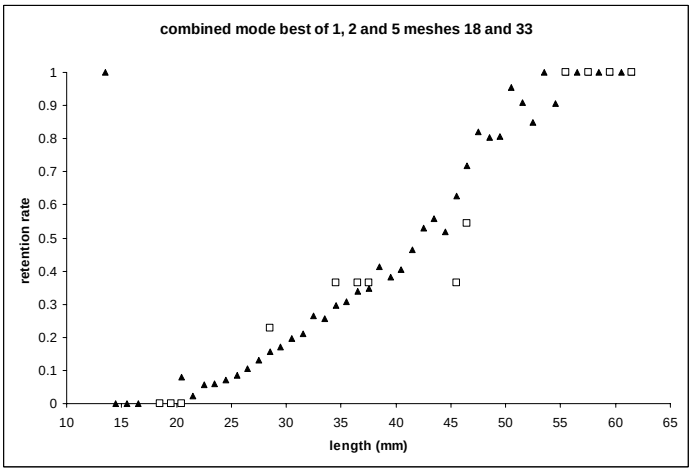

Fig. 7

These results are very convincing but it is clear that a better set penetration data based on a large number of *Nephrops* having higher resolution in length classes is needed before we try to refine the analysis further.

Main experiments.

Based on the pilot experiment we decided to base to main experiment on contact modes 1, 2 and 5 only while we increased the number of meshes to 160. Table 10 shows the mesh data using the syntax for mesh description used in the FISHSELECT software tool.

Table 10

ID=1;Type=D;m=70;oa=15;ID=2;Type=D;m=70;oa=20;ID=3;Type=D;m=70;oa=30;ID=4;Type=D;m=70;oa=35;
ID=5;Type=D;m=70;oa=40; ID=6;Type=D;m=70;oa=45;ID=7;Type=D;m=70;oa=50;ID=8;Type=D;m=70;oa=55;
ID=9;Type=D;m=70;oa=60;ID=10;Type=D;m=70;oa=65;ID=11;Type=D;m=70;oa=70;ID=12;Type=D;m=70;oa=75;
ID=13;Type=D;m=70;oa=80;ID=14;Type=D;m=70;oa=85;ID=15;Type=D;m=70;oa=90;ID=16;Type=D;m=80;oa=15;
ID=17;Type=D;m=80;oa=20;ID=18;Type=D;m=80;oa=25;ID=19;Type=D;m=80;oa=30;ID=20;Type=D;m=80;oa=55;
ID=21;Type=D;m=80;oa=85;ID=22;Type=D;m=90;oa=15;ID=23;Type=D;m=90;oa=20;ID=24;Type=D;m=90;oa=25;
ID=25;Type=D;m=90;oa=30;ID=26;Type=D;m=90;oa=35;ID=27;Type=D;m=90;oa=40;ID=28;Type=D;m=90;oa=45;
ID=29;Type=D;m=90;oa=50;ID=30;Type=D;m=90;oa=55;ID=31;Type=D;m=90;oa=60;ID=32;Type=D;m=90;oa=65;
ID=33;Type=D;m=90;oa=70;ID=34;Type=D;m=90;oa=75;ID=35;Type=D;m=90;oa=80;ID=36;Type=D;m=90;oa=85;
ID=37;Type=D;m=90;oa=90;ID=38;Type=D;m=100;oa=20;ID=39;Type=D;m=100;oa=55;ID=40;Type=D;m=100;oa=85;
ID=41;Type=D;m=110;oa=20;ID=42;Type=D;m=110;oa=55;ID=43;Type=D;m=110;oa=85;ID=44;Type=D;m=120;oa=15;
ID=45;Type=D;m=120;oa=20;ID=46;Type=D;m=120;oa=25;ID=47;Type=D;m=120;oa=30;ID=48;Type=D;m=120;oa=35;
ID=49;Type=D;m=120;oa=40;ID=50;Type=D;m=120;oa=45;ID=51;Type=D;m=120;oa=50;ID=52;Type=D;m=120;oa=55;
ID=53;Type=D;m=120;oa=60;ID=54;Type=D;m=120;oa=65;ID=55;Type=D;m=120;oa=70;ID=56;Type=D;m=120;oa=75;
ID=57;Type=D;m=120;oa=80;ID=58;Type=D;m=120;oa=85;ID=59;Type=D;m=130;oa=20;ID=60;Type=D;m=130;oa=55;
ID=61;Type=D;m=130;oa=85;ID=62;Type=D;m=140;oa=20;ID=63;Type=D;m=140;oa=55;ID=64;Type=D;m=140;oa=85;
ID=65;Type=D;m=160;oa=15;ID=66;Type=D;m=160;oa=20;ID=67;Type=D;m=160;oa=25;ID=68;Type=D;m=160;oa=30;
ID=69;Type=D;m=160;oa=35;ID=70;Type=D;m=160;oa=40;ID=71;Type=D;m=160;oa=45;ID=72;Type=D;m=160;oa=50;
ID=73;Type=D;m=160;oa=55;ID=74;Type=D;m=160;oa=60;ID=75;Type=D;m=160;oa=65;ID=76;Type=D;m=160;oa=70;
ID=77;Type=D;m=160;oa=75;ID=78;Type=D;m=160;oa=80;ID=79;Type=D;m=160;oa=85;ID=80;Type=D;m=180;oa=15;
ID=81;Type=D;m=180;oa=55;ID=82;Type=D;m=180;oa=85;ID=83;Type=D;m=200;oa=15;ID=84;Type=D;m=200;oa=55;
ID=85;Type=D;m=200;oa=85;ID=86;Type=S;b=100;ID=87;Type=S;b=90;ID=88;Type=S;b=80;ID=89;Type=S;b=70;
ID=90;Type=S;b=60;ID=91;Type=S;b=50;ID=92;Type=S;b=40;ID=93;Type=S;b=35;ID=94;Type=S;b=30;
ID=95;Type=R;b=90;a=10;ID=96;Type=R;b=90;a=15;ID=97;Type=R;b=90;a=20;ID=98;Type=R;b=90;a=30;
ID=99;Type=R;b=90;a=50;ID=100;Type=R;b=90;a=70;ID=101;Type=R;b=120;a=10;ID=102;Type=R;b=120;a=15;
ID=103;Type=R;b=120;a=20;ID=104;Type=R;b=120;a=30;ID=105;Type=R;b=120;a=50;ID=106;Type=R;b=120;a=70;
ID=107;Type=R;b=200;a=10;ID=108;Type=R;b=200;a=15;ID=109;Type=R;b=200;a=20;ID=110;Type=R;b=200;a=30;
ID=111;Type=R;b=200;a=35;ID=112;Type=R;b=200;a=40;ID=113;Type=R;b=200;a=45;ID=114;Type=R;b=200;a=50;
ID=115;Type=R;b=200;a=60;ID=116;Type=R;b=200;a=70;ID=117;Type=H;b=50;k=100;oa=145;
ID=118;Type=H;b=50;k=100;oa=130;ID=119;Type=H;b=50;k=100;oa=105;ID=120;Type=H;b=50;k=100;oa=90;
ID=121;Type=H;b=50;k=100;oa=60;ID=122;Type=H;b=50;k=100;oa=40;ID=123;Type=H;b=15;k=30;oa=145;
ID=124;Type=H;b=15;k=30;oa=130;ID=125;Type=H;b=15;k=30;oa=105;ID=126;Type=H;b=15;k=30;oa=90;
ID=127;Type=H;b=15;k=30;oa=80;ID=128;Type=H;b=15;k=30;oa=60;ID=129;Type=H;b=15;k=30;oa=40;
ID=130;Type=H;b=17.5;k=35;oa=145;ID=131;Type=H;b=17.5;k=35;oa=130;ID=132;Type=H;b=17.5;k=35;oa=105;
ID=133;Type=H;b=17.5;k=35;oa=90;ID=134;Type=H;b=17.5;k=35;oa=80;ID=135;Type=H;b=17.5;k=35;oa=60;
ID=136;Type=H;b=17.5;k=35;oa=40;ID=137;Type=H;b=20;k=40;oa=145;ID=138;Type=H;b=20;k=40;oa=130;
ID=139;Type=H;b=20;k=40;oa=105;ID=140;Type=H;b=20;k=40;oa=90;ID=141;Type=H;b=25;k=50;oa=145;
ID=142;Type=H;b=25;k=50;oa=130;ID=143;Type=H;b=25;k=50;oa=105;ID=144;Type=H;b=25;k=50;oa=90;
ID=145;Type=H;b=30;k=60;oa=145;ID=146;Type=H;b=30;k=60;oa=130;ID=147;Type=H;b=30;k=60;oa=105;
ID=148;Type=H;b=30;k=60;oa=90;ID=149;Type=H;b=30;k=60;oa=80;ID=150;Type=H;b=30;k=60;oa=70;
ID=151;Type=H;b=30;k=60;oa=60;ID=152;Type=H;b=30;k=60;oa=40;ID=153;Type=H;b=35;k=70;oa=145;
ID=154;Type=H;b=35;k=70;oa=130;ID=155;Type=H;b=35;k=70;oa=105;ID=156;Type=H;b=35;k=70;oa=90;
ID=157;Type=H;b=40;k=80;oa=145;ID=158;Type=H;b=40;k=80;oa=130;ID=159;Type=H;b=40;k=80;oa=105;
ID=160;Type=H;b=40;k=80;oa=90;

Fig. 8 shows a photo of the mesh plates.

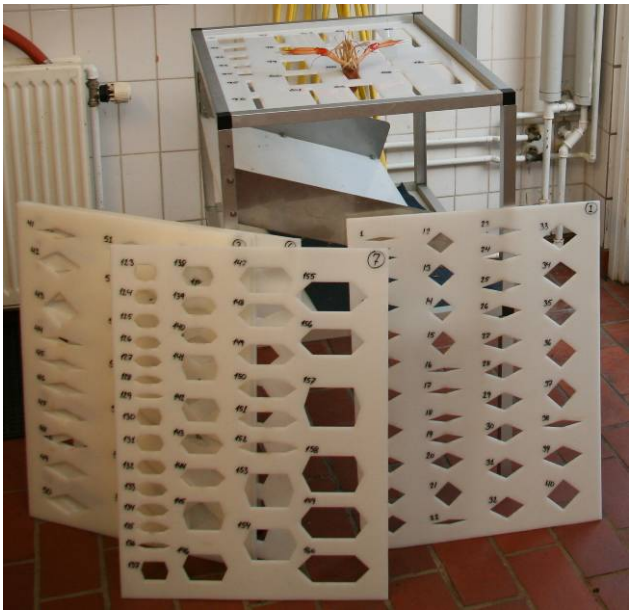

Fig. 8

In total we analyzed 70 individuals yielding a total of 3x70x160=33600 penetration results. Fig. 9 shows the length distribution of the *Nephrops* used in the main experiment.

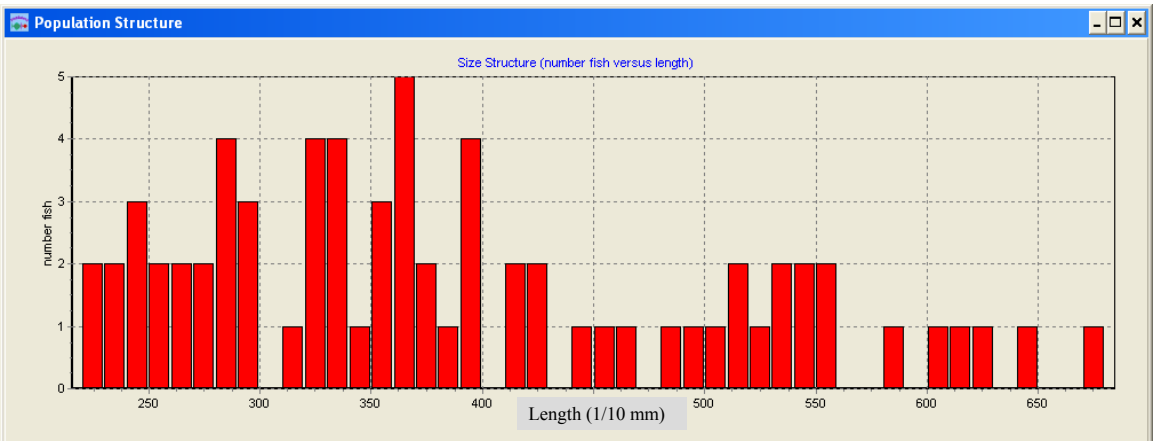

Fig. 9

As we also wish to link mesh penetration to the morphology of *Nephrops* we have identified different morphological measures besides length, sex and weight. We acquire these by use of a small Mechanical MorphoMeter and the flatbed scanner. Some of the measures are read directly from pictures obtained by placing the *Nephrops* directly on the scanner. Thus for each of the 70 *Nephrops* we made 7 scans. Two of the scans included using the mechanical MorphoMeter and were directly linked the decisive cross sections for contact modes 1 (Fig. 10) and 5 (Fig. 11).

Fig. 10

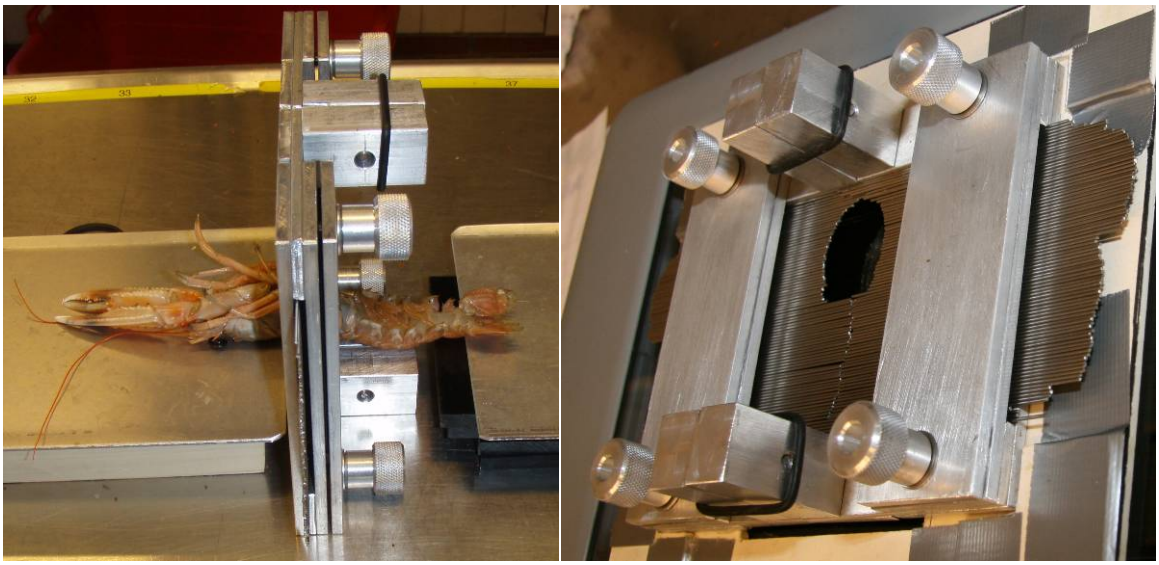

Fig. 11

Fig. 12 shows scannings of Nephrops made without the MorphoMeter.


Fig. 12

The main experiment was carried out within this project. But we were not able to conduct the analysis of the data within the limits of the project.

Discussion.
The analysis of the main experiment data shall include rerunning the analysis of Table 7 to 9 because more confidence can be gained on results based on the more extensive penetration data set. The analysis shall also include comparisons with other results from experimental fishing in order to gain a better foundation for the level of importance of the different modes. Hopefully, these analyses will confirm that using combinations of contact modes 1, 2 and 5 can explain experimental results obtained for other gear designs.

It is expected that between haul variation is high for this species as the selective properties of the codend is partly determined by its geometry and *Nephrops* tend to pack if there are no or very few round fish in the catch and this will affect codend geometry. The combination of species in the specific haul is therefore expected to contribute to the between haul variation. Another source of variation is found in cases where analysis is based on few individuals coursed by use of sub-sampling or low catch rates. We will attempt to estimate this variation by varying in the level of importance of the three contact modes between hauls.

Based on the data in the main experiment, prediction on the size selective properties of different nettings with respect to *Nephrops* can be made in two ways:
1) As in the pilot study where we do not link analysis to cross section morphology;
2) As in the analyses of fish species in FISHSELECT where we do link it to cross section morphology.
The latter will, if successful give a method that is more general and more robust with respect to extrapolation. It will also provide the deepest inside with respect to gain of

knowledge about basic size selective mechanisms for *Nephrops*. On the other hand the first is simpler and less time consuming to carry through.

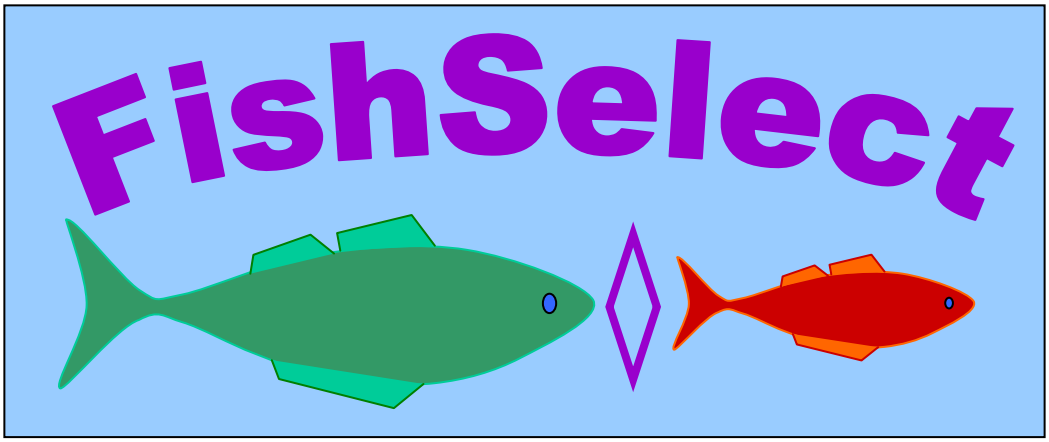

A9

A SHORT GUIDE

TO

THE

FISHSELECT SOFTWARE TOOL

Introduction

This manual gives a short overview of the facilities implemented in the FISHSELECT software tool. It shows the different windows in the tool and how to navigate between them. It also briefly describes what the different windows can be used to do. The software tool is implemented using the development tool Delphi from Borland Software Corporation. FISHSELECT software tool can be run on a powerful personal computer having a Microsoft Windows operating system.

Briefly, FISHSELECT is a methodology to assess the morphological conditions for different species of fish and crustaceans relevant in the process of mesh (and grid) penetration in towed fishing gears. It is based on a combination of laboratory experiments with freshly caught individuals, data collection, data analysis and computer simulations. The FISHSELECT software tool supports all these tasks.
The four main elements (a to d) in the FISHSELECT methodology are described below.

a. Laboratory experiments and data collection.
   Length and weight are recorded for each individual. Cross sections that potentially could influence the ability of the species to penetrate meshes or grids are recorded with regard to shape and size. This is done by use of a specially designed mechanical tool (MorphoMeter), scanning with a flatbed scanner and digital image analysis. Based on different geometrical shapes, the cross sections are automatically described by a few parameters. The values of the parameters are linked to the length of the individuals by applying regression analysis. All data are recorded and analysed in the FISHSELECT software tool.

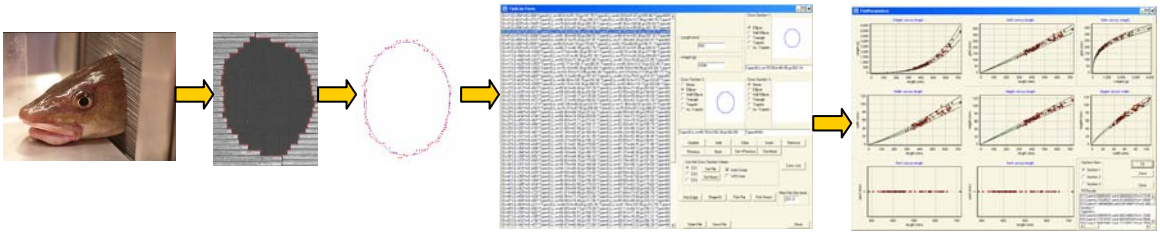

   Template plates with holes imitating a large number of different meshes are used. For each individual it is tested and recorded whether or not it can pass through a given mesh. Fish are always oriented head first and pulled by the force of gravity alone.

b. Simulation of laboratory experiments on mesh penetration.
By use of built-in facilities in the simulation tool, the experimental morphological descriptions of the cross sections and information about the mesh holes are combined and this feature enables a simulation of the experimental penetration experiments. The model facilities allow inclusion and exclusion of different cross sections as well as different ways to account for compression or distortion of the cross sections during the penetration attempts.
Subsequently, the tool is used to compare the experimental results with the corresponding simulated results. The same set of fish is run through a series of simulations using different combinations of cross sections and different compressions/distortions. This procedure enables the user to identify the cross sections most important for mesh penetration of the given species. Furthermore, this procedure improves the understanding on how and to what extent these cross sections are compressed or distorted during penetration.

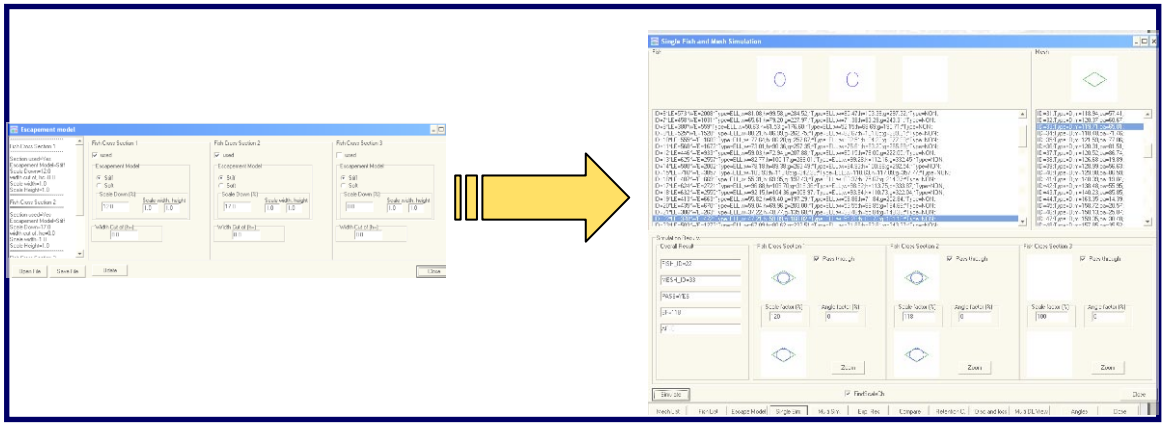

In this way, it is established which cross section information to use and how to use these to simulate penetration through any mesh for the species being studied. These informations are compiled in what is called the penetration model.

c. Establishment of morphological relationships
There is a built-in functionality to describe the relationship between fish length and the parameters describing the cross sections and fish length. The output contains the fit statistics and variance of the parameter values.

Morphological relationships

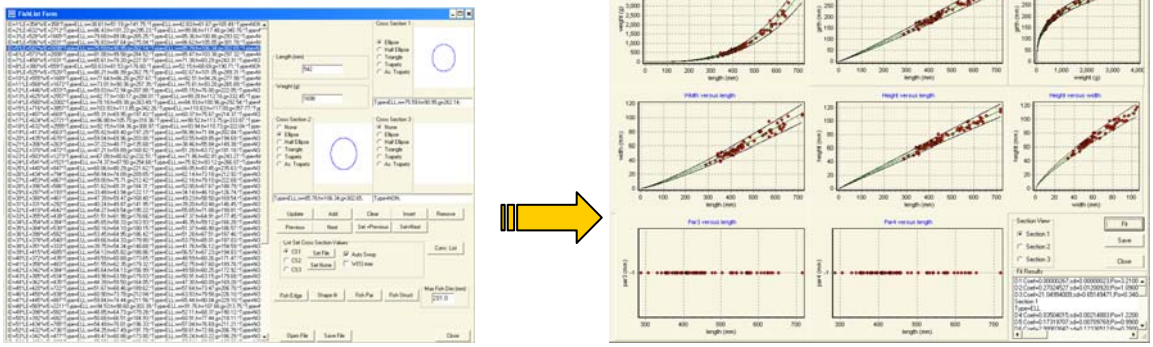

This information can then be used to construct a virtual population of the species having similar morphological characteristics with respect to mesh penetration ability as the fish tested experimentally. The between-individuals-variation in the relationship between length and the parameter values describing the cross sections shapes and sizes will also be included in the virtual population.

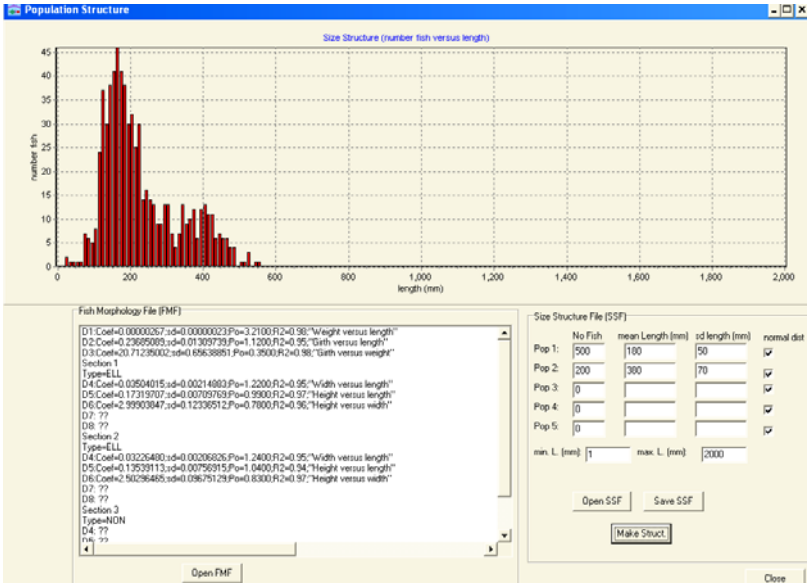

d. Estimation of basic selectivity of netting panels

Data for the virtual population of fish and data for mesh panels of interest are combined to make a new series of simulations with the established penetration model. The built-in functionality enables the user to estimate the basic selective properties (selection curves) for the selected netting panels for the species being studied. For a specific panel, it also enables a prediction of weather or not there is a reasonable balance between the selective properties of the netting panel and the minimum landing size (MLS) for the species.

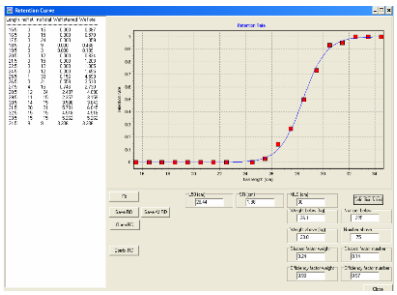

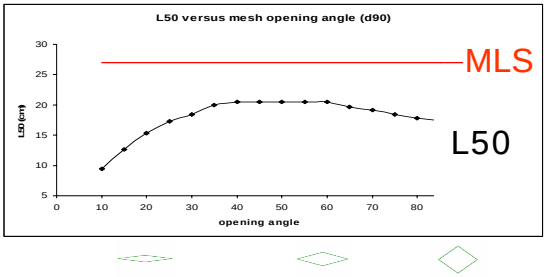

Thus if information on the large scale population structure of a species is available for a particular fishery, the built-in functionality gives a first indicative prediction of the consequences on discard / loss of marketable fish, of using the netting panel in combination with the chosen MLS.

Table 1 contains a list of the different windows in FISHSELECT tool and on which page in this manual they are shown and described. To ensure the functionality of the program, the order of filling in values, should follow the order of the list below.

Main Window.

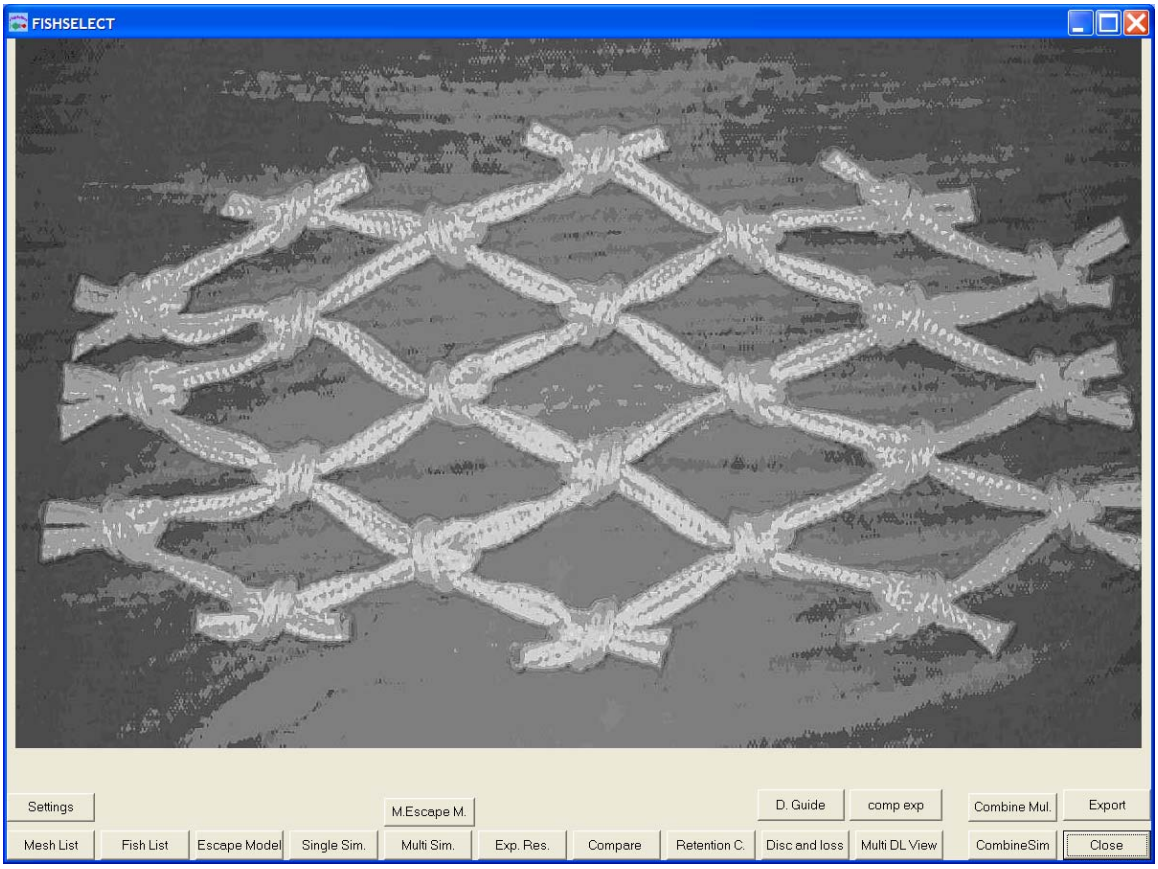

When starting FISHSELECT from Microsoft Windows the **Main Window** shows up. The user controls what goes on in FISHSELECT by using the mouse to activate the buttons in the lower part of the window.

Mesh List window

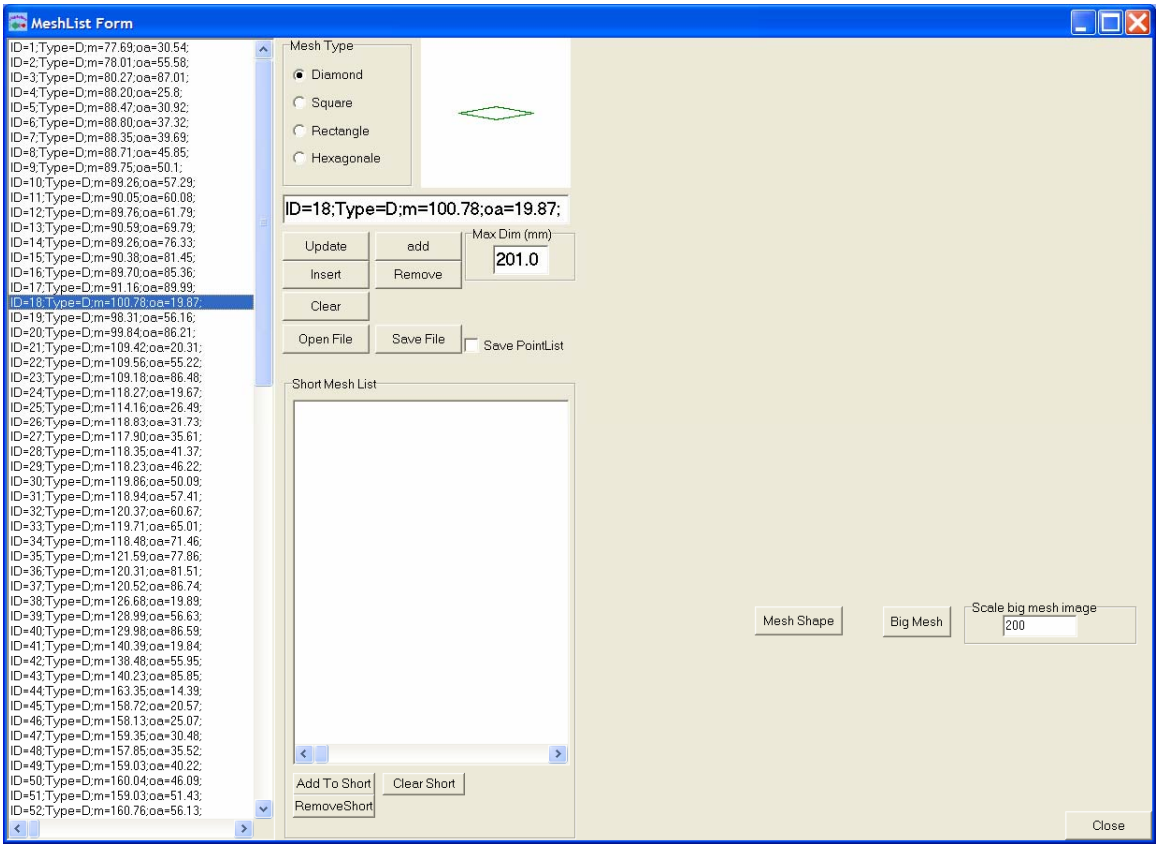

Access: from **Main Windows** by clicking on the **Mesh List** button.

Use the **Mesh List Window** to define the different mesh shapes and sizes used in the experiment in the laboratory and/or in the simulations.
A special syntax language and an associated interpreter for the syntax has been developed and implemented in the software tool. The list is saved in a text-file format with the extension MLF (Mesh List File) and data are thus accessible outside the program.
Four mesh types are implemented: D (Diamond), S (Square), R (Rectangle), H (Hexagonal). Mesh type is selected by setting the appropriate radio button in the **Mesh Type Panel**. Use the buttons **Update**, **Add**, **Insert**, **Remove**, **Clear** to define the mesh list. Use button **Open File** to open an existing Mesh List File. Use button **Save File** to save the current mesh list to a MLF file.

The **Short Mesh List Panel** makes it possible to select a subset of meshes from the current mesh list. It is possible to run simulations in the **Multiple Simulation Window** for that subset only instead of for the full list. Use button **Add To Short** to add the marked mesh in the full mesh list to the short list. Use button **Remove Short** to remove the marked mesh in the short mesh list from the short list. Use button **Clear Short** to clear the short list.

Use button **Mesh Shape** to access the **Mesh Shape Window**.
The button **Big Mesh** automatically saves a JPG-picture of the marked mesh in the mesh list.

Mesh Shape Window

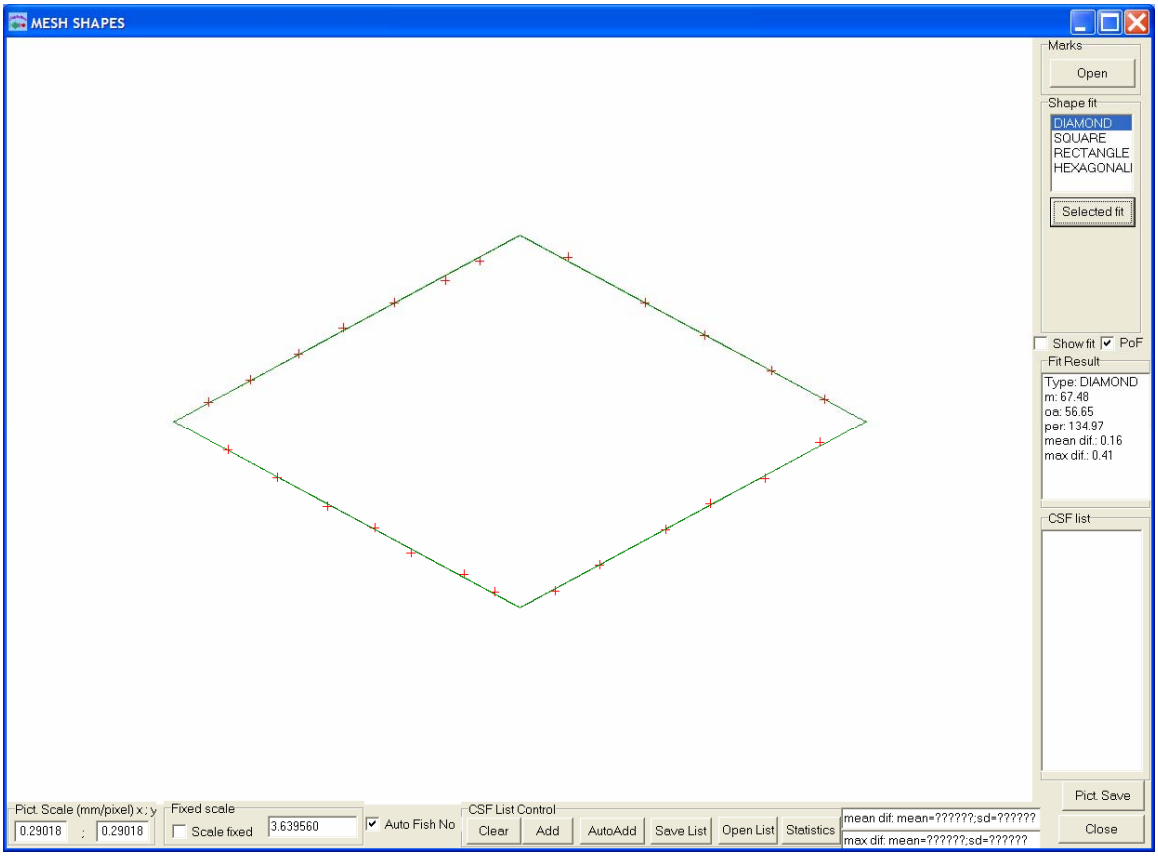

Access: from **Mesh List Window** by activating button **Mesh Shape**.

If measured shape data for a mesh have been saved as a set of coordinate points (x,y) in a file complying with the MKS (MarKS file) format like that generated in the **Fish Edge Window,** the file can be viewed as x,y points (the red crosses) in this window. In the **Shape fit Panel** select the mesh type to try to fit to the coordinate points. The main result from the fit is shown in the **Fit Result Panel**. In the example above a diamond shape is fitted to the points. Mesh size m is found to be 67.48 mm and the opening angle oa to be 56.65 ˚. The mean difference between the points and the fitted diamond shape is 0.16 mm while the maximal difference is found to be 0.41 mm. The fitting procedure is based on a least square technique.
When opening a MKS file, the screen view is automatically scaled to optimum size. If one wants to compare MKS files of meshes of different sizes this may be impractical. The automatic scaling can be disabled by checking the checkbox **Scale fixed**.

Fish List Window

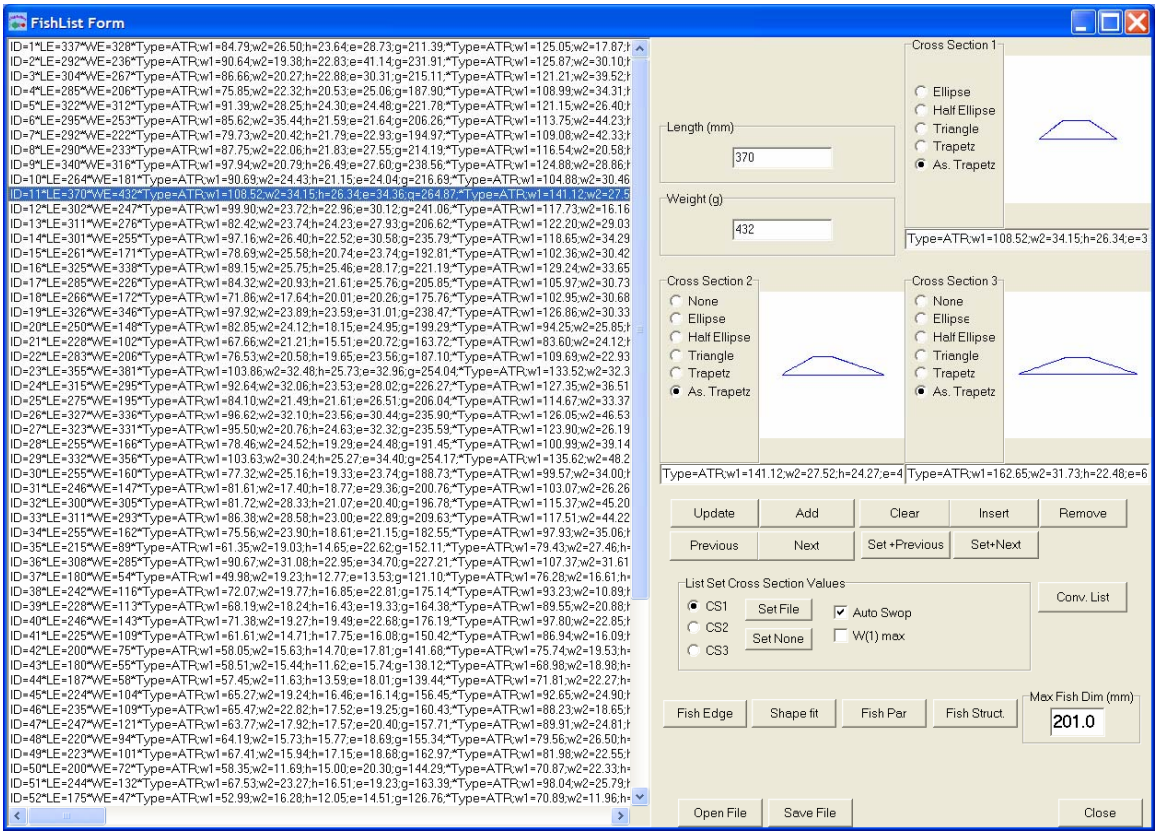

Access: from **Main Window** by activating button **Fish List**.

Use the **Fish List Window** to organize a list of different individual fish definitions used in the experiment in the laboratory and/or in the simulations.
A special syntax language and an associated interpreter for the syntax has been developed and implemented in the software tool. The list is saved in a text-file format with the extension FLF (Fish List File) which makes data accessible outside the program. Use the buttons **Update**, **Add**, **Insert**, **Remove**, **Clear** to define the mesh list. Use button **Open File** to open an existing Fish List File. Use button **Save File** to save the current fish list to a FLF file.
Parameters defining shapes and sizes of up to three different cross sections (CS1, CS2, CS3) can be included for each fish. The parameters of the cross sections are obtained in the Fish Shape Fit Window.

Fish Edge Window

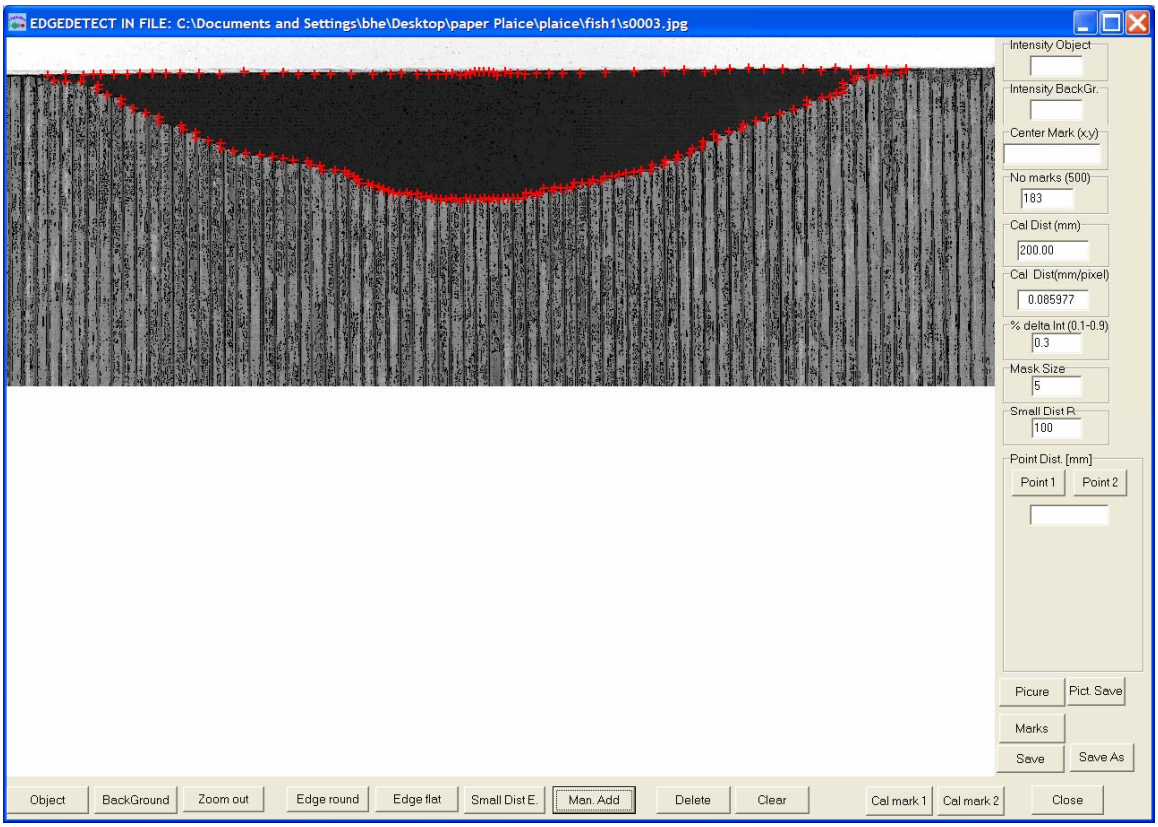

Access: from **Fish List Window** by activating button **Fish Edge**.

Use the **Fish Edge Window** to extract the Cross Section outline contour from a scanned image of the mechanical MorphoMeter by applying the built-in image analysis functions (buttons **Edge round**, **Edge flat**, **Small Dist E.**, **Man. Add**, **Delete**, **Clear**). Click the button **Object** and then click the mouse to mark the centre of the object (centre of cross section). Use button **BackGround** in the same way to define the background colour intensity (on the Morphometer Sticks). The detected contour is marked by the red crosses (Marks). Data are saved in a text-file with extension MKS and can be accessed from other programs as well. Remember to calibrate the pixel to mm relation by using the calibration marks in the picture together with the facilities in the window.

Fish Shape Fit Window

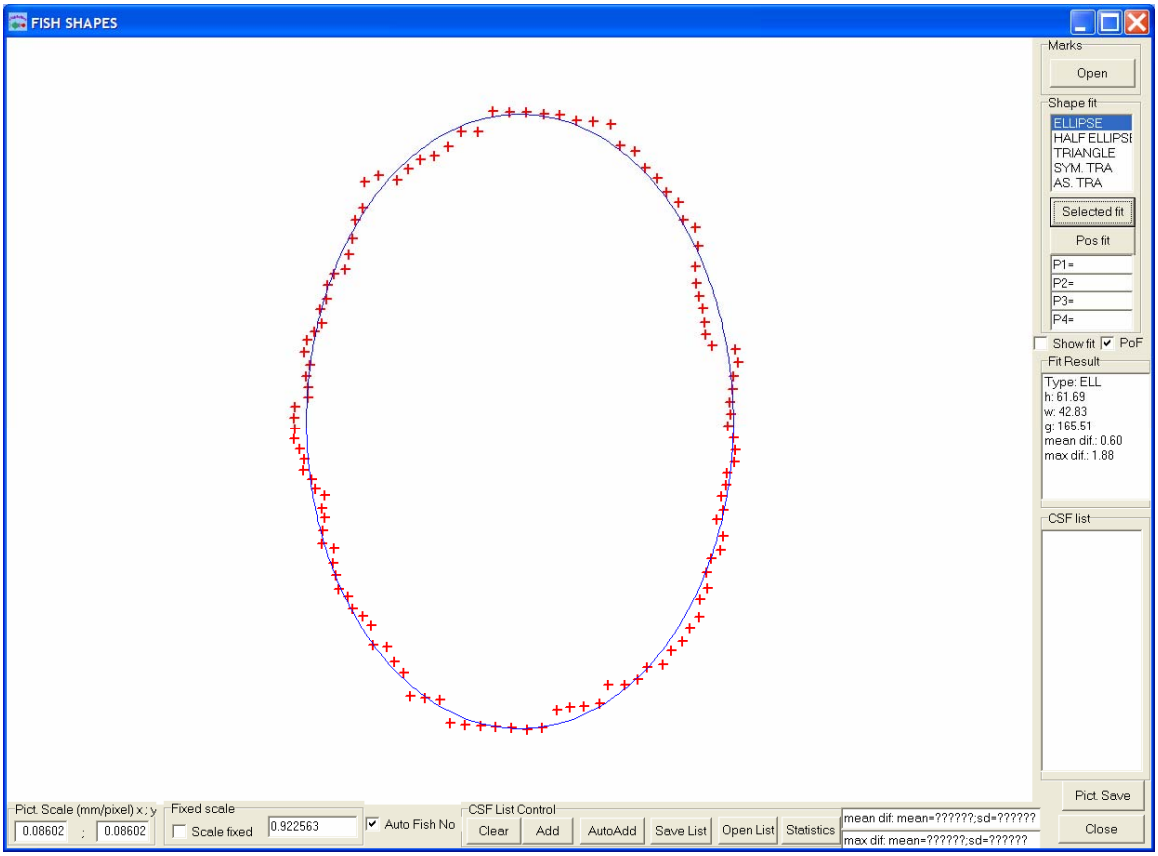

Access: from **Fish List Windows** by activating button **Shape Fit**.

Use the **Fish Shape Window** to fit basic geometrical shapes to the mks-files defining the fish cross section shape and size.
Five cross section shape types are implemented: ELL (Ellipse), HEL (half ellipse), TRI (Triangle), TRA (Symmetrical Trapezoid), ATR (Asymmetrical Trapezoid).
The main result from the fit is shown in the **Fit Result Panel**. In the shown example, an ellipsoid is fitted to the points. Cross section height (h) is found to be 61.69 mm, width (w) is 42.83 mm and circumference (g) is found to be 165.51mm. The mean difference between the points and the fitted ellipsoid is 0.60 mm while the maximum difference is found to be 1.88 mm. The fitting procedure is based on a least square technique.

Fish Parameters Window

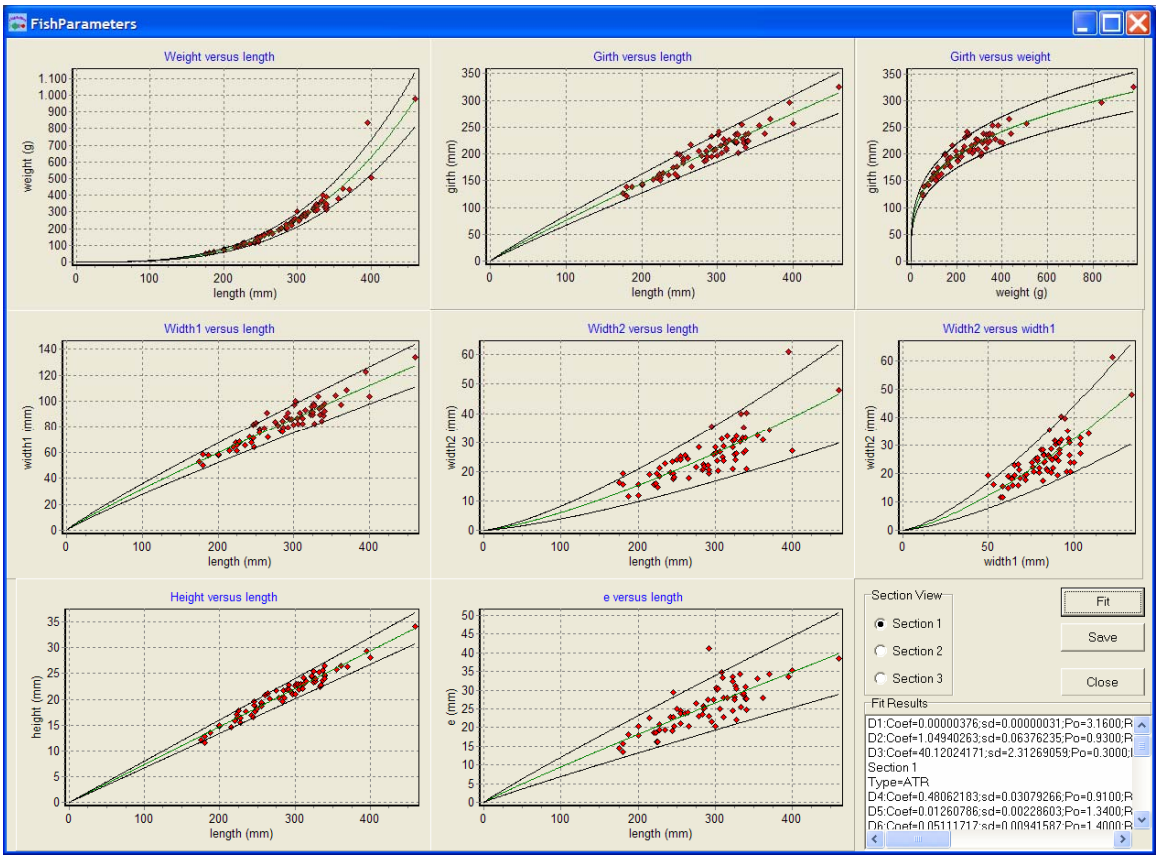

Access: from **Fish List Window** by activating button **Fish Par**.

Use the **Fish Parameters Window** to estimate the mean and standard deviation of the parameters describing the relations between fish length, fish weight and cross section shape measures.

The example shows plots of the parameters, when asymmetrical trapezoids are fitted to the cross section measures of Cs1 (cross section immediately behind the head) for a batch of plaice. Use the button **Fit** to estimate the relationships, which are shown in the **Fit Results** panel. The plots show the mean relationships (center line) and mean ±2 times standard deviation.

Fish Size Structure Window

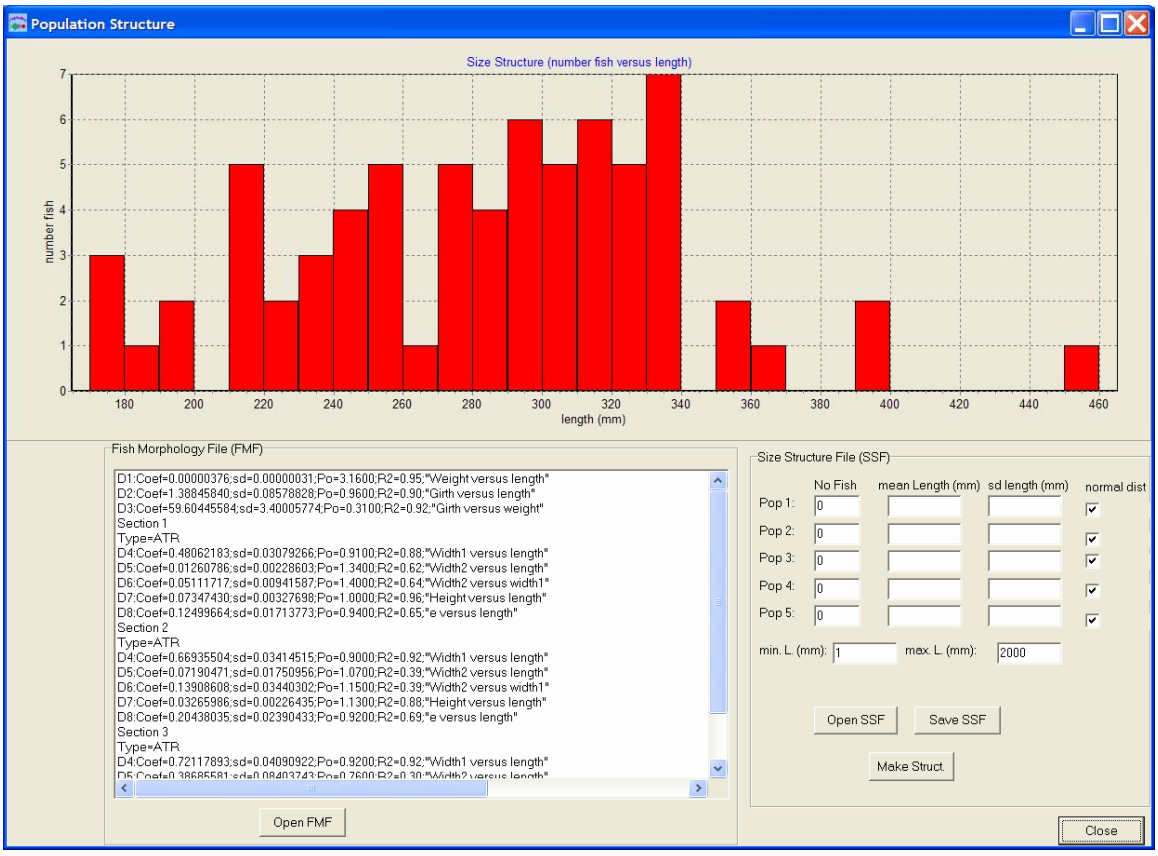

Access: from **Fish List Window** by activating button **Fish Struct**.
The window is used to check size structure of fish examined in the lab and to create a virtual population of fish.

Penetration Model Window

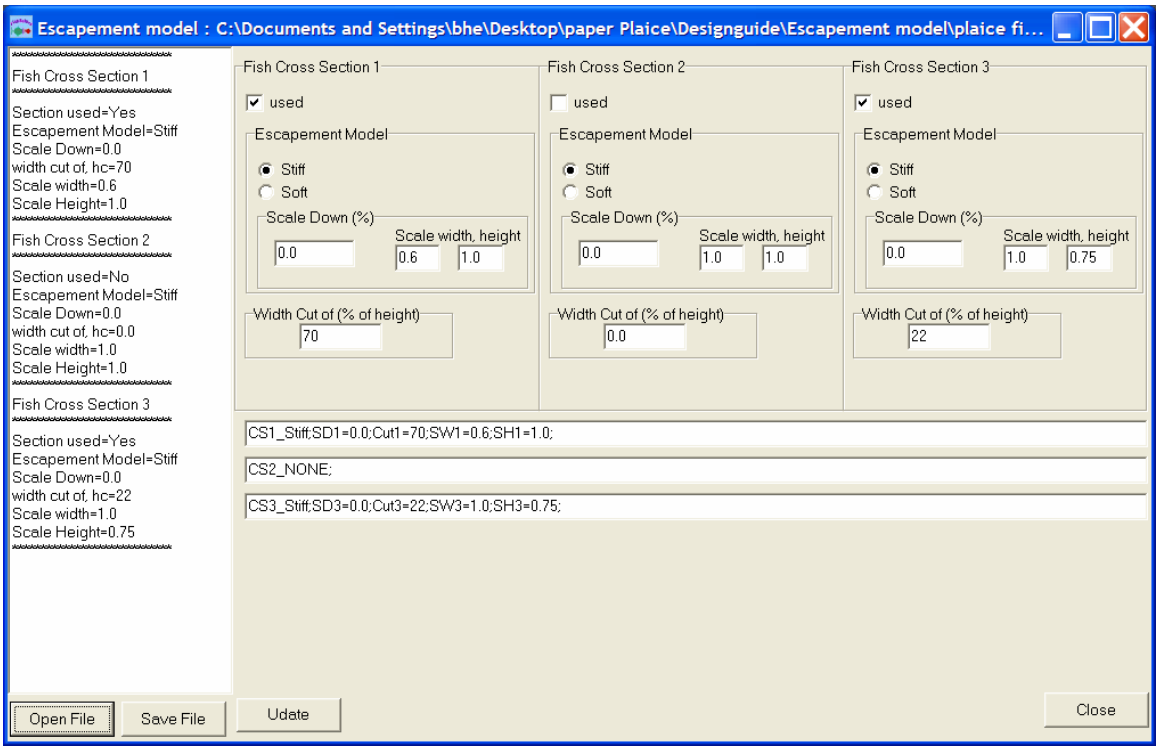

Access: from **Main Window** by activating button **Escape Model**.
The window is used to enter the penetration model that is used in the subsequent simulations. The model is saved as a text file with the extension EMF.

Single Simulation Window

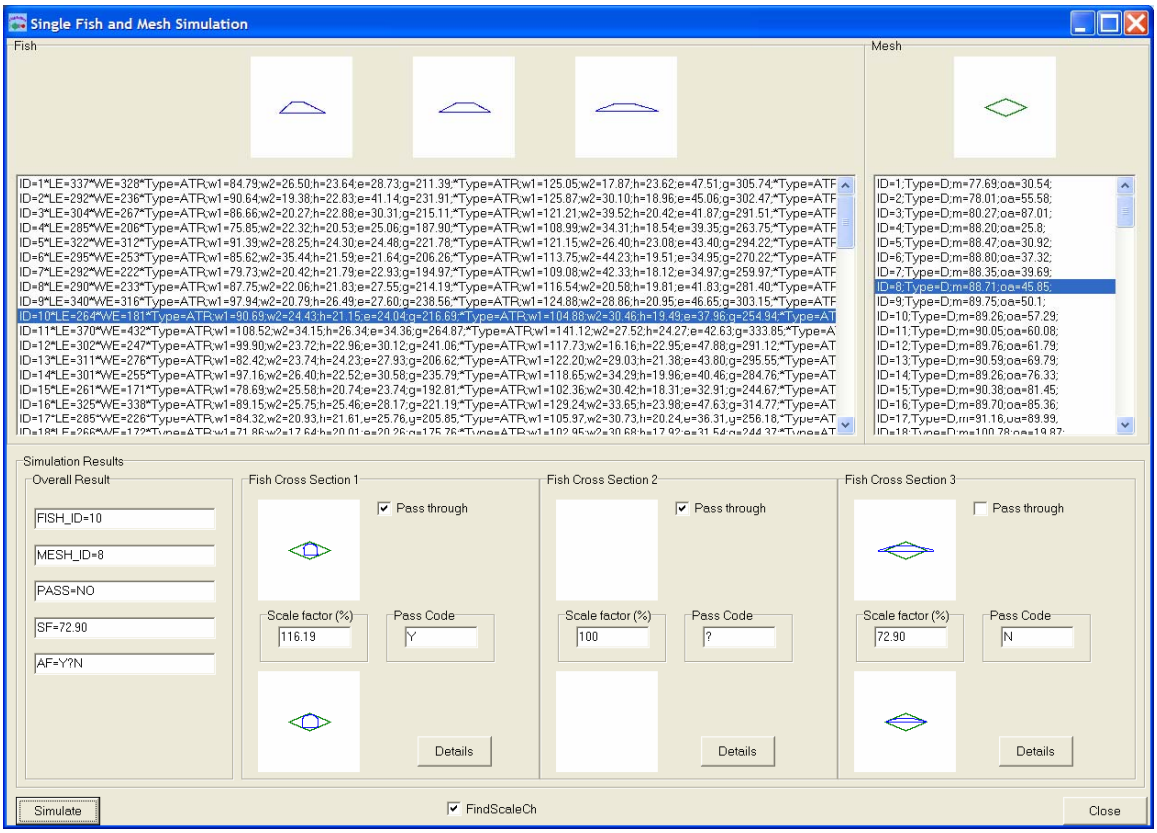

Access: from **Main Window** by activating button **Single Sim**. Can also be accessed through: **Multiple Simulation Window**, **Simulation Result Matrix Window**, **Compare Simulation and Experimental Penetration Result Window**, **Compare Result Matrix Window**.

The window is used to test penetration of one fish in one mesh by use of the penetration model shown in the **penetration model window**.

Simulation Detail Window

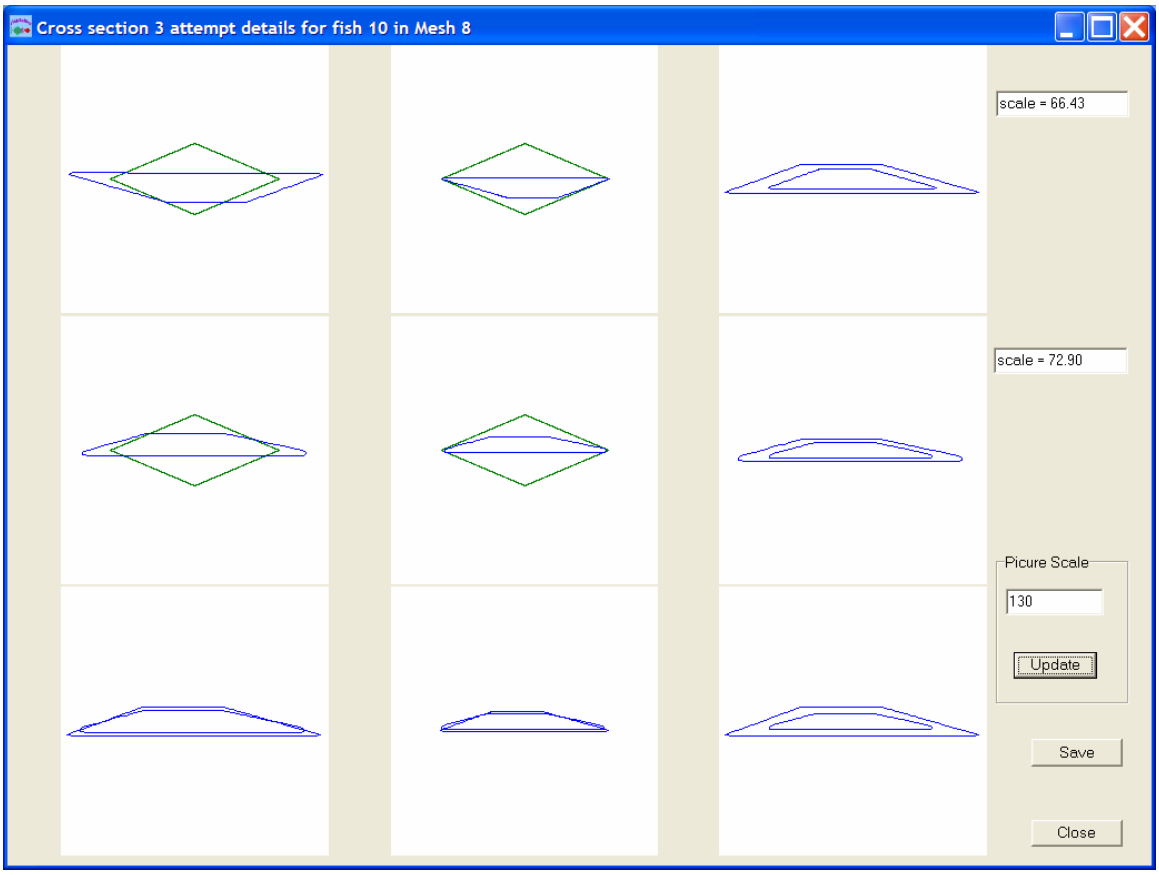

Access: from **Single Simulation Window** by activating button **Details**.
The window illustrates the scaling needed to:

- fit the original cross section to the mesh (upper row)
- fit the cross section compressed according to the penetration model, to the mesh (middle row)

Bottom row illustrates the effect on the cross section of compression, cutting and downscaling.

Multiple Simulation Window

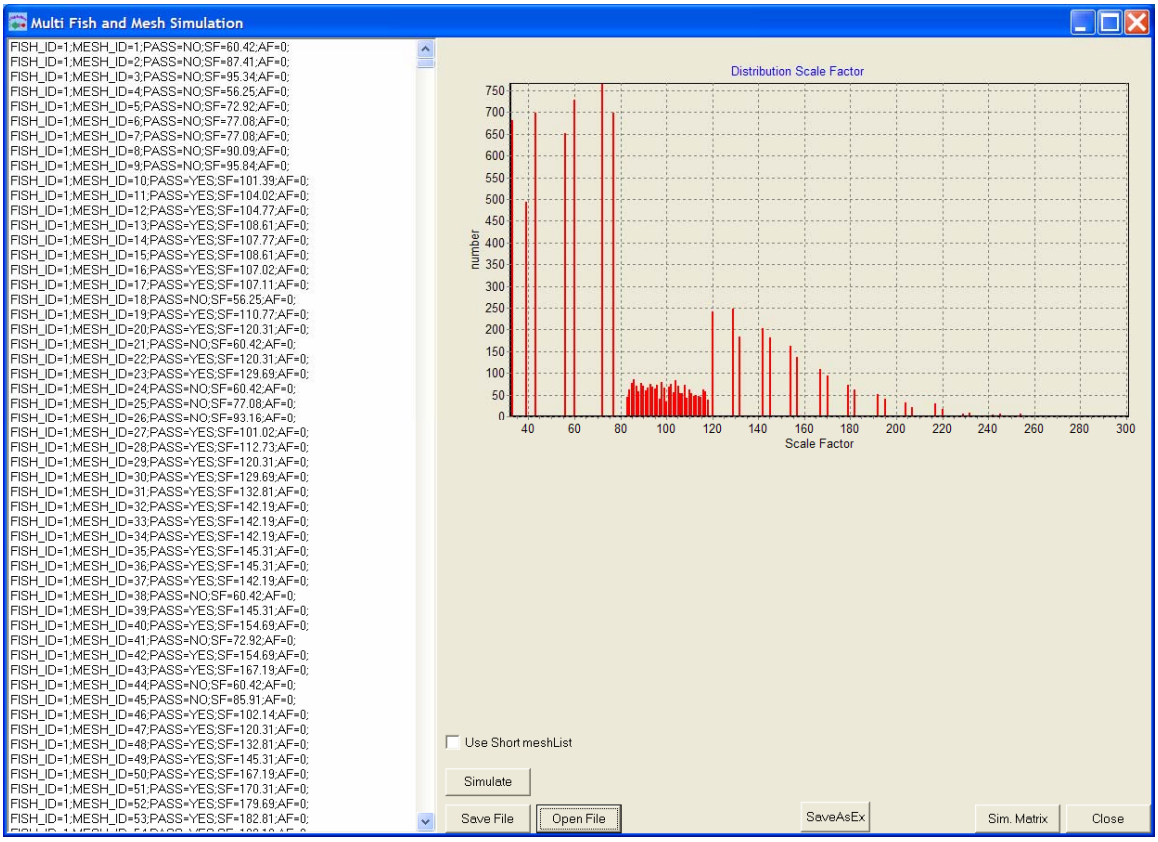

Access: from **Main Window** by activating button **Multi Sim**.
The window is used to test all fish in all meshes using the penetration model shown in the **penetration model window**. Results can be saved as a text file with the extension MSF.

Simulation Results Matrix Window

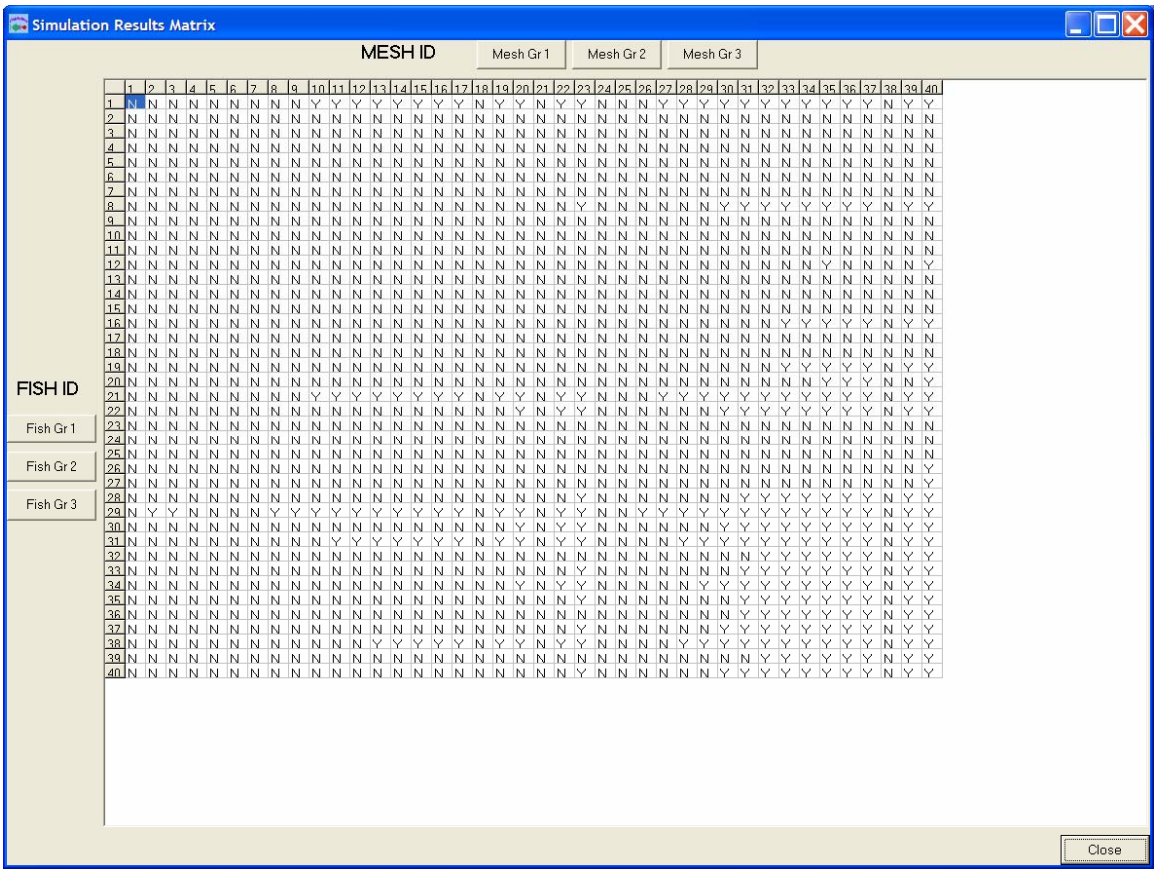

Access: from **Multiple Simulation Window** by activating button **Sim Matrix**.
The window shows the simulated penetration results obtained in the **Multiple Simulation Window**. Y indicates success and N indicates failure. Scroll by clicking the **Mesh Gr** or **Fish Gr** buttons.

Experimental Results Penetration Window

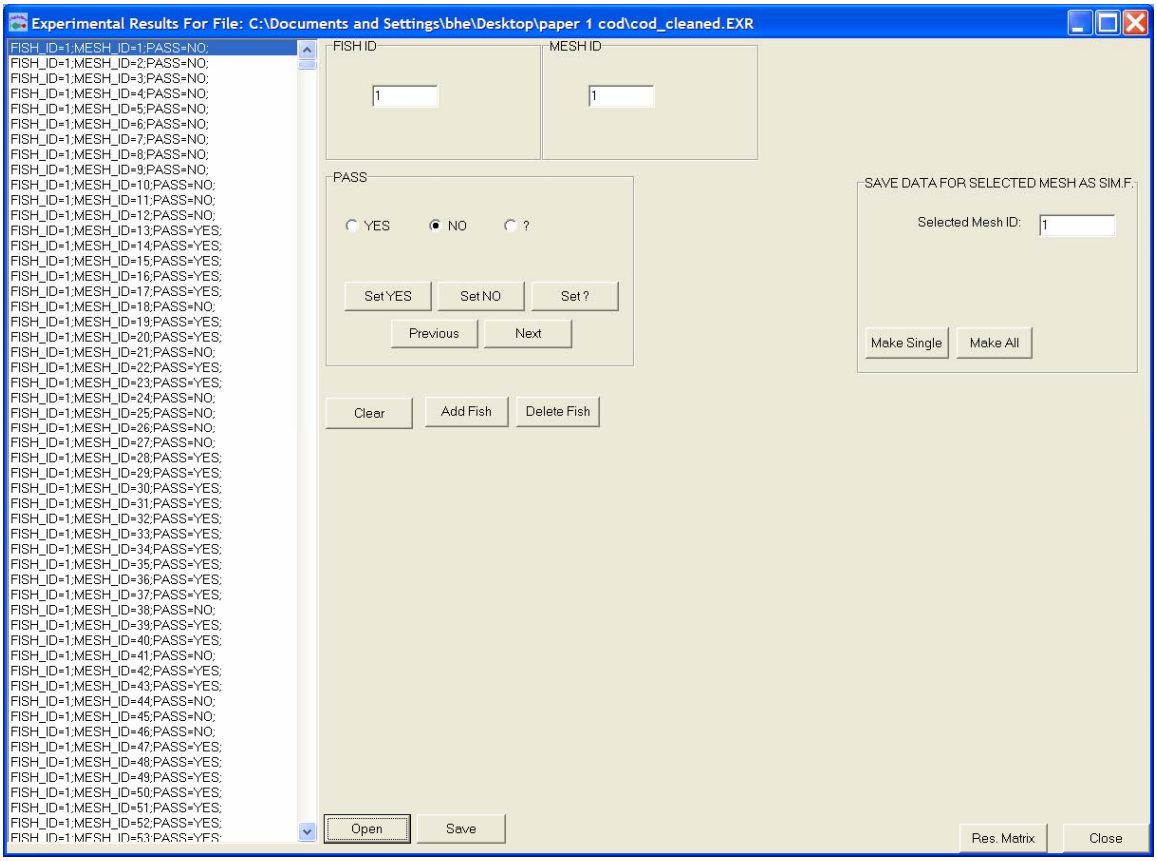

Access: from **Main Window** by activating button **Exp. Res**.
The window is used to simultaneously enter experimental results. If a fish is able to pass through a given mesh, the **SetYes** button is clicked. If it doesn't pass through the mesh click the **SetNo** button. In cases where the result is assessed to be unreliable it should be entered as a question mark. In the subsequent analyses, question marks will be treated as missing values. The results can be saved as a text file with the extension EXR.

Experimental Results Matrix Window

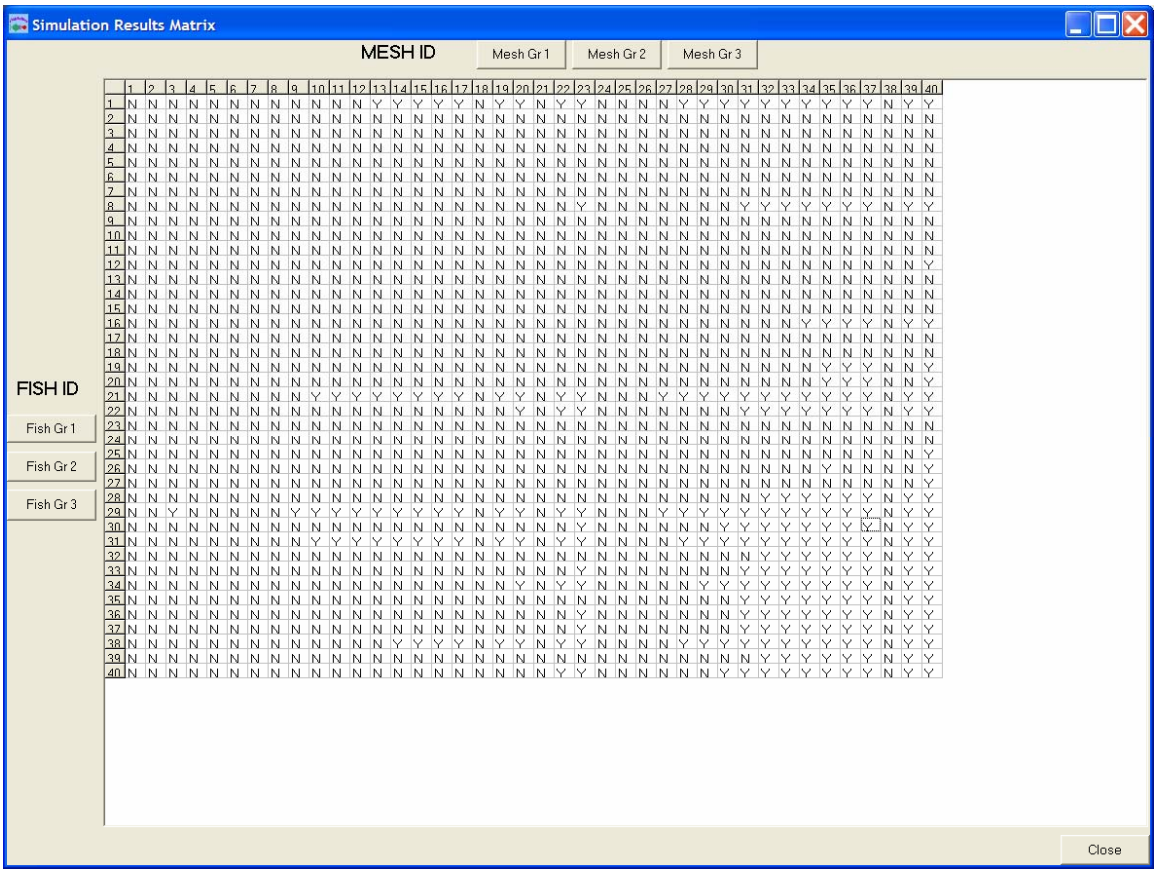

Access: from **Experimental Result Window** by activating button **Res. Matrix**.
The window shows the experimental results. Y indicates success and N indicates failure.
Scroll by clicking the **MeshGr** or **FishGr** buttons.

Compare Simulation and Experimental Penetration Results Window

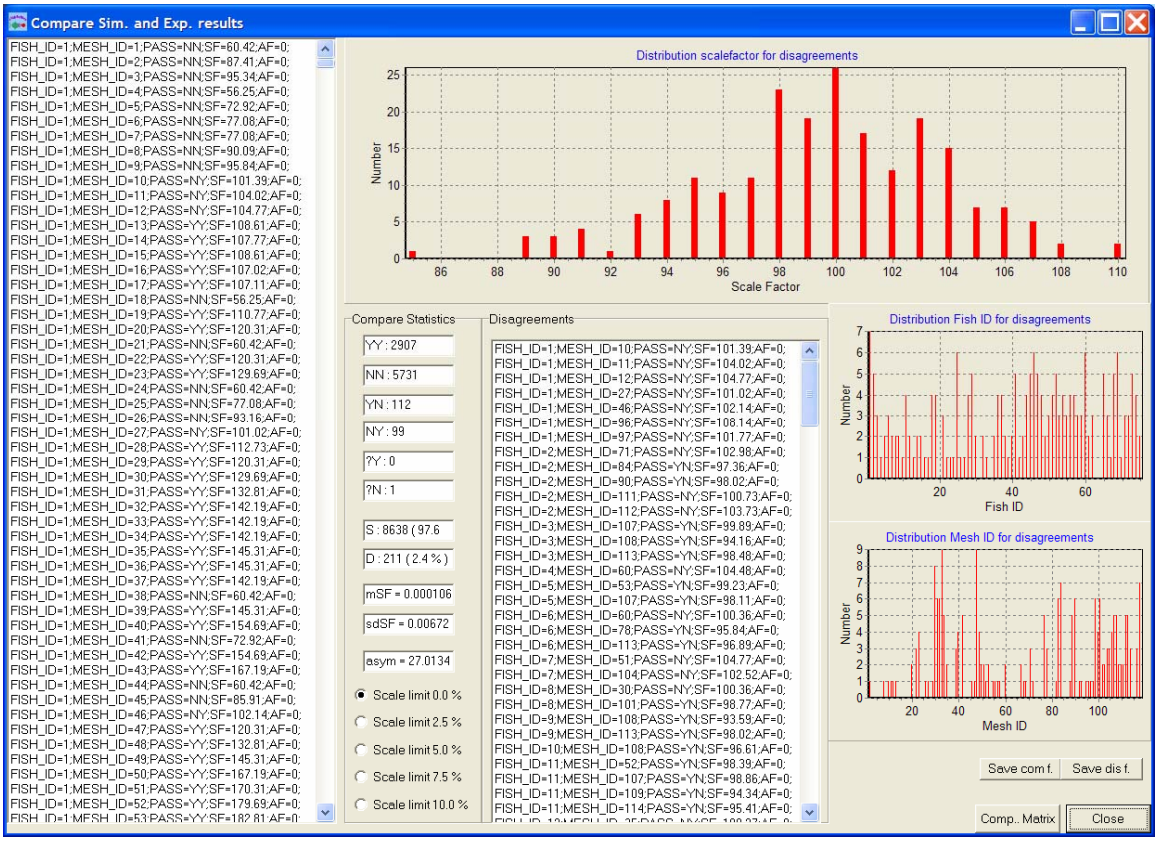

Access: from **Main Window** by activating button **Compare**.
In this window, the simulated results are held against the experimental. It gives an overview of agreements and disagreements and is used to evaluate the tested penetration model. The complete comparison file is shown in the left most panel and can be saved as a text file with the extension CSE. In the **compare statistics panel** the number of agreements (YY and NN) and disagreements (YN, NY, ?Y and ?N) are given. The first letter is the experimental result and the second letter is the simulated result. The agreements are summed up and shown as the S-value while the summed up disagreement is given as the D value. To limit the number of shown disagreements in the **Disagreement panel** check a scale limit different from 0%. The higher the scale limit, the bigger the disagreement. This feature is an important tool for data validation. The disagreements shown in the **Disagreement panel** can be saved as a text file with the extension DIS.

Compare Results Matrix Window

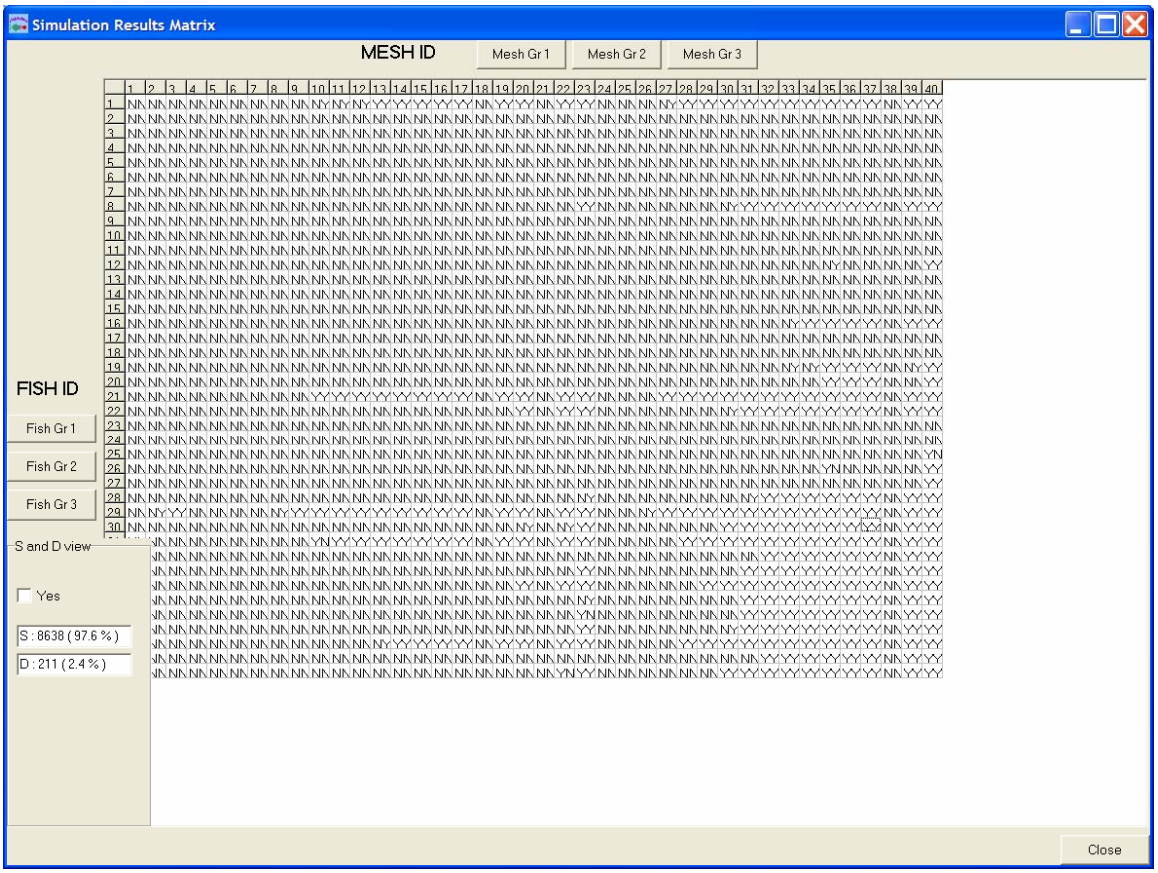

Access: from **Compare Simulation and Experimental penetration Results Window** by activating button **Comp. Matrix**.
Matrix view of the comparison of simulated and experimental results. First letter in each box is the experimental result, second letter is the simulated result. Scroll by clicking the **MeshGr** or **FishGr** buttons.

Multiple Penetration Models Simulation Window

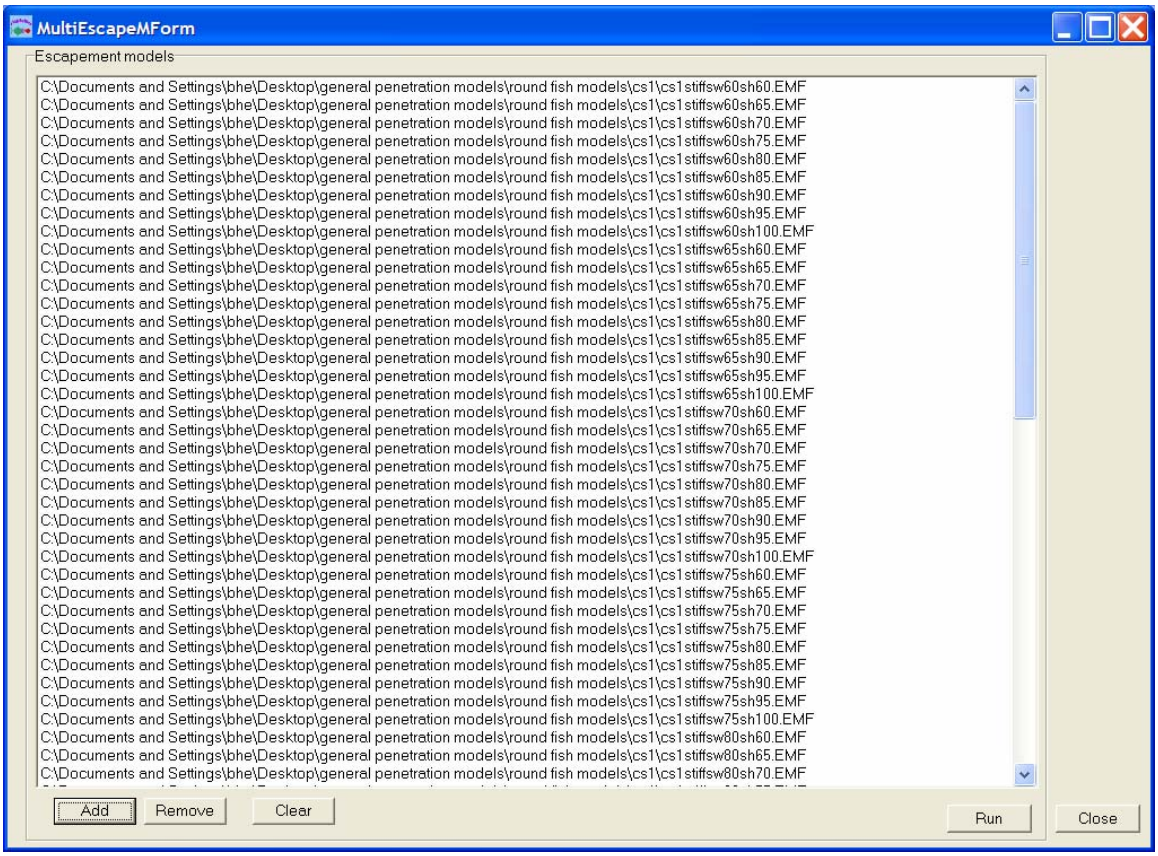

Access: from **Main Window** by activating button **M. Escape M**.

In order to identify the penetration model that can be used to simulate penetration results most accurately it is most efficient to run the different cross sections separately. This window allows the user to run a series of different compressions and cuttings.
The output is a list of all the tested penetration models and their DA values (degree of agreement).

Combine Cross section Simulations Window

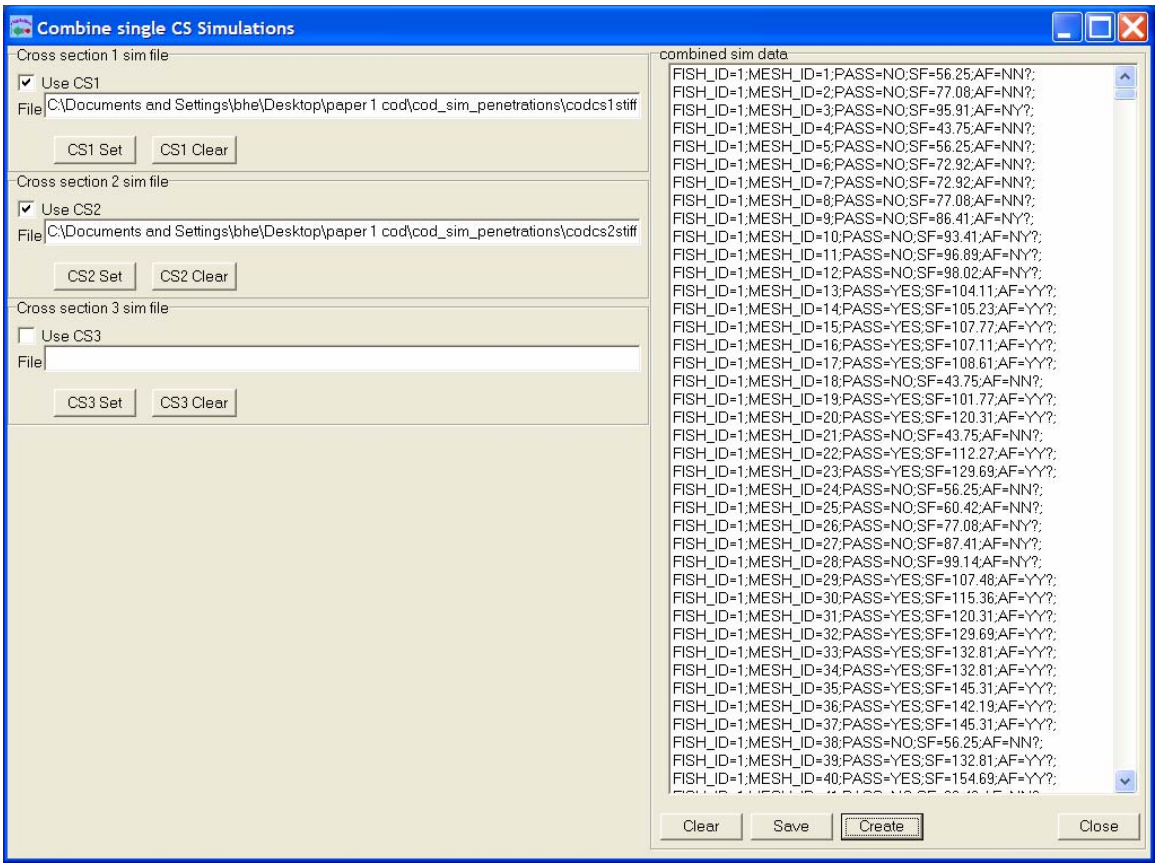

Access: from **Main Window** by activating button **Combine Sim**.
Simulated results based on the different cross sections can be combined in this window. This is relevant if the user only needs to compare one or few penetration models for each cross section. Else see **Compare Multiple Combinations Models Window.**

Compare Multiple Combinations Models Window

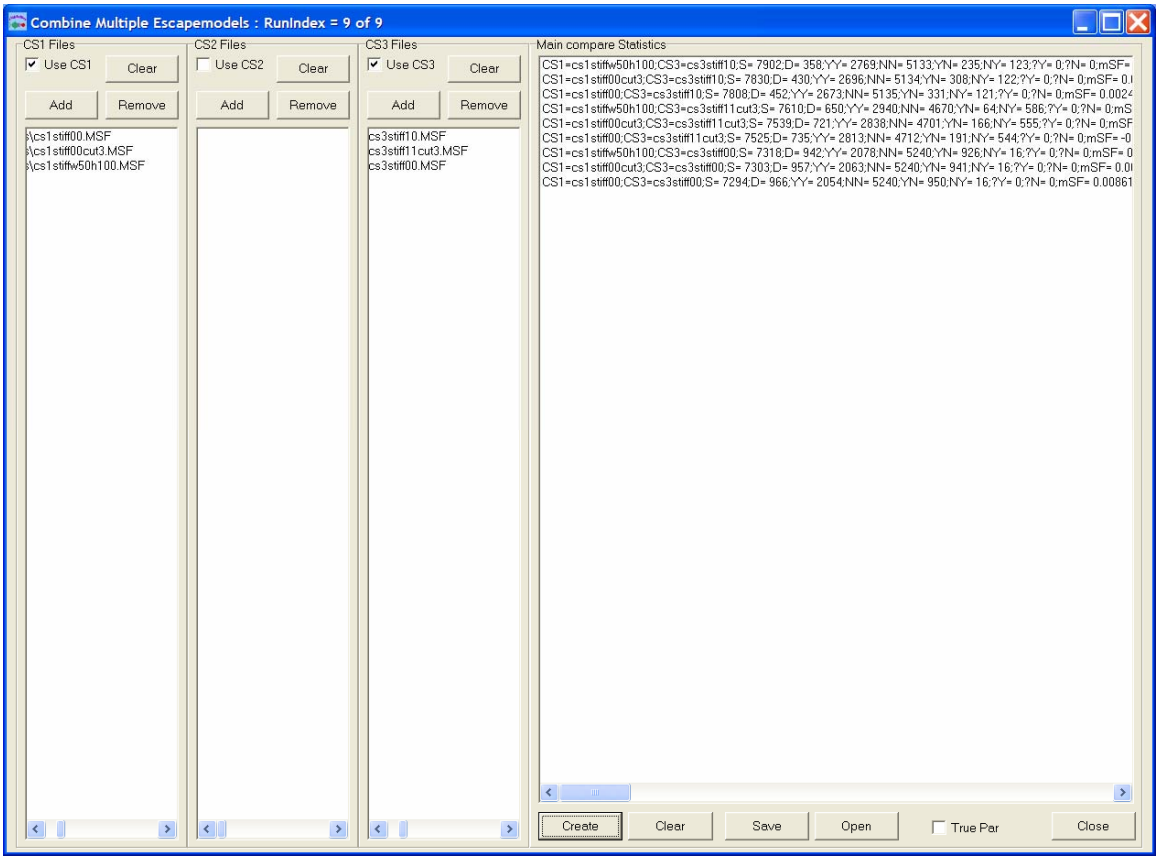

Access: from **Main Window** by activating button **Combine Mul**.
This window allows combination of series of different penetration models for all cross sections. The output lists all combination with a value of disagreement and can be saved as a text file with the extension MCF.

Retention Estimation Window

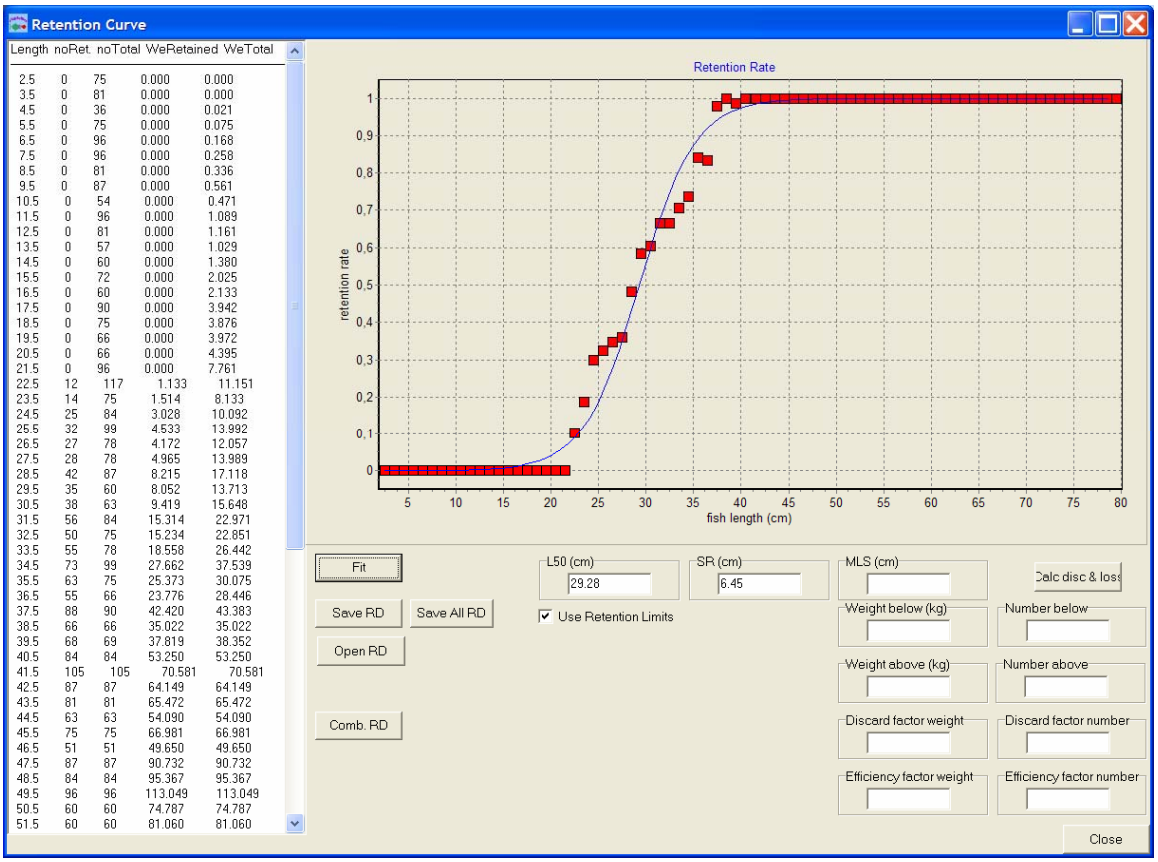

Access: from **Main Window** by activating button **Retention C**.
A sigmoid selection curve is fitted to data simulated by use of a virtual population, the mesh under investigation and the penetration model found to predict penetration most accurately. Click the **SaveAllRD** for use when creating the design guide in the **Design Guide Window**.

Combine Retention Data Window

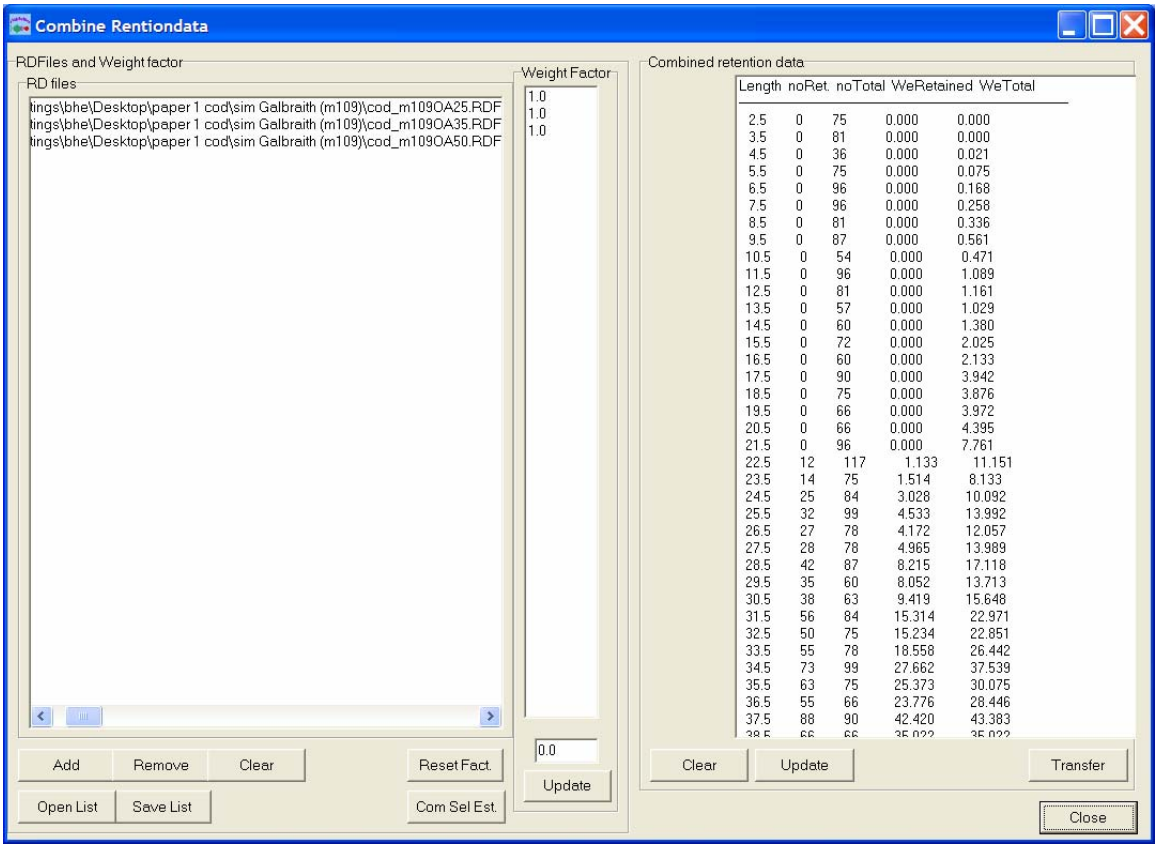

Access: from **Retention Estimation Window** by activating button **Comb. RD**.
Selection parameters for series of meshes present in the netting panel under investigation (e.g. 90 mm diamond meshes with different opening angles) is combined in order to obtain selection parameters for the entire codend. It is possible to weight the selection parameters differently. A build in feature automatically tests different combinations of weighting – click the **Com Sel Est** button!
The retention data can be fitted to a selection curve by clicking the **Transfer** buttom and return to the **Retention Estimation Window**.

Compare Selection Estimates

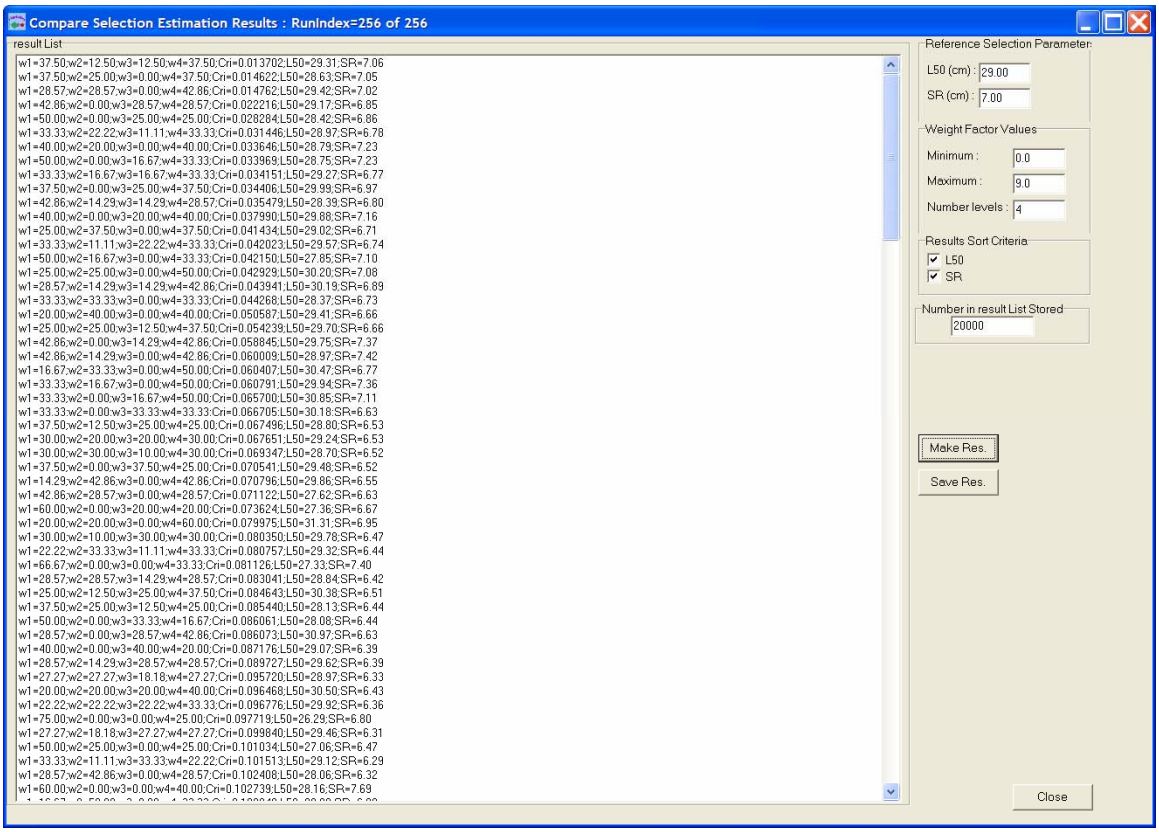

Access: from **Combine Retention Data Window** by activating button **Com. Sel. Est**.
In cases where the weighting of different mesh configurations e.g. opening angles in a 90 mm diamond mesh codend is unknown, it may be useful to test different combinations of weightings against selection parameters obtained in field experiments.
It uses the meshes shown in the **Combine Retention Data Window**. Insert L50 and SR in the upper right corner and define the levels of weighting that is likely to occur. Minimum limit should be 0 which opens for the possibility that the specific mesh is without importance for the grand result. The computing is time consuming and the number of levels should be kept low.
The generated list is shown in the panel and is prioritized showing the combination of weighting that results in parameter estimates closests to the ones given.
The prioritization is based on the *Cri*-value:

$$Cri = \sqrt{\left(\left(\frac{simL_{50} - refL_{50}}{refL_{50}}\right)^2 + \left(\frac{simSR - refSR}{refSR}\right)^2\right)}$$

where simL50 and refL50 are simulated and reference L50 respectively. The same syntax is used for SR. For a perfect match with the experimental results (simL50 = refL50 and simSR = refSR) Cri will be zero.

Design Guide Window

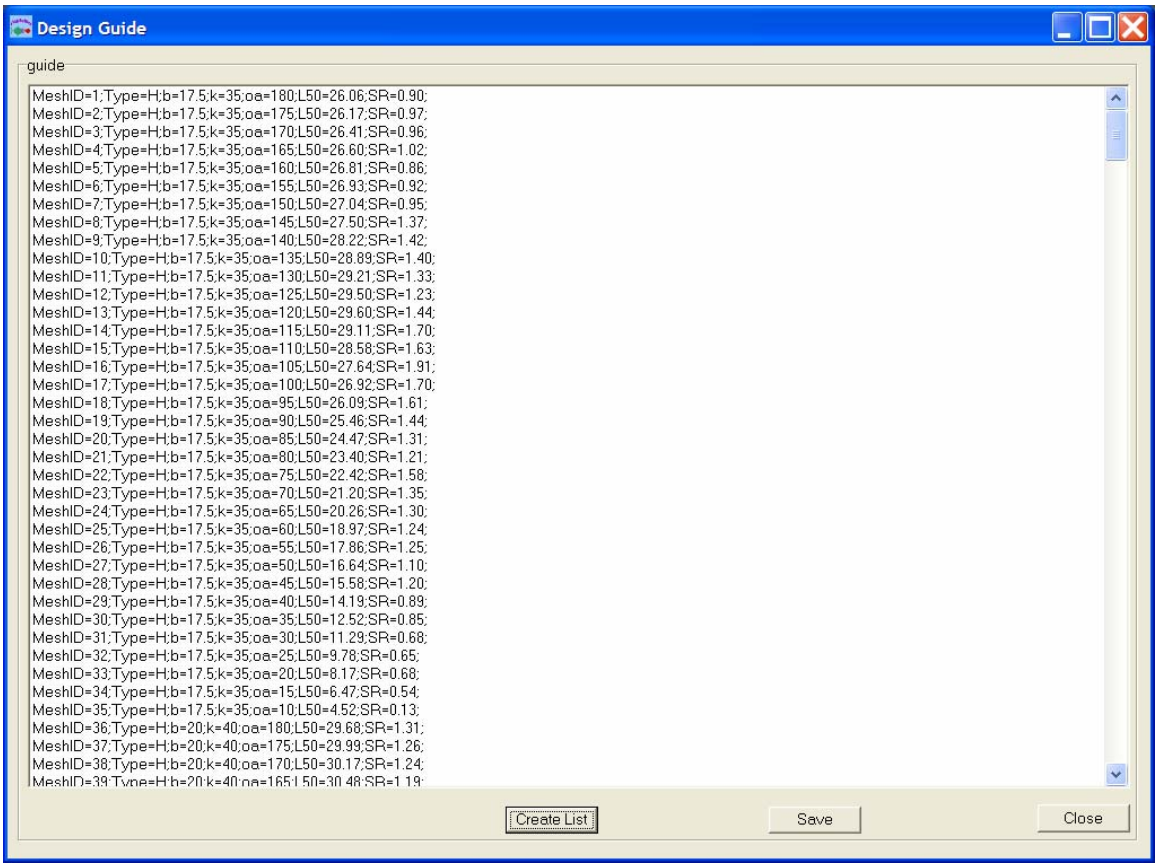

Access: from **Main Window** by activating button **D. Guide**.
The features build in in this window, creates the design guide. The list of L50's and SR's can be plotted as an isoplot. When clicking the **Create List** button, the program prompts for one of the retention data files created in the **Retention Estimation Window**.

Compare Experimental Penetration Results Window

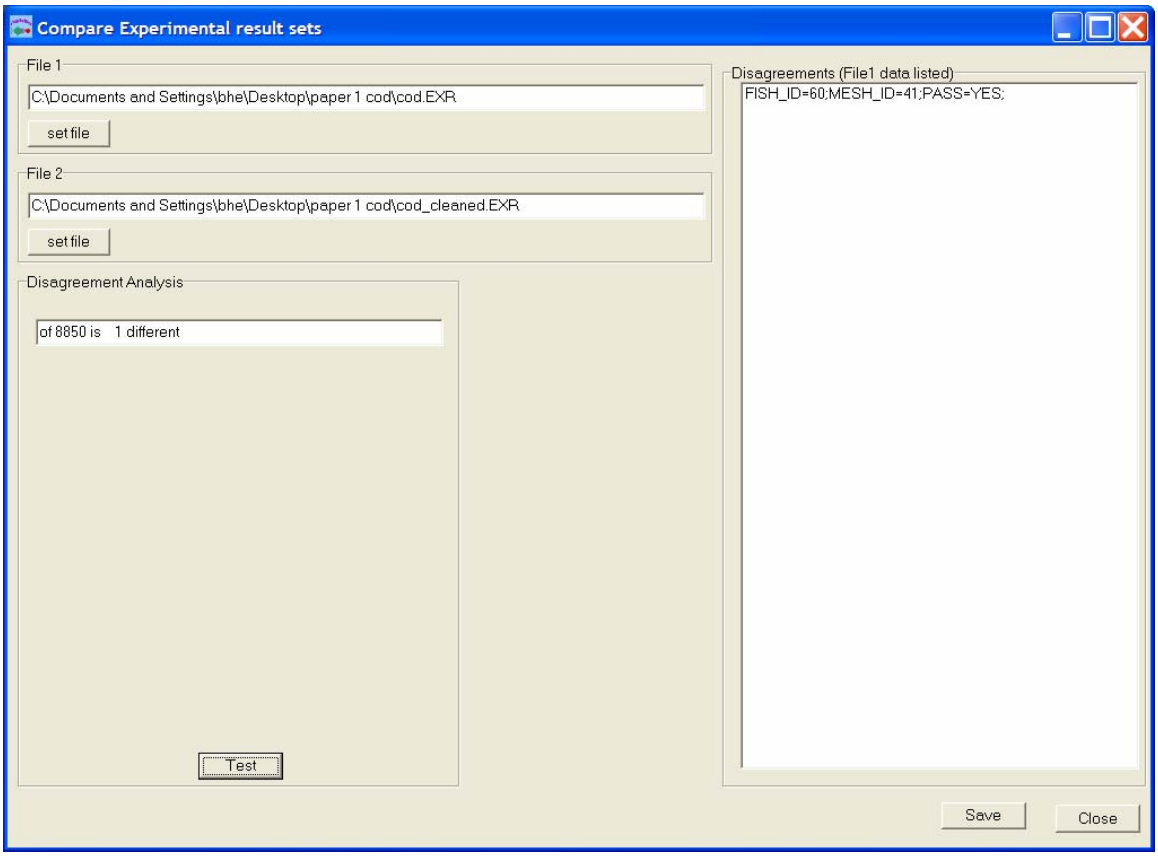

Access: from **Main Window** by activating button **Comp. Exp**.
In order to validate the penetration experiment a number of fish should repeatedly be tested. To test whether a change in results happen e.g. as a consequence of degradation of the fish, the two files listing the experimental results are held against each other.

Export Data Window

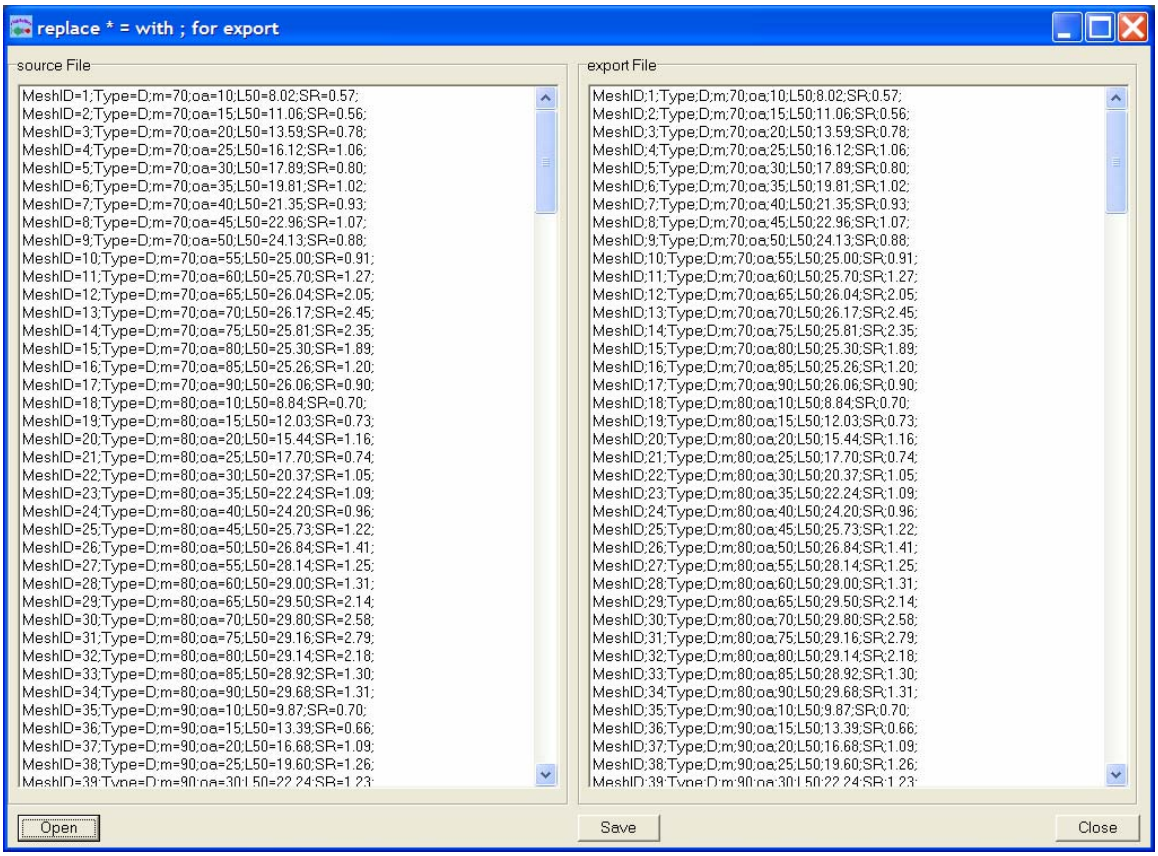

Access: from **Main Window** by activating button **Export**.
This feature is used to change the syntax used in all FISHSELECT files into a format which is easily read in e.g. Microsoft Excel.

Settings Window

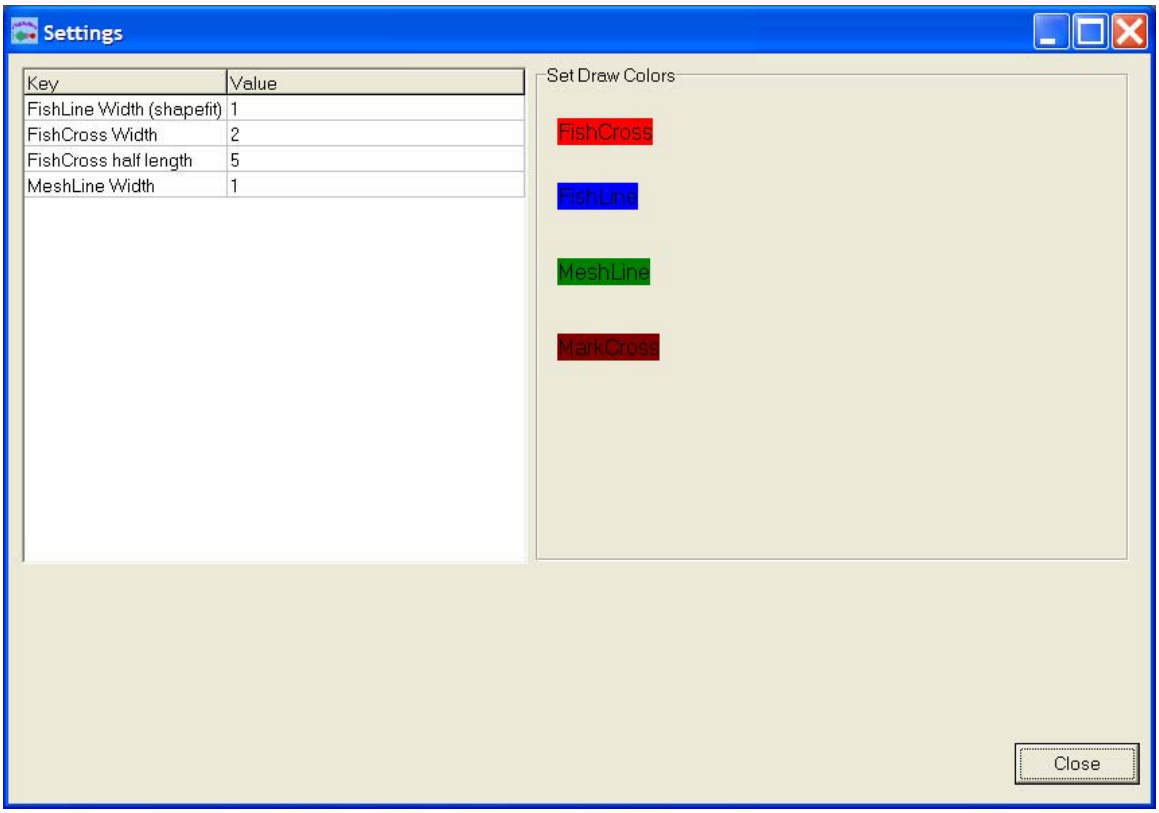

Access: from **Main Window** by activating button **Settings**.
Use this window to change colors in marks and lines.

Colour Dialog

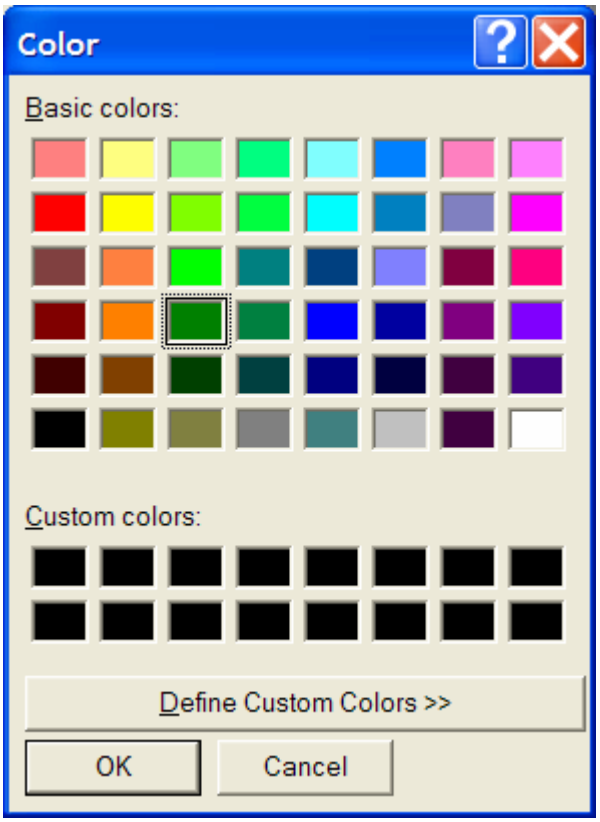

Access: from **Settings Window** by activating one of the **colour buttons**.

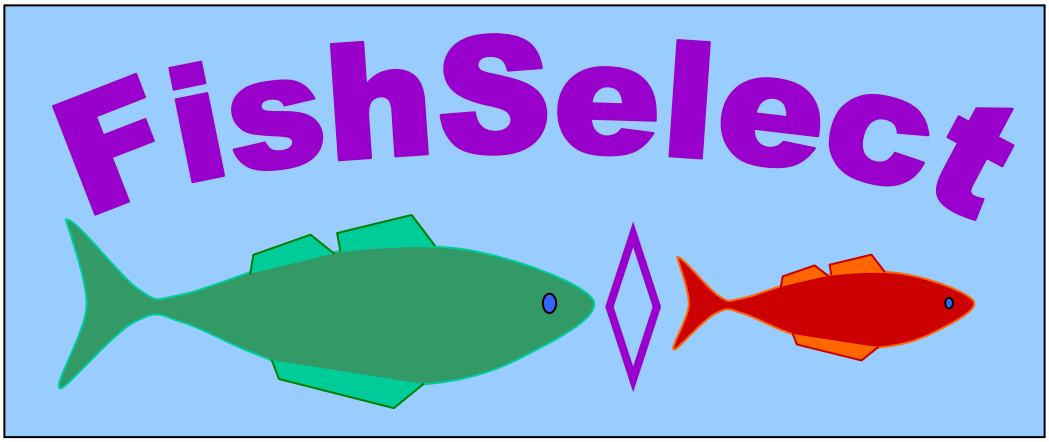

A10

Note on mesh templates and nettings.

To investigate the morphological conditions for mesh penetration it is important that the mesh shapes used in the fall through experiments reflect meshes encountered in connection with cod-end selection for nettings in use today in or future trawl fisheries. Due to drag forces caused by the catch build-up in the cod-end are the mesh bars, which are not perpendicular to the towing direction, non-deformable for the fish. The softer fish cross section can however deform during a mesh penetration. Therefore the FISHSELECT methodology is mainly based on using mesh shapes which are non-deformable called stiff meshes. The justification for this approximation is described in detail in the FISHSELECT methodology (appendix A1). One practical benefit from using stiff meshes in the fall through experiments is that they are more well-defined compared to more flexible and deformable meshes. Thus establishing the species dependent conditions for mesh penetrations based on the fall through experiments, morphological description of the fish and geometrical description of the mesh is less complex.
To emulate stiff trawl meshes we for most of the experiments carried out in this project used 5 mm water-resistant cardboard plates (500 mm times 700 mm). With a sharp knife and a ruler we manual cut out the holes in the plates to emulate different diamond, square, rectangle and hexagonal shapes meshes of different sizes (Fig. 1). The edge of the mesh holes were strengthened with “Dock-tape”.

Fig. 1.

To handle the plates in the fall through experiments a special table for the plates was designed and produced (Fig. 2).


Fig. 2.

During the first series of experiments (Cod and Plaice) mesh plates with a total of 118 different stiff mesh shapes were used. This was later extended to 132 (Sole, Lemon Sole, Turbot and Haddock). One problem with the cardboard-plates were that due to the lack of stiffness in the material the density of meshes on each plate were limited which resulted in many plates were necessary to cover a reasonable amount of different mesh sizes and shapes. A consequence of this was an increased handling of the plates during the fall through experiments. Further is the production accuracy of the manually cut holes lower than machine made ones. This was somewhat compensated by measuring the manually cut holes (see later). Wherefore, for the last experiments (*Nephrops*) a new set of mesh plates (Fig. 3) was designed and produced in PE-plates in a computer controlled water-cutting machine. The number of mesh holes was then increased to 160 but the number of plates reduced from 21 to 7.

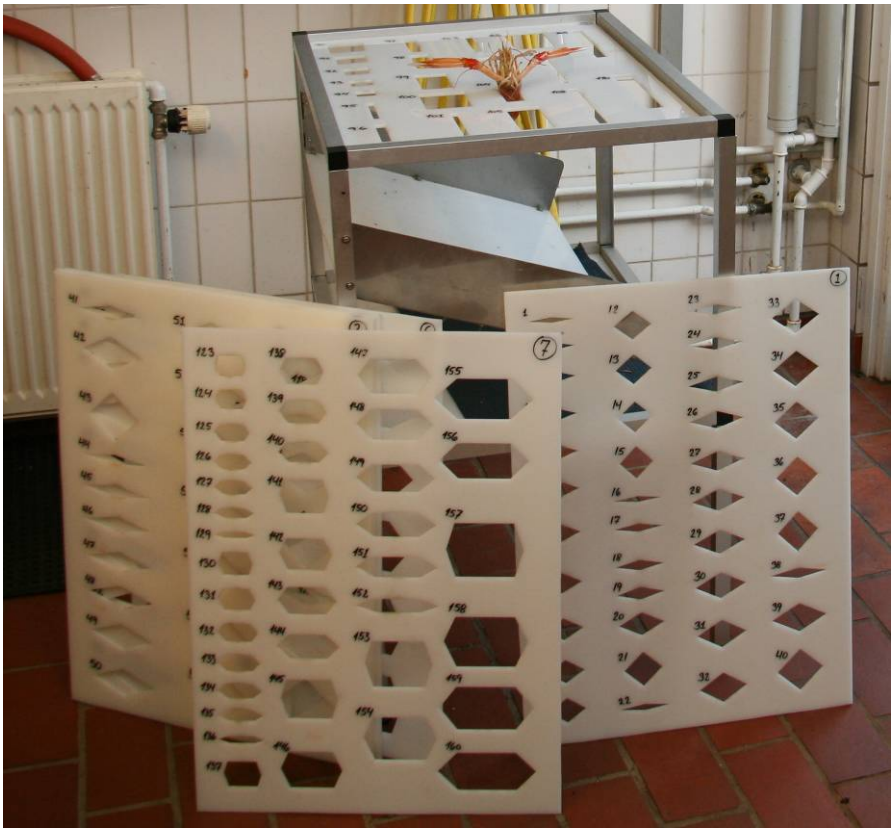

Fig. 3.

To get a precise measure of the actual size and shapes of the mesh holes in the plates was a measuring technique was developed. It consisted of first scanning each mesh hole using a flatbed scanner in 300 times 300 dpi. Having pre-calibrated the relationship between the size of pixels in the resulting scanning pictures and the geometrical measures in mm the scanned images could be used as basis for assessing the actual size and shape of the mesh holes. An image-analysis functionality was build into the FISHSELECT software tool which enabled acquiring the edge of the mesh hole inform of a series of points around the edge. Fig. 4 demonstrates this.

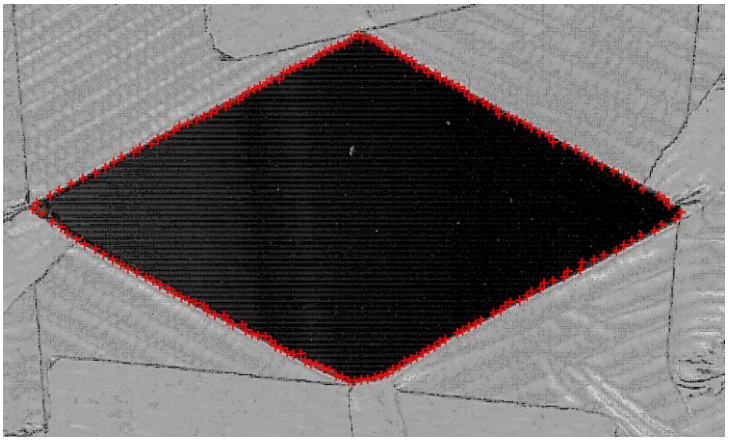

Fig. 4 scanned mesh digitized edge

Further a functionality to fit different basic mesh shapes to the edge-points using a least-squares technique was implemented in the software tool. In this way the parameters describing the different mesh holes best could be identified. Fig. 5 shows this for a diamond mesh identifying the mesh by: m = 98.20 mm (mesh size); oa (opening angle) = 56.28 degree; max dif=1.22; mean dif = 0.23.

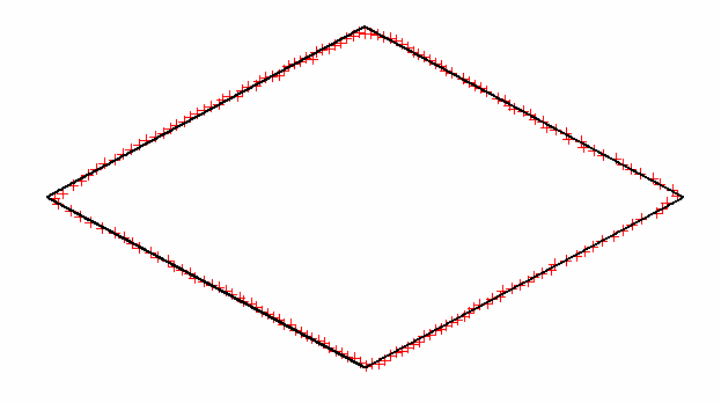

Fig. 5.

Table 1 contains the result of applying this method for all the 132 mesh templates in the extended cardboard set.

Table 1.

ID=1;Type=D;m=77.69;oa=30.54;ID=2;Type=D;m=78.01;oa=55.58;ID=3;Type=D;m=80.27;oa=87.01;
ID=4;Type=D;m=88.20;oa=25.8;ID=5;Type=D;m=88.47;oa=30.92;ID=6;Type=D;m=88.80;oa=37.32;
ID=7;Type=D;m=88.35;oa=39.69;ID=8;Type=D;m=88.71;oa=45.85;ID=9;Type=D;m=89.75;oa=50.1;
ID=10;Type=D;m=89.26;oa=57.29;ID=11;Type=D;m=90.05;oa=60.08;ID=12;Type=D;m=89.76;oa=61.79;
ID=13;Type=D;m=90.59;oa=69.79;ID=14;Type=D;m=89.26;oa=76.33;ID=15;Type=D;m=90.38;oa=81.45;
ID=16;Type=D;m=89.70;oa=85.36;ID=17;Type=D;m=91.16;oa=89.99;ID=18;Type=D;m=100.78;oa=19.87;
ID=19;Type=D;m=98.31;oa=56.16;ID=20;Type=D;m=99.84;oa=86.21;ID=21;Type=D;m=109.42;oa=20.31;
ID=22;Type=D;m=109.56;oa=55.22;ID=23;Type=D;m=109.18;oa=86.48;ID=24;Type=D;m=118.27;oa=19.67;
ID=25;Type=D;m=114.16;oa=26.49;ID=26;Type=D;m=118.83;oa=31.73;ID=27;Type=D;m=117.90;oa=35.61;
ID=28;Type=D;m=118.35;oa=41.37;ID=29;Type=D;m=118.23;oa=46.22;ID=30;Type=D;m=119.86;oa=50.09;
ID=31;Type=D;m=118.94;oa=57.41;ID=32;Type=D;m=120.37;oa=60.67;ID=33;Type=D;m=119.71;oa=65.01;
ID=34;Type=D;m=118.48;oa=71.46;ID=35;Type=D;m=121.59;oa=77.86;ID=36;Type=D;m=120.31;oa=81.51;
ID=37;Type=D;m=120.52;oa=86.74;ID=38;Type=D;m=126.68;oa=19.89;ID=39;Type=D;m=128.99;oa=56.63;
ID=40;Type=D;m=129.98;oa=86.59;ID=41;Type=D;m=140.39;oa=19.84;ID=42;Type=D;m=138.48;oa=55.95;
ID=43;Type=D;m=140.23;oa=85.85;ID=44;Type=D;m=163.35;oa=14.39;ID=45;Type=D;m=158.72;oa=20.57;
ID=46;Type=D;m=158.13;oa=25.07;ID=47;Type=D;m=159.35;oa=30.48;ID=48;Type=D;m=157.85;oa=35.52;
ID=49;Type=D;m=159.03;oa=40.22;ID=50;Type=D;m=160.04;oa=46.09;ID=51;Type=D;m=159.03;oa=51.43;
ID=52;Type=D;m=160.76;oa=56.13;ID=53;Type=D;m=160.54;oa=60.74;ID=54;Type=D;m=160.56;oa=66.13;
ID=55;Type=D;m=161.10;oa=71.33;ID=56;Type=D;m=160.77;oa=76.62;ID=57;Type=D;m=159.68;oa=80.65;
ID=58;Type=D;m=160.97;oa=85.57;ID=59;Type=D;m=177.19;oa=15.68;ID=60;Type=D;m=180.96;oa=56.47;
ID=61;Type=D;m=182.90;oa=86.00;ID=62;Type=D;m=195.97;oa=15.85;ID=63;Type=D;m=200.40;oa=55.71;
ID=64;Type=D;m=200.30;oa=86.89;ID=65;Type=S;b=34.67;ID=66;Type=S;b=40.07;ID=67;Type=S;b=50.14;
ID=68;Type=S;b=60.23;ID=69;Type=S;b=69.69;ID=70;Type=S;b=80.08;ID=71;Type=S;b=89.95;
ID=72;Type=S;b=100.27;ID=73;Type=R;b=90.59;a=9.81;ID=74;Type=R;b=90.96;a=14.49;
ID=75;Type=R;b=91.35;a=19.33;ID=76;Type=R;b=91.05;a=29.19;ID=77;Type=R;b=91.23;a=49.01;
ID=78;Type=R;b=91.79;a=68.83;ID=79;Type=R;b=120.42;a=8.99;ID=80;Type=R;b=121.67;a=14.85;
ID=81;Type=R;b=122.15;a=19.38;ID=82;Type=R;b=121.61;a=29.57;ID=83;Type=R;b=122.40;a=48.84;
ID=84;Type=R;b=121.93;a=69.02;ID=85;Type=R;b=202.66;a=9.89;ID=86;Type=R;b=203.93;a=14.28;
ID=87;Type=R;b=203.45;a=19.02;ID=88;Type=R;b=200.19;a=29.96;ID=89;Type=R;b=203.26;a=49.13;
ID=90;Type=R;b=203.62;a=69.37;ID=91;Type=H;b=17.49;k=35.25;oa=142.05;ID=92;Type=H;b=17.61;k=36.17;oa=130.44;
ID=93;Type=H;b=18.06;k=36.51;oa=103.65;ID=94;Type=H;b=17.02;k=35.71;oa=86.08;
ID=95;Type=H;b=20.25;k=39.95;oa=147.81;ID=96;Type=H;b=20.35;k=39.75;oa=126.92;
ID=97;Type=H;b=19.96;k=39.31;oa=107.59;ID=98;Type=H;b=19.98;k=40.81;oa=91.84;
ID=99;Type=H;b=25.37;k=50.15;oa=143.40;ID=100;Type=H;b=24.91;k=49.24;oa=126.33;
ID=101;Type=H;b=26.22;k=48.60;oa=102.92;ID=102;Type=H;b=26.04;k=48.05;oa=89.54;
ID=103;Type=H;b=29.74;k=59.42;oa=143.88;ID=104;Type=H;b=30.53;k=60.21;oa=128.98;
ID=105;Type=H;b=29.86;k=59.42;oa=105.49;ID=106;Type=H;b=29.94;k=59.80;oa=88.85;
ID=107;Type=H;b=35.15;k=68.93;oa=142.28;ID=108;Type=H;b=34.18;k=70.03;oa=128.34;
ID=109;Type=H;b=35.29;k=69.42;oa=106.33;ID=110;Type=H;b=35.62;k=69.47;oa=89.76;
ID=111;Type=H;b=40.78;k=80.51;oa=145.98;ID=112;Type=H;b=40.66;k=79.42;oa=129.65;
ID=113;Type=H;b=40.34;k=80.04;oa=105.87;ID=114;Type=H;b=41.03;k=80.19;oa=88.19;
ID=115;Type=H;b=49.89;k=99.69;oa=141.66;ID=116;Type=H;b=50.59;k=99.35;oa=127.28;
ID=117;Type=H;b=50.47;k=99.31;oa=106.32;ID=118;Type=H;b=50.97;k=98.67;oa=88.05;
ID=119;Type=D;m=66.38;oa=26.86;ID=120;Type=D;m=67.25;oa=29.74;ID=121;Type=D;m=67.66;oa=37.95;
ID=122;Type=D;m=67.59;oa=41.83;ID=123;Type=D;m=67.81;oa=44.22;ID=124;Type=D;m=67.61;oa=51.56;
ID=125;Type=D;m=68.85;oa=55.10;ID=126;Type=D;m=69.35;oa=63.60;ID=127;Type=D;m=70.11;oa=64.87;
ID=128;Type=D;m=68.44;oa=69.86;ID=129;Type=D;m=69.33;oa=74.24;ID=130;Type=D;m=68.80;oa=79.65;
ID=131;Type=D;m=70.12;oa=85.60;ID=132;Type=D;m=69.69;oa=89.67;

Where Type identifies which basic mesh shape is applied for the description: D (diamond); S (square); R (rectangle); H (hexagonal).

Another important aspect is to investigate if these basic shapes are reasonable approximations to the actual shapes in trawl netting used today especially in cod-end. To get an impression of this we procured different samples of netting panels. These panels were stretched differently over a flatbed scanner. Pictures of real netting meshes could then be acquired and analyzed the same way as the holes in the mesh plates including fitting the various basic shapes to the digitized mesh shapes.
Fig. 6 to 9 illustrates this for the different diamond mesh netting panels. Fig. 6 shows three different diamond netting panels as an example.

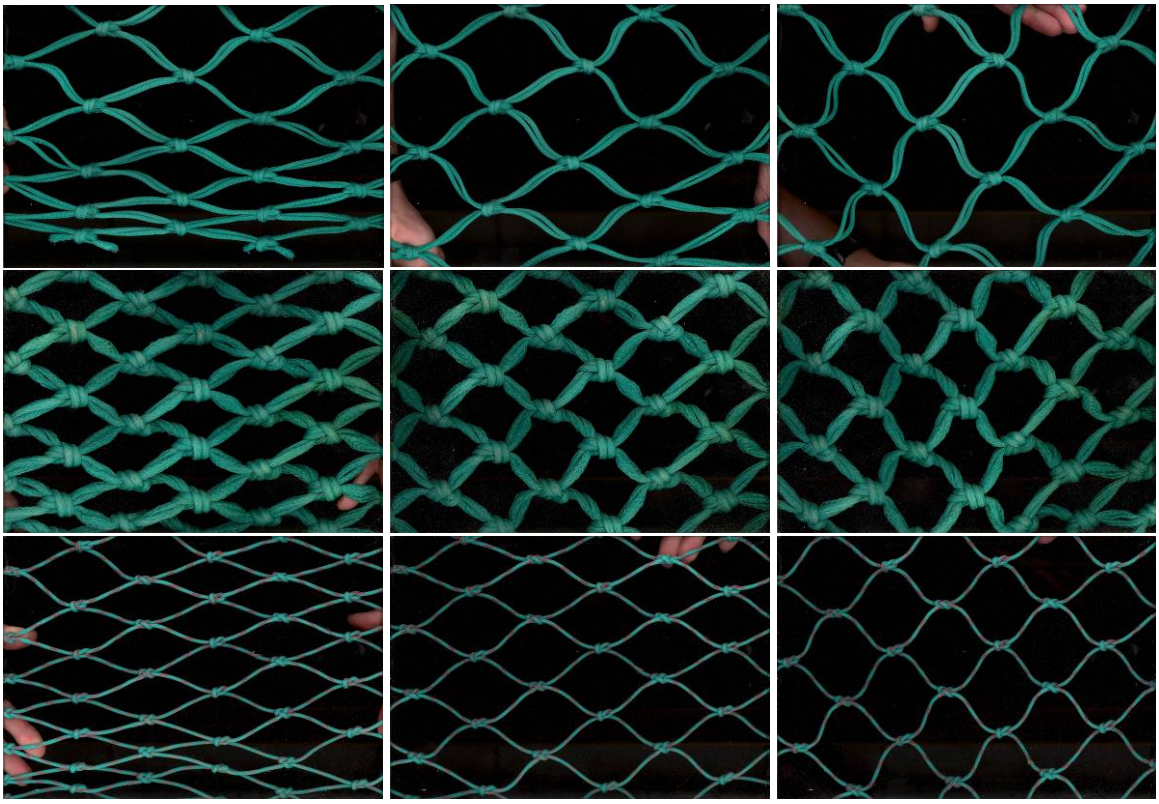
Fig. 6.

The first row show a netting panel with a relative big mesh size compared to the twine thickness which is also double. The second row is also for double twine netting but here the mesh size is small compared to the twine thickness. Here it is evident that the knot size affects the mesh shape more. The third row is for a single twine netting panel with relative big mesh size compared to the twine thickness. The first column in Fig. 6 represents a situation where the stretching load is perpendicular (vertical in the pictures) to towing direction when used as normal netting is relative small. In the second column the stretching load perpendicular is increased resulting in an increased opening angel of the meshes. In the third column the perpendicular load is further increased and it is clearly seen that the knot geometry affects the mesh shape more in this situation especially for the second netting where the twine is thick compared to the mesh size. This situation will have some similarities to when the netting panels are used as T90 netting (90 degree turned).
Fig. 7 shows a situation where the image-analysis functionality build in to the FISHSELECT software tool has been applied to digitize the inside mesh shape for a mesh in the first row and column of Fig. 6.

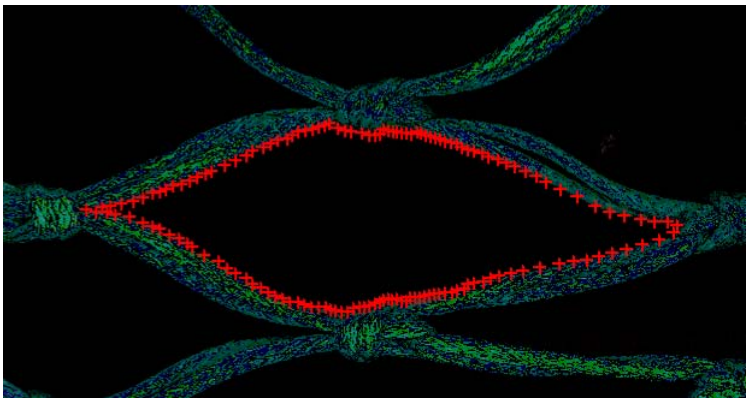

Fig. 7

In Fig. 8 the process detecting the mesh shape by image-analysis shown in Fig. 7 has been carried of for one mesh in each of the situations in Fig. 6. Further we show results from fitting a diamond basic shape to one mesh from each of the differently stretched netting panels shown in Fig.6.

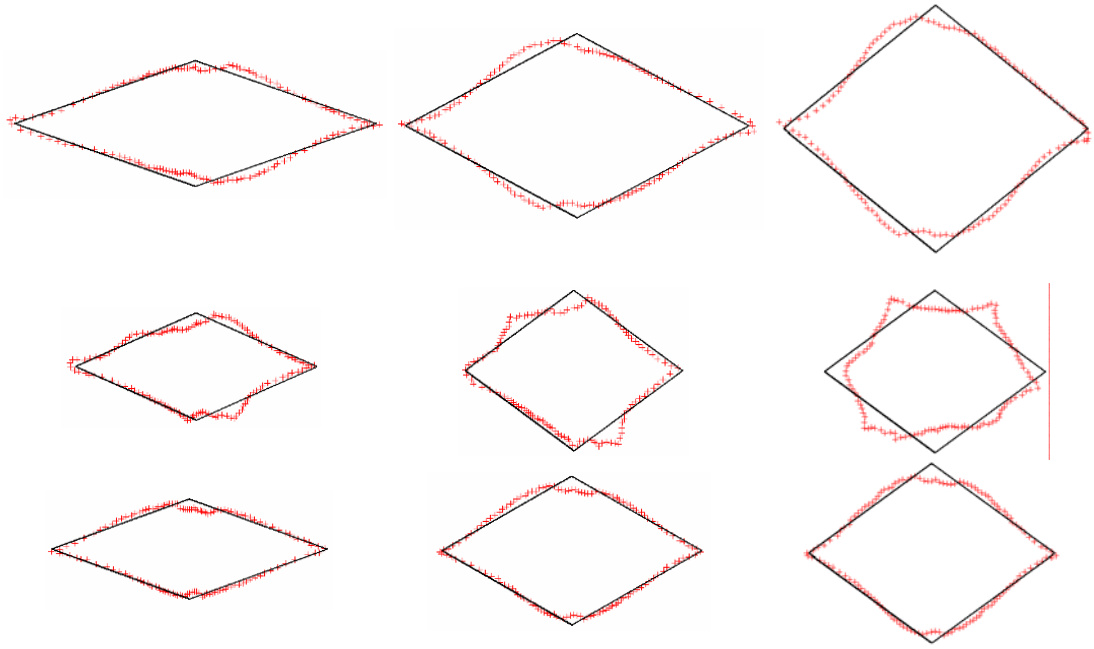

Fig. 8.

From Fig. 8 it is evident that the diamond shape is not a perfect description of mesh shapes in real netting especially for the results in the second row (panel with thick twine compared relative to mesh size) it seems as it represents a reasonable approximation. In general the poorest description is in column three where the nettings are overstretched perpendicular. Table 2 summaries the main fit data for the results shown in Fig. 8 (see FISHSELECT methodology for explanation of parameters).

Table 2

m=127.82 mm oa=38.25 degrees mean dif.=1.75 mm max dif.=4.64 mm	m=129.95 mm oa=56.34 degrees mean dif.=1.70 mm max. dif=4.79 mm	m=130.86 mm oa= 78.31 degrees mean dif.=1.78 mm max. dif.= 5.65 mm
m=87.87 mm oa= 47.69 degrees mean dif.=1.61 mm max. dif.=5.56mm	m=89.85 mm oa=72.75 degrees mean dif.=1.78 mm max. dif.=7.02 mm	m=91.47 mm oa=72.80 degrees mean dif.=3.14 mm max. dif.=8.08 mm
m=97.90 mm oa=39.85 degrees mean dif.=1.04 mm max. dif.=3.31 mm	m=99.67 mm oa=59.53 degrees mean dif.=1.15 mm max. dif.=4.17 mm	m=101.46 mm oa=72.48 degrees mean dif.=1.21 mm max. dif.=4.88 mm

Table 2 also confirmed that the poorest description is in column three where the maximal difference for all designs is found there.
One way to improve the description of the real mesh shapes for the overstretched meshes could be to use a hexagonal basic shape as suggested by Herrmann et al. (2007) for T90 netting. In Fig. 9 we show the results for the situations in column 3 of Fig. 6.

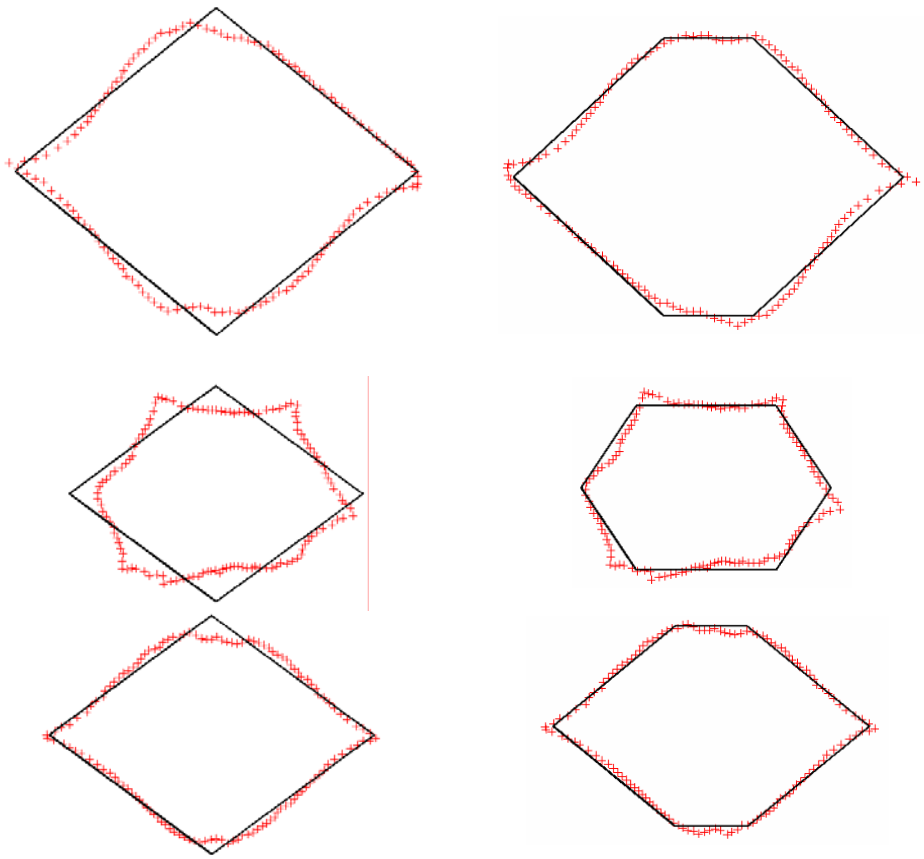

Fig. 9.
The first column in Fig. 9 repeats the results from Fig. 8 column three while the second column show the results from fitting a hexagonal shape to the data. Fig. 9 illustrates how the description for the big mesh openings (high oa) can be improved greatly by using a hexagonal basic shape in stead of a diamond. Table 3 summaries the results from fitting the hexagonal shape.

Table 3.

k=22.46 mm b=51.55 mm oa=85.48 degrees mean dif.=1.24 mm max. dif.=4.56 mm
k=35.14 mm b=24.87 mm oa=112.29 degrees mean dif.=1.42 mm max. dif.=5.33 mm
k=18.31 mm b=39.61 mm oa=78.88 degrees mean dif.=0.81 mm max. dif.=2.89 mm

From the above results we conclude that a simple diamond shape will be able to give an acceptable description of the mesh shapes for diamond mesh nettings in most situations. For situations where this is not the case (thick twine, T90 stretched) a hexagonal shape seems to offer an acceptable description. Based on this we are confident to simulate stiff diamond meshes of real netting by stiff diamonds or stiff hexagonal as in the mesh templates.

Panels of square mesh nettings are used in several trawl designs today. Fig. 10 shows the scanned images for three different square mesh panels.

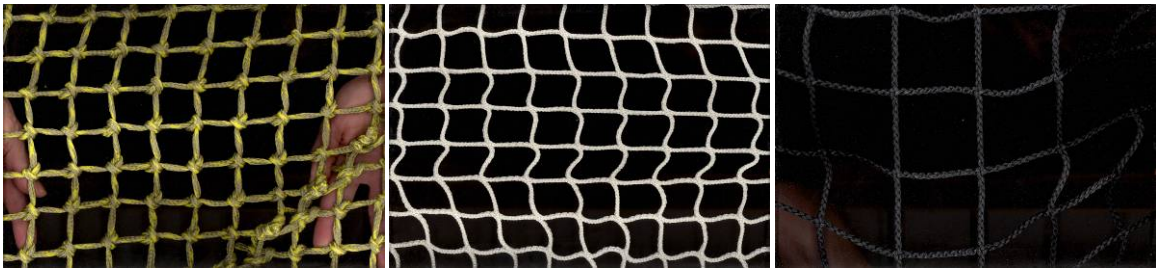

Fig. 10.

Fig. 11 shows edge detection of the inside contour in FISHSELECT software tool. Leftis a knotted panel and right a knotless panel.

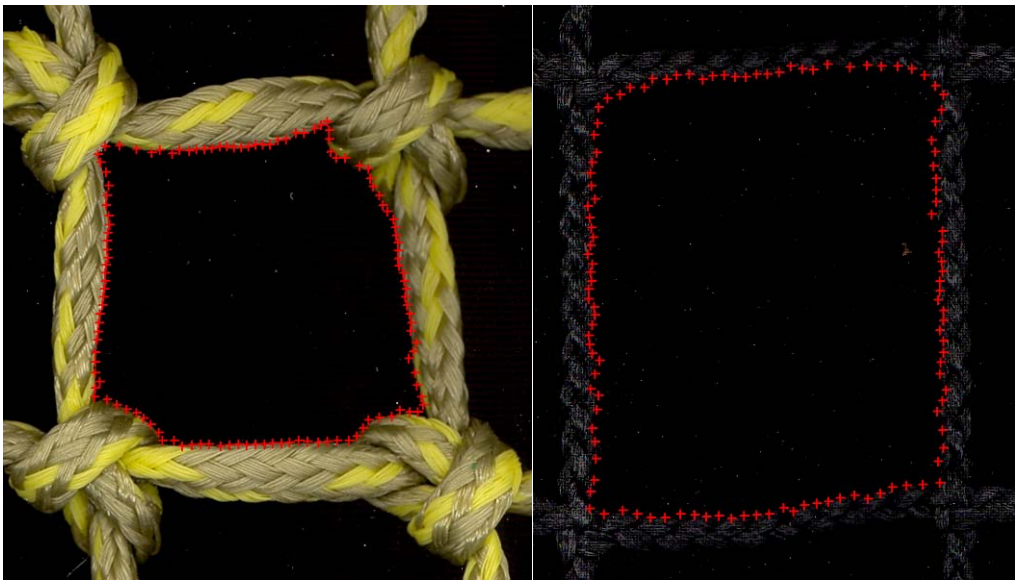

Fig. 11.

Fig. 12 shows fit of a square shape to a mesh in a square mesh panels (column right). In the left column is a diamond shape is fitted for the stretching situation. The diamond shape represents a better description which is confirmed quantitatively by the fit data in Table 4.

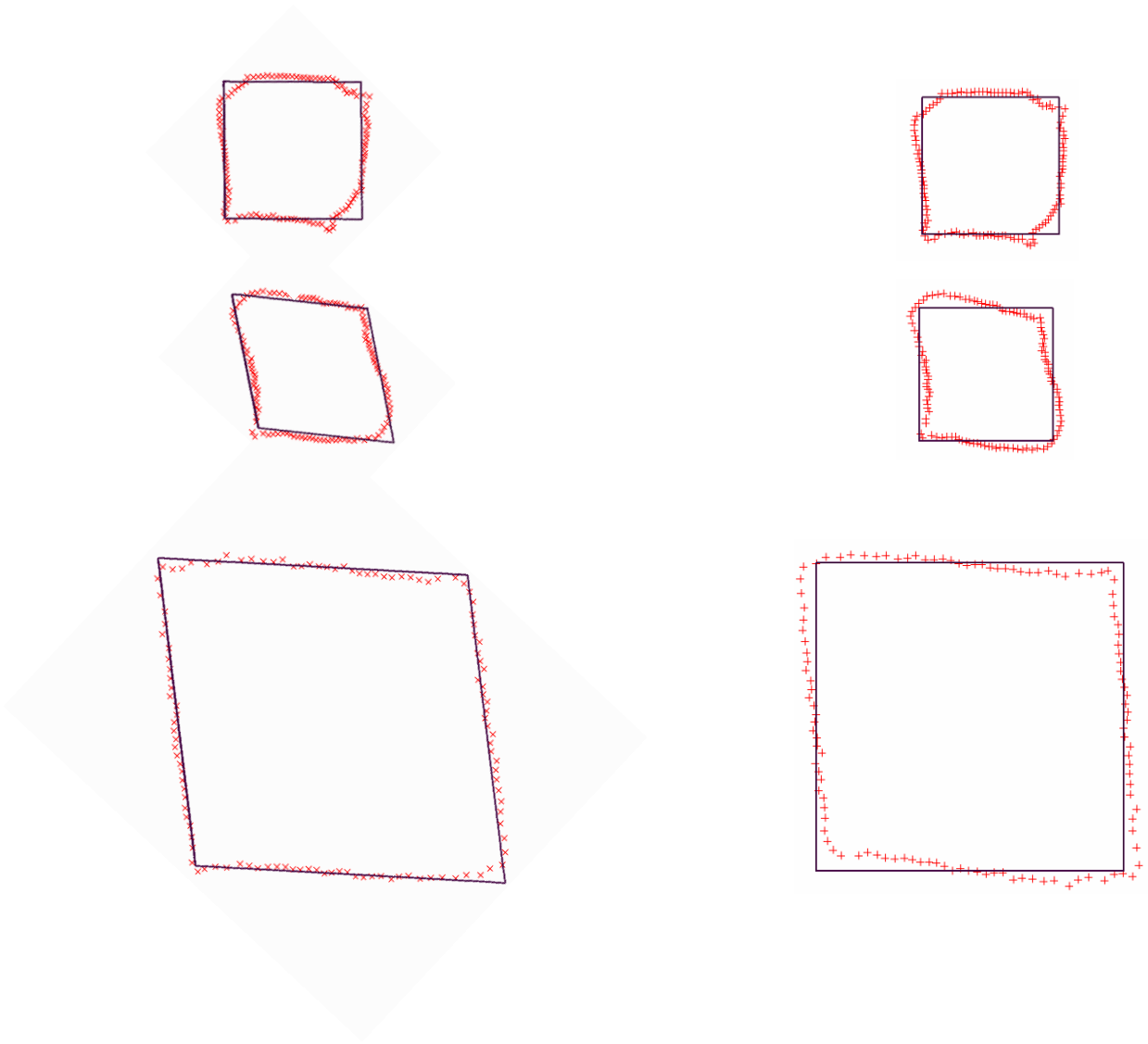

Fig. 12.

Table 4.

m=56.34 oa=89.20 degrees mean dif.=0.89 mm max. dif=3.12 mm	b=28.08 mm mean dif.=0.91 mm max. dif.=3.30 mm
m=56.02 mm oa=72.65 degrees mean dif.=0.85 mm max. dif.=2.25 mm	b=27.20 mm mean dif.=1.44 mm max. dif=3.42 mm
m=127.27 mm oa=79.93 degrees mean dif.=0.66 mm max. dif.=3.33 mm	b=63.01 mm mean dif.=1.68 mm max. dif=4.65 mm

As can be seen from Fig. 12 and Table 4 is it possible to achieve a reasonable description of the square mesh panels meshes by applying a basic diamond shape or a square shape.

Based on the results we conclude that by using basic shapes: diamond, square, rectangle and hexagonal we should be able to cover meshes used today and meshes realistic to implement in the future.
It should be noted that the FISHSELECT software tool image-analysis and parametric shape fitting functionalities applied can also be applied to images obtained from underwater recordings of nettings towed in experimental fishing and from flume tank test.
It should also be noted that the FISHSELECT methods will be able to handle general mesh shapes as for example digitized non-parametric as obtained from images of real netting.

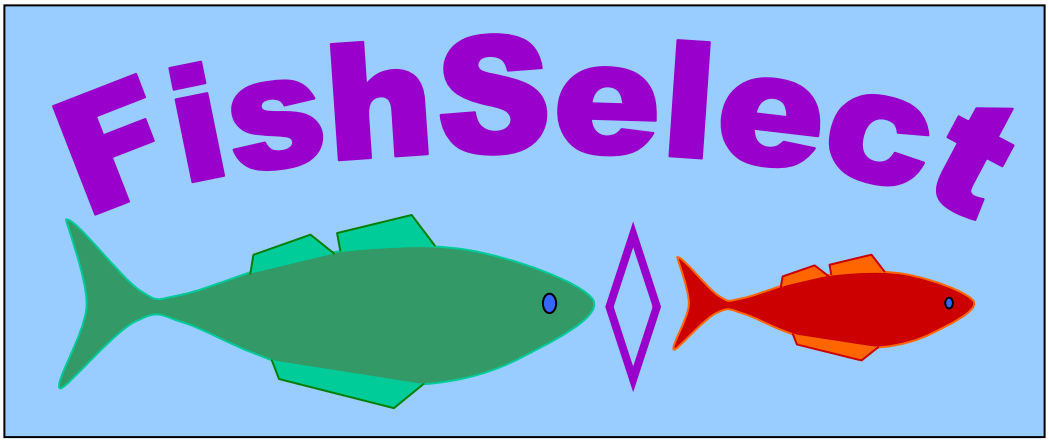

A11

Note on development of tools and methods for acquiring cross section shapes.

To apply the FISHSELECT methodology it is necessary with an efficient and reasonably accurate method and tool to assess cross section shapes and size on species of round and flat fish. It is also desirable if these could be able to handle Nephrops as well.

During the project two basically different methods have been investigated:

1) a mechanical contact based method – mechanical MorphoMeter
2) an optical non-contact based method – laserline MorphoMeter

1. Mechanical MorphoMeter.

The mechanical MorphoMeter is based on a large number of sensing sticks that are pushed into contact with the cross section being measured. This leaves a replica of the cross section contour in the MorphoMeter. This is then scanned into a computer with a flatbed scanner and by applying image-analysis based on edge detection the contour is digitized at a large number of points along the contour. The mechanical MorphoMeter and its application for flat fish and round fish measurements are described in detail in the FISHSELECT methodology report(appendix A1). Two different sizes of the mechanical MorphoMeter were developed during this project using sensing sticks of different diameter (2.5 mm and 0.8 mm) (Fig. 1).

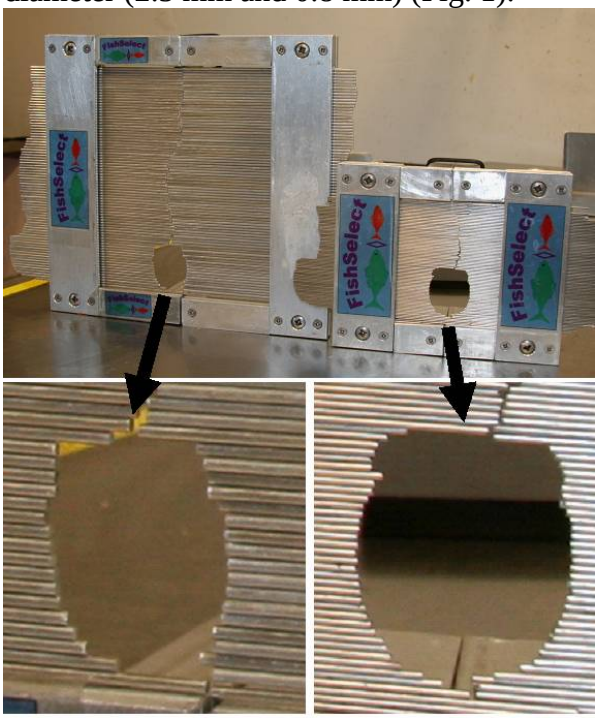

Fig. 1

The large mechanical MorphoMeter was developed first and applied to the fish species cod, plaice, turbot, haddock, sole, lemon sole and provided sufficiently accurate assessment of the cross sections. For Nephrops we wanted better resolution and therefore

the small MorphoMeter was developed and applied to Nephrops. For large turbots it was necessary to use the large MorphoMeter in a special wide twin version (Fig. 2).

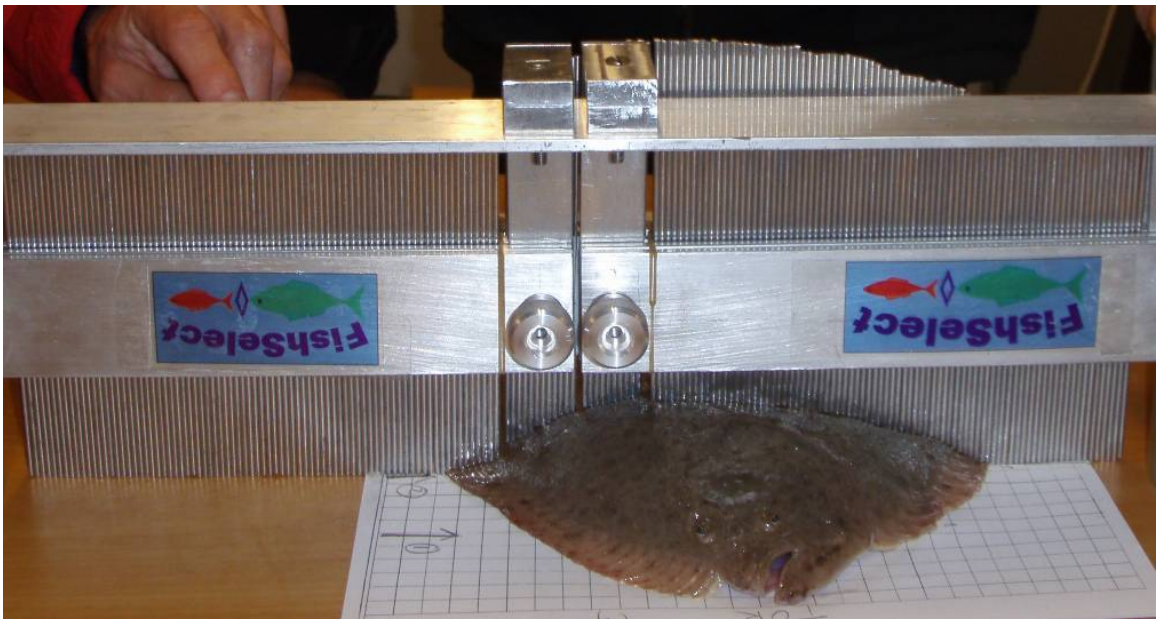

Fig. 2

The setup shown in Fig. 2 was achieved by assembling two MorphoMeters into one.

Two off-the-shelf flatbed scanners and a laptop computer have been procured to acquire images of the cross sections from the mechanical MorphoMeter. To handle the large datasets of scanned images two external terabyte hard discs have been procured.

2. Laserline MorphoMeter.

With the successful application of the mechanical MorphoMeter it was possible to obtain the data required for the species investigated in this project without using the laserline MorphoMeter. This was fortunate, since it was not possible within the limits of the project to complete the development of the laserline MorphoMeter. However, the laserline MorphoMeter method could become much more efficient than the mechanical method when finally developed. The rest of this appendix describes the work carried out with the development of the laserline MorphoMeter in this project.

The laserline MorphoMeter is based on using a laser with line-generating optics to mark the cross section being measured. A fraction of the laserlight is diffusly reflected from the surface of the fish to produce a light curve, the shape of which depends on the cross section shape being measured and of the viewing angle. Fig. 3 shows this using a laser with 660 nm wavelength.

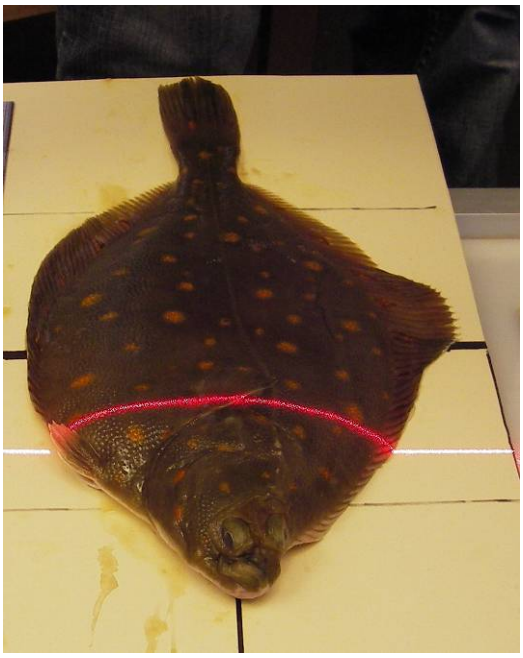

Figure 3. Image of the laserlight curve on a plaice.

By aquiring an image of the laserlight curve with a digital camera being placed in a known angle relative to the laser the principle of active triangulation can be applied. Fig. 4 shows the triangulation setup.

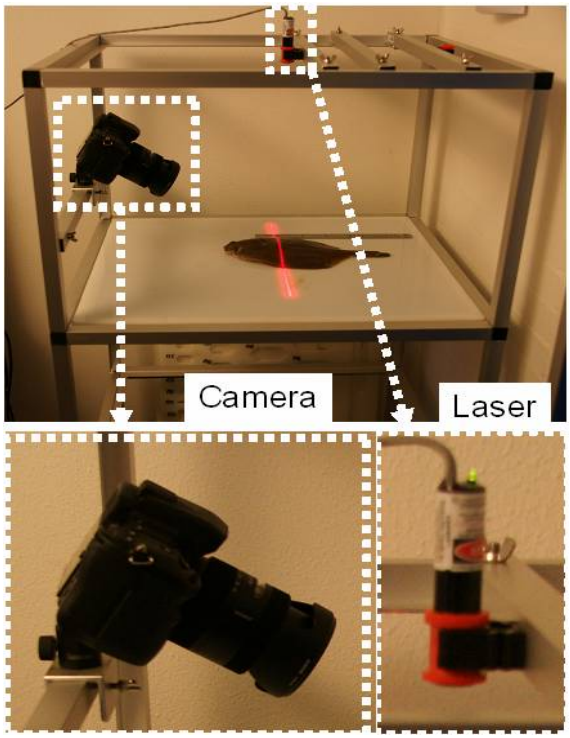

Figure 4. Triangulation setup.

Due to the high coherence of the laserlight and the diffuse reflection in the fish surface the image of the line appears both speckled and somewhat smeared-out. Through image-

analysis the position of the center curve of the laserline can be determined with sub-pixel precision by averaging pixel dependent color and intensity information over several pixels along the curve at several positions across the curve. Fig. 5 shows the average intensity acquired along the yellow marked line on a plaice with the image-analysis functionality developed for the laserline MorphoMeter.

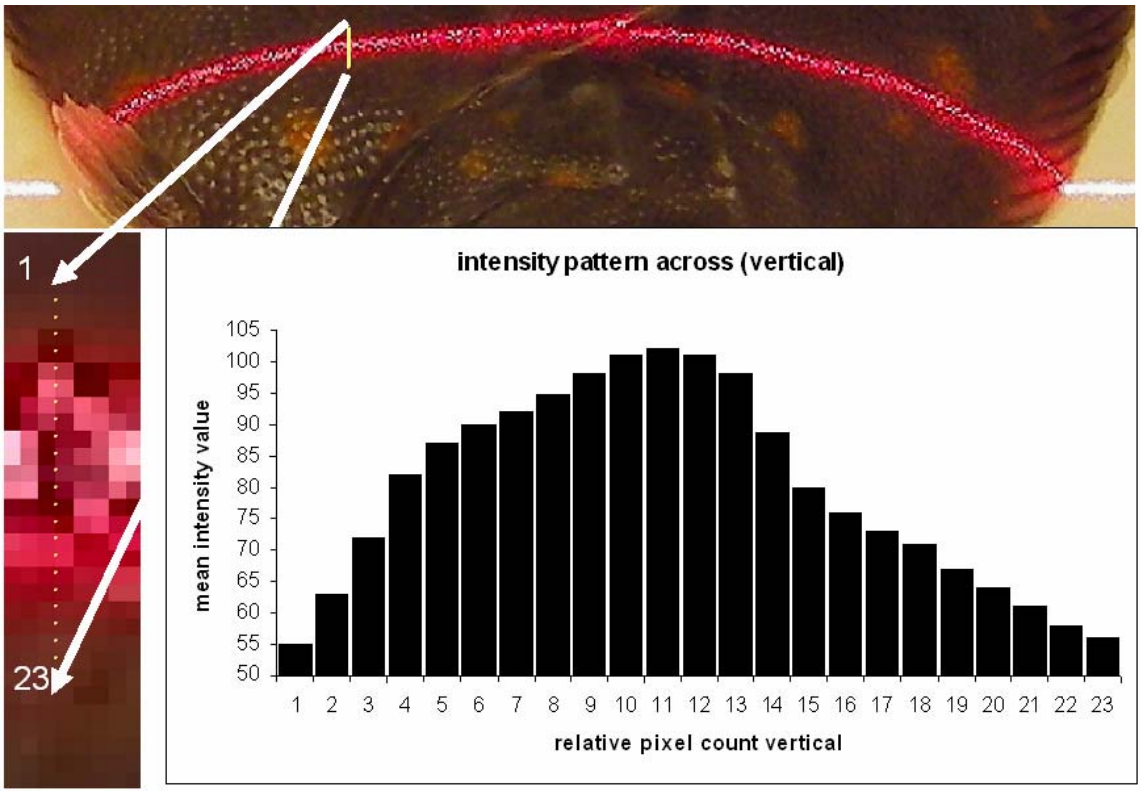

Fig. 5

When the position of the centre curve has been estimated across the full image it is possible to calculate the cross section of the fish in the plane defined by the laserbeam. This is done with a mathematical model that uses information about the position of the laser relative to the camera and information about the how to transform from pixel coordinates to distances in mm within in the camera object space (see next section).

The setup in Fig. 4 is presently best suited to acquire cross sections of flat fish with a single laser and a single camera, but has been prepared to be part of the project to develop methods including several laser-camera systems similar to those in Fig 4. For roundfish the same basic principle can be applied at least two or preferably three times around the cross section. The preferable design thus requires three lasers and three cameras in known positions relative to each other.

3 Conversion from laser light-sheet coordinates to camera pixel coordinates.

This section will treat triangulation for the simplified case, where we assume that the laser light-sheet defines a plane (x-y-plane) that is vertical, the fish lies on a horizontal plane (x-z-plane), the optical axis (zc-axis) of the camera is perpendicular to the

intersection line (x-axis, xc-axis) between the light-sheet plane and the fish plane, and the intersection point ((x, y, z) = (xc, yc, zc) = (0, 0, 0) (origin O)) between the two lines is situated approximately below the centerline of the fish. The zc-axis makes an angle vc with the horizontal plane. Figure 6 outlines the geometry:

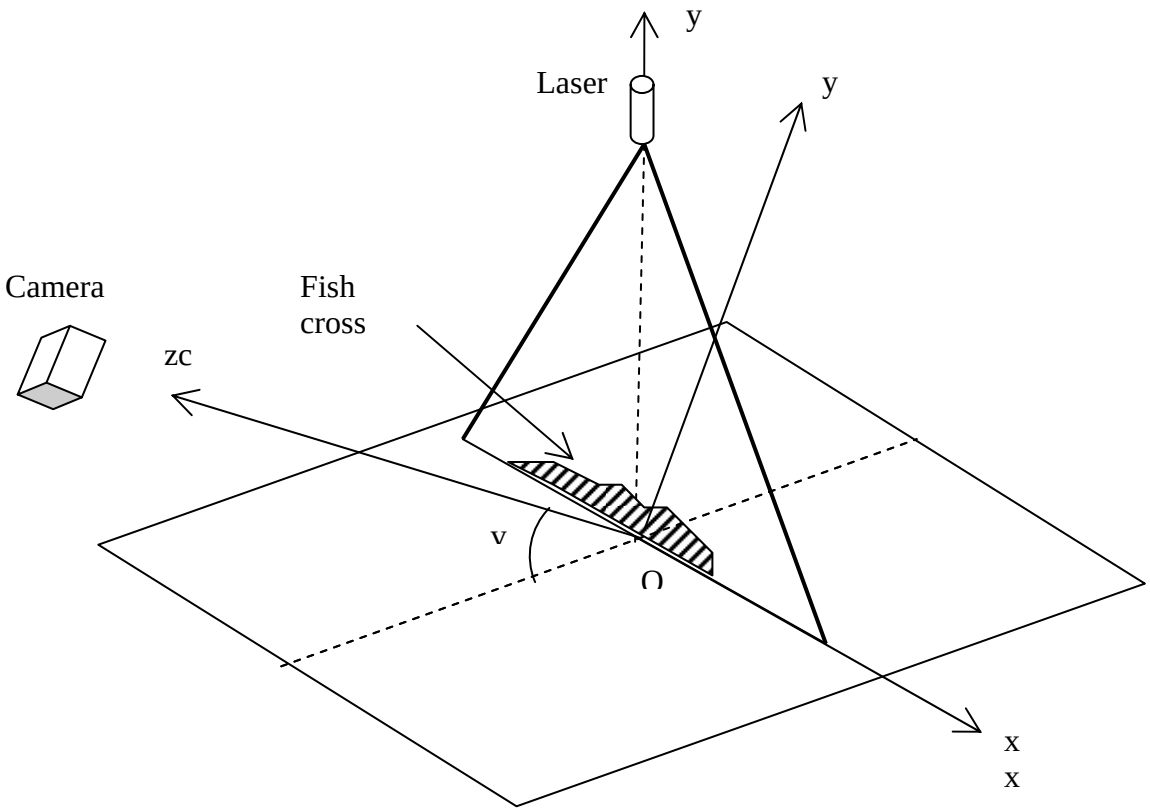

Figure 6. Outline of the laserline MorphoMeter conversion geometry

Assuming a simple pinhole camera model for the camera the following relations are valid between a point (xc, yc, zc) in the camera object space and the corresponding image pixel point (xp, yp) in the camera image plane:

$$xp = k*xc/r$$
$$yp = k*yc/r$$
$$r = \mathrm{sqrt}((d - zc)^2 + xc^2 + yc^2)$$

For any point (x, y) on the fish cross section in the laser light-sheet plane the corresponding point in the camera object space will be:

$$xc = x$$
$$yc = y*\cos(vc)$$
$$zc = y*\sin(vc)$$

where d is the distance between the camera model pinhole position and the point O, k is a constant that depends on the pinhole distance from the image plane (mainly dependent on the focal length of the camera lens and the object distance) and the pixel size of the

camera chip. Those parameters are determined by calibration with object of known size in the camera space. To obtain the cross section curve from the curve on the image the inverse relations of those above are calculated.

4. Laserline source.

Traditionally point-laser sources have been turned in to line sources by simply mounting cylindrical lenses on the laser to fan out the point source in one direction. A major weakness of such a design is that line width and intensity is very variable along the line, which makes measuring systems based on this technique inaccurate. Over the last two decades an alternative based on holographic optics has become available that does not suffer from this weakness. We have based the laserline MorphoMeter on this technology and chosen a 35 mW laser with a wavelength of 660 nm, and checked that this wavelength results in diffuse reflection with sufficient contrast to the background on most of the relevant fish species to create images of a quality where the centre curve of the light can be extracted precisely. The image creation has been tested with plaice as well as haddock and mackerel (Fig. 7).

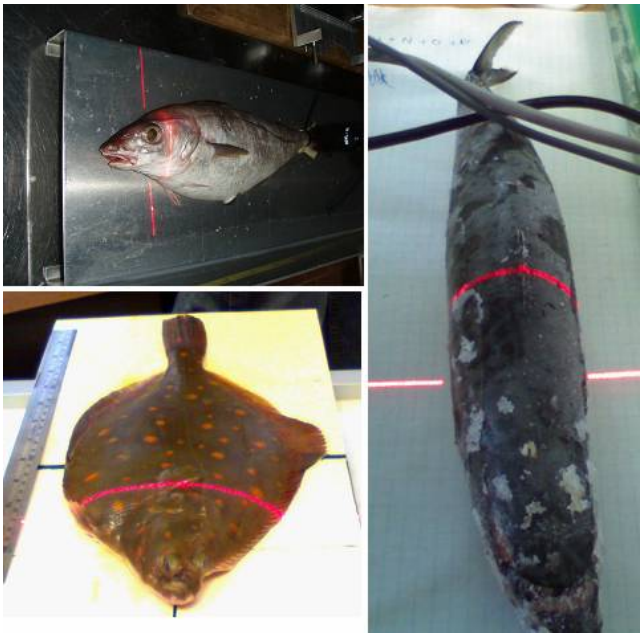

Fig. 7

Fig. 7 shows that the chosen laser wavelength can produce clearly visible curves of diffusly reflected light on those species of fish.

5. Image acquisition.

The simplest way to acquire the image of the diffuse reflected laser light is to use a digital camera connected to a laptop computer with an USB-connection. By using off-the-shelf standard consumer products instead of specialized industry products we can benefit from the fast development in resolution and significantly lower prices of this type of cameras over the past few years. We have procured and tested two different off-the-shelf camera-systems for the laserline MorphoMeter:

1) high resolution web camera (Fig. 8 left) based on a 2 megapixel CCD with normal 8-bit colour depth.
2) high precision and resolution digital camera (Fig. 8 right) based on a 12.4 megapixel CCD with increased 12-bit colour depth.

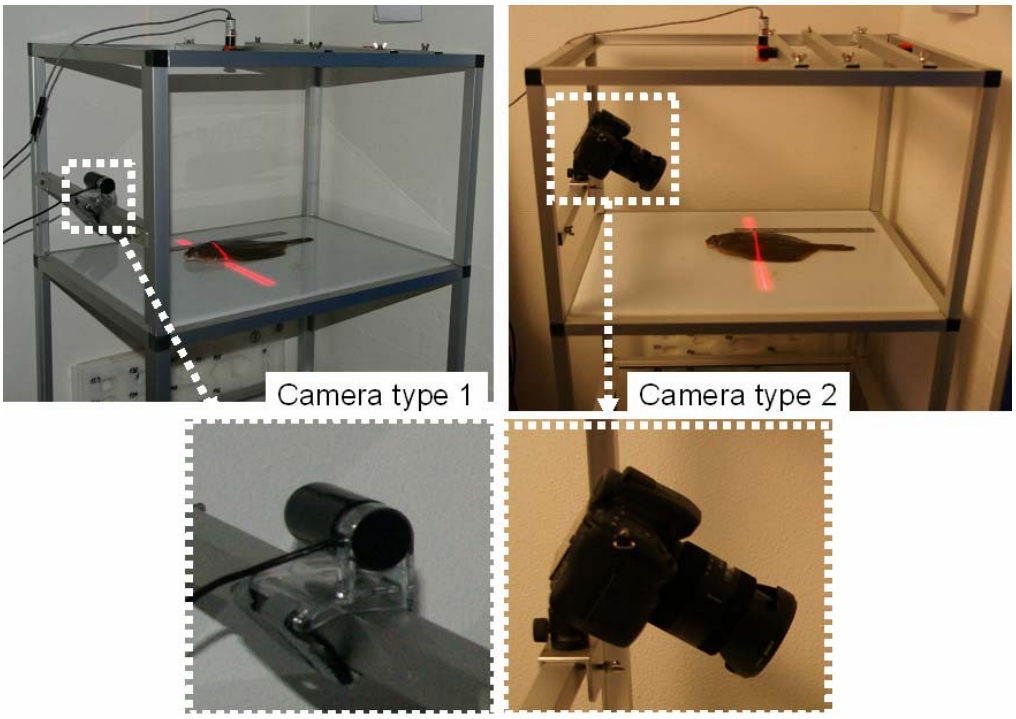

Fig. 8

Fig. 9 shows images acquired using the to different camera systems under two different background lighting situations. A and B are for camera type 1 while C and D are for camera type 2. A and C show situations with relatively high background light intensity while B and D show situations with relatively low background light intensity.

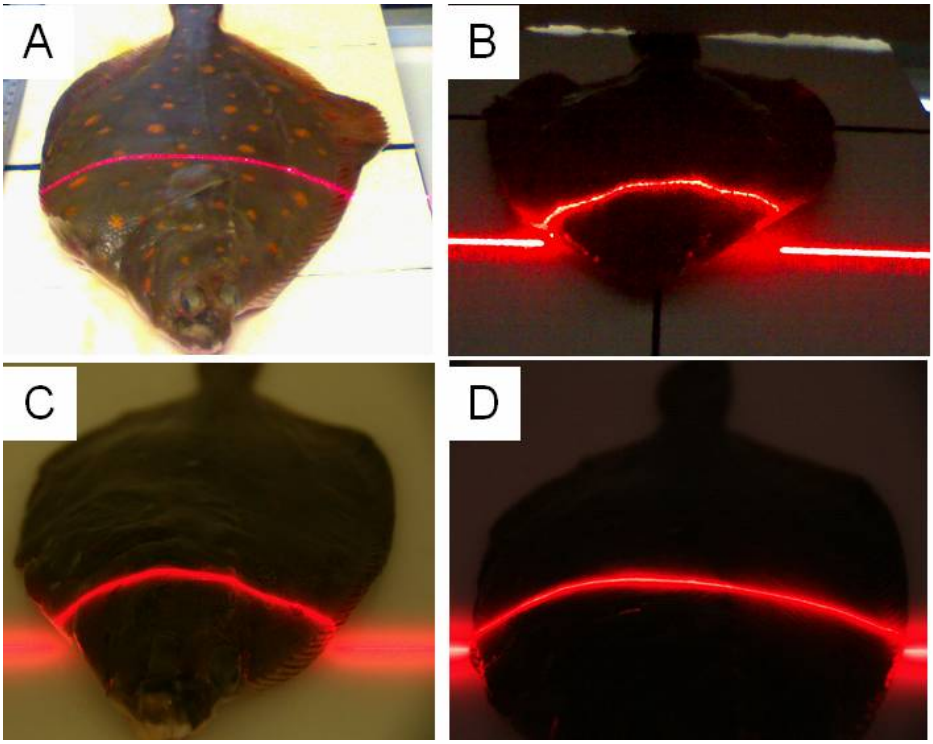

Fig. 9

Fig. 9 documents the significantly better quality of the image of the reflected laserlight under varying background lightings in camera type 2 compared to type 1. Zoomed detail images of the laserlight lines in the images of Fig. 9 are shown in Fig. 10.

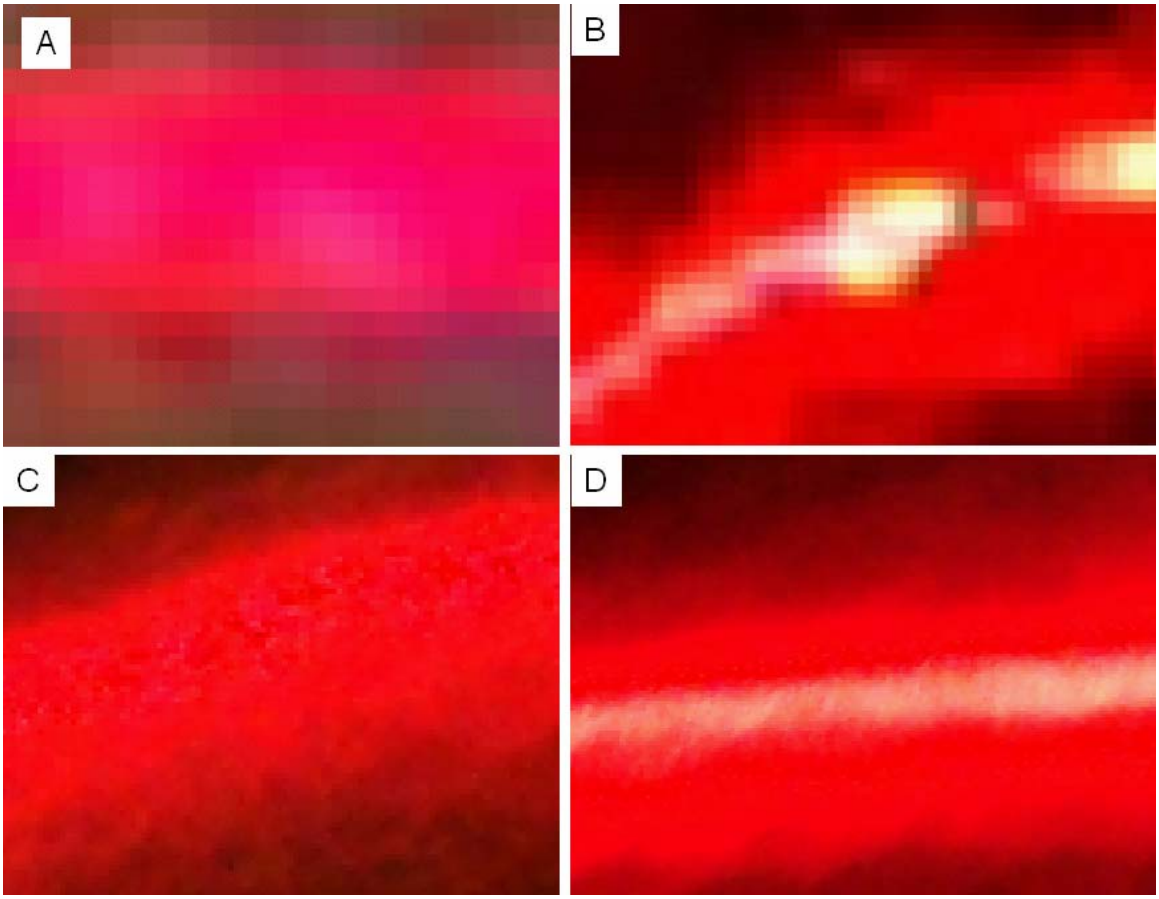

Fig. 10

They clearly show the superior quality of the camera type 2 images. The increased number of pixels within the laserline width combined with the higher dynamic range of the CCD chip of camera 2 is also evident giving a significantly better estimate of the centerline position. It is therefore recommended to base the laserline MorphoMeter on camera type 2.

6. Conclusion.

Although we have not been able to complete the development and implementation of the laserline MorphoMeter within this project, we think that the results we have obtained indicate that the method is feasible. Compared to the mechanical MorphoMeter we expect it will have an advantage of being much faster to measure many cross sections of a large number of individuals. This would be very time-consuming process using the mechanical MorphoMeter. For very small individuals, where the resolution of even the small mechanical MorphoMeter is too coarse to give the required accuracy of the cross section, it would also be beneficial to use the laserline MorphoMeter.

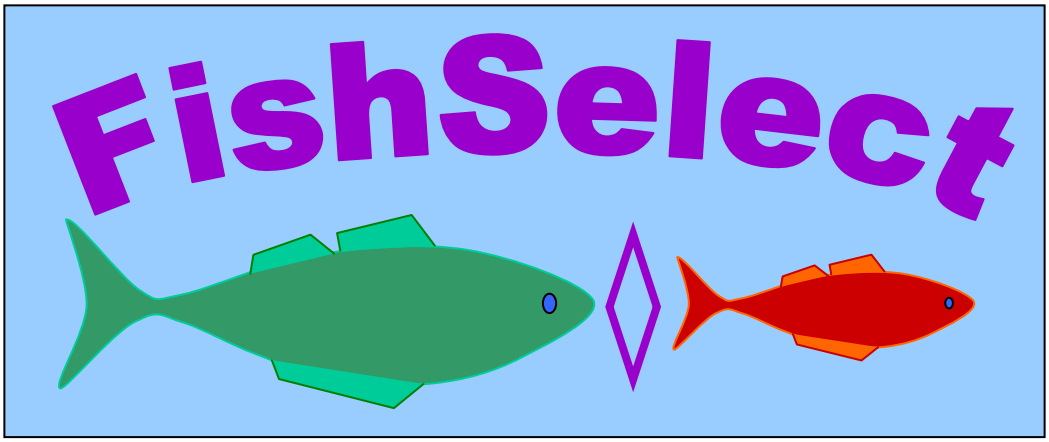

A12

ICES FTFB Dublin 2007

FISHSELECT
Development of methodology

Technical University of Denmark
Danish Institute for Fisheries Research
Section of Fisheries Technology

Bent Herrmann, Bo Lundgren, Ludvig A. Krag, Rikke P. Frandsen, Niels Madsen, Karl-Johan Stæhr

Introduction

In towed fishing gear like trawl, mesh size regulations aim at retaining marketable fish and releasing juvenile fish. Different species have different morphological characteristics such as cross-section shape and in mixed species fisheries, finding the optimal combination of mesh size and shape is a complex procedure depending on species composition as well as defined minimum landing sizes (MLS).
We present a new methodology, FISHSELECT, developed to make a first prediction of the basic selective properties of different netting panels. The methodology identifies species specific morphological features that are important for mesh penetration and data on these features are processed in an integrated software tool.

Conditions for mesh penetration:

1) The morphological condition. The geometrical relation between the cross-section size and shape of the fish and mesh size and shape must be such that the fish is able to pass through the mesh with or without deformation.
2) The behavioral condition. The fish must either actively attempt to pass through the mesh or be forced mechanically towards it. An important element is that the fish is able to meet the netting oriented in an optimal way to penetrate it.

View point

The first step in the process of designing a new selective fishing gear for a specific fishery should contain a procedure of selecting netting designs that fulfill at least the morphological condition for fish below MLS. If this condition is not fulfilled then, regardless of the behavioral response, the fish will be retained by the fishing gear. The morphological condition for netting penetration is thus an important aspect of the selection process in a fishing gear. Assessment of its effect may thus provide a first indicative prediction of the consequences on discard and catch efficiency of deploying different netting designs in a specific fishery.

Methodology

1) Laboratory experiments

For selected species, morphological characteristics important for mesh penetration are identified and cross-sections at corresponding positions are assessed. Each fish is labeled and its length and weight are recorded. Cardboard templates with pre-cut holes of a large range of different sizes and shapes are used to imitate different mesh designs. With the templates held horizontally we test and record if the fish, head first and under influence of gravity, can or cannot pass through the imitated meshes. The fish is rotated to the optimal orientation for penetration.

Assessing fish cross-sections

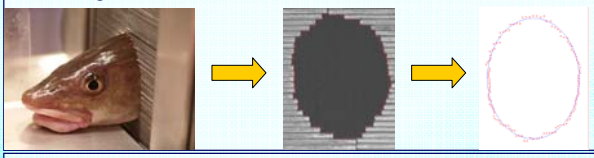

Sensing tool is used to capture cross-section of a cod. The image is digitized and fitted to parametric shapes that can be described by few parameters.

Fall-through experiments

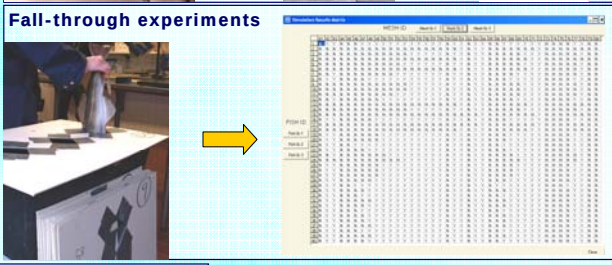

A cod is guided through a "mesh" and the success (Y) or failure (N) is recorded. Each fish and each "mesh" is provided with a unique ID.

Defining escapement model and 1st run of simulations

Up to 3 different cross-sections can be used and the fish only penetrates the mesh if all chosen cross-sections passes. The limiting cross-section may differ between area or season.

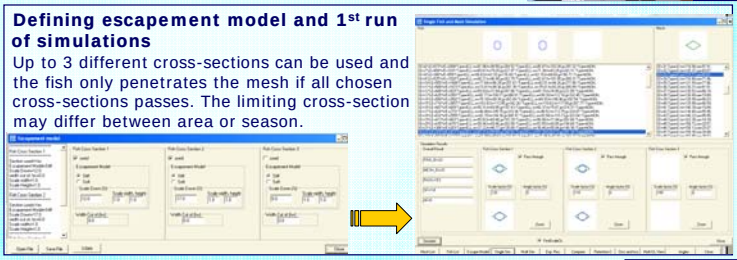

2) Simulating experiments

We have constructed a flexible simulation model that employ information on fish cross-sections obtained from the laboratory experiments and data on a predefined mesh geometry. The tool predicts chances of mesh penetration by relating these informations and by up- and down scaling the size of the fish. For validation, a scenario identical to the setup in the lab is simulated using the same fish and the same selection of mesh shapes and sizes. Repetitive simulations using different escapement models with options for degree of compression (~scaling) and for geometrical description of the fish cross-sections are run.

3) Comparison

The penetration results from the laboratory experiments are compared with the results from the simulated experiments. If the degree of agreement for a given set of the options described in 2) is high for the large majority of meshes and fish, the setup is accepted. This means that the choice of morphological features to be measured as well as the method used for measuring is suitable for the purpose. Furthermore, the modeling of the morphology and the options for mesh penetration for the species under investigation is reasonable.

Comparing simulations and experiments

Results from the fall-through experiments are held against simulated data and the degree of agreement is estimated. In the shown setup there is a 96% agreement between simulated and experimental data.

S: ok, D: not ok
YY: sim. and exp. both Y (S)
NN: sim, and exp. both N (S)
YN: sim. N and exp. Y (D)
NY: sim. Y and exp. N (D)

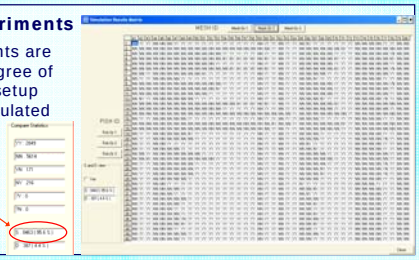

Measuring more fish!

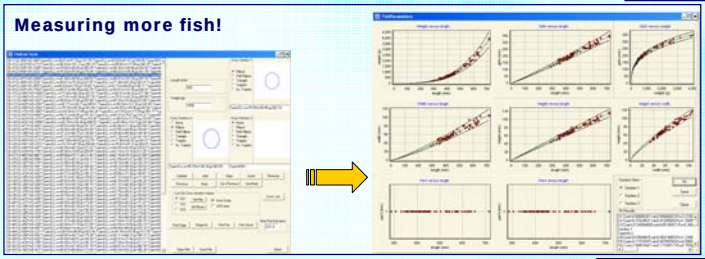

4) Establishment of morphological relationships

If 3) is successful, the features found to be important will be measured on a larger sample of fish. Hereby, more reliable relationships between these measures and the length of fish are established and the statistical variations are quantified.
These relationships can then be applied to estimate the morphological data for a fish population of any size structure. The population structure may be arbitrary or based on data from standard surveys.

5) Predictions

A new series of simulations incorporate the model established in 3) and the morphological relationships established in 4) and output predictions on basic selective properties for different netting designs and specified populations of fish. Together with information on distribution of fishing effort in the specific fishery, these predictions may provide indicative information on the consequences on discard rates and catch efficiencies of applying different netting designs in towed fishing gears. Also the effect of altering the minimum landing size can be investigated.

Combining all informations

A virtual fish population, a validated escapement model and data on mesh geometry are used to predict basic selective properties of a new gear and its consequences on discard and loss of marketable Fish.

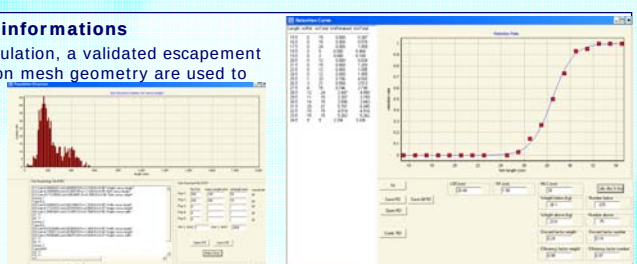

FISHSELECT

Study of cod (*Gadus morhua*)

ICES FTFB Dublin 2007

Technical University of Denmark
Danish Institute for Fisheries Research
Section of Fisheries Technology

Ludvig A. Krag, Bent Herrmann, Rikke P. Frandsen, Karl-Johan Stæhr, Niels Madsen, Bo Lundgren

Introduction: The cod stocks in Kattegat/Skagerrak are at a critical level. Cod is caught in most fisheries both as a target species and as unwanted by-catch. The minimum landing size (MLS) and the technical regulations specifying legal mesh sizes and types varies between the Kattegat/Skagerrak. For a sustainable exploitation of a marine resource like the cod stock, a meaningful relationship between the mesh size regulation and the MLS is necessary. We use the FISHSELECT methodology to provide the cross-section data that will affect cod's ability to penetrate different mesh sizes and types. The cross-sections are used to simulate the selection of cod in the mesh sizes and types used today in Kattegat/Skagerrak. Some preliminary results are reported.

Size distribution of cod used in the experiments

75 freshly caught cod in the length range 29 cm – 72 cm were kept alive in tanks and anaesthetized just before use.

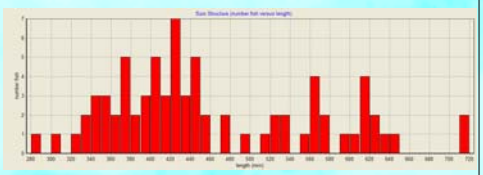

Meshes templates used in the experiments

Templates with 118 meshes of different types (diamonds, squares, rectangular and hexagonal), openings and sizes were used in the penetration experiments.

Assessing cross section shapes

A mechanical sensing tool was used to asses the cross section contours of each individual at two positions.

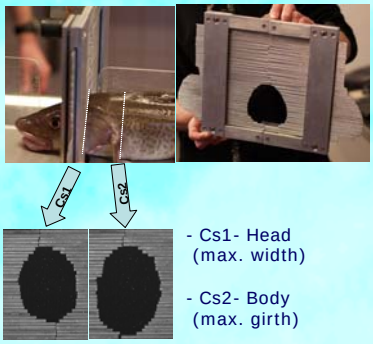

- Cs1- Head (max. width)
- Cs2- Body (max. girth)

Digitizing and parametric fitting

Each cross section was digitized using a scanner and the image analysis function-ality of FISHSELECT. The cross section contours was parameterized as ellipses with given width and height.

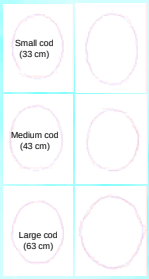

Results for different sized cods

Red crosses: Digitized contours.
Blue shapes: Fitted ellipses.

An ellipse is a reasonable representation for all sizes of cod examined both at Cs1 and Cs2.

Establishment of morphological relationships

Length based regressions were fitted ($w,h = aL^b$) for both cross sections.

Good R^2 values were obtained.

Black curves: Simulated variance represents data variance well.

Relationships can therefore be used to simulate new population structures.

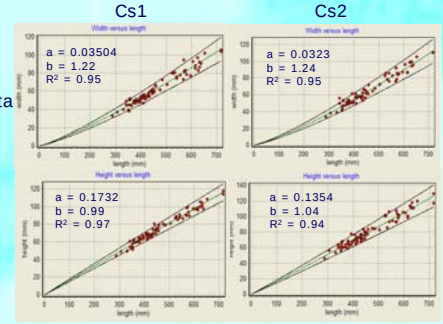

Penetration experiments

75 cod were tested in 118 meshes, which gives 8850 penetration trials. 3020 succeeded and 5830 did not.

Simulation of penetration experiments

The results were compared with simulated penetration using different escapement models with two different levels of cross section compression tested on Cs1 or Cs2:

1) **stiff** compression – fish is assumed to be compressed symmetrically, the cross section is not able to take shape after the mesh during a penetration attempt.
2) **soft** compression – the fish is assumed to be able to take shape fully after the mesh during a penetration attempt.

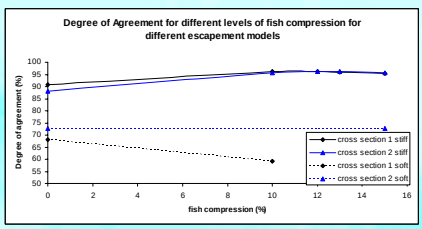

Conclusion on simulation of penetration experiments

With Cs1 and max 10% stiff compression the simulations correctly predicted the experimental penetration results in 8515 of the 8850 results or 96.2% agreement. Nearly the same level of agreement could be obtained with Cs2 and max 15% stiff compression.

With a simple (soft) escapement model based on comparing cross section circumferential length of the fish to the inside circumferential length of the mesh, the degree of agreement was considerably lower (down to 59.1 %).

Conclusion: With Cs1 an max 10% compression and modeling the cross section by an ellipse leads to a good agreement between laboratory experiments and simulation results for cod.

Prediction of cod-end selection

We can predict the basic selective properties for different netting designs based on the established morphological relations and the 10% stiff compression model based on the elliptical description of cross section 1. In Kattegat/Skagerrak, the mesh size regulation for diamond mesh cod-ends is 90 mm (**d90**), while the legal alternative in square mesh cod-ends used to be 70 mm (**s70**). MLS for cod in Skagerrak is 40 cm. We investigated if there were a reasonable agreement between the legal netting designs and the MLS. We assumed that the shapes of the diamond meshes is not distorted by the fish during mesh penetration. The justification for this have been investigated by Herrmann & O' Neill (2005;2006) who found comparable results from computer simulations and sea trials except for very small catch weights. For the square mesh cod-end we make similar assumptions where the cod-end bars parallel to the cod-end axis can not be distorted by fish making escape attempts. The mesh bars perpendicular to the cod-end axis were modeled to be distorted into a hexagonal shape by fish trying to penetrate, if the perimeter of the cod-end was less than the sum of the length of the mesh bars around.

Diamond mesh cod-end d90

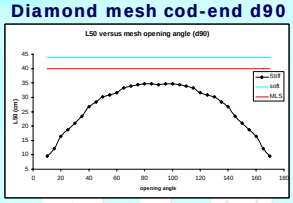

Black curves: The 50% retention length (L50) as a function of the mesh opening angle.
Red line: MLS.
With L50 below MLS for all opening angles there is a poor relationship between MLS and the technical regulations.
Blue line: L50 if the fish is able to deform the shape of the mesh fully (soft mesh).

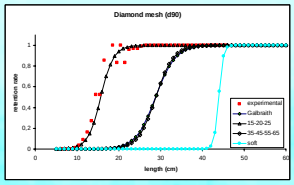

Black triangles and diamonds: Selection curves for different mesh opening distributions. Red: Our sea trial data. Green: Experimentally based results from Galbraith et al. (1994).

The comparisons show that it is possible to explain apparently contradictory experimental results by differences in the mesh opening distribution introduced by e.g. different catch weights (see Herrmann & O' Neill, 2005).

Light blue curve: Selection if the meshes were fully deformable (soft). The experimental results show that full distortion is not a realistic scenario.

Square mesh cod-end s70

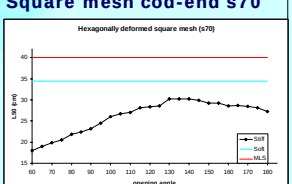

Green: Selection curve for a fully open square mesh. Open and filled diamonds: Selection curve for a distribution of perpendicular mesh distortions. Red: Our sea trial data.

The comparisons show that it is possible to explain the experimental data.

Light blue curve: Selection if the mesh shape were fully deformable (soft). The experimental results show that this is not a realistic scenario.

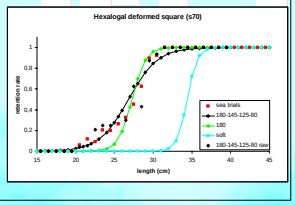

References: **Galbraith, R.D., Fryer, R.J., Maitland, K.M.S., 1994**. Demersal pair trawl cod-end selectivity models. Fish. Res. 20: 13-27. **Herrmann, B. & O'Neill, F.G., 2005**. Theoretical study of the between-haul variation of haddock selectivity in a diamond mesh cod-end. Fish. Res. 74: 243-252. **Herrmann, B. & O'Neill, F.G., 2006.** Theoretical study of the influence of twine thickness on haddock selectivity in diamond mesh cod-ends. Fish. Res. 80: 221-229.

FISHSELECT

Study of Plaice *(Pleuronectes platessa)*

ICES FTFB Dublin 2007

Technical University of Denmark
Danish Institute for Fisheries Research
Section of Fisheries Technology

Rikke P. Frandsen, Bent Herrmann, Ludvig A. Krag, Karl-Johan Stæhr, Bo Lundgren & Niels Madsen

Abstract

The plaice stocks in Kattegat/Skagerrak have decreased in recent years. Plaice is caught in demersal fisheries both as target species and as by-catch, and minimum landing size (MLS) in these waters is 27 cm. For a sustainable exploitation of a resource like plaice, the interactions between regulations on mesh size and MLS need to be documented and taken into account. We use the FISHSELECT methodology to identify the morphological characteristics and corresponding cross-sections that are expected to affect the selective properties in different mesh sizes and types. The cross-sections are used to simulate selection of plaice in the net designs used in Kattegat/Skagerrak today and preliminary results show a mis-match between mesh and MLS.

Experiments and development of the model

Size distribution of plaice used in the experiments

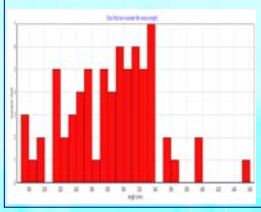

70 plaice measuring 18-46 cm were examined in laboratory experiments.

It is important that the morphology of the fish measured is close to that of live fish. We conducted these experiments in the laboratory with a supply of wild-stock plaice kept in tanks. Fish were anaesthetized when removed from the tanks.

Mesh templates used in the experiments

Templates with 118 meshes of different shape and size were used in the fall-through experiments. The mesh shapes examined were diamond, square, rectangular and hexagonal. For each shape and size, a series of different openings were laid out in order to reflect the mesh configurations found in a codend.

Assessing cross-sections

A mechanical sensing tool was used to assess the cross-section at three different positions:
CS1: At the highest point of the head
CS2: At the anal spine
CS3: At the maximum width of the fish ignoring the fins

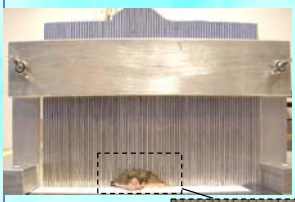

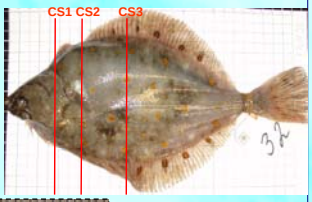

Sensing tool at CS1

Digitizing and parametric fitting of cross-sections

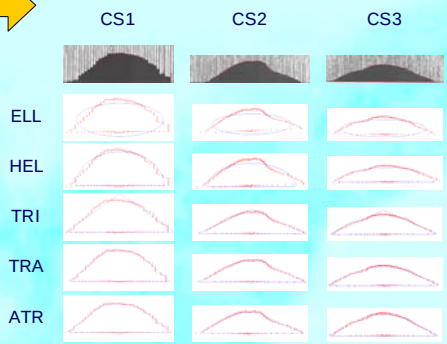

Each cross-section outline was scanned and the contour extracted with the image analysis function in the FISHSELECT software tool.

To reduce the number of parameters needed to describe the shape of the cross-section, five different basic shapes were fitted to the contour:

1) ellipsoid (ELL)
2) half ellipsoid (HEL)
3) triangle (TRI)
4) symmetrical trapezoid (TRA)
5) asymmetric trapezoid (ATR)

The best fit for all cross-sections was found when using the asymmetric trapezoid.

Simulating fall-through experiments and comparing results

The fins of plaice are fully deformable and the highest degree of agreement between results from the fall-through experiments and the simulation model were obtained when fins were ignored from the cross-sections. The three cross-sections were chosen based on practical experience both from the laboratory and from fishing. They were all expected to be essential for the prediction of whether a fish can penetrate a given mesh. This was confirmed by the simulation study since the highest degree of agreement between experiments and simulations was obtained for a model taking all 3 cross-sections into account.

In contrast to cod, the highest degree of agreement was found when fish compression during penetration was assumed to be zero – this may be due to a harder bone structure and the lack of swim bladder in the plaice and is therefore expected to be the case for all flat fish. With the asymmetric trapezoid fit and the above mentioned definitions included in the escapement model, the degree of agreement between experiments and simulations was 94.6%.

Establishment of morphological relationships

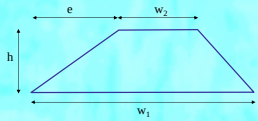

As asymmetric trapezoids, the cross-sections can be described by four parameters: W_1, W_2, h and e.

Data on these parameters versus length for all fish were plotted. A power model based on fish length (e.g. $h=a*l^b$) was fitted to data. Relationships were obtained for the three cross-sections CS1 – CS3. Results from CS1 and CS3 are shown.

For the relationships between length and parameters W1 and h, the power model fitted data well with R^2 above 0.74. Parameters W2 and e are sensitive to actual shape and more variable and R^2 is therefore lower.

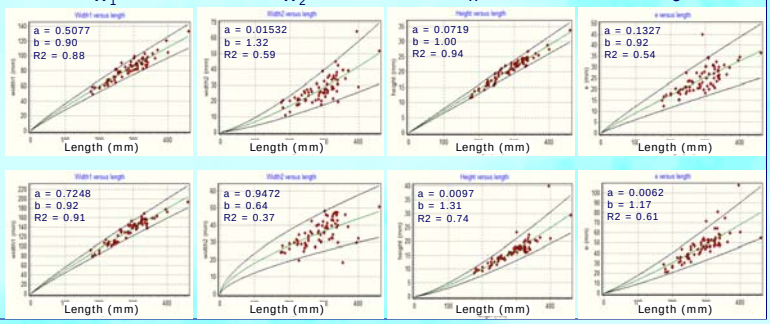

Predictions of codend selection

Based on the morphological relationships and the escapement model in FISHSELECT, we are able to predict the basic selective properties for different netting designs. In Kattegat/Skagerrak, mesh size regulation is 90 mm for diamond mesh codends (**D90**). Until recently, a 70 mm full square mesh codend (**S70**) was legal as well. We investigate if there is a reasonable match between these netting designs and the MLS by estimating 50% retention length (L50) for all the different configurations a 90mm diamond mesh and a 70mm square mesh can take on respectively. If L50 for all configurations is much smaller than MLS, the risk of discard is expected to be high. Conversely, if it is much larger than MLS there is a risk of loosing marketable fish. Whether these risks actually result in a high discards or loss of marketable fish, depend on the size structure of the population.

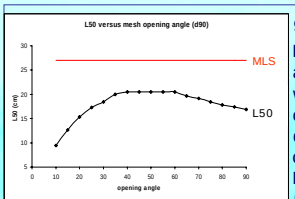

90 mm diamond mesh

L50 depends on the opening angle of the diamond mesh with highest values for openings ranging from 35-65 degrees. Highest L50 is 20.5 cm which is well below the MLS of 27 cm, indicating a mismatch that will increase the risk of a high discard.

70 mm square mesh

If square meshes are deformable in the low-tension perpendicular direction of the netting, they may take on an approximately hexagonal shape, when a fish tries to penetrate. The degree of deformation is defined by the opening angle (0=full deformation / stretched mesh; 180=no deformation / square mesh).
L50 depends on the opening angle, but never exceeds a value of 17.2 cm, well below the MLS. This indcates a severe mismatch that will increase the risk of a high discard.

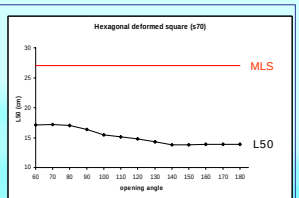

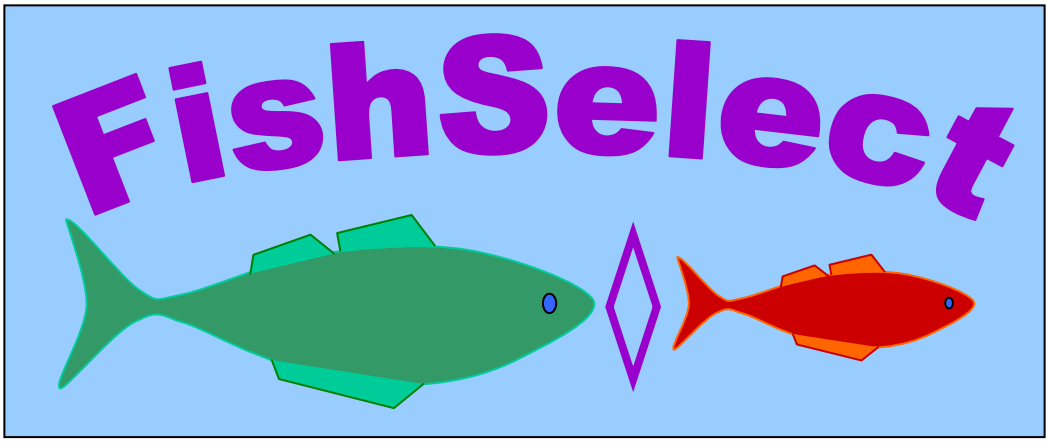

A13

Note on FISHSELECT newspaper articles.

During the project there has been some newspaper coverage of the project specific on FISHSELECT below is a list followed by some of the articles.

Newspaper	Date	Title of the FISHSELECT article
DTU-avisen	1.06.2007	Intelligent nets protect fish stocks
DTU-avisen	1.06.2007	Intelligente net skåner fiskene – Pap, hoppykniv og avanceret computerteknologi skal mindske bifangst af undermålsfisk
MetroXpress	11.06.2007	Forskere udvikler intelligente fiskenet
Fiskeri Tidende	28.06.2007	Ny metode til at mindske bifangst – Avanceret computerteknologi skal mindske bifangst af undermålsfisk
Fiskeri Tidende	28.06.2007	Tværfaglighed skaber resultater
Fiskeri Tidende	28.06.2007	21 papstykker og en hobbykniv
Ingeniøren	10.08.2007	Flere fisk skal undslippe fiskenet – Computersimuleringer skal finde frem til de bedste fiskenet
Nordjyske Stifttidende	19.08.2007	De vil ha' færre fisk i nettet
FiskerBladet	7.11.2007	Ny metode til at mindske bifangst

DTU AVISEN

1. JUNI 2007 NR. 6

2. SEKTION

DTU IN ENGLISH

Intelligent nets protect fish stocks

329 fish, 21 pieces of cardboard, one Stanley knife and advanced computer technology may reduce the bycatch of undersized fish

For each fish sold at the fishmongers, many others have often been thrown back into the ocean. They were either too small or of a variety that was not the target catch. Fish that have been brought on deck have a lower survival rate. Discarding fish is thus poor exploitation of fish stocks.

Now an interdisciplinary research team at the Danish Institute for Fisheries Research in Hirtshals has developed an entirely new method that makes it possible to assess whether fish under the minimum size can escape through the mesh of a trawl net.

Preliminary results of the group's work suggest that the mesh sizes and minimum sizes used in fisheries in Skagerrak and Kattegat do not work as intended. For instance, Dover sole larger than the minimum size escape through the mesh, while lemon sole, turbot and cod under the minimum size are caught.

Body structure is key

The basic premise behind the project entitled FishSelect is that you have to know and be able to describe the body structure of a species of fish in order to assess whether the fish will be caught in the mesh of a trawl net, explains Bent Herrmann, head of project and senior researcher at the Danish Institute of Fisheries Research.

„Traditionally, only length is considered when dealing with the size of fish in fisheries. It is the minimum size that determines whether a fish may be caught or must be discarded. But what actually determines whether a fish gets caught in a trawl net or whether it can escape through the mesh is not the length of the fish but the size of the cross-section. Is it long and thin or short and fat, and how much can the cross-section be compressed? We have developed a method of determining and describing this," says Mr. Herrmann.

Fishing from the computer

One of the concrete results of the project, which began two years ago, will be a database containing the ratio between length and cross-section for all the major species of fish in Danish fisheries. With this in hand, it will be possible to use a newly developed simulation program to quickly calculate the probability that a 20-centimeter-long cod can escape a net with a given mesh size.

„This can save both time and money in the future, when developing and testing new tools for fisheries. Instead of sailing out to sea to test equipment in experimental fishery, it will be possible to do some of the work in front of the computer. At the same time, the simulation program would generally be useful for determining whether the proper ratio has been achieved between the mesh sizes used in fisheries today and the minimum sizes that are set for fish," adds Ludvig Ahm Krag, project participant, biologist and former fisherman.

4

Dynamo forsvarede VM-titlen

Woops – vi gjorde det igen. Endnu et mesterskab og to hædersbevisninger røg til DTU's økoracere ved VM for energirigtige biler – Shell EcoMarathon. Først i sidste forsøg lykkedes det DTU Dynamo at sætte konkurrenterne til vægs.

5

Gratis på nettet overalt

Snart bliver det muligt for studerende på DTU at gå gratis på nettet, uanset hvor i verden de befinder sig. Eduroam hedder systemet, der er planlagt til at kunne servicere alle studerende efter sommerferien.

11

44 millioner til Food DTU

Danmark får et nyt center for forskning i sund og sikker mad. Food DTU er et forskningscenter, der åbner med ti projekter inden for friskere kantinemad over catering og sygdomsforebyggende fødevarer til sikkerhed i frosne færdigretter.

DTU AVISEN

4 JUNI 2007 NR. 6

SIMULERING LINE REEH

Ved hjælp af en række miljøpinde, som forsigtigt presses ind til de har kontakt til fisken, aftrykkes et aftryk af fiskens form. Aftrykket bliver efterfølgende scannet ind i en computer til videre billedbehandling. Målet er at skabe nye fiskegarn, der nedbringer bifangster og beskytter fiskebestandene.

Intelligente net skåner fiskene

Pap, hobbykniv og avanceret computerteknologi skal mindske bifangst af undermålsfisk

For hver fisk, som sælges hos fiskehandleren, er der ofte smidt mange andre fisk tilbage i havet igen. Enten er for små eller er af en art, som man slet ikke fiskede efter.

Fisk, som én gang har været på dækket, har ringe chancer for at overleve. Udsmid af fisk, også kaldet discard, er derfor en dårlig udnyttelse af fiskebestandene.

Nu har en tværfaglig forskergruppe ved Danmarks Fiskeriundersøgelser i Hirtshals udviklet en helt ny metode, som gør det muligt hurtigt at vurdere om fisk under mindstemålet kan slippe fri gennem maskerne i et trawl.

Foreløbige resultater af gruppens arbejde tyder på, at de maskestørrelser og mindste-

➡ side 2

DTU

UDGIVER I DTU AVISEN UDGIVES AF DANMARKS TEKNISKE UNIVERSITET (DTU), ANKER ENGELUNDS VEJ 1, 2800 LYNGBY. DTU KAN KONTAKTES PÅ TLF. 45 25 25 25 OG VIA WWW.DTU.DK. REDAKTIONEN KAN KONTAKTES PÅ TLF. 45 25 10 11 / 45 25 12 99. MAIL: REDAKTION@DTUAVISEN.DK **UDKOMMER** I DTU AVISEN UDSENDES DEN FØRSTE MANDAG I HVER MÅNED, OG IKKE I SOMMERPERIODEN. **DEADLINE FOR NÆSTE NUMMER** I 16. AUGUST 2007. **UDGIVELSE** I 3. SEPTEMBER 2007.
ANSV. REDAKTØR I DAN JENSEN. **REDAKTØR** I MICHAEL STRANGHOLT. **REDAKTION** I PETER HOFFMANN, LINE REEH, METTE MINOR ANDERSEN, MARIA SKOU, MOGENS BISGAARD, MICHAEL AAGAARD OG LEIF SØNDERBERG PETERSEN.
ANNONCER I IDA BANGERT. MAIL: ANNONCER@DTUAVISEN.DK **DESIGN & TRYK** I DATAGRAF **OPLAG** I 10.000 EX.

→

> **Der er helt klart lidt Georg Gearløs over det. Men det virker!"**
>
> RIKKE FRANDSEN, BIOLOG

mål, som man bruger i fiskeriet i Skagerrak og Kattegat ikke fungerer efter hensigten. Blandt andet kan gråtunger større end mindstemålet slippe fri gennem maskerne, mens rødspætte, pighvar og torsk under mindstemålet bliver fanget.

Kropsbygningen er afgørende

Grundtanken i projektet, som har titlen FishSelect, er, at man er nødt til at kende og kunne beskrive en fiskearts kropsbygning for at kunne vurdere, om en fisk vil blive fanget i maskerne i et trawl, forklarer projektleder og seniorforsker ved Danmarks Fiskeriundersøgelser, Bent Herrmann.

„Traditionelt taler man kun om længde, når man beskæftiger sig med fisks størrelse i fiskeriet. Det er mindstemålet som bestemmer, om en fisk må landes eller skal smides ud igen. Men det, der faktisk afgør, om en fisk bliver fanget i et trawl eller om den kan undslippe gennem maskerne, er ikke fiskens længde, men hvor meget den fylder i tværsnit. Er den lang og slank eller kort og tyk og hvor meget kan tværsnittet komprimeres? Det har vi udviklet en metode til at bestemme og beskrive," siger Bent Herrmann.

På fisketur fra computeren

Et af de konkrete resultater af projektet, som startede for to år siden, bliver en databank over forholdet mellem længde og tværsnit for alle de vigtige arter i dansk fiskeri. Med den i hånden vil man ved hjælp af et nyudviklet simuleringsprogram, hurtigt kunne beregne sandsynligheden for, at fx en torsk på 20 cm kan undslippe et trawl med en given maskestørrelse.

„Det kan spare både tid og penge i fremtiden, når man udvikler og tester nye redskaber til fiskeriet. I stedet for at tage på havet for at teste udstyret ved forsøgsfiskeri, vil man kunne klare en del af arbejdet foran computeren. Samtidig vil simuleringsprogrammet generelt kunne bruges til at undersøge om vi har den rette sammenhæng mellem de maskestørrelser, som vi bruger i fiskeriet i dag og de mindstemål på fisk, som er fastsat," supplerer projektdeltager, biolog og tidligere fisker, Ludvig Ahm Krag.

Udstyr fra bunden

Fordi det er helt nyt at forsøge at registrere og beskrive den del af fisks kropsbygning, der har betydning for maskepassage, eksisterede der ikke måleredskaber, som forskerholdet kunne gribe til.

Derfor har holdet udviklet metode og udstyr helt fra bunden, oplyser biolog Karl-Johan Stæhr, som også indgår på projektholdet:

„Ved de første pilotforsøg skar vi alle fiskene over og målte deres tværsnit. Men det var for langsommelig og ustabil en metode. Vi måtte tænke kreativt – og fik god hjælp fra vores kolleger hos DTU's IT- og teknikafdeling til at udtænke og konstruere et brugbart instrument."

Løsningen blev et instrument, som endnu ikke har fået et navn. Det består af en række målepinde, som forsigtigt presses ind til de har kontakt til fisken, så pindende efterlader et aftryk af fiskens form. Aftrykket bliver efterfølgende scannet ind i en computer til videre billedbehandling.

„Ved hjælp af et specielt udviklet billedbehandlingsprogram med kant-detektions software kan vi ud fra aftrykket bestemme fiskenes tværsnitskontur og beskrive dem med nogle få dækkende parametriske værdier i forhold til fiskens længde. Torsks tværsnit kan for eksempel beskrives ved hjælp af en ellipse med en højde og bredde, mens fladfisk kan beskrives via en asymmetrisk trapez," forklarer Bent Herrmann.

Når fiskenes tværsnit er registreret kan forskerne ved hjælp af et integreret simuleringsprogram, forudsige, hvor store maskerne skal være for at en fisk af den pågældende størrelse kan undslippe.

Fisk, forvaltning og modeller

Projektleder Bent Herrmann er oprindeligt uddannet civilingeniør og har en PhD-grad i udvikling af simuleringsmodeller, som kan forudsige fisks mulighed for at undslippe fra forskellige trawl og fiskeredskaber.

Med på holdet har han en række biologkolleger med stor erfaring i, hvad der skal til for at et fiskeredskab fungerer til havs – og med indgående kendskab til, hvordan arbejdet med forvaltningen af fiskebestandene foregår.

„Udfordringerne i projektet er mange og vi har haft brug for meget forskellige kompetencer – fra indsigt i fiskeredskaber til viden om, hvordan vi fangede og opbevarede de levende fisk som vi skulle bruge – for ikke at nævne arbejdet med at udvikle metoder, måleinstrumenter og computermodeller."

21 papstykker og en hobbykniv

For at kunne kalibrere og validere simuleringsprogrammet har forskerne opfundet endnu en effektiv, men simpel løsning. Den består af 21 store stykker vandfast specialpap, hvori der er skåret huller, som svarer til forskellige maskestørrelser og faconer. Dem bruger holdet til rent fysisk at undersøge, hvilke størrelse masker, som fisk af forskellige arter og længde kan passere igennem.

Samtidig kan forskerne se, hvilke dele af fiskens krop som evt. går på kanten og forhindrer fisken i at komme ud gennem maskerne. Fx blev holdet hurtigt klar over, at det ikke nødvendigvis er tværsnittet med den største omkreds, der er afgørende for, om en fisk kan passere en maske. I nogle masker er det højden af en fladfisks hoved der er begrænsende, mens det i andre masketyper er det bredeste tværsnit på kroppen, fortæller biolog og projektdeltager Rikke Frandsen:

„Der er helt klart lidt Georg Gearløs over det og vi blev da også drillet i al venskabelighed af kollegerne, da vi troppede op med 21 stykker pap. Men det virker!"

For hver fiskeart har forskerne haft fat i 70 fisk af forskellige længde. Hver fisk har de testet om kan komme igennem 120 forskellige huller. Det bliver til over 8000 resultater per fiskeart. Undervejs har der været flere nyttige overraskelser, fortæller biolog Rikke Frandsen.

„Vi har for eksempel opdaget, at torsk kan komme igennem forholdsvis små masker i forhold til deres tværsnitsstørrelse. Hovedet er hårdt, men resten af kroppen er meget fleksibel og kan komprimeres ret meget. Omvendt er rødspætters kompression, hvis man lige ser bort fra finnerne, næsten lig nul. Måske fordi de har et stivere skelet og fordi de mangler svømmeblære."

Videndeling med Europa

Foreløbig har forskerne målt og registreret længde og tværsnit på udvalgte punkter og mulig passage gennem masker af forskellige størrelse og form for 5 fiskearter: torsk, rødspætte, rødtunge, gråtunge og pighvar. Målet er at opmåle samtlige af de fiskearter, som er vigtige for dansk fiskeri, så det er ikke sidste gang at holdet er trukket i det blå arbejdstøj.

Projekt FishSelect er finansieret af det nationale udviklingsprogram for bæredygtigt fiskeri og selektive fangstmetoder. Forskerne bag FishSelect, der også inkluderer seniorforskerne Bo Lundgren og Niels Madsen, har søgt om midler fra EU's 7. rammeprogram i samarbejde med 11 europæiske partnere til at fortsætte arbejdet, når den nuværende bevilling udløber senere på året.

Forskerne håber blandet andet at kunne dele deres resultater og metoder med kolleger i andre lande via en række workshops.

„Teknologien kan overføres og anvendes i alt fra det nordeuropæiske fiskeri helt ned til Middelhavet og Egyptens rejefiskeri," vurderer projektleder Bent Herrmann.

For at kunne kalibrere og validere simuleringsprogrammet har forskerne opfundet endnu en effektiv, men simpel løsning: 21 store stykker vandfast special-pap med huller, som svarer til forskellige maskestørrelser og faconer, bruger Ludvig Ahm Krag og Rikke Frandsen til at undersøge, hvilke størrelse maskar, som fisk af forskellige arter og længde kan passere igennem.

Bent Herrmann overfører data fra måleudstyret til simuleringsprogrammet, der kan bruges til at designe mere effektive og ikke mindst skånsomme fiskenet.

> **Teknologien kan overføres og anvendes i alt fra det nordeuropæiske fiskeri helt ned til Middelhavet og Egyptens rejefiskeri"**
>
> BENT HERRMANN, SENIORFORSKER

Ny metode til at mindske bifangst

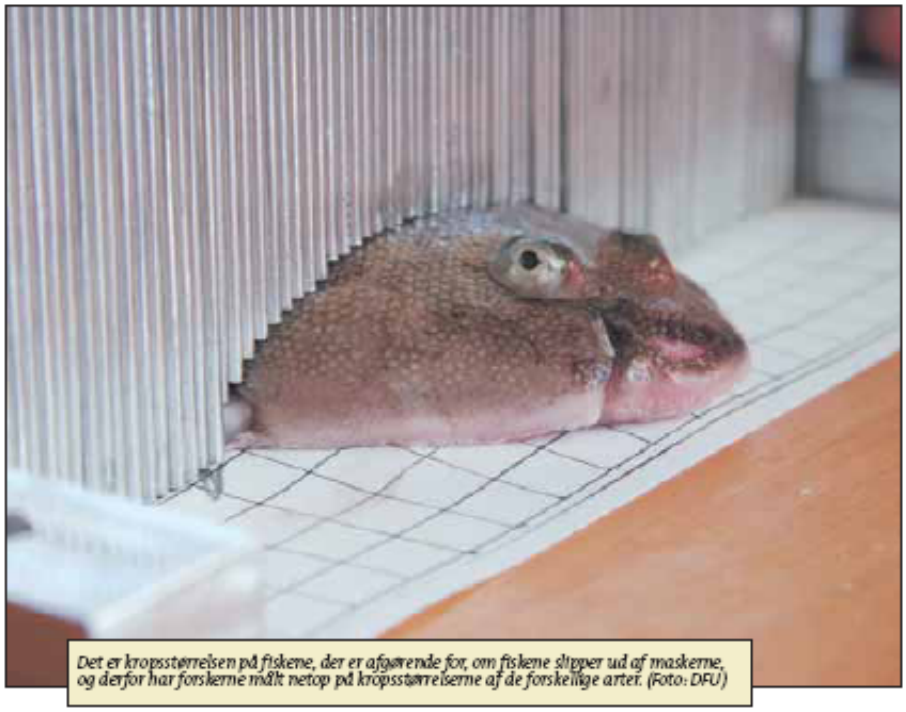

Det er kropsstørrelsen på fiskene, der er afgørende for, om fiskene slipper ud af maskerne, og derfor har forskerne målt netop på kropsstørrelserne af de forskellige arter. (Foto: DFU)

Avanceret computerteknologi skal mindste bifangst af undermålsfisk

Af Line Rode, Danmarks Fiskeriundersøgelser

En tværfaglig forskergruppe ved Danmarks Fiskeriundersøgelser – DFU - i Hirtshals har udviklet en helt ny metode, som gør det muligt hurtigt at vurdere, om fisk under mindstemålet kan slippe fri gennem maskerne i et trawl.

Foreløbige resultater af gruppens arbejde tyder på, at de maskestørrelser og mindstemål, som man bruger i fiskeriet i Skagerrak og Kattegat, ikke fungerer efter hensigten. Således kan gråtunger større end mindstemålet slippe fri gennem maskerne, mens rødspætte, pighvar og torsk under mindstemålet bliver fanget.

Kropsbygningen er afgørende

Grundtanken i projektet, som har titlen FishSelect, er, at man er nødt til at kende og kunne beskrive en fiskearts kropsbygning for at kunne vurdere, om en fisk vil blive fanget i maskerne i et trawl, forklarer projektleder og seniorforsker ved DFU, Bent Herrmann:

- Traditionelt taler man kun om længde, når man beskæftiger sig med fisks størrelse i fiskeriet. Det er mindstemålet, som bestemmer, om en fisk må landes eller skal smides ud igen. Men det, der faktisk afgør, om en fisk bliver fanget i et trawl, eller om den kan undslippe gennem maskerne, er ikke fiskens længde, men hvor meget den fylder i tværsnit. Er den lang og slank eller kort og tyk, og hvor meget kan tværsnittet komprimeres? Det har vi udviklet en metode til at bestemme og beskrive.

På fisketur fra computeren

Et af de konkrete resultater af projektet, som startede for to år siden, bliver en databank over forholdet mellem længde og tværsnit for alle de vigtige arter i dansk fiskeri. Med den i hånden vil man ved hjælp af et nyudviklet simuleringsprogram hurtigt kunne beregne sandsynligheden for, at en torsk på for eksempel 20 centimeter kan undslippe et trawl med en given maskestørrelse

- Det kan spare både tid og penge i fremtiden, når man udvikler og tester nye redskaber til fiskeriet. I stedet for at tage på havet for at teste udstyret ved forsøgsfiskeri, vil man kunne klare en del af arbejdet foran computeren. Samtidig vil simuleringsprogrammet generelt kunne bruges til at undersøge, om vi har den rette sammenhæng mellem de maskestørrelser, som vi bruger i fiskeriet i dag, og de mindstemål på fisk, som er fastsat, supplerer projektdeltager, biolog og tidligere fisker Ludvig Ahm Krag.

Udstyr helt fra bunden

Fordi det er helt nyt at forsøge at registrere og beskrive den del af fisks kropsbygning, der har betydning for maskepassage, eksisterede der ikke måleredskaber, som forskerholdet kunne gribe til. Derfor har holdet udviklet metode og udstyr helt fra bunden, oplyser biolog Karl-Johan Stæhr, som også indgår på projektholdet:

- Ved de første pilotforsøg skar vi alle fiskene over og målte deres tværsnit. Men det var for langsommelig og ustabil en metode. Vi måtte tænke kreativt – og fik god hjælp fra vores kolleger hos DFU's IT- og teknikafdeling til at udtænke og konstruere et brugbart instrument, siger Karl-Johan Stæhr.

Løsningen blev et instrument, som endnu ikke har fået et navn. Det består af en række målepinde, som forsigtigt presses ind, til de har kontakt til fisken, så pindene efterlader et aftryk af fiskens form. Aftrykket bliver efterfølgende scannet ind i en computer til videre billedbehandling.

- Ved hjælp af et specielt udviklet billedbehandlingsprogram med kant-detektions-software, kan vi ud fra aftrykket bestemme fiskenes tværsnitskontur og beskrive dem med nogle få dækkende parametriske værdier i forhold til fiskens længde. Torsks tværsnit kan f.eks. beskrives ved hjælp af en ellipse med en højde og bredde, mens fladfisk kan beskrives via en asymmetrisk trapez, forklarer Bent Herrmann.

Når fiskenes tværsnit er registreret, kan forskerne ved hjælp af et integreret simuleringsprogram forudsige, hvor store maskerne skal være, for at en fisk af den pågældende størrelse kan undslippe.

Videndeling med Europa

Foreløbig har forskerne målt og registreret længde og tværsnit på udvalgte punkter og mulig passage gennem masker af forskellige størrelse og form for fem fiskearter: torsk, rødspætte, rødtunge, gråtunge og pighvar. Målet er at opmåle samtlige af de fiskearter, som er vigtige for dansk fiskeri, så det er ikke sidste gang, at holdet er trukket i det blå arbejdstøj.

Projekt FishSelect er finansieret af det nationale udviklingsprogram for bæredygtigt fiskeri og selektive fangstmetoder. Forskerne bag FishSelect, der også inkluderer seniorforskerne Bo Lundgren og Niels Madsen, har søgt om midler fra EU's 7. rammeprogram i samarbejde med 11 europæiske partnere, til at fortsætte arbejdet, når den nuværende bevilling udløber senere på året.

Forskerne håber blandt andet at kunne dele deres resultater og metoder med kolleger i andre lande via en række workshops.

- Teknologien kan overføres og anvendes i alt fra det nordeuropæiske fiskeri helt ned til Middelhavet og Egyptens rejefiskeri, vurderer projektleder Bent Herrmann.

fakta

Udsmid

Udsmid – eller discard som det også kaldes med et låneudtryk fra engelsk – sker oftest, fordi fiskene enten er for små – under mindstemålet – eller fordi de er en art, som ikke må landes på grund af opbrugte eller lave kvoter.

Problemet er, at fisk, som først har været oppe på fiskefartøjets dæk, har ringe chancer for at overleve, selv om de bliver smidt ud igen umiddelbart efter fangsten. Udsmid af fisk – som ofte er ganske velegnet til konsum – er derfor dårlig udnyttelse af fiskebestandene. Det giver også et problem i forhold til kvoterne og rådgivningen om fiskekvoter, fordi udsmid er "usynligt" – det vil sige, det er svært at bestemme, hvor mange fisk, der reelt tages ud af bestanden.

21 papstykker og en hobbykniv

Opfindsomheden hos forskerne har været stor – blandt andet er der brugt 21 stykker pap til at måle fiskenes størrelse rent fysisk, inden resultaterne bliver brugt i computeren. (Foto: DFU)

Af Line Rooh, Danmarks Fiskeriundersøgelser

For at kunne kalibrere og validere et nyudviklet simuleringsprogram – der kan beregne sandsynligheden for at fisk kan slippe gennem netmaskerne - har forskerne opfundet endnu en effektiv, men simpel løsning. Den består af 21 store stykker vandfast special-pap, hvori der er skåret huller, som svarer til forskellige maskestørrelser og faconer.

Dem bruger holdet til rent fysisk at undersøge, hvilke størrelse masker fisk af forskellige arter og længde kan passere igennem.

Samtidig kan forskerne se, hvilke dele af fiskens krop som evt. går på kanten og forhindrer fisken i at komme ud gennem maskerne. Fx blev holdet hurtigt klar over, at det ikke nødvendigvis er tværsnittet med den største omkreds, der er afgørende for, om en fisk kan passere en maske.

I nogle masker er det højden af en fladfisks hoved, der er begrænsende, mens det i andre masketyper er det bredeste tværsnit på kroppen, fortæller biolog og projektdeltager Rikke Frandsen:

- Der er helt klart lidt Georg Gearløs over det, og vi blev da også drillet i al venskabelighed af kollegerne, da vi troppede op med 21 stykker pap. Men det virker!

For hver fiskeart har forskerne haft fat i 70 fisk af forskellige længde. For hver fisk har de testet, om den kan komme igennem 120 forskellige huller. Det bliver til over 8000 resultater pr. fiskeart. Undervejs har der været flere nyttige overraskelser, fortæller biolog Rikke Frandsen.

- Vi har for eksempel opdaget, at torsk kan komme igennem forholdsvis små masker i forhold til deres tværsnitsstørrelse. Hovedet er hårdt, men resten af kroppen er meget fleksibel og kan komprimeres ret meget. Omvendt er rødspætters kompression, hvis man lige ser bort fra finnerne, næsten lig nul. Måske fordi de har et stivere skelet og fordi de mangler svømmeblære.

Tværfaglighed skaber resultater

Af Line Rooh, Danmarks Fiskeriundersøgelser

Projektleder Bent Herrmann er oprindeligt uddannet civilingeniør og har en Ph.D.-grad i udvikling af simuleringsmodeller, som kan forudsige fisks mulighed for at undslippe fra forskellige trawl og fiskeredskaber.

Med på holdet har han en række biolog-kolleger med stor erfaring i, hvad der skal til, for at et fiskeredskab fungerer til havs - og med indgående kendskab til, hvordan arbejdet med forvaltningen af fiskebestandene foregår.

Netop det, at arbejdet er foregået på tværs af faggrænser, er en af de ting, som har været med til at skabe resultater i projektet:

- Udfordringerne i projektet er mange, og vi har haft brug for meget forskellige kompetencer – fra indsigt i fiskeredskaber til viden om, hvordan vi fangede og opbevarede de levende fisk, som vi skulle bruge – for ikke at nævne arbejdet med at udvikle metoder, måleinstrumenter og computermodeller.

Flere fisk skal undslippe fiskenet

Computersimuleringer skal finde frem til de bedste fiskenet

Af Mette Holt
meh@ing.dk

For hver fisk fanget er flere fisk typisk fanget og smidt tilbage i havet. Men det vil ny forskning fra Danmarks Fiskeriundersøgelser gøre op med. Computersimuleringer skal forudsige de mest effektive fiskenet, for bifangsten er ødelæggende for fiskebestanden.

»Fisk, der er hevet op med trawl, er typisk døde eller så beskadiget, at de har svært ved at overleve, når de kommer tilbage i havet. Derfor vil vi udvikle bedre net, så fiskene kan undslippe trawlet nede i vandet,« siger seniorforsker *Bent Herrmann*, som leder forskningsprojektet på Danmarks Fiskeriundersøgelser i Hirtshals.

Forskerne er ved at indsamle en lang række data om alt lige fra forskellige fiskearters størrelse ved forskellige aldre til fiskenes bøjelighed – data som skal være grundlaget for en model, der skal forudsige netmaskernes størrelse og facon, så de rette fisk tilbageholdes, mens de små fisk smutter gennem nettet.

Ca. halvdelen af den mængde fisk, der fanges i eksempelvis Kattegat, er uønsket bifangst, oplyser Bent Herrmann. Enten fordi fiskene er "undermålsfisk", dvs. fisk der ikke opfylder mindstemålet, eller de er af uønsket art. F. eks. oplever fiskerne i Kattegat og Skagerrak, at rødspætter, torsk og pighvar under mindstemålet fanges i de godkendte net, mens gråtunger over mindstemålet slipper igennem nettet. For mindstemålene for de forskellige arter, der fanges sammen, spiller ikke optimalt sammen.

Forskningen glæder fiskerne.

»Vi har hårdt brug for, at der bliver forsket i bedre måder til at selektere de uønskede fisk fra på havbunden, så de overlever,« siger formand for Danmarks Fiskeriforening, *Flemming Kristensen*.

Han understreger dog, at størrelse alene ikke er afgørende for, om fisken undslipper nettet.

»En torsk søger nedad mod bunden, når den bliver fanget. Så man skal også inddrage fiskens adfærd i forskningen,« siger han.

Netmasker af pap

En hel række faktorer spiller ind på, hvor stor bifangsten er. Herunder hvor mange forskellige arter, der forekommer i det pågældende hav – på en bestemt årstid. Men det primære er ifølge Bent Herrmann forholdet mellem netmaskernes geometri og størrelse og fiskenes tværsnitsfacon og bredde.

Med en række papskabeloner har forskerne simuleret netmasker og undersøgt hvilke fiskearter, der smutter gennem hvilke netfaconer, og hvor på kroppen fiskene eventuelt støder mod nettet. Her har forskerne så med et specialkonstrueret måleapparat bestemt fiskenes facon og størrelse i tværsnittet.

»I dag bruger fiskerne primært diamantformede netmasker, men det er ikke nødvendigvis det bedste,« siger Bent Herrmann.

Derfor har forskerne også undersøgt, hvordan fiskene passerer kvadratiske, rektangulære og heksagonale faconer. En anden relevant faktor, som forskerne også har undersøgt manuelt, er komprimering af fiskene. En levende fisk er ikke stiv, men kan deformeres på forskellig vis. Det gør jagten på det optimale net mere kompliceret.

F.eks. er en rødspætte, bortset fra finnerne, utrolig stiv, mens en torsk er blød i det og kan deformeres ret meget.

Alle data bliver lagt ind i et simuleringsprogram, som forskerne har udviklet. Udfra dette, kan forskerne forudsige det optimale design af fiskenettene.

Nye net og nye mindstemål

Når forskningsprojektet afsluttes ved årets udgang, vil forskerne komme med anbefalinger for de mest optimale netmasker i forskellige trawl.

Projektet er finansieret af et program for bæredygtigt fiskeri og fangstmetoder.

Bent Herrmann og de seks andre forskere har allieret sig med 11 andre forskningsgrupper i Europa. □

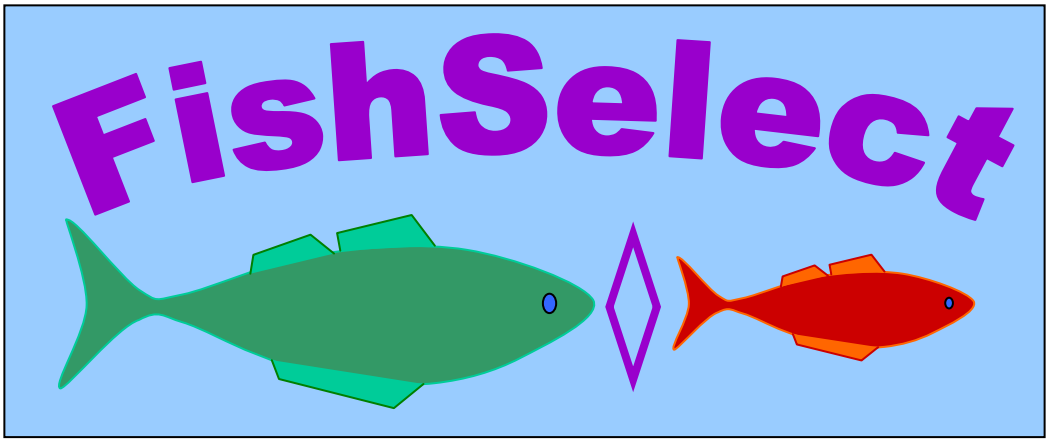

A14

Danish Institute for Fisheries Research

ICES 2006 BOSTON

Simulation of catch and discard for a fishing gear
Demonstrating the PRESEMO software

Bent Herrmann, Niels Madsen, Ludvig A. Krag, Rikke P. Frandsen, Bo Lundgren, Daniel Priour and Finbarr G. O'Neill

Introduction

An individual-based structural model of the fish catching process in the cod-end of a demersal trawl has been developed and implemented in a software package called PRESEMO (Herrmann 2005a). A typical simulation of a single haul can be carried out within a few minutes on a personal computer.

Fish input data
Morphological data:
Length, weight, cross section shape

Behaviour data:
swimming time since entry, time between escape attempts, exhaustion time

Data for the individual fish is assigned randomly on the basis of distributions defined on population level.

PRESEMO – Simulation of haul

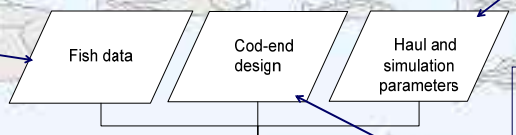

Haul and simulation parameters
Towing time, time for hauling to surface, escape model

Cod-end data
Cod-end design data:
mesh size, number of meshes, twine characteristics

Cod-end shape data:
Externally generated information on how the shape of the cod-end changes as result of the catch build up. Imports data produced by FEMNET (Priour, 2001) or by the method described in O'Neill 1999.

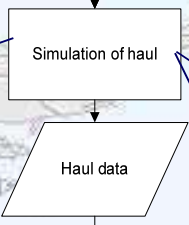

Simulation of a haul
A haul is simulated using a time step integration technique over the fishing process.
At each time step:
cod-end shape is updated based on current catch weight
For each fish the position is updated and checks for escape attempts and exhaustion are carried out
The weight of exhausted fish are added to the catch weight
An escape attempt is considered successful if the fish can pass through the mesh at its position, given the fish cross section and the mesh size and shape.

Simulation of haul
The process is continually visualized, that is, the entry time, the movement-pattern and the escape attempts of individual fish are shown as well as changes in the cod-end shape.

Processing of haul data
The numbers of caught and escaped fish are split into species and length classes and selection data calculated
The logistic function is automatically fitted to the simulated selection data to obtain estimates for L50 and SR
Catch and escape data to together with information on minimum landing size form the basis for prediction of catch efficiency and discard.

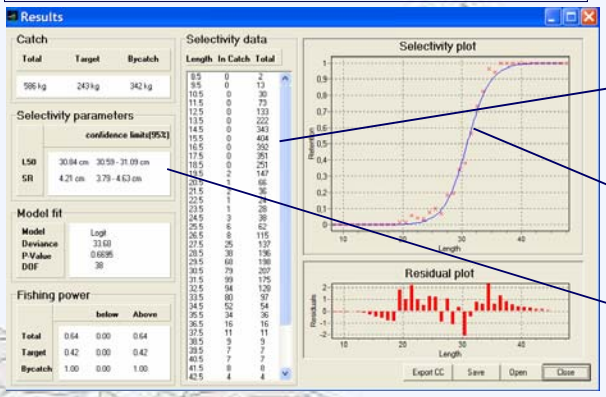

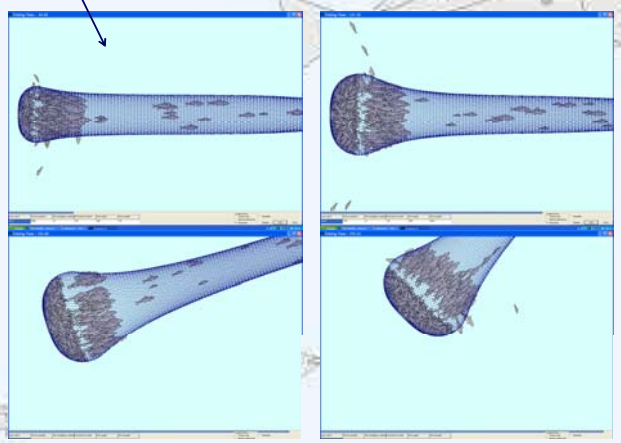

Stochastic simulation

A built-in facility enables repeated simulations for the same cod-end using randomly varying parameter values that affect the catch and escapement processes. This enables investigation of the performance of a cod-end under a range of different fishing conditions.

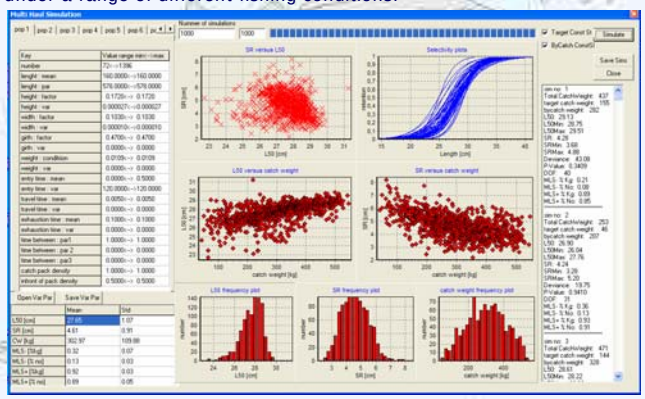

Using the stochastic simulation technique where parameters describing fish entry pattern and population sizes were varied randomly between hauls it was possible to generate between-haul variability of haddock selection similar to result from sea trials (Herrmann & O'Neill, 2005).

	O'Neill and Kynoch, 1996 experimental results	PRESEMO simulations of experimental results
$L50$ (cm)	28.69	28.63
sd_{L50} (cm)	0.98	1.07
SR (cm)	5.26	5.14
sd_{SR} (cm)	1.02	0.96

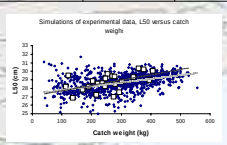

Comparison of different cod-end designs

A built-in facility to simulate and compare the performance of different cod-end designs under the same range of conditions, enables a quick and cheap examination of the consequences of implementing different gear designs in different fisheries. This was used to study the selection of haddock in different cod-end designs of different mesh size or different number of meshes along the circumference. Predictions were compared to predictions of empirical models of Galbraith et al. 1994 (in Herrmann, 2005b).

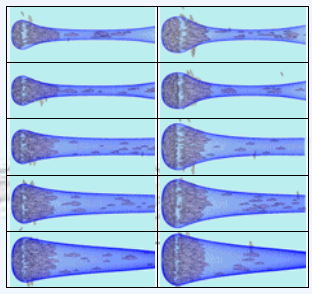

Shape of cod-ends. Catch weight from left: 150 and 500 kg, meshes around from top: 60, 80, 100, 120 and 160.

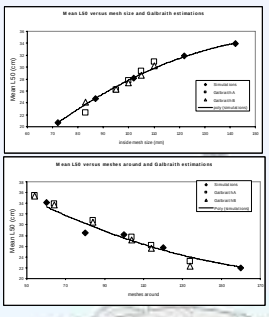

Cod-ends with round straps

Using FEMNET together with PRESEMO it is possible to investigate the influence of attachments like round straps on the cod-end selection process (Herrmann et al., 2006).

References

Galbraith, R.D., Fryer, R.J., Maitland, K.M.S., 1994. Demersal pair trawl cod-end selectivity models. Fish. Res. 20: 13-27
Herrmann, B., 2005a. Effect of catch size and shape on the selectivity of diamond mesh cod-ends: I Model development. Fish. Res. 71: 1-13
Herrmann, B., 2005b. Modelling and simulation of size selectivity in diamond mesh trawl cod-ends. PhD. Thesis. Aalborg University, Denmark. ISBN 87-91200-50-4
Herrmann, B. & O'Neill, F.G., 2005. Theoretical study of the between-haul variation of haddock selectivity in a diamond mesh cod-end. Fish. Res. 74: 243-252
Herrmann, B., Priour, D., Krag, L.A., 2006. Theoretical study of the effect of round straps on the selectivity in a diamond mesh cod-end. Fish. Res. 80: 148-157
O'Neill, F.G., 1999. Axissymmetrical trawl cod-ends made from netting of generalized mesh shape. IMA J. Appl. Math. 62: 245-262
O'Neill, F.G., Kynoch, R.J., 1996. The effect of cover mesh size and cod-end catch size on cod-end selectivity. Fish. Res. 28: 291-303
Priour, D., 2001. Introduction of mesh resistance to opening in a triangular element for calculation of nets by the finite element method. Com. Num. Meth. 17: 229-237

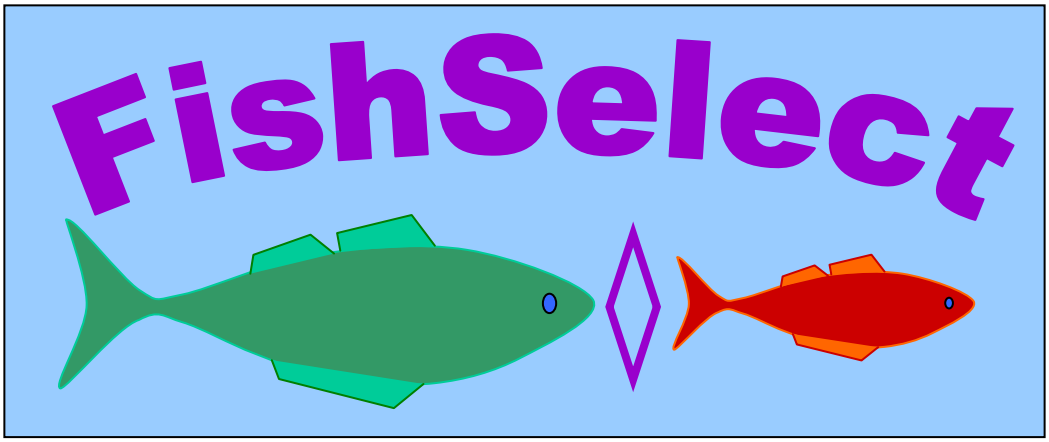

A15

PRESEMO—a predictive model of codend selectivity—a tool for fishery managers

F. G. O'Neill and B. Herrmann

O'Neill, F. G., and Herrmann, B. 2007. PRESEMO—a predictive model of codend selectivity—a tool for fishery managers. – ICES Journal of Marine Science, 64: 1558–1568.

The codend selectivity simulation model PRESEMO is a predictive model based on an understanding of the physical, biological, and behavioural mechanisms that underpin codend selection. In this paper, PRESEMO is used to predict the selectivity of a large range of codends of varying design. In particular, the selectivity of codends with mesh sizes in the range 80–160 mm, number of meshes around in the range 60–140, and netting twine thickness in the range 3–6 mm are predicted and, where possible, the predictions are validated with experimental data. Using the simulated data, the codend selectivity parameters are expressed in terms of the gear design parameters and in terms of both catch size and gear design parameters. The potential use of these results in a management context and for the development of more selective gears is highlighted by plotting iso-l_{50} and iso-sr curves used to identify gear design parameters that give equal estimates of the 50% retention length and the selection range, respectively. It is emphasized that this approach can be extended to consider the influence of other design parameters and, if sufficient relevant quantitative information exists, biological and behavioural parameters. As such, the model presented here will provide a better understanding of the selection process, permit a more targeted approach to codend selectivity experiments, and assist fishery managers to assess the impact of proposed technical measures that are introduced to reduce the catch of undersized fish and unwanted bycatch.

Keywords: catch weight, codend selectivity, mesh size, number of meshes around, PRESEMO, stochastic simulation, twine thickness.

Received 1 September 2006; accepted 15 April 2007; advance access publication 23 July 2007.

F. G. O'Neill: Fisheries Research Services, Marine Laboratory, 375 Victoria Road, Aberdeen AB9 11DB, UK. B. Herrmann: Danish Institute for Fisheries Research, North Sea Centre, DK-9850 Hirtshals, DK. Correspondence to F. G. O'Neill: tel: +44 1224 295343; fax: +44 1224 295511; e-mail: B.Oneill@marlab.ac.uk.

Introduction

Mesh size regulations for codends in trawls aim to reduce fishing mortality by allowing small fish to escape through the meshes. In recent years, the minimum mesh size of the codends fished in the North Sea has been increased many times. Restrictions also exist on the maximum number of meshes around and the maximum twine thickness. Many studies have investigated the influence of these parameters, and some have developed empirical models that relate these parameters to the selectivity of the codend (Reeves *et al.*, 1992; Galbraith *et al.*, 1994). These models are used by fishery managers to assess the effect on future stocks of proposed codend technical measure changes. We must be very careful, however, in applying these models to cases outside the range of data from which they have been parameterized. Indeed, these models should not be extrapolated. Nevertheless, it is still necessary to be able to respond quickly to perceived changes in the fish stocks and to be able to consider alternative gear designs without having to carry out new experimental trials for each proposed design.

In this paper, we use the codend selectivity model PRESEMO to predict the haddock selectivity of a large range of diamond mesh codends of varying design. In particular, the selectivity of codends with mesh sizes in the range 80–160 mm, number of meshes around in the range 60–140 meshes, and made from double braided polyethylene (PE) twines of thicknesses in the range 3–6 mm are predicted. Where possible, the predictions are validated with experimental data. Because PRESEMO is a predictive model, that is, based on an understanding of the physical, biological, and behavioural mechanisms that underpin codend selection, we are confident of its predictions outside the experimental data range.

We analyse the simulated selectivity data in two ways: first in terms of the mesh size, the number of meshes around, and the twine thickness, and then in terms of these design parameters and the catch size. We also plot iso-l_{50} and iso-sr curves, which identify the combination of design parameters that give equal estimates of the 50% retention length (l_{50}) and the selection range (sr), respectively.

Methods

As explained in Herrmann (2005), PRESEMO is an individual-based structural model of the selection process in the codend of a trawl fishing gear. It models different populations of fish entering the codend during a tow. Each fish is assigned a weight and a maximum width and height according to its length, and is assumed to be of elliptical cross section. Each is also allocated a travel time down the codend, a time it can swim in the codend without being exhausted, a time between escape attempts, and a

Table 1. Fish population data used in the PRESEMO simulations.

	Population 1	Population 2	Population 3	Population 4	Population 5	Population 6
Species	Haddock	Haddock	Haddock	Bycatch	Bycatch	Bycatch
Number of fish	10–3000	5–2000	5–400	0–600	0–400	0–200
Mean length (mm)	160.0	298.0	500.0	240.0	290.0	500.0
Length variance (mm^2)	578.0	737.0	5561.0	1600.0	1200.0	1600.0
Entry interval (% of entry period)	25–100	25–100	25–100	25–100	25–100	25–100
Entry period (minute)	240	240	240	240	240	240

Only data that differ from those used by Herrmann and O'Neill (2005) are listed. Populations 1–3 describe the target species (haddock), and Populations 4–6 describe the other species of fish entering the codend. The values for number of fish and entry interval indicate the range within which these variables varied randomly between hauls.

Table 2. Haddock selectivity results from covered codend experiments.

Data source	*m* (mm)	*n*	*t* (mm)	*w* (kg)	l_{50} (cm)	sr (cm)	Data source	*m* (mm)	*n*	*t* (mm)	*w* (kg)	l_{50} (cm)	sr (cm)
Lowry and Robertson (1996)	95.1	100	3.5	196	24.90	4.70	Dahm *et al.* (2002)	95	100	4	519	27.27	4.48
	95.1	100	3.5	213	25.20	3.50		95	100	4	840	27.38	7.74
	95.1	100	3.5	182	25.80	3.40		95	100	4	596	26.73	4.45
	95.1	100	3.5	130	24.80	4.10		95	100	4	339	26.67	3.57
	95.1	100	3.5	177	25.20	3.70		95	100	4	351	28.67	4.49
	95.1	100	3.5	149	25.20	4.90		95	100	4	370	27.67	3.73
	95.1	100	3.5	149	24.70	4.10		95	100	4	325	27.27	3.76
	100	100	5.2	211	23.9	3.1		95	100	4	836	27.76	3.45
	100	100	5.2	207	24.5	4.1		95	100	4	583	26.50	4.81
	100	100	5.2	212	24.4	4.0		95	100	4	773	25.20	3.80
	100	100	5.2	172	23.2	4.0	Kynoch *et al.* (2004)	111	100	5	411	29.07	3.85
	100	100	5.2	172	22.3	4.7		111	100	5	506	30.18	3.79
	100	100	5.2	192	23.9	6.0		111	100	5	573	28.10	4.89
O'Neill and Kynoch (1996)	100	100	3.5	359	30.32	5.91		111	100	5	545	30.99	4.04
	100	100	3.5	342	29.30	4.83		111	100	5	336	30.75	4.06
	100	100	3.5	191	28.16	4.35		111	100	5	708	31.40	4.61
	100	100	3.5	270	29.40	4.12		111	100	5	549	30.15	3.95
	100	100	3.5	245	28.25	4.09		111	100	5	486	29.87	4.11
	100	100	3.5	294	27.49	4.28		111	100	5	567	29.86	3.42
	100	100	3.5	275	26.99	4.77		111	100	5	433	31.07	4.11
	100	100	3.5	396	28.93	5.11		111	100	5	502	32.85	5.89
	100	100	3.5	377	30.22	4.72		111	100	5	544	30.86	5.46
	100	100	3.5	254	29.64	4.18		111	100	5	422	32.00	5.52
	100	100	3.5	171	27.80	4.75		111	100	5	639	29.60	5.00
	100	100	3.5	137	26.83	4.98		121	100	5	522	31.97	6.37
	100	100	3.5	217	27.23	4.87		121	100	5	720	32.26	5.09
	100	100	3.5	205	28.82	6.46		121	100	5	425	32.44	5.17
	100	100	3.5	113	28.19	7.82		121	100	5	519	33.48	5.44
	100	100	3.5	221	28.53	5.06		121	100	5	466	32.02	5.42
	100	100	3.5	280	28.44	6.02		121	100	5	483	32.70	5.51
	100	100	3.5	279	29.33	4.32		121	100	5	336	33.72	5.02
	100	100	3.5	122	29.46	7.37		121	100	5	365	34.20	4.54
	100	100	3.5	237	28.61	5.28		121	100	5	329	34.97	4.68
	100	100	3.5	407	30.00	5.56		121	100	5	314	35.36	4.68
	100	100	3.5	247	29.14	6.30		121	100	5	247	35.11	5.69
	100	100	3.5	302	28.79	5.91		121	100	5	525	32.78	4.90

Continued

Table 2. *Continued*

Data source	*m* (mm)	*n*	*t* (mm)	*w* (kg)	l_{50} (cm)	sr (cm)	Data source	*m* (mm)	*n*	*t* (mm)	*w* (kg)	l_{50} (cm)	sr (cm)
Kynoch *et al.* (1999)	96.7	100	3.66	507	29.62	4.06	Galbraith *et al.* (1994)	82.6	104	3.50	680	20.52	6.68
	96.7	100	3.66	559	32.38	3.81		85.5	64	3.50	950	28.70	8.14
	96.7	100	3.66	617	31.96	5.52		82.6	104	3.50	1360	22.43	8.90
	93.7	100	5.47	2763	24.21	6.21		85.5	64	3.50	100	29.87	3.48
	93.7	100	5.47	536	25.64	2.97		85.5	64	3.50	1560	30.37	3.67
	93.7	100	5.47	579	26.01	3.34		82.6	104	3.50	1390	16.57	5.58
	93.7	100	5.47	593	27.82	3.23		85.5	64	3.50	2240	27.78	6.26
	93.7	100	5.47	376	26.06	3.32		82.6	104	3.50	1770	17.41	6.78
	93.7	100	5.47	661	27.03	3.47		85	134	3.50	5100	18.57	3.49
Dahm *et al.* (2002)	94.6	100	4	323	27.68	6.32		96.3	114	3.00	2650	20.98	9.35
	94.6	100	4	662	31.77	5.60		85	134	3.50	1770	18.58	6.00
	94.6	100	4	94	26.47	4.61		96.3	114	3.00	650	29.50	5.02
	94.6	100	4	190	28.59	5.04		85	134	3.50	1600	16.43	6.12
	94.6	100	4	315	24.65	4.65		96.3	114	3.00	610	23.72	11.50
	94.6	100	4	167	24.45	5.55		98.6	84	3.00	580	31.82	6.05
	94.6	100	4	352	26.95	5.42		108.7	84	4.00	710	37.42	4.89
	94.6	100	4	196	27.43	4.47		98.6	84	3.00	650	29.97	6.19
	94.6	100	4	311	22.53	2.82		108.7	84	4.00	410	25.44	7.71
	94.6	100	4	172	28.00	5.13		108.8	104	4.00	1500	26.76	5.39
	94.6	100	4	265	24.48	3.41		108.8	104	4.00	1330	31.24	5.15
	94.6	100	4	254	25.83	3.81		110.6	64	4.00	1700	34.77	10.08
	94.6	100	4	171	28.39	7.46		98.5	54	3.50	1160	37.19	4.47
	94.6	100	4	186	27.56	3.32		110.6	64	4.00	270	39.64	7.18
	94.6	100	4	385	27.42	5.25		98.5	54	3.50	240	30.17	4.12
	94.6	100	4	758	31.25	4.54		108.8	104	4.00	370	28.36	4.51
	94.6	100	4	512	32.58	5.50		108.7	84	4.00	240	35.58	7.13
	94.6	100	4	771	28.37	5.02		108.8	104	4.00	710	28.14	8.90
	94.6	100	4	683	28.22	7.04		108.7	84	4.00	340	38.57	4.55
	95	100	4	822	23.52	6.15		108.8	104	4.00	200	25.78	6.72
	95	100	4	685	23.02	4.42		110.6	64	4.00	1330	31.71	6.05
	95	100	4	1233	30.78	5.90		110.6	64	4.00	710	39.54	9.19
	95	100	4	573	25.29	3.99		98.6	84	3.00	1970	30.65	6.84
	95	100	4	673	28.11	4.50		98.6	84	3.00	850	34.47	3.61
	95	100	4	574	27.95	4.79		98.5	54	3.50	820	29.59	5.27
	95	100	4	370	27.02	5.39		98.5	54	3.50	850	29.38	5.49
	95	100	4	1056	28.79	4.95		96.3	114	3.00	1260	28.32	4.39
	95	100	4	490	26.92	4.29		108.7	84	4.00	880	35.77	6.12
	95	100	4	321	27.20	5.73		85.0	134	3.50	2210	21.16	4.39
	95	100	4	319	28.65	4.94		85.0	134	3.50	2450	20.78	3.12
	95	100	4	408	27.95	3.89		82.6	104	3.50	1460	24.65	3.76

m, mesh size; *n*, number of meshes around; *t*, twine thickness; and *w*, catch weight in the codend.

packing density for swimming in front of the catch. An escape attempt is deemed successful if the fish can pass through the mesh opening at the point of the codend where the attempt takes place. The openness of a mesh is a function of the codend geometry and is calculated using the methods of O'Neill (1997, 1999). Fish that do not escape fall back and become part of the catch when their exhaustion time is reached. The codend shape is continually updated as the catch builds up during the tow. At the end of a simulation, a logistic function is automatically fitted to the simulated selection data to obtain estimates of l_{50} and sr.

PRESEMO requires information on codend geometry, fish behaviour, the escape process, the fish population structure, and the fish morphology. The following parameter settings/descriptions were used.

Codend geometry

The codends examined were made of 3-, 4-, 5-, and 6-mm double braided PE netting, had 60, 80, 100, 120, and 140 open meshes around, and had mean inside mesh sizes of 80, 100, 120, 140, and 160 mm. All combinations of these design parameters were

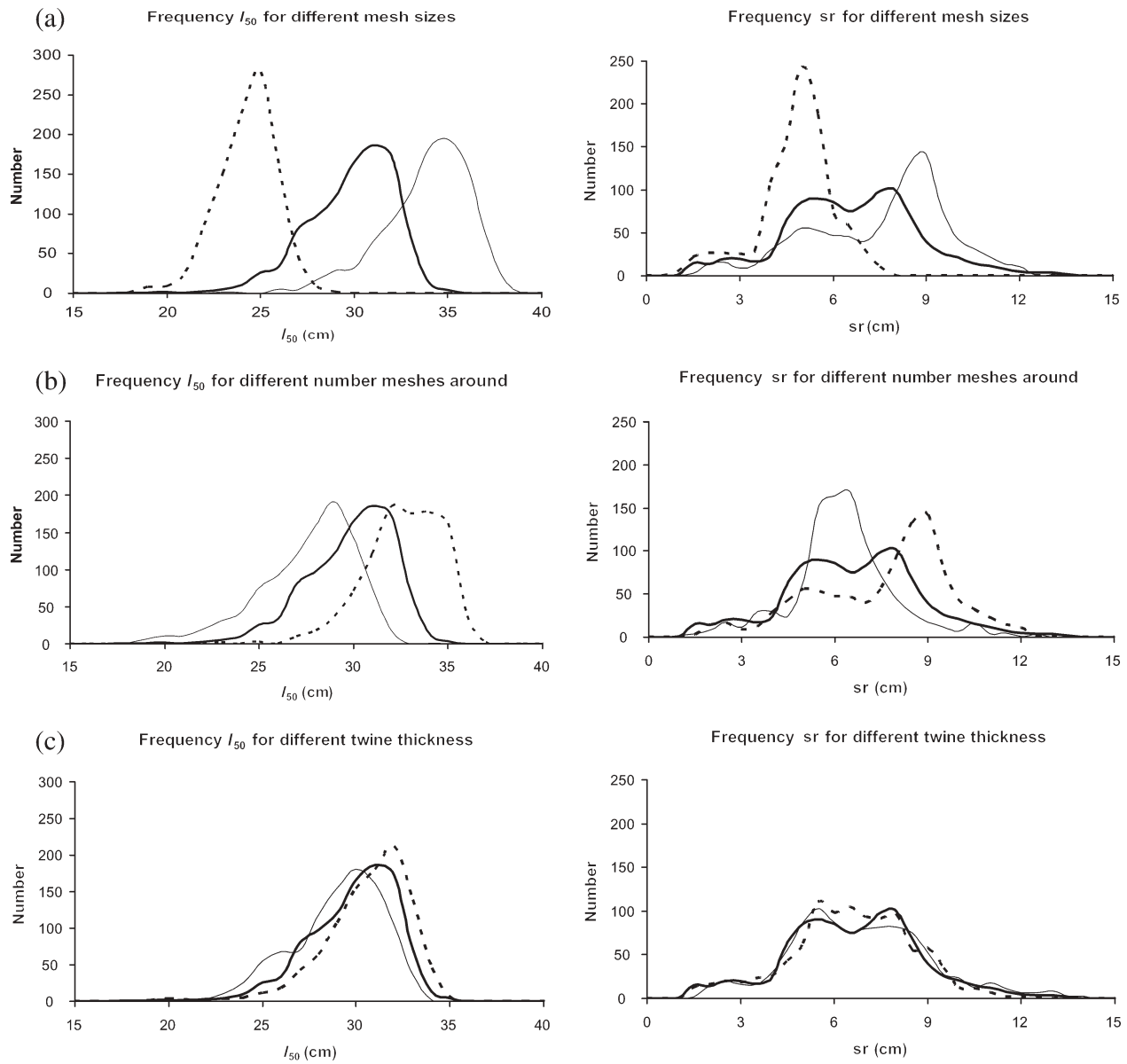

Figure 1. Plots of the frequency distribution of simulated selectivity parameters for 9 of the 100 codends examined. The thick line indicates the codend where $m = 100$, $n = 100$, and $t = 4$ in all plots. (a) The dashed line indicates the codend where $m = 80$, $n = 100$, and $t = 4$, and the thin line indicates that $m = 120$, $n = 100$, and $t = 4$. (b) The dashed line indicates that $m = 100$, $n = 80$, and $t = 4$, and the thin line indicates that $m = 100$, $n = 120$, and $t = 4$. (c) The dashed line indicates that $m = 100$, $n = 100$, and $t = 3$, and the thin line indicates that $m = 100$, $n = 100$, and $t = 5$.

investigated, giving 100 different codends that were used in the simulations. The following relationships were used to relate the knot centre to knot-centre mesh size, m_{kc}, and the twine bending stiffness, EI, with the twine thickness, t, and the inside mesh size, m_i,

$$m_{kc} = 2.8t + m_i(\text{mm})$$

$$\text{EI} = 12 \times 10^{-6} t^2 (\text{N m}^2)$$

where t, m_{kc}, and m_i are all measured in millimetres, and m_i is assumed to be normally distributed and have a standard deviation of 3% of its mean value (Herrmann and O'Neill, 2006). These relationships are from an unpublished analysis of 3-, 4-, 5-, and 6-mm double braided PE carried out by the first author using the analysis of O'Neill (2002). Estimates of the geometry of these codends, for a range of catch weights, were then calculated using the methods of O'Neill (1997, 1999), assuming a 3.0-knot towing speed. As no codend shape data were available for zero catch, the shape for zero catch was assumed to be the same as for a 20-kg catch.

Simulation of selection

Herrmann and O'Neill (2005) outlined a protocol for using PRESEMO that takes between-haul variability into account. In their study, only catch weights up to 500 kg were considered.

Table 3. The regression coefficients for Model 1 fitted to the simulated data for l_{50} and sr, where mesh size, m, and twine thickness, t, are expressed in millimetres.

Term	l_{50}			sr		
	Estimate	s.e.	$Pr(>\|t\|)$	Estimate	s.e.	$Pr(>\|t\|)$
(Intercept)	−6.83E + 01	1.64E + 00	<2e-16	−4.87E + 01	1.22E + 00	<2e-16
m	1.91E + 00	3.05E-02	<2e-16	1.04E + 00	2.66E-02	<2e-16
n	5.91E-01	2.41E-02	<2e-16	2.66E-01	9.00E-03	<2e-16
t	−4.71E + 00	2.13E-01	<2e-16	2.36E + 00	1.60E-01	<2e-16
m^2	−9.62E-03	2.26E-04	<2e-16	−6.34E-03	1.99E-04	<2e-16
n^2	−2.09E-03	1.94E-04	<2e-16	−4.32E-03	1.17E-04	<2e-16
mn	−8.96E-03	1.41E-04	<2e-16	[a]	–	–
mt	3.52E-02	3.25E-03	<2e-16	7.43E-03	2.75E-03	0.00697
nt	3.83E-02	3.16E-03	<2e-16	−3.71E-02	2.58E-03	<2e-16
m^3	1.79E-05	5.99E-07	<2e-16	1.44E-05	5.29E-07	<2e-16
n^3	1.35E-06	5.99E-07	0.024541	−4.51E-06	1.97E-07	<2e-16
mnt	−1.65E-04	9.09E-06	<2e-16	[a]	–	–
m^2n	1.81E-05	4.29E-07	<2e-16	1.06E-05	3.79E-07	<2e-16
m^2 t	−4.07E-05	1.09E-05	0.000176	−1.33E-04	9.59E-06	<2e-16
n^2 m	1.94E-05	4.29E-07	<2e-16	1.04E-05	3.65E-07	<2e-16
n^2 t	−1.10E-04	1.09E-05	<2e-16	1.82E-04	9.28E-06	<2e-16
t^2 m	−8.81E-04	1.88E-04	2.85E-06	2.30E-03	1.66E-04	<2e-16
t^2n	4.61E-04	2.23E-04	0.038829	−1.81E-03	1.97E-04	<2e-16

For l_{50}: $r^2 = 0.8584$, d.f. = 99982. For sr: $r^2 = 0.3234$, d.f. = 99984. [a]Indicates that non-significant terms have been eliminated.

Here, we want to consider catch sizes up to 1200 kg and, therefore, have had to change some of the input parameter values. In particular, the number of fish in the target and bycatch populations entering the codends during a simulated tow was increased. The towing time also was increased to prevent the density of fish in the codend from becoming too large, and the population size structure was changed to ensure that codends with large mesh sizes retained a sufficient number of both target and bycatch fish. Table 1 summarizes the fish data used in the simulations. Herrmann and O'Neill (2005) also described a model of fish escape during the early part of a tow, when the tension in the mesh bars is low. In a subsequent paper (Herrmann and O'Neill, 2006), they relate their fish escape model to twine thickness, and it is this model that is applied here.

Between-haul variability is modelled by varying the size, spatial distribution, and structure of the target and bycatch population between each simulation (Herrmann and O'Neill, 2005). For each codend design, 1000 such simulations are made, from which 1000 estimates of l_{50}, sr, and total catch weight are calculated. As there are 100 codend designs, 100 000 hauls are simulated.

Experimental data

For the comparison of simulated results with similar experimental ones, we have chosen published haddock selectivity data from Galbraith *et al.* (1994), Lowry and Robertson (1996), O'Neill and Kynoch (1996), Kynoch *et al.* (1999, 2004), and Dahm *et al.* (2002). These data are summarized in Table 2, and represent results from a number of different cruises and a number of different codend designs. To facilitate sufficient comparisons, the experimental data are from codends whose mesh size, number of meshes around, and twine thickness differ from the simulated codends by as much as ±5 mm, ±5 meshes, and ±1 mm, respectively. These studies provided selectivity estimates for 152 individual, covered codend hauls.

Analysis of simulated data

In order to use and interpret the simulated data in a relatively straightforward way, two types of cubic polynomials were fitted to the estimates of l_{50} and sr. The first of these (Model 1) used mesh size, m, number of open meshes around, n, and twine thickness, t. The total catch weight at the end of the haul, w, is treated as a random effect, and l_{50} and sr are expressed as follows:

$$l_{50} = \sum_{\substack{0\le i,j,k\le 3\\ i+j+k\le 3}} \lambda_{ijkl} m^i n^j t^k \quad \text{sr} = \sum_{\substack{0\le i,j,k\le 3\\ i+j+k\le 3}} \mu_{ijkl} m^i n^j t^k. \qquad (1)$$

In the second (Model 2), w is considered to be a fixed effect, and l_{50} and sr are expressed as:

$$l_{50} = \sum_{\substack{0\le i,j,k,l\le 3\\ i+j+k+l\le 3}} \lambda_{ijkl} m^i n^j t^k w^l \quad \text{sr} = \sum_{\substack{0\le i,j,k,l\le 3\\ i+j+k+l\le 3}} \mu_{ijkl} m^i n^j t^k w^l. \qquad (2)$$

Results

Simulated data

Figure 1 plots the distributions of l_{50} and sr for a selection of the simulated data. In Figure 1a, the number of meshes around is 100 open meshes, twine thickness is 4 mm, and the mesh size is 80, 100, and 120 mm, respectively. While it is clear that the mean l_{50} and sr increase with mesh size, there is considerable overlap (especially for sr) of the frequency distributions. In Figure 1b, the mesh size is 100 mm, the twine thickness is 4 mm, and the

Table 4. The regression coefficients for Model 2 fitted to the simulated data for l_{50} and sr, where mesh size, m, and twine thickness, t, are expressed in millimetres and catch weight, w, in tonnes.

Term	l_{50}			sr		
	Estimate	s.e.	$Pr(>\|t\|)$	Estimate	s.e.	$Pr(>\|t\|)$
(Intercept)	−4.1700E + 01	1.5600E + 00	<2e-16	−2.40E + 01	1.64E + 00	<2e-16
m	1.4100E + 00	2.2400E-02	<2e-16	5.93E-01	2.63E-02	<2e-16
n	4.2200E-01	1.6900E-02	<2e-16	2.87E-01	1.58E-02	<2e-16
t	−9.9600E-01	5.7800E-01	8.49E-02	−7.42E-01	4.16E-01	0.074545
w	−4.2700E + 01	1.3400E + 00	<2e-16	−2.38E + 01	1.58E + 00	<2e-16
m^2	−6.6300E-03	1.5800E-04	<2e-16	−3.60E-03	1.86E-04	<2e-16
n^2	−1.8100E-03	1.2800E-04	<2e-16	−1.38E-03	6.82E-05	<2e-16
t^2	−3.5200E-01	1.1200E-01	1.65E-03	1.35E-01	4.12E-02	0.001015
w^2	3.7800E + 00	8.3400E-01	6.00E-06	−7.98E + 00	9.80E-01	3.66E-16
mn	−7.9000E-03	1.0400E-04	<2e-16	−3.79E-03	1.22E-04	<2e-16
mt	1.0500E-02	2.7400E-03	1.30E-04	9.85E-03	3.22E-03	0.002212
mw	5.5200E-01	1.2800E-02	<2e-16	3.37E-01	1.50E-02	<2e-16
nt	2.8100E-02	2.4200E-03	<2e-16	−1.07E-02	2.84E-03	0.000161
nw	2.7800E-01	9.6100E-03	<2e-16	1.29E-01	1.12E-02	<2e-16
tw	−7.3400E-01	2.6200E-01	5.13E-03	1.98E + 00	3.08E-01	1.36E-10
m^3	1.1500E-05	4.1000E-07	<2e-16	8.03E-06	4.81E-07	<2e-16
n^3	3.6300E-06	3.9900E-07	<2e-16	[a]	–	–
t^3	2.7400E-02	7.9600E-03	5.69E-04	[a]	–	–
w^3	4.0700E + 00	2.3900E-01	<2e-16	−1.55E + 00	2.81E-01	3.43E-08
mnt	−1.9600E-04	6.8700E-06	<2e-16	−1.29E-04	8.06E-06	<2e-16
mnw	1.4500E-04	4.3300E-05	7.96E-04	−1.41E-03	5.08E-05	<2e-16
mtw	1.6900E-02	9.6500E-04	<2e-16	1.82E-02	1.13E-03	<2e-16
ntw	4.9600E-03	7.7400E-04	1.47E-10	−1.90E-02	9.09E-04	<2e-16
m^2n	1.7600E-05	3.1700E-07	<2e-16	1.07E-05	3.72E-07	<2e-16
m^2t	4.0600E-05	7.5900E-06	8.68E-08	−6.44E-05	8.91E-06	4.84E-13
m^2w	−1.5600E-03	4.3500E-05	<2e-16	−1.29E-03	5.11E-05	<2e-16
n^2m	1.4800E-05	3.2000E-07	<2e-16	1.29E-05	3.75E-07	<2e-16
n^2t	−9.3900E-05	7.3000E-06	< 2e-16	1.93E-04	8.57E-06	<2e-16
n^2w	−1.1000E-03	3.6100E-05	< 2e-16	−3.12E-04	4.18E-05	8.80E-14
t^2m	−1.1700E-03	2.0500E-04	1.39E-08	9.79E-04	2.41E-04	4.85E-05
t^2n	1.0500E-03	1.9500E-04	7.44E-08	−2.38E-03	2.28E-04	<2e-16
t^2w	−1.0800E-01	2.3600E-02	5.01E-06	8.59E-02	2.76E-02	0.001872
w^2m	−1.6100E-01	4.6000E-03	< 2e-16	6.92E-02	5.40E-03	<2e-16
w^2n	−8.9600E-03	2.9500E-03	2.35E-03	8.98E-02	3.46E-03	<2e-16
w^2t	−2.9200E-01	7.2600E-02	5.89E-05	−1.13E + 00	8.52E-02	<2e-16

For l_{50}: $r^2 = 0.939$, d.f. = 99965. For sr: $r^2 = 0.4857$, d.f. = 99967. [a]Indicates that non-significant terms have been eliminated.

number of meshes around is 80, 100, and 120. Here we see, as expected, a decrease in l_{50} with increasing number of meshes around and a greater degree of overlap. In Figure 1c, the number of meshes around is 100 open meshes, the mesh size is 100 mm, and the twine thickness is 3, 4, and 5 mm. Although there is a considerable degree of overlap between the distributions, we can still identify that l_{50} decreases with increasing twine thickness, whereas there is no real difference in the sr distributions.

These plots not only highlight the extent of between-haul variability and the relative influence of the gear design parameters on codend selection, but also emphasize the difficulties that may be encountered in designing experiments to test a given hypothesis.

Analysis of simulated data and comparison with experimental data

The coefficient estimates of Models 1 and 2 are shown in Tables 3 and 4, respectively. The validation of these models is a two-stage procedure. First, we must demonstrate that the cubic expressions are a good fit to the simulated data and second, that their predictions are a good fit to the experimental data. Table 5 shows some comparisons of the predictions of Model 1 with the average simulated values for all the codends made from 4-mm double PE. These show that the cubic model is a good fit to the catch-averaged simulated data and that the low r^2 value for sr (Table 3) is caused by the large variation of this parameter. A similar analysis for Model 2 identifies a small but systematic lack of fit for the extreme values

Table 5. The catch-averaged simulated selectivity parameters and the estimates using Model 1 for all 4-mm double braided polyethylene codends. m is mesh size and n is number of meshes around. l_{50} and sr are the catch-averaged simulated parameter estimates, w is average catch weight of simulated hauls, and values in italics are the corresponding standard deviations. pl_{50} and $p$sr are the selectivity estimates predicted using Model 1, and $\Delta l_{50} = l_{50} - pl_{50}$, and Δsr = sr $-$ $p$sr.

Codend design		l_{50} (cm)		sr (cm)		w (kg)		pl_{50} (cm)	Δl_{50} (cm)	$p$sr (cm)	Δsr (cm)
m	***n***										
80	60	25.49	*1.05*	6	*0.92*	701	*306*	25.25	0.24	5.88	0.12
80	80	24.91	*1.23*	4.98	*1.1*	716	*308*	24.86	0.05	5.14	−0.16
80	100	23.77	*1.56*	4.58	*1.2*	711	*299*	23.96	−0.19	4.79	−0.21
80	120	22.26	*1.77*	4.4	*1.07*	713	*314*	22.59	−0.33	4.6	−0.2
80	140	21.13	*1.83*	4.45	*1.08*	731	*322*	20.83	0.3	4.37	0.08
100	60	33.8	*1.73*	8.42	*1.96*	508	*217*	33.32	0.48	8.13	0.29
100	80	32.14	*2.03*	7.31	*2.22*	535	*210*	31.48	0.66	7.02	0.29
100	100	29.33	*2.35*	6.39	*2.16*	587	*233*	29.43	−0.1	6.45	−0.06
100	120	27.06	*2.62*	6.02	*1.7*	656	*238*	27.24	−0.18	6.22	−0.2
100	140	24.36	*2.6*	5.5	*1.43*	694	*267*	24.96	−0.6	6.11	−0.61
120	60	38.33	*1.92*	8.46	*2.32*	440	*174*	38.74	−0.41	8.84	−0.38
120	80	35.7	*2.48*	7.29	*2.38*	452	*179*	35.74	−0.04	7.52	−0.23
120	100	33.34	*2.36*	7.06	*2.1*	504	*179*	32.83	0.51	6.92	0.14
120	120	30.34	*2.72*	7.23	*2.06*	560	*204*	30.09	0.25	6.82	0.41
120	140	27.46	*2.99*	7.09	*1.8*	630	*232*	27.58	−0.12	6.99	0.1
140	60	41.9	*2.41*	8.38	*2.78*	387	*151*	42.36	−0.46	8.71	−0.33
140	80	37.95	*2.51*	6.94	*2.11*	426	*160*	38.48	−0.53	7.35	−0.41
140	100	34.99	*2.64*	7.03	*1.84*	463	*165*	35.01	−0.02	6.88	0.15
140	120	32.48	*2.88*	7.59	*2.09*	517	*183*	32.02	0.46	7.07	0.52
140	140	29.98	*3.1*	8.1	*2.21*	558	*196*	29.57	0.41	7.71	0.39
160	60	45.58	*2.94*	8.51	*3.26*	337	*111*	45.03	0.55	8.41	0.1
160	80	40.46	*2.96*	7.01	*2.16*	400	*143*	40.57	−0.11	7.19	−0.18
160	100	36.36	*2.82*	6.91	*1.78*	440	*158*	36.83	−0.47	7.01	−0.1
160	120	33.76	*3.05*	7.67	*2.03*	477	*179*	33.87	−0.11	7.67	0
160	140	31.63	*3.2*	8.87	*2.49*	540	*189*	31.77	−0.14	8.95	−0.08

l_{50} and sr are the catch-averaged simulated parameter estimates, w is average catch weight of simulated hauls, and values in italics are the corresponding s.d. pl_{50} and $p$sr are the selectivity estimates predicted using Model 1, and $\Delta l_{50} = l_{50} - pl_{50}$, and Δsr = sr $-$ $p$sr.

of the design parameters, indicating that the cubic model may not model the simulated data accurately enough when catch is a fixed effect.

Some comparisons of predictions of these models with the experimental data of Table 2 are presented in Figure 2. The dashed lines are 95% confidence limits (i.e. $\pm$ 2 s.d.) of the simulated average parameter estimates for each codend, examples of which are found in Table 5. The data points are the relevant individual experimental haul estimates of Table 2, and the unbroken lines are the relevant empirical model predictions of the studies of Galbraith *et al.* (1994), Lowry and Robertson (1996), and Kynoch *et al.* (1999). Triangles are the predictions using Model 1, where catch weight is assumed to be a random effect, and the small square symbols are the predictions using Model 2, where catch is a fixed effect and given a value of 442 kg (the average catch weight of the experimental hauls, excluding catches >1300 kg).

In general, the predictions of Models 1 and 2 provide a reasonable estimate of the experimental data and the empirical models in the literature. In particular, the l_{50} predictions are a very good reflection of the experimental results. Most experimental data points are within the 95% range of the simulated data, indicating that the simulations can explain a large portion of the variation found in the experimental data, although the plots of sr suggest that the model predictions may overestimate the between-haul variability.

A few experimental results are outside the predicted confidence bands. In Figure 2a, two l_{50} values are very small. Examining the experimental data in greater detail reveals that the catch weights in these hauls were 1390 and 1770 kg, while the cover contained only 100 and 140 kg. We are unable to explain or reproduce the large sr value of Figure 2d.

In Figures 3 and 4, we use Models 1 and 2 to generate iso-l_{50} and iso-sr curves. These are curves of constant l_{50} and sr and can be used to identify the set of parameter pairs to achieve a given selective performance. Figure 3 plots the iso-l_{50} and iso-sr curves in terms of the mesh size and the number of meshes around for codends made from 4-mm (Figure 3a) and 6-mm (Figure 3b) double-braided PE. This figure is very informative and, by looking along any horizontal or vertical line, we can see how the selectivity parameters will vary with either mesh size or number of meshes around. By comparing Figures 3a and 3b, we can further see the effect of increasing twine diameter. These

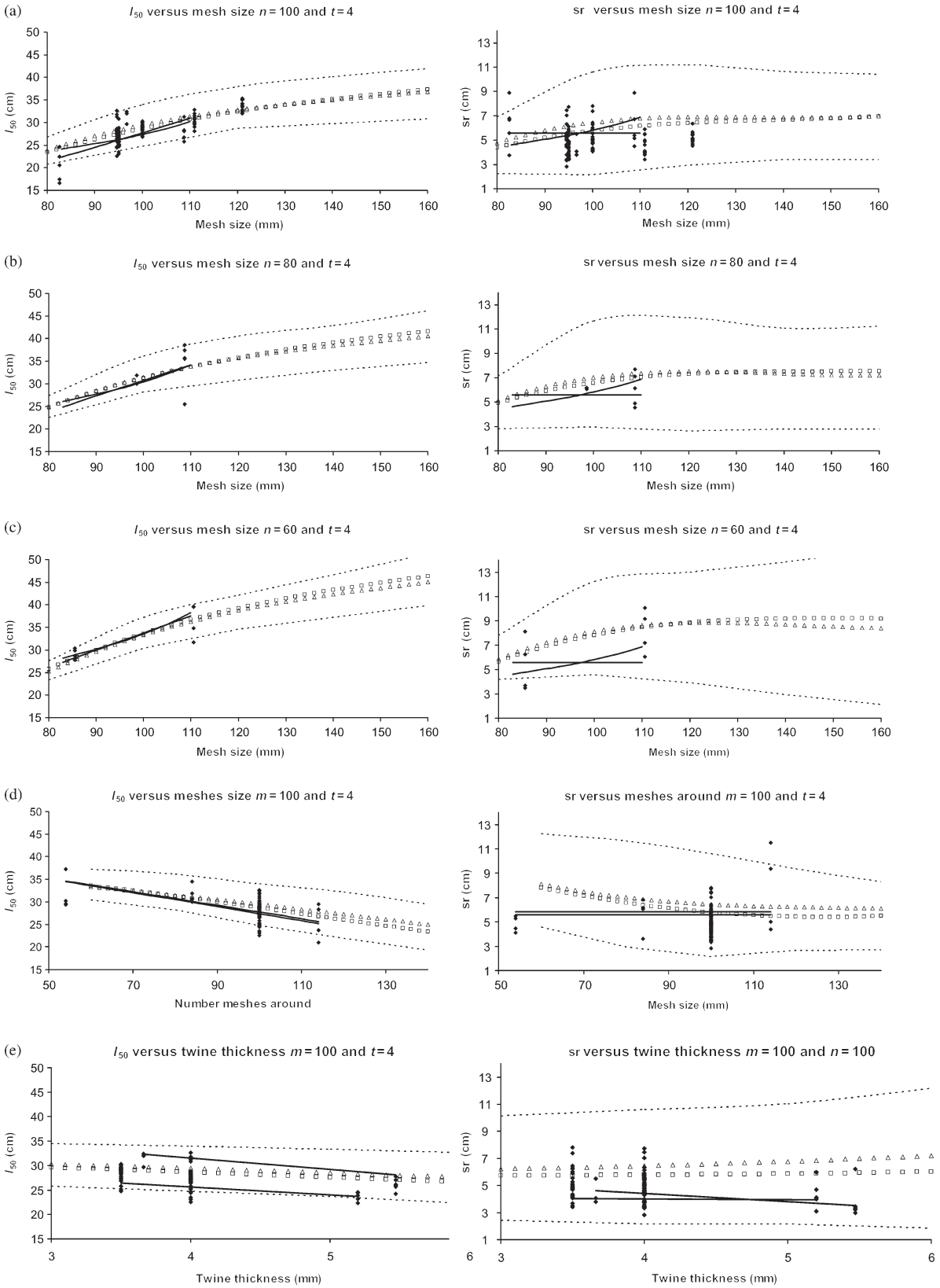

Figure 2. Comparisons of predictions of Models 1 and 2 with experimental data of Table 2. The dashed lines are 95% confidence limits (± 2 s.d.) of simulated average parameter estimates for each codend. The data points correspond to individual experimental haul estimates. The unbroken lines are the relevant empirical model predictions of the studies of Galbraith *et al.* (1994), Lowry and Robertson (1996), and Kynoch *et al.* (1999). Triangles are the predictions using Model 1, where catch weight is assumed to be a random effect, and the small square symbols are the predictions using Model 2, where catch is a fixed effect and given a value of 442 kg (the average catch weight of the experimental hauls, excluding catches >1300 kg).

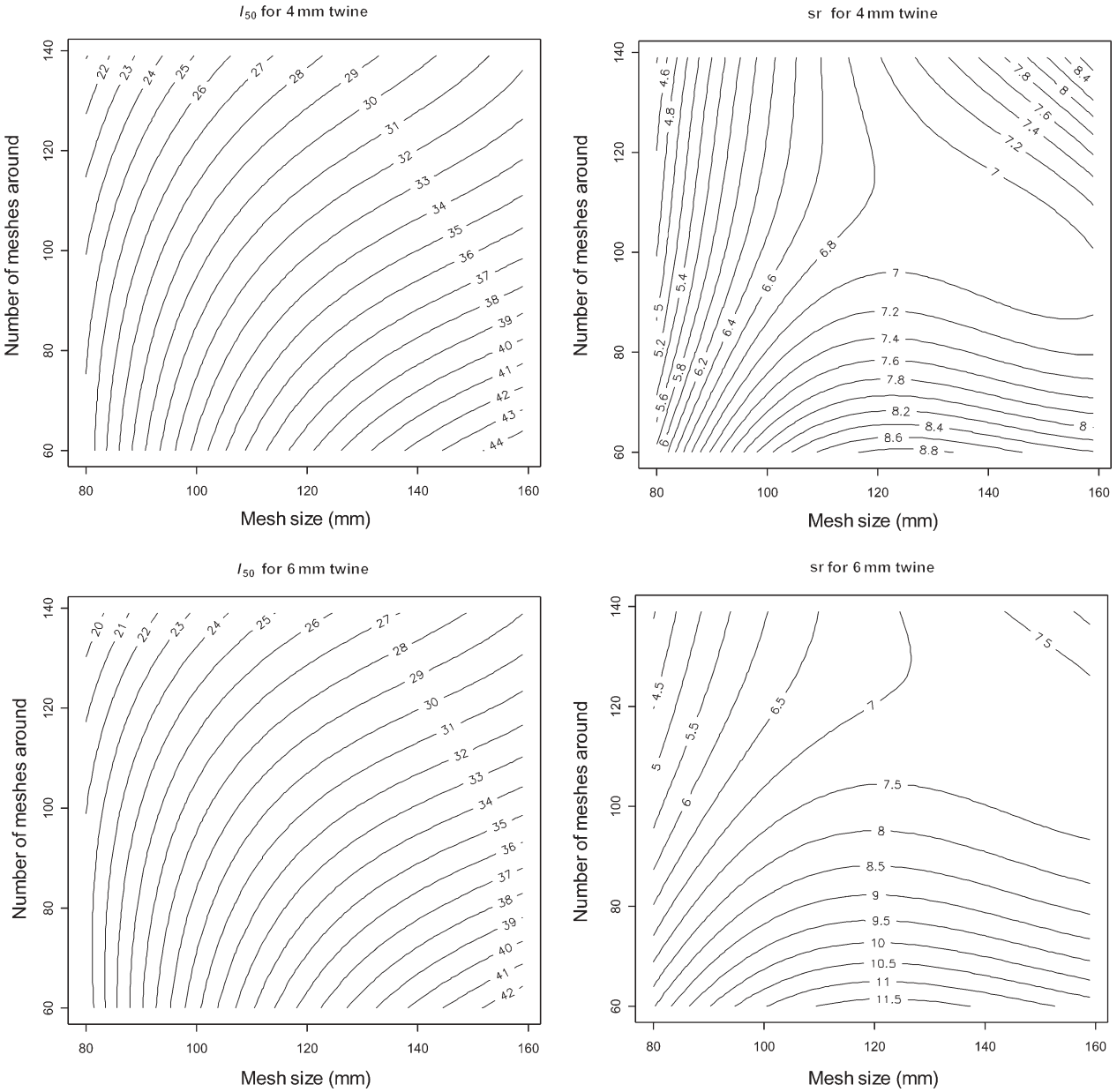

Figure 3. Plots of the iso-l_{50} and iso-sr curves using Model 1 in terms of mesh size and number of meshes around for codends made from (a) 4-mm and (b) 6-mm double braided polyethylene (PE).

plots are based on Model 1, which assumes that catch is a random effect.

The contours drawn in Figure 4 are based on Model 2, which considers catch to be a fixed effect. This model permits an explicit examination of the effect of catch size, and we can see from the figure how the dependence of the selectivity parameters on mesh size and number of meshes around varies as the catch size increases from 400 to 800 kg.

Discussion

The aim of this paper is to provide a means of predicting codend selectivity outside the range of available experimental data. To do this, we employed the codend selectivity model PRESEMO to simulate the haddock selectivity of a large range of diamond-mesh codends. We then fitted a cubic model to this simulated dataset and expressed the selectivity parameters in terms of the gear design parameters and, in the case of Model 2, the catch size. We validated these models, as much as we could, with available experimental data. Because PRESEMO is a structural model, based on an understanding of the underlying physical, biological, and behavioural mechanisms that govern codend selection, we believe that its predictions outside the range of available experimental data are reasonably accurate. At the very least, we are more confident of these predictions than we would be of extrapolating the empirical models that have been developed by other authors. The obvious question then is, how far beyond the experimental data range can we accept the predictions of PRESEMO? Although there is no easy answer, we would be reasonably confident of the results presented here, at least up to mesh sizes of 140 mm and 140 meshes around. The issue of twine thickness is

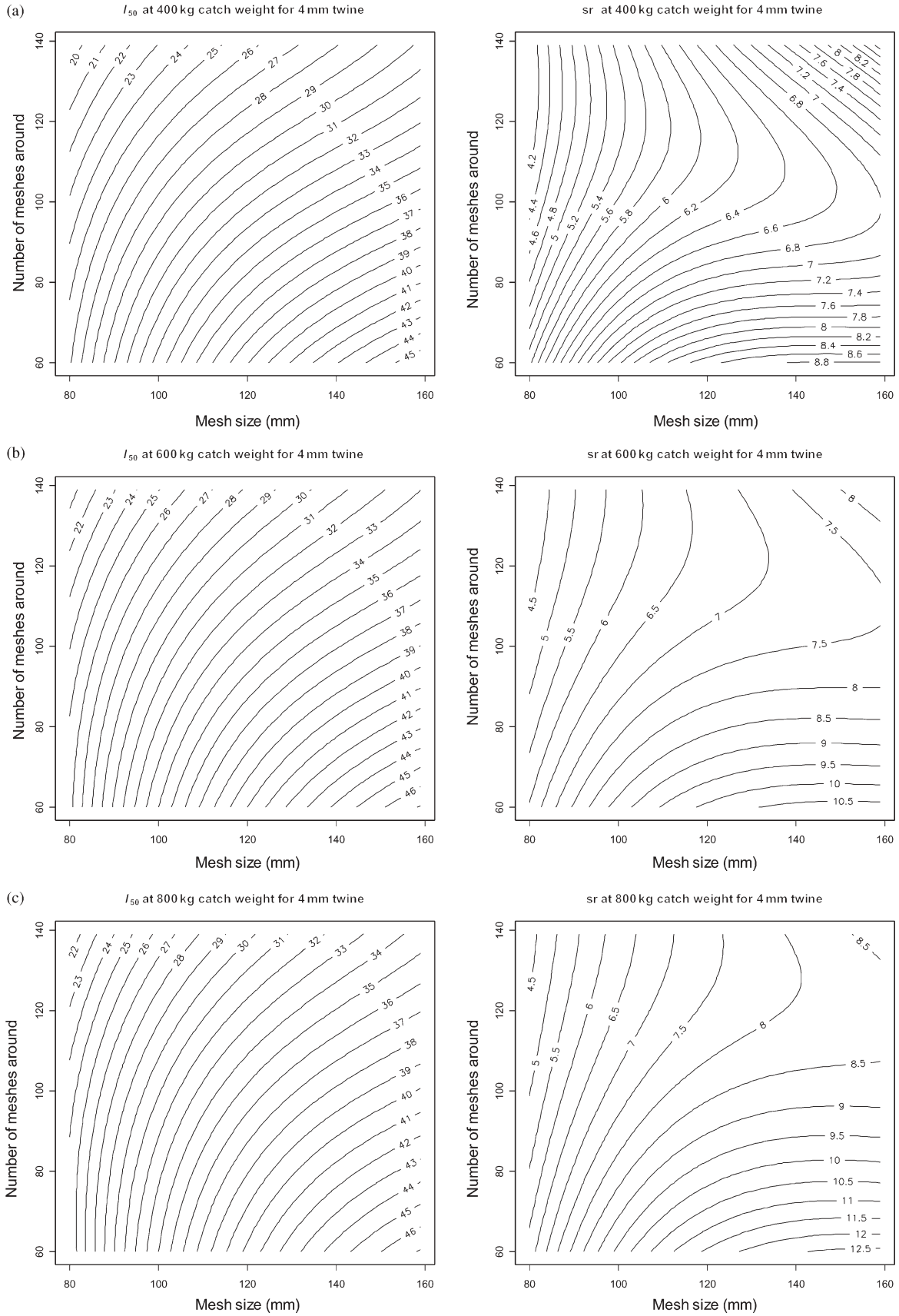

Figure 4. Plots of the iso-l_{50} and iso-sr curves using Model 2 in terms of mesh size and number of meshes around for codends made from 4-mm double braided PE and at catch weights of (a) 400, (b) 600, and (c) 800 kg.

more difficult because twine bending stiffness also depends on the material type, twine construction, and any subsequent treatments. Furthermore, our model of twine deformation assumes a linear relationship between bending moment and twine curvature, which may not hold for composite twines, where there will be friction between the component fibres, each of which is likely to bend non-linearly [see O'Neill (2002) for a full discussion].

As a general rule, however, if this approach is to be applied to a given fishery, it will be necessary to ensure that the PRESEMO input parameters pertain to the fishery in question and that there is as much validation with experimental data as possible. Therefore, it should be possible for fishery managers to make reliable assessments of the effect of proposed codend technical measure changes, to respond quickly to changes in the fish stocks, and to be able to consider alternative gear designs without having to carry out new experimental trials for each proposed design.

Model 1 may be considered more useful. Not only is it simpler and an accurate description of the simulated data, it also implicitly takes into account changes in catch size that may arise as a result of changes of codend selectivity. Thus, it may provide more accurate assessments of the effect on future stocks of technical measure changes.

Model 2 is also useful and could be used, for example, to distinguish between fisheries where catch sizes differ. However, there is some evidence that the predictions of Model 2 exhibit a small but systematic lack of fit to the simulated data at extreme values of the design parameters. This indicates that the form of the expressions of Equation (2) may not be sufficiently flexible, which probably can be remedied by using a higher order expansion or an appropriate surface fitting routine (e.g. cubic splines).

One concern regarding the simulated haul data is that the variance of sr is overestimated. It may be possible to address this by altering some of the PRESEMO input parameters (Herrmann and O'Neill, 2005). The contour plots and the iso-curves are a particularly useful way of presenting the results. They provide a quick and easy means of identifying the different combinations of gear design parameters that have a given selective performance and can be extended to consider the influence of other design parameters, such as mesh shape, twine material and—as discussed by Herrmann and O'Neill (2006), if sufficient quantitative information exists—to factors such as light levels, fish condition/swimming ability, and water turbidity.

Acknowledgements

This work has been carried out with financial support from the Commission of the European Communities, on the specific RTD programme—Quality of Life and Management of Living Resources, "Development of predictive model of codend selectivity". It does not necessarily reflect the Commission's view and in no way anticipates its future policy in this area. The authors acknowledge the great debt they owe the partners in the EU projects PREMECS and PREMECS II. Financial support was also given from a project under the development programme for sustainable fishery financed by the Directorate for Food, Fisheries and Agri Business, Denmark.

References

Dahm, E., Wienbeck, H., West, C. W., Valdemarsen, J. W., and O'Neill, F. G. 2002. On the influence of towing speed and gear size on the selective properties of bottom trawls. Fisheries Research, 55, 103–119.

Galbraith, R. D., Fryer, R. J., and Maitland, K. M. S. 1994. Demersal pair trawl cod-end selectivity models. Fisheries Research, 20: 13–27.

Herrmann, B. 2005. Effect of catch size and shape on the selectivity of diamond mesh cod-ends. I. Model development. Fisheries Research, 71: 1–13.

Herrmann, B., and O'Neill, F. G. 2005. Theoretical study of the between haul variation of haddock selectivity in a diamond mesh cod-end. Fisheries Research, 74: 243–252.

Herrmann, B., and O'Neill, F. G. 2006. Theoretical study of the influence of twine thickness on haddock selectivity in diamond mesh cod-ends. Fisheries Research, 80: 221–229.

Kynoch, R. J., Ferro, R. S. T., and Zuur, G. 1999. The effect on juvenile haddock by-catch of changing cod-end twine thickness in EU trawl fisheries. MTS Journal, 33: 61–72.

Kynoch, R. J., O'Dea, M. C., and O'Neill, F. G. 2004. The effect of strengthening bags on cod-end selectivity of a Scottish demersal trawl. Fisheries Research, 68: 249–257.

Lowry, N., and Robertson, J. H. B. 1996. The effect of twine thickness on cod-end selectivity of trawls for haddock in the North Sea. Fisheries Research, 26: 353–363.

O'Neill, F. G., and Kynoch, R. J. 1996. The effect of cover mesh size and cod-end catch size on cod-end selectivity. Fisheries Research, 28: 291–303.

O'Neill, F. G. 1997. Differential equations governing the geometry of a diamond mesh cod-end of a trawl net. Journal of Applied Mechanics, 64: 1631–1648.

O'Neill, F. G. 1999. Axissymmetrical trawl cod-ends made from netting of generalized mesh shape. IMA Journal of Applied Mathematics, 62: 245–262.

O'Neill, F. G. 2002. Bending of twines and fibres under tension. Journal of the Textile Institute, 93: 1–10.

Reeves, S. A., Armstrong, D. W., Fryer, R. J., and Coull, K. A. 1992. The effects of mesh size, cod-end extension length and cod-end diameter on the selectivity of Scottish trawls and seines. ICES Journal of Marine Science, 49: 279–288.

doi:10.1093/icesjms/fsm101